THE ROLE OF NOTCH SIGNALING IN VASCULAR DEVELOPMENT AND HOMEOSTASIS

by

Linda Ya-ting Chang

B.Sc., University of British Columbia, 2003

A THESIS SUBMITTED IN PARTIAL FULFILLMENT OF THE REQUIREMENT FOR THE DEGREE OF

DOCTOR OF PHILOSOPHY

in

The Faculty of Graduate Studies

(Experimental Medicine)

THE UNIVERSITY OF BRITISH COLUMBIA

(Vancouver)

July 2010

ABSTRACT

The vasculature is essential for the delivery of oxygen and nutrients and the removal of metabolic wastes from tissues of the body. The embryonic vasculature is developed through the processes of vasculogenesis, angiogenesis, and arteriogenesis. Once the vasculature is fully developed and stabilized, the adult vasculature shows very little proliferation or cell death. Nevertheless, the endothelium, which lines the lumen of the blood vessels, is actively involved in the control of vascular tone, permeability, blood flow, coagulation, inflammation and tissue repair. An injury to the endothelium is important for progression of diseases such as atherosclerosis and the sepsis syndrome. The Notch signaling pathway has emerged in the recent decade as an important player in multiple vascular processes and endothelial behaviors. This thesis examines the role of the Notch signaling pathway in embryonic arteriogenesis and endothelial survival signaling.

The first part of this thesis investigates the developmental source of vascular smooth muscle cells. This study presents the first *in situ* observation of an immediate smooth muscle precursor cell present in all embryonic arteries. This $Tie1^{+}/CD31^{+}/VE\text{-}cadherin^{-}$ precursor requires Notch signaling to differentiate into vascular smooth muscle cells and to ensure vascular stability of newly formed arteries. However, Notch activation is not required in the precursor cells to maintain the medial layer of the arteries once the vessel is invested with vascular smooth muscle cells.

In the second part of this thesis, the mechanism of Notch-induced endothelial survival signaling is examined. In endothelial cells, Notch signaling activates phosphotidylinositol-3 kinase (PI3K) through up-regulation of a secreted factor. Activity of PI3K is required to offset the parallel apoptotic signaling induced by Notch activation and to maintain endothelial survival through the up-regulation of Slug, a direct Notch target with anti-apoptotic activity. Upon treatment with apoptotic stimuli, Notch activation shows context-dependent effects on

endothelial survival. Inhibition of PI3K activity and Slug expression by a stimulus abolishes Notch-induced endothelial survival and increases apoptotic death.

The work presented in this thesis shows that the Notch signaling pathway is essential for the stability of the vasculature through regulation of vascular smooth muscle cell differentiation and endothelial cell survival.

TABLE OF CONTENTS

LIST OF TABLES

LIST OF FIGURES

LIST OF ABBREVIATIONS

ADAM	a disintegrin and metelloprotease domain
AGM	aorta-gonad-mesonephros
APH1	anterior pharynx-defective 1
AVC	atrio-ventricular canal
AVM	arteriovenous malformation
CADASIL	cerebral autosomal dominant arteriopathy with subcortical infarcts and leukoencephalopathy
caspase	cysteinyl aspartyl-directed proteases
CD	cluster of differentiation
CDK8	cyclin-dependent kinase-8
CIR	CBF1-interacting co-repressor
COUP-TFII	chicken ovalbumin upstream promoter transcription factor II
CSL	CBF-1, Suppressor of Hairless Su(H), Lag-1
Dll	delta-like ligand
dnMAML	dominant-negative form of mastermind-like1
E10.5	embryonic day 10.5
ECM	extracellular matrix
EGF	epidermal growth factor
EndMT	endothelial-to-mesenchymal transdifferentiation
ER	endoplasmic reticulum
ES cell	embryonic stem cell
FACS	fluorescence activated cell sorting
FBXL14	F-box and leucine-rich repeat protein 14
FGF	fibroblast growth factor
Flk-1	fetal liver kinase 1

GAPDH	glyceraldehyde 3-phosphase dehydrogenase
GCN5	general control of amino-acid synthesis
GFP	green fluorescent protein
GOF	gain of function
Grl	gridlock
GSI	gamma-secretase inhibitor
GSK-3β	glycogen synthase kinase -3 beta
HAT	histone acetyl-transferases
HDAC	histone deacetylase complex
Hes	hairy/enhancer of Split
Hey	hairy/enhancer of Split related with YRPW
HMEC	human dermal microvascular endothelial cells
HUVEC	human umbilical vein endothelial cells
IAP	inhibitor of apoptosis protein
ISV	intersomitic vessel
LDL	low density lipoprotein
LOF	loss of function
LPS	lipopolysaccharide
MAML	mastermind-like
MCM	minichromosome maintenance
Mdm2	mouse double minute 2
MEF2D	myocyte-specific enhancer factor 2D
Msx2	muscle segment homeobox 2
mTOR	mammalian target of rapamycin
Myf-5	myogenic factor 5
MyoD	myogenic differentiation antigen 1
NFκB	nuclear factor of kappa-light-chain in B-cells

NLS	nuclear localization signal
P10	post-natal day 10
PCAF	p300/CBP-associated factor
PDGFR	platelet-derived growth factor receptor
PEN2	presenilin enhancer 2
PI3K	phosphotidylinositol-3 kinase
Pofut	protein o-fucosyl transferase
Ppa	partner of paired
PTEN	phosphatase and tensin homolog
RNAi	RNA interference
ROS	reactive oxygen species
RT-PCR	reverse transcription polymerase chain reaction
SKIP	ski-interacting protein
SMA	α-smooth muscle actin
Smad3	mothers against decapentaplegic homolog 3
SMRT	silencing mediator for retinoic acid and thyroid hormone receptor
SRF	serum response factor
TACE	tumor necrosis factor-a converting enzyme
TGF-β	transforming growth factor-beta
TNF	tumor necrosis factor
VE-cadherin	vascular endothelial cadherin
VEGF	vascular endothelial growth factor
VEGFR-2	vascular endothelial growth factor receptor-2
VSMC	vascular smooth muscle cells
YFP	yellow fluorescent protein

ACKNOWLEDGEMENTS

I would like to thank my parents, Jei-seng and Chang-hua Chang, for their support and understanding. I would not be able to dedicate myself wholeheartedly to my studies if you haven't been there for me, even if sometimes I was not there for you. I would also like to thank my sister Judy, for being my "lay-person" and editor through all the scholarship applications and her constant reminder that "science is cool".

I am grateful for my supervisor Dr. Aly Karsan for all these years of guidance, support and stimulating conversations. I have learnt so much about science in the environment that he has provided me. His excitement towards science is one of the many things that I will take away from this experience.

I would like to thank our collaborators Drs. Daniel Dumont and Mira Puri for providing the transgenic mice used in this thesis and the many valuable comments. Thank you to Dr. Laura Benjamin also for providing the VEtTA transgenic mouse.

I would also like to thank my supervisory committee members, Drs. Kelly McNagny, Catherine Pallen and Andrew Weng for their thought-provoking comments, useful suggestions, and dedication to my graduate school education and my projects.

Many thanks to Denise MacDougal for her assistance with flow cytometry and friendship over the years. Also I would like to thank the staff at the BCCRC flow core, animal resource center and transgenic core facilities for their expert help.

I am also grateful for the members of my laboratory, past and present, for their unfailing friendship, support, help and sessions of scientific musings through the years. I would not have enjoyed science and the graduate school experience without them. There are really memories that would last a lifetime. They have helped to build my skill set and confidence as a scientist-in-training. Thanks to Megan Fuller, Michelle Ly, Fred Wong and

Michelle Higginson also for their help with my projects. I especially like to thank Dr. Michela Noseda, whose dedication and enthusiasm to science is something I marvel at. Without her inspiration, I would not be where I am today.

Finally, I express my gratitude towards the Michael Smith Foundation of Health Research for providing the Graduate Studentships, which allow me to attend conferences and purchase useful reference books. Thanks to the Stem Cell Network, the Heart and Stroke Foundation of BC & Yukon, and the Canadian Institutes of Health Research for funding the research projects.

Chapter 1. INTRODUCTION

The vasculature is one of the most important and complex organs in mammals and is essential for the delivery of oxygen and nutrients and the removal of metabolic wastes from tissues of the body. The vasculature is the first functional system to form during development and its disruption during development leads to early embryonic death. The development of vascular system is a carefully orchestrated event that results in a network of vessels with various calibers and functions. Multiple cell types are generated as the result of vascular development: the endothelial cells which form the inner vessel wall and the mural cells which associate with and coat the endothelial tubes. In the normal adult vasculature, there is very little endothelial cell proliferation or cell death. However, the homeostasis of the adult vasculature requires active maintenance. Endothelial survival signaling is important due to the constant assault from apoptotic stimuli in the blood stream encountered by the endothelium. One of the signaling pathways involved in regulating the vasculature is the Notch signaling pathway, whose role has been demonstrated in cell type specification, contact inhibition and homeostasis establishment (reviewed by (Iso, Hamamori et al. 2003; Karsan 2005; Gridley 2007)). This dissertation will discuss the role of Notch signaling in the establishment of the vasculature in the embryo as well as the maintenance of a stable vascular system in the adult.

1.1. Vascular development and homeostasis

Formation of the cardiovascular system is an early and essential process during embryogenesis (Figure 1.1). The development of the vasculature initiates with the differentiation of endothelial cells, which are the specialized epithelial cells lining the lumen of the blood vessels, from mesodermal precursor cells called angioblasts. The cluster of endothelial cells then assembles into the primary capillary plexus, a network of uniformly sized endothelial tubes. This process is termed **vasculogenesis** (reviewed in (Flamme, Frolich et al. 1997; Drake, Hungerford et al. 1998)). This primitive plexus is then remodeled into a network of blood vessels of various diameters by the process of **angiogenesis,** during which vessels are pruned and new vessels are formed by either intussusception or sprouting. During angiogenic sprouting, the extracellular matrix (ECM) is broken down, cells sprout from the pre-existing endothelial tube, and endothelial cells then proliferate, migrate, and form into a new tubular structure (Folkman 1984). Finally, the new endothelial tube is stabilized by deposits of ECM and the recruitment of mural cells. In the case of artery formation, the mature arteries are surrounded by layers of vascular smooth muscle cells (VSMC) by the process of **arteriogenesis** (Carmeliet 2000). Interestingly, once stabilized, the adult vasculature is quiescent (Hobson and Denekamp 1984) with the exception of wound healing, menstruation (Reynolds, Killilea et al. 1992) or in pathological angiogenesis, such as in tumor growth (Hanahan and Folkman 1996) and rheumatoid arthritis (Colville-Nash and Scott 1992). The homeostasis of the mature vasculature is actively maintained by signaling pathways as the endothelium is constantly under stimulation by factors in the blood and the surrounding tissue.

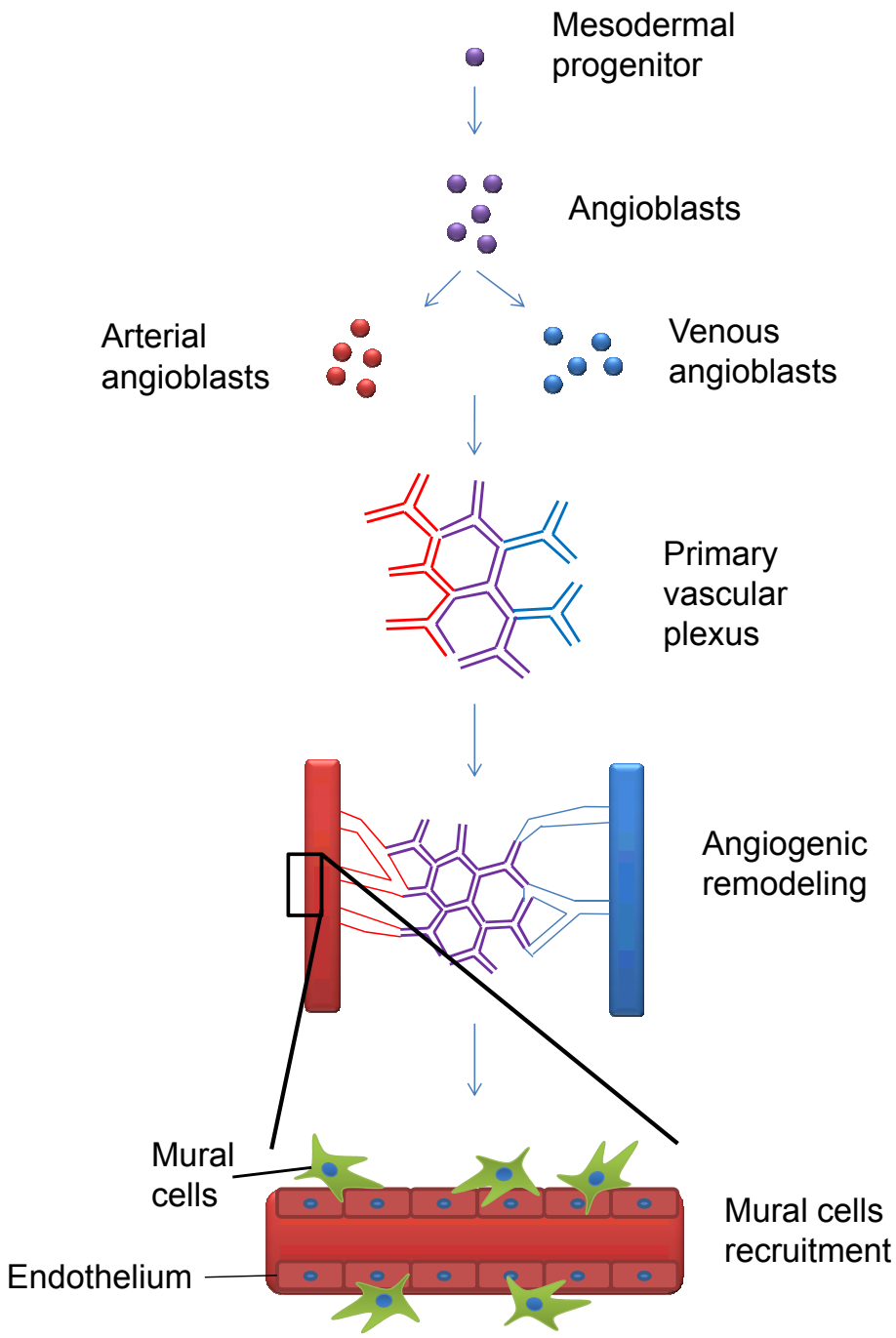

Figure 1.1. Embryonic vascular development. Endothelial precursors, called angioblasts, are differentiated from mesodermal progenitors. Angioblasts are further specified to arterial or venous fate. Angioblasts differentiate into endothelial cells, which form the endothelial tubes of the primary vascular plexus. The primary plexus undergoes angiogenic remodeling to form a vascular system complete with arteries, veins, capillaries, and other vessels of various calibers. The nascent blood vessels are stabilized by the recruitment of mural cells such as pericytes or vascular smooth muscle cell.

1.1.1. Vasculogenesis and angiogenesis

The site of the first vascular structure formed during embryogenesis is the yolk sac, where mesodermal precursors from the primitive streak of the embryo migrate to form the blood island (Ferguson, Kelley et al. 2005). Angioblast differentiation in the blood island results in endothelial-lined lumen filled with primitive blood cells (Haar and Ackerman 1971). These endothelial cords then fuse to form the primary capillary plexus of the yolk sac. The extraembryonic vasculogenesis is temporally and spatially distinct from the intraembryonic vasculogenesis (Ferguson, Kelley et al. 2005). In the embryo proper, endothelial cell precursors also reside in the mesodermal layer in early embryonic development, more specifically in the paraxial and the lateral plate mesoderm (Wilting and Becker 2006). There is evidence of multipotent progenitor cells derived from the mesoderm that can differentiate into endothelial cells, such as the hemangioblasts (Vogeli, Jin et al. 2006) or fetal liver kinase-1 (Flk-1)-expressing cardiovascular progenitors (Yang, Soonpaa et al. 2008). These progenitors migrate to the site of vessel formation taking cues from the surrounding tissues. Endothelial specification of the angioblast is followed by lumen formation to generate an endothelial tube capable of containing the circulating blood (Coffin, Harrison et al. 1991). The first vessels formed through vasculogenesis in the embryo proper are the dorsal aorta and the cardinal vein (Flamme, Frolich et al. 1997).

The arterial endothelium is phenotypically and functionally different from the venous endothelium. The arteries bring oxygenated blood at high pressure from the heart to the rest of the organism through smaller caliber arterioles and capillaries. The veins return the low-oxygen blood back to the pulmonary system. It was long believed that variation in hemodynamic force and oxygenation from the blood flow differentiates the arterial system from the venous system. Interestingly, “arterial” and “venous” angioblasts with differential arterial and venous markers (see Table 1.1) were observed from the mesoderm prior to the establishment of blood flow, suggesting that the specification between artery and veins is

regulated by genetic factors as well as blood flow (Wang, Chen et al. 1998; Adams, Wilkinson et al. 1999). Many of the markers specifying arteriovenous fate are components of signaling pathways, such as Notch/Delta-like ligand (Dll) and Eph receptor/Ephrin, proposing the involvement of those signaling pathways in the arteriovenous cell fate decision.

Table 1.1. Mammalian arterial and venous endothelial markers during vascular development

Arterial endothelial marker	Venous endothelial marker
EphrinB2 (Wang, Chen et al. 1998)	EphB4 (Wang, Chen et al. 1998)
Neuropilin1 (Herzog, Kalcheim et al. 2001)	Neuropilin2 (Herzog, Kalcheim et al. 2001)
Notch4 (Villa, Walker et al. 2001)	COUP-TFII (You, Lin et al. 2005)
Dll4 (Villa, Walker et al. 2001)	
CD44 (Wheatley, Isacke et al. 1993)	

The primary capillary plexus is a network of endothelial tubes with uniform diameters, which is further remodeled into a functional system of vessels of various calibers by angiogenesis. This process is readily observed in the formation of yolk sac vasculature and the embryonic cephalic vasculature (Coffin and Poole 1988). Vascular remodeling involves the regression of branches from large vessels like the artery, vessels splitting by intussusceptive growth and new capillary sprouting from pre-existing vessels. In the embryo proper, the intersomitic vessels are formed by new capillaries sprouting from the dorsal aorta (Poole and Coffin 1989). Angiogenic sprouting requires a sequence of highly coordinated endothelial activities, starting with the disruption of ECM around the formation of the new sprout, followed by the guided migration and proliferation of endothelial cells, the re-establishment of the ECM, and finally the stabilization of the nascent vessel with the recruitment of mural cells, such as pericytes and VSMC (Carmeliet 2003). The endothelial cell is an anchorage-dependent cell type, for which contact with ECM or neighboring cells is required for survival. During sprouting, additional survival signaling will be necessary as the endothelial cells obtain a migratory morphology and break away from their neighbors (Liu,

Ahmad et al. 2000). Angiogenic sprouting is regulated by cytokines from the surrounding tissue, bidirectional signaling between mural cells and the endothelium, and cell-cell contact dependent signaling between adjacent endothelial cells.

The initiation of a new angiogenic sprout requires a specialized endothelial cell, called a tip cell. This cell is more “explorative” than the endothelial cells still residing in the monolayer of the original vessel. It is characterized by the appearance of filopodia, which are outstretched actin filament-containing protrusions that also contain vascular endothelial growth factor receptor-2 (VEGFR-2) (Gerhardt, Golding et al. 2003). The tip cell has the ability to respond to the changing gradient of vascular endothelial growth factor (VEGF) and guide the new sprout by migrating towards the area of high VEGF concentration. Following the tip cell is the stalk cell, which proliferates and elongates the sprout as the tip cell migrates (Gerhardt, Golding et al. 2003). The stalk cell also forms the lumen and later recruits mural cells. While tip cell formation is required for the generation of a new sprout, excessive tip cell specification may create a defective vascular network (Suchting, Freitas et al. 2007). In order for productive angiogenesis to occur, there must be signals present to direct the tip cell and stalk cell fate. These signals will be discussed in later sections.

1.1.2. Embryonic arteriogenesis

The process of arteriogenesis is essential for the establishment of a proper embryonic vasculature. VSMC play an important role in the overall stability of the vasculature. During development, they provide structural support for the nascent arteries and are also involved in bidirectional signaling with the endothelium. In the absence of VSMC or pericytes, developing murine vasculature becomes unstable and exhibits a hemorrhagic phenotype along with embryonic lethality (Hungerford and Little 1999; Li, Sorensen et al. 1999). Diseases like hereditary hemorrhagic telangiectasia may be affected by poor VSMC development (Li, Sorensen et al. 1999).

VSMC development occurs between embryonic day 9.5 (E9.5) and E11.5 for major arteries (Takahashi, Imanaka et al. 1996). A detailed study on the differentiation of VSMC during early murine vascular development was performed with immunohistochemistry labeling of α-smooth muscle actin (SMA) (Takahashi, Imanaka et al. 1996). The first artery to associate with VSMC in the embryo proper is the dorsal aorta starting at E9.5. The ventral portion of the dorsal aorta is the first to recruit smooth muscle covering, followed by the dorsal region. Smooth muscle development is also more advanced in the thoracic region of the fused dorsal aorta compared to the paired dorsal aortae either rostral or caudal to it. VSMC development of the internal carotid artery initiates at E10.5 with only discontinuous VSMC coverage (Takahashi, Imanaka et al. 1996). The pharyngeal arch arteries also exhibit discontinuous SMA staining in the ventral region at E10.5, while there is still no VSMC around the endothelial tube in the extremities, such as the caudal artery of the tail (Takahashi, Imanaka et al. 1996). One day later, at E11.5, most arteries, including the vertebral artery and some veins are covered with at least a discontinuous layer of VSMC.

VSMC of developing vessels present themselves as a heterogeneous population with a wide range of phenotypes at different stages of differentiation for different vascular beds (Owens, Kumar et al. 2004). As more studies are performed to examine the origin of embryonic VSMC, it becomes clear that the heterogeneity may be generated by the mosaic origin of the VSMC precursors (Majesky 2007). This observation adds layers of complexity in deciphering the molecular and cellular signaling pathways involved in VSMC differentiation as each developmental source may utilize different mechanisms to become mature VSMC. However, the work presented in this thesis proposes a local common VSMC precursor whose differentiation is regulated through Notch signaling.

1.1.2.1. Sources of vascular smooth muscle cells during development

From lineage-tracing experiments using either a genetic reporter or cross-species-transplants, various embryonic tissues have been shown to be sources of VSMC during development (reviewed in (Gittenberger-de Groot, DeRuiter et al. 1999; Majesky 2007)) (Figure 1.2). While most of the early experiments were done in avian models, there has been an emergence of mammalian (mostly murine) models in recent years. In addition, the use of embryonic stem cells has also advanced our knowledge of progenitor cell differentiation and the molecular signaling pathways involved. The combination of both lines of investigation has shed light on the mosaic origin of VSMC.

The first study to identify a tissue-specific source of VSMC focused on the avian neural crest cells, and found that this progenitor cell type incorporated into the cardiovascular system as VSMC of the ascending aorta, the aortic arch and the carotid arteries and the mesenchyme of the septum dividing the aorta and the pulmonary artery (Le Lievre and Le Douarin 1975; Kirby, Gale et al. 1983). Later studies using cell fate tracing during mammalian development confirmed the observations made in chick embryos (Jiang, Rowitch et al. 2000; Li, Chen et al. 2000). It is especially noteworthy that the boundary between neural crest-derived VSMC and VSMC from other sources is very distinct as no neural crest-derived VSMC are found in the neighboring subclavian arteries, coronary arteries and descending aorta (Jiang, Rowitch et al. 2000; Li, Chen et al. 2000).

VSMC that arise from a distinct source are also found in the walls of coronary arteries. Cell fate tracing in avian development using cells transduced with β-galactosidase viral vector showed that progenitor cells from the pro-epicardium can give rise to cells of the mature epicardium, the coronary endothelium and also the VSMC of the coronary arteries (Mikawa and Gourdie 1996). This observation was confirmed in later studies using chick-quail chimera (Gittenberger-de Groot, Vrancken Peeters et al. 1998; Perez-Pomares, Macias et al. 1998) or

adenovirus tagged epicardium (Dettman, Denetclaw et al. 1998). Again, the boundary of pro-epicardium-derived VSMC is very distinct. The VSMC of the ascending aorta, which is physically connected to the coronary artery, are from another source.

The cells of the vasculature come from the mesodermal germ layer of the developing embryo. During avian development, both the splanchnic mesoderm (Wiegreffe, Christ et al. 2009) and the somites (Pouget, Gautier et al. 2006) have been shown to differentiate into VSMC of the dorsal aorta. However, the processes are mutually exclusive and sequential. The splanchnic mesoderm contains progenitor cells that can differentiate into endothelial cells, smooth muscle cells and hematopoietic cells (Pardanaud, Luton et al. 1996). During early embryogenesis, the dorsal aorta is constructed by splanchnic mesoderm-derived endothelial cells and VSMC (Hungerford, Owens et al. 1996). As the vessel matures, the dorsal endothelium is replaced by somite-derived endothelial cells (Pouget, Gautier et al. 2006). Somite-derived endothelial and VSMC will proceed to replace splanchnic mesoderm-derived cells in the dorsal aorta as development advances. Cell fate tracing with either a lateral plate mesoderm-specific promoter or a paraxial mesoderm-specific promoter in murine embryos reveals similar observations (Wasteson, Johansson et al. 2008). Clonal analysis in murine embryogenesis also shows that VSMC of the descending aorta share common somite-derived precursor cells with the dorsal skeletal muscle (Esner, Meilhac et al. 2006). While the somitic precursors migrate ventrally towards the dorsal aorta, it does not migrate in the rostral-caudal axis (Esner, Meilhac et al. 2006), suggesting that VSMC of different segments of the dorsal aorta differentiate independently from each other. In the adult thoracic and abdominal aorta, cell tracing also shows that aortic VSMC are of somitic origin (Wasteson, Johansson et al. 2008). These studies suggest that in both murine and avian development, VSMC of the descending aorta first comes from the splanchnic mesoderm and are later replaced by somitic cells.

Examination of these tissue-derived VSMC showed a common theme: within a tissue, only a subset of cells has the ability to differentiate into VSMC. During avian dorsal aorta development, while cells from the mesoderm can migrate to the site of dorsal aorta formation, only a small percentage of mesoderm cells actually integrate as a part of the dorsal aorta (Pouget, Gautier et al. 2006), suggesting the existence of a vascular progenitor cell within the tissue that is predisposed towards a vascular fate.

Several studies have been done to isolate and culture VSMC progenitor cells from mammalian sources. Among them, the mesoangioblasts (Minasi, Riminucci et al. 2002) and the embryonic stem cell (ES cell)-derived cardiovascular progenitors (Yamashita, Itoh et al. 2000; Yang, Soonpaa et al. 2008) both express the same marker, Flk-1, a receptor for VEGF. Mesoangioblasts are mesodermal progenitors isolated from E9.5 mouse embryonic dorsal aorta (Minasi, Riminucci et al. 2002). Mesoangioblast can incorporate into developing chick embryos as VSMC, skeletal muscle, cardiomyocytes and osteocytes, showing multipotency in the mesodermal lineages (Minasi, Riminucci et al. 2002). The mesoangioblasts also expresses hemo-angioblastic markers such as cluster of differentiation (CD)34, MEF2D (myocyte-specific enhancer factor 2D) and cKit and a subpopulation of mesoangioblasts is also positive for SMA expression (Minasi, Riminucci et al. 2002).

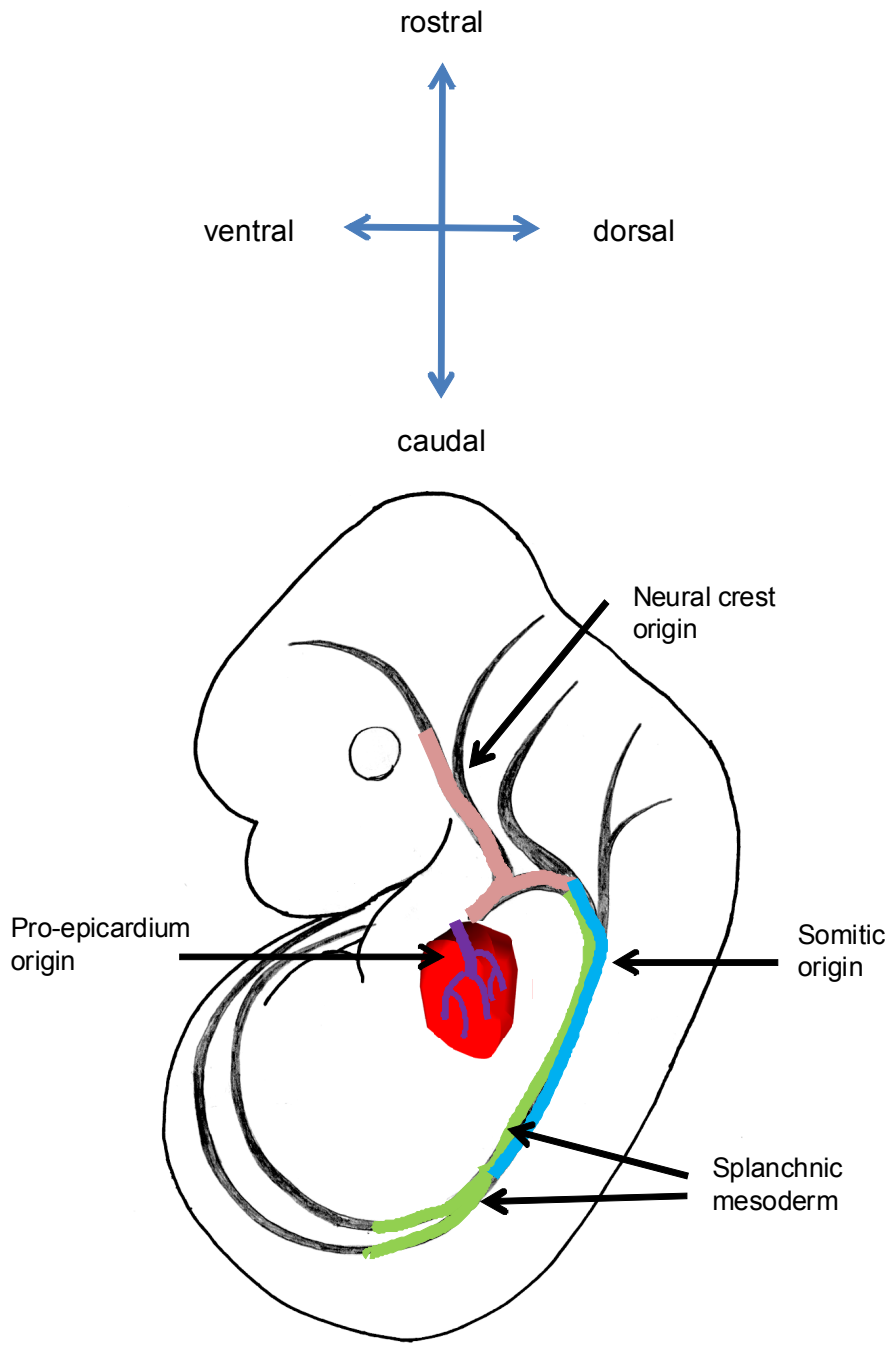

Figure 1.2. Mosaic origin of vascular smooth muscle cells. Vascular smooth muscle cells (VSMC) are derived from different tissue origin depending on the vascular bed. The arterial VSMC of the coronary artery comes from the pro-epicardial origin. The ascending aorta, the aortic arch and the carotid arteries are derived from the neural crest cells. The descending aorta is first populated by VSMC of the splanchnic mesoderm origin, which are later replaced by somite-derived VSMC. However, VSMC of the caudal region of the abdominal aorta remains to be of the splanchnic mesoderm origin.

Flk-1 positive progenitor cells can also be generated from differentiating ES cells and can further differentiate into endothelial cells, mural cells and cardiomyocytes (Kattman, Huber et al. 2006). Flk-1 positive cells can also form vascular tubes in three-dimensional culture and be incorporated into the developing chick vasculature as both endothelial cells and mural cells (Yamashita, Itoh et al. 2000). When the Flk-1 promoter is used in lineage tracing experiments, endothelial cells, hematopoietic cells, cardiomyocytes and surprisingly, skeletal muscle cells, are found to come from Flk-1 positive progenitors; however, no VSMC was observed to have come from Flk-1^+ cells (Motoike, Markham et al. 2003). A similar Flk-1 positive progenitor can be isolated from differentiating human ES cells by a cytokine-regulated protocol (Yang, Soonpaa et al. 2008). Both progenitor cells can be expanded *ex vivo* and are capable of incorporating into developing avian vasculature as endothelial and smooth muscle cells. However, there is still a lack of direct *in vivo* evidence and *in situ* tracking of an immediate vascular progenitor cell that can differentiate into VSMC within the mammalian development system.

Anatomically, the endothelium is the cell type most closely associated with VSMC. Interestingly, the endothelium has been shown to be a possible source of VSMC through the process of endothelial-mesenchymal transdifferentiation (EndMT) in an avian developmental model (DeRuiter, Poelmann et al. 1997). Endothelial cell fate tracing with dye-uptake and co-localization of endothelial and smooth muscle markers suggests that the smooth muscle layer closest to the endothelium may come from an endothelial source (Arciniegas, Neves et al. 2005). In pulmonary hypertension, EndMT has also been suggested to be a mechanism for pathological arterial neointimal thickening (Arciniegas, Frid et al. 2007). However, there are no studies examining the endothelium as a possible source of smooth muscle progenitor cells during mammalian development. Experiments from our lab and others have shown that mammalian endothelial cells can be induced to undergo EndMT *in vitro* (Noseda, McLean et

al. 2004; Deissler, Lang et al. 2006; Kitao, Sato et al. 2009). This thesis will further investigate the *in vivo* significance of this observation.

1.1.3. Endothelial homeostasis in pathogenesis

Once the cardiovascular system is fully developed, the adult vasculature remains seemingly quiescent with the exception of physiological processes like wound healing and menstruation. In adult macrovessels, only 0.1% of the endothelial cells are undergoing mitosis (Schwartz and Benditt 1977), while endothelial programmed cell death (apoptosis) is a rare event in healthy individuals (Alvarez, Gips et al. 1997). Still, the endothelium is actively involved in the control of vascular tone, permeability, blood flow, coagulation, inflammation and tissue repair (reviewed in (Cines, Pollak et al. 1998)). Endothelial dysfunction has been linked to a variety of cardiovascular diseases.

Interestingly, when signaling pathways required for vascular development are disrupted in the adult endothelium, this can result in disturbances in vascular homeostasis and sometimes even death. For example, adult mice with endothelial-specific inactivation of the VEGF gene show increased mortality compared to littermate control mice (Lee, Chen et al. 2007). The VEGF mutants exhibit systemic vascular pathologies such as hemorrhages, abnormal accumulation of ECM and appearance of microinfarcts in multiple organs. Examination of the endothelium in VEGF mutants shows morphological changes typical of apoptosis (Lee, Chen et al. 2007).

Disruption of vascular homeostasis from deregulated apoptosis and growth has systemic and detrimental effect on the overall health of the individual. This thesis will examine the mechanism of endothelial survival when stimulated with agents that damage the vasculature.

1.1.3.1. Apoptosis

Apoptosis, often referred to as “programmed cell death”, can be morphologically identified by the plasma-membrane vesiculation (also called membrane blebbing), nuclear condensation, nuclear fragmentation and an appearance of overall cell shrinkage of an apoptotic cell (Kerr, Wyllie et al. 1972). The cellular material is encapsulated within vesicles (called apoptotic bodies) and is quickly phagocytosed without leading to an inflammatory response (Kerr, Wyllie et al. 1972). Apoptosis can be triggered by either an environmental source (extrinsic) or an intracellular stress (intrinsic) (reviewed by (Adams 2003)). The extrinsic apoptotic pathway often leads to activation of the intrinsic mechanism and both pathways result in the activation of a family of cysteinyl aspartyl-directed proteases (caspases), where a cascade of caspase activation leads to cleavages of many intracellular proteins during apoptosis (Thornberry and Lazebnik 1998). Pro-apoptotic stimuli can activate apoptotic pathways by interacting with the death receptor pathways, inducing expression or activity of proteins involved in the intrinsic pathway, or inhibiting survival signaling pathways within the cell. On the other hand, anti-apoptotic stimuli can activate survival pathways and/or induce expression of anti-apoptotic protein within the cell, such as the proteins in the Inhibitor of Apoptosis Protein (IAP) family or the Bcl-2 family.

Maintenance of the adult vasculature is especially challenging because the endothelium is under constant assault of stimuli that are present in the blood. The survival of individual endothelial cells and the maintenance of homeostasis require a local balance of pro- and anti-apoptotic agents. Each of these stimuli has the capability to activate intracellular signaling events within the endothelial cells. Therefore, an intracellular balance of pro- and antiapoptotic signals must also be reached to prevent unwanted activation of the apoptotic cascade (Stefanec 2000). Endothelial apoptosis in the vasculature is associated with the initiation and/or progression of serious diseases, often leading to mortality. Thus, by broadening our understanding of the mechanisms by which different stimuli cause endothelial

apoptosis, we may be able to perturb the progression of vascular disease by maintaining endothelial integrity.

1.1.3.2. Diseases associated with endothelial apoptosis

Many of the commonly known risk factors of cardiovascular disease are pro-apoptotic in endothelial cells. Therefore, it is not surprising that endothelial apoptosis exacerbates the progression of some diseases. This section introduces two distinct endothelial apoptotic stimuli examined in this thesis and their associated vascular disorders.

Atherosclerosis is a disease that can lead to cardiac infarct, stroke or peripheral vascular disease. It is characterized by the build-up of the atherosclerotic plaque at the vessel wall. Over time, the plaque can grow and constrict the vessel, causing reduced blood flow. Endothelial apoptosis has been observed both in the atherosclerotic plaque and just downstream of the plaque in patients suffering from carotid atherosclerosis (Alvarez, Gips et al. 1997; Tricot, Mallat et al. 2000). Moreover, apoptotic endothelial cells show increased adherence to platelets and leukocytes (Bombeli, Schwartz et al. 1999; Schwartz, Karsan et al. 1999), which may contribute to the progression of plaque formation. One of the risk factors for atherosclerosis is hyperhomocysteinemia (Clarke, Daly et al. 1991; McCully 1996), where patients experience an elevated plasma concentration of total homocysteine. Homocysteine is a metabolic product in the conversion between methionine and cysteine. Serum homocysteine levels can be increased through genetic mutation of enzymes in the homocysteine metabolic pathway or through dietary deficiency of vitamin B's required for homocysteine metabolism. High level of homocysteine can induce endothelial apoptosis by increasing intracellular reactive oxygen species (ROS) (Lee, Kim et al. 2005), upregulating p53 and Noxa, increasing endoplasmic reticulum (ER) stress (Zhang, Cai et al. 2001), activating the intrinsic apoptotic pathway through mitochondria destabilization (Tyagi, Ovechkin et al. 2006), and decreasing signaling through the phosphotidylinositol 3-kinase

(PI3K) pathway (Suhara, Fukuo et al. 2004). Homocysteine-induced endothelial apoptosis is most likely the result of interaction between multiple pro-apoptotic signaling pathways (see Table 1.2).

Table 1.2. Signaling pathway activation by homocysteine and lipopolysaccharide.

	Intracellular reactive oxygen species	**p53 pathway**	**Intrinsic apoptosis pathway**	**PI3K pathway**
Homocysteine	Increase ROS (+)[1]	Increase p53 activity (+)	Activates intrinsic apoptotic pathway (+)	Decrease PI3K activity (-)
Lipopolysaccharide	Increase ROS (+) Increase NO (-)[2]	Increase p53 acitivity (+)	Activates intrinsic apoptotic pathway (+)	Increase PI3K activity (+)

Another human disease that is associated with endothelial death is sepsis. Sepsis is a systemic inflammatory disorder whose complications include systemic vascular collapse, multi-organ failure and acute respiratory distress (Bannerman and Goldblum 2003). Endotoxin, also known as lipopolysaccharide (LPS), is present on gram-negative bacteria and is a mediator of the sepsis syndrom (Parrillo 1993). LPS-stimulation induces endothelial apoptosis *in vitro* (Bannerman and Goldblum 2003). Endothelial apoptosis leads to detachment of cells from the vessel, activation of the coagulation pathway, and increase in vascular permeability. These endothelial defects may exacerbate the effect of LPS, especially in the lung, where respiratory distress can be caused by edema. When a caspase inhibitor is administrated after LPS injection, there is a reduced level of acute lung injury and decreased endothelial apoptosis (Kawasaki, Kuwano et al. 2000). LPS activates apoptosis in endothelial cells through generation of ROS and activation of both the extrinsic (Bannerman, Tupper et al. 2001) and intrinsic apoptotic pathways (Munshi, Fernandis et al. 2002; Wang, Akinci et al.

[1] Increase in pathway activation
[2] Decrease in pathway activation

2007). However, LPS-induced endothelial apoptosis is more readily observed with inhibition of endogenous anti-apoptotic proteins FLIP and Mcl-2 (Bannerman, Tupper et al. 2001). Interestingly, LPS stimulation in endothelial cells also activates pro-survival pathways such as nitric oxide synthesis (Huang, Kuo et al. 1998) and PI3K activation (Wong, Hull et al. 2004). The overall apoptotic phenotype in LPS-stimulated cells may require other pro-apoptotic signals to tip the balance between two opposing signals (Table 1.2).

1.1.4. Signaling pathways in vascular development and homeostasis

Many signaling pathways are involved in generation of the complex vascular system, and some of these pathways are also required to maintain adult vessel homeostasis. The fibroblast growth factor (FGF) pathway is important for the specification of mesodermal progenitors and angioblasts (Cox and Poole 2000; Ciruna and Rossant 2001). Signaling through the VEGF pathway is required for multiple steps in vascular development, including angioblast migration, endothelial tube formation, and arterial endothelial cell specification (Coultas, Chawengsaksophak et al. 2005). In the adult, the VEGF signal is required for endothelial survival and regulation of vascular permeability (Lee, Chen et al. 2007). The Eph receptors and their ligands in the Ephrin family play integral roles in the arteriovenous specification of angioblast and endothelial cells (Wang, Chen et al. 1998; Adams, Wilkinson et al. 1999). The transforming growth factor-β (TGF-β) pathway is required for proper vessel patterning during angiogenesis and pericyte recruitment (Darland and D'Amore 2001; Pardali and ten Dijke 2009). The Tie/Angiopoietin signaling between mural cells and endothelial cells induces sprouting angiogenesis (Koblizek, Weiss et al. 1998) and enhances vessel stability. Lastly, examination of mutants in the Notch signaling pathways shows that Notch activation is essential for vascular development by regulating multiple endothelial processes (Iso, Hamamori et al. 2003). This thesis will examine the role of Notch signaling in both vascular smooth muscle development and endothelial cell survival.

1.2. Notch signaling pathway

Development is the spatially and temporally controlled process whereby the complexity of a multi-cellular organism is built from one single cell. There are surprisingly few signaling pathways which govern the multifaceted processes of development (Gerhart 1999), and those that exist are often evolutionarily well-conserved (Pires-daSilva and Sommer 2003). One of these pathways is the Notch signaling pathway. Many components of this pathway have been shown to be conserved through the Metazoan lineage, from worms to humans (Gazave, Lapebie et al. 2009). At different stages of development, Notch signaling is found to be essential for processes that include asymmetric cell-fate decision, boundary formation, and lateral inhibition (reviewed by (Bray 1998; Artavanis-Tsakonas, Rand et al. 1999; Baron, Aslam et al. 2002; Hurlbut, Kankel et al. 2007)), all of which are involved in creating the diversity of cell types and their organization in an organism.

1.2.1. Notch signaling overview

There are four identified Notch receptors in mammals, Notch1-4. The receptor is first translated as one single 300 kDa polypeptide, which is then processed by a furin-like convertase in the trans-Golgi network (Blaumueller, Qi et al. 1997; Logeat, Bessia et al. 1998). The processed receptor is expressed on the cell surface as a transmembrane heterodimer held together non-covalently by a calcium-dependent interaction (Rand, Grimm et al. 2000). Notch signaling is activated when transmembrane receptors interact with transmembrane ligands (Jagged1/2 and Dll1/3/4 in mammals) on neighboring cells. This physical interaction via the epidermal growth factor (EGF)-like repeats in the extraceullular domain of the receptor (Rebay, Fleming et al. 1991) is cell-cell contact dependent. Receptor-ligand interaction leads to the cleavage of the Notch receptor at an extracellular site (termed S2) by metalloprotease TACE (TNF-α converting enzyme; also known as ADAM17, a member of a disintegrin and metalloprotease domain family) (Brou, Logeat et al. 2000) or

Kuzbanian (Kuz, or ADAM10) (Rooke, Pan et al. 1996). Evidence supporting the subsequent transendocytosis of the extracellular domain of Notch receptor into the ligand-expressing cells exists (Parks, Klueg et al. 2000; Morel, Le Borgne et al. 2003), although it is unknown whether this process is required for Notch receptor activation.

Following the cleavage at S2, the Notch receptor is further processed by the γ-secretase complex. Presenilin is the enzymatic subunit of γ-secretase, which also contains nicastrin, PEN2 (presenilin enhancer 2) and APH1 (anterior pharynx-defective 1) (Ray, Yao et al. 1999; Goutte, Tsunozaki et al. 2002; Hu, Ye et al. 2002; Lopez-Schier and St Johnston 2002; Kimberly, LaVoie et al. 2003). This second proteolytic cleavage in the transmembrane domain of Notch receptor (S3) releases the intracellular domain of Notch (NotchIC) into the cytoplasm (De Strooper, Annaert et al. 1999). NotchIC, which contains two putative nuclear localization signals (NLS) (Stifani, Blaumueller et al. 1992), translocates to the nucleus where it interacts with DNA-binding protein CSL (CBF-1, Suppressor of Hairless Su(H), Lag-1) (Tamura, Taniguchi et al. 1995). The nuclear localization of NotchIC has been shown to be required for its activity (Kopan, Nye et al. 1994; Schroeter, Kisslinger et al. 1998).

In the absence of Notch activation, CSL is a transcriptional repressor (Dou, Zeng et al. 1994; Waltzer, Logeat et al. 1994) that binds to the DNA sequence 5'-C(T)GTGGGAA-3' with high affinity (Tun, Hamaguchi et al. 1994) and recruits co-repressor proteins SMRT/N-CoR (silencing mediator for retinoic acid and thyroid hormone receptor/nuclear repressor), CIR (CBF1-interacting co-repressor), and SKIP (Ski-interacting protein) to target promoters. The CSL-co-repressor complex then recruits histone deacetylase complex (HDAC) to deacetylate histones at the promoter, leading to repression of target transcription (Kao, Ordentlich et al. 1998; Hsieh, Zhou et al. 1999). Interaction between NotchIC and CSL leads to the displacement of the co-repressors and the recruitment of co-activator Mastermind-like (MAML) (Jeffries, Robbins et al. 2002; Wu, Sun et al. 2002), which in turn recruits other co-activators such as CBP/p300 (Oswald, Tauber et al. 2001; Fryer, Lamar et al. 2002), PCAF

(p300/CBP-associated factor) and GCN5 (general control of animo-acid synthesis) (Kurooka and Honjo 2000), all of which have histone acetyl-transferase (HAT) activity. The co-activator complex opens up the chromatin and allows active transcription of target genes (summarized in Figure 1.3).

The target genes of Notch signaling are highly cell type-dependent. There are two classically defined families of Notch targets, the Hes (hairy/enhancer of Split) and the Hey (hairy/enhancer of Split related with YRPW) transcription repressors (Iso, Sartorelli et al. 2001). From *in vitro* experiments in endothelial cells Hes1, Hey1, and Hey2 have all been shown to be Notch signaling targets (Shawber, Das et al. 2003; MacKenzie, Duriez et al. 2004). In addition, EphrinB2, an arterial specific marker, is also a target of Notch activation in endothelial cells (Shawber, Das et al. 2003). Recently, studies on the role of Notch activation in EndMT have also identified many mesenchymal genes as targets of Notch signaling (Noseda, Fu et al. 2006; Jin, Hansson et al. 2008; Niessen, Fu et al. 2008). I will discuss the Notch-induced mesenchymal transformation in more detail in later sections

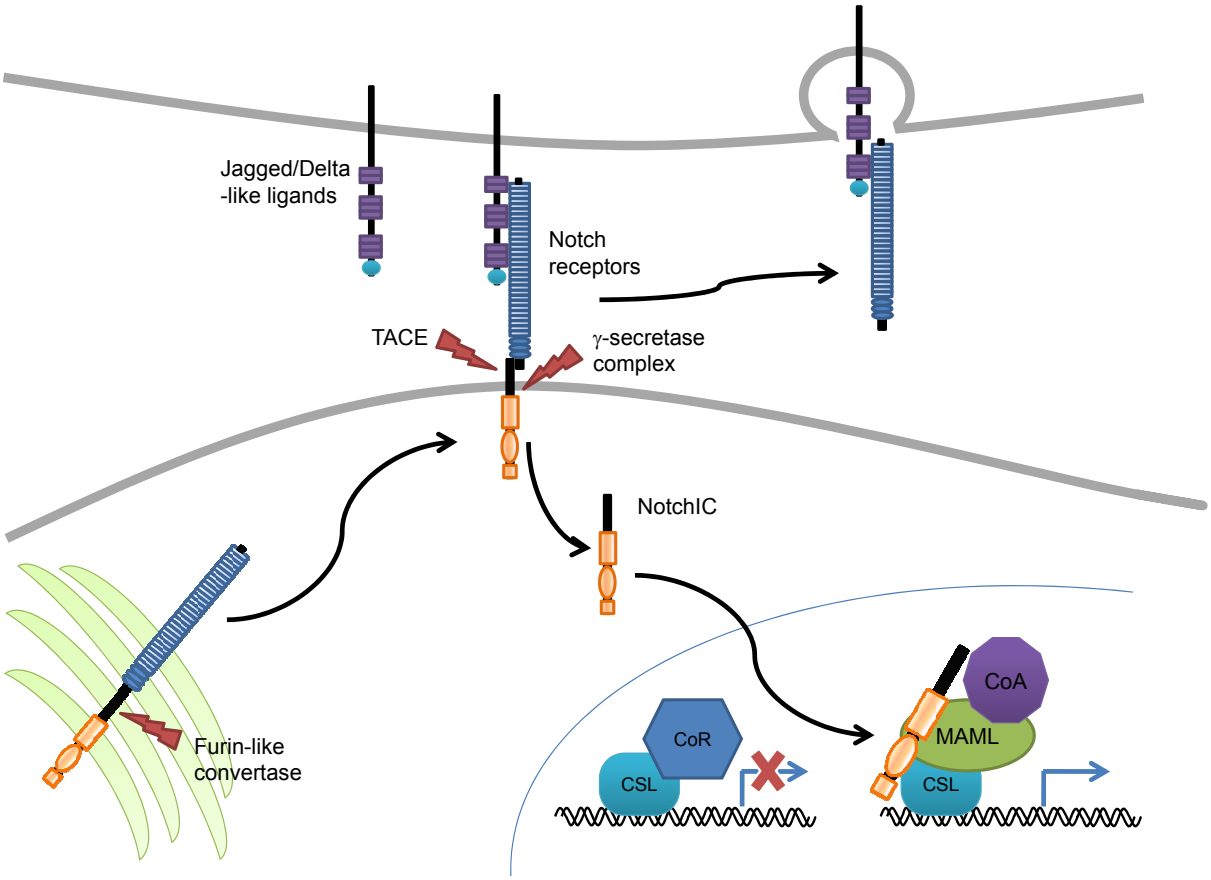

Figure 1.3. A simplified view of the Notch signaling pathway. The receptor is processed by a furin-like convertase in the trans-Golgi network. The processed receptor is expressed on the cell surface as a transmembrane heterodimer. Notch signaling is activated when the receptors (Notch1-4 in mammals) interact with transmembrane ligands (Jagged1/2 and Dll1/3/4 in mammals) on neighboring cells through the extraceullular domain of the receptor. Receptor-ligand interaction leads to the cleavage of the Notch receptor by metalloprotease TACE. There is evidence supporting the subsequent trans-endocytosis of the extracellular domain of Notch receptor into the ligand-expressing cells. Following the cleavage at S2, Notch receptor is further processed by the γ-secretase complex. This second proteolytic cleavage releases the intracellular domain of Notch (NotchIC) into the cytoplasm. NotchIC translocates to the nucleus after it is untethered from the membrane. Once in the nucleus, NotchIC then interacts with DNA-binding protein CSL. CSL, in the absence of Notch activation, is a transcription repressor. Interaction between NotchIC and CSL leads to the displacement of the co-repressors and the recruitment of co-activator MAML. The co-activator complex opens up the chromatin and allows active transcription of target genes. There are two classically defined families of Notch targets, the Hes and the Hey transcription repressors.

1.2.2. Modifiers of Notch signaling

Since Notch plays an important role in development where spatiotemporal control of signals is essential, activation of the pathway must be tightly regulated. Interestingly, the expression of the Notch receptors is found to be ubiquitous while receptor activation and downstream signaling show stringent regulation. One method by which Notch signaling is modulated is through ligand expression. At the initiation of angiogenesis, VEGF activates VEGF receptors, which in turn up-regulate transcription of Dll4 in endothelial cells. Thus, through activation of Notch receptor on neighboring endothelial cells by cell-to-cell contact, the Dll4-expressing cell can regulate the angiogenic process (Lobov, Renard et al. 2007).

In addition to the cleavage by a furin-like convertase, other modifications are made to Notch receptors in the ER and the trans-Golgi network. The extracellular domain of Notch is o-fucosylated by protein o-fucosyl transferase (Pofut) in the ER (Okajima and Irvine 2002). Pofut expression is also required for proper protein folding and cellular membrane sorting of the receptor (Sasamura, Ishikawa et al. 2007). The Pofut1-null mouse shows phenotypes indicative of systemic Notch signaling defects (Okamura and Saga 2008). After the addition of the first fuctose, additional modifications can be made by extending the carbohydrate chain. Through glycosylation of EGF repeats, the Fringe family of glycosyl transferases can alter the affinity of Notch receptor to ligands and favor signals from Dll at the expense of Jagged ligands (Panin, Papayannopoulos et al. 1997; Bruckner, Perez et al. 2000). In this fashion, additional regulation of the Notch signal can be made without altering the expression of ligands or receptors.

Another method of regulating ligand activity is through post-translational modification of the ligands. Expression of E3 ligases Mind bomb and Neuralized are required for Notch ligand activity (Itoh, Kim et al. 2003). Mind bomb and Neuralized are involved in the mono-ubiquitination and Epsin-mediated endocytosis of Notch ligands Jagged and Delta-like. This

post-translational modification is necessary for ligand-induced Notch activation. One possible mechanism is that some additional modifications to the ligands are necessary, and endocytosis drives the process by localizing the ligand and enzymes in the same endosome compartment to facilitate ligand modification. The second scenario is that ligand ubiquitination and endocytosis is required for creating a mechanical strain on the receptor upon ligand binding. This mechanical pulling force may lead to conformational changes in the receptor, revealing the S2 site for TACE cleavage. The transendocytosis of cleaved Notch receptor that follows may then enable γ-secretase cleavage of the remaining membrane-tethered receptor (Pratt, Wentzell et al. 2010).

The membrane-localized receptors are also ubiquitinated and endocytosed. Endocytosis of Notch receptor can either lead to activation or de-activation of the receptor. Notch receptor is mono-ubiquitinated after TACE cleavage before it can be cleaved by the γ-secretase complex (Gupta-Rossi, Six et al. 2004). Impaired endocytosis blocks Notch signaling independent of ligand-activation (Vaccari, Lu et al. 2008). However, the requirement for this process in overall Notch activation is still unclear. Receptor endocytosis can also negatively regulate Notch signaling by the degradation of unused receptor in the proteasome. E3 ligases such as Numb have been implicated to ubiquitinate Notch, which leads to degradation of Notch receptor (McGill, Dho et al. 2009).

Once the NotchIC-coactivator complex is assembled in the nucleus and transcription of the targets is activated, there must be a way to dampen the signal when it is no longer required. The co-activator complex recruits kinases such as cyclin-dependent kinase 8 (CDK8) (Fryer, White et al. 2004) and glycogen synthase kinase-3β (GSK-3β) (Espinosa, Ingles-Esteve et al. 2003); NotchIC has been shown to be a substrate for both kinases. Phosphorylation of NotchIC leads to its eventual ubiquitination and degradation by SEL10 E3 ligase (Oberg, Li et al. 2001; Wu, Lyapina et al. 2001). The presence of these modulator molecules spatiotemporally regulates a ligand-specific activation of Notch receptor.

1.2.3. Experimental methods of blocking Notch signaling *in vivo*

Notch activation requires the relay of signals from the surface of neighboring cells to the promoters of the target genes in the nucleus. The multi-step process allows for the development of tools to interfere with the transduction of the signal at multiple points in order to study the endogenous function of this pathway. In the study of mammalian development and adult biological processes, transgenic and knock-out mouse models are widely used, although each has its advantages and pitfalls. These models will be discussed in a later section. Chemical or antibody-based inhibition of Notch signaling also holds promise for therapeutic application. However, the inevitable off-target effects of chemical inhibitors need to be closely examined.

Both receptors and ligands of the Notch signaling pathway are transmembrane proteins whose functions are dependent on their extracellular domains. Recent animal studies have used antibodies against either Notch receptors or ligands to block the interaction and activation of the pathway. In mouse tumor models, Dll4 antibody is found to deregulate angiogenesis and block tumor growth in one model (Ridgway, Zhang et al. 2006), while decreasing the tumor-initiating population in another model (Hoey, Yen et al. 2009). Antibodies against Notch1 (Aste-Amezaga, Zhang et al. 2010) and Notch4 (Dontu, Jackson et al. 2004) receptors have been shown to block signaling *in vitro*. Antibody treatment is a specific method for signal inactivation, however, accessibility of the tissue and the systemic nature of the treatment may be concerns.

Notch signaling can also be blocked by chemical inhibitors for γ-secretase (Geling, Steiner et al. 2002). Gamma-secretase inhibitors (GSI) were first developed as a treatment for Alzheimer's disease. The use of GSI as a Notch blocker has been widely applied and accepted in *in vitro* experiments and has also been used in animal experiments involving rodent models. Since it requires systemic administration, Notch signaling in multiple systems

is affected. The most often observed side effect of GSI treatment is the expansion of intestinal goblet cells (Milano, McKay et al. 2004; Wong, Manfra et al. 2004). Overall, systemic GSI treatment is not a specific method of Notch inhibition, but small molecule inhibitors may provide better tissue penetration and diffusion compared to blocking antibodies.

Several dominant negative molecules of the Notch pathway components have been developed. While they are widely used for *in vitro* experiments, few constructs are used for transgenic mouse generation. Truncated Dll1 is shown to have dominant negative activity in vertebrae formation (Cordes, Schuster-Gossler et al. 2004). Dominant-negative CSL and MAML1 are both shown to block CSL-dependent Notch signaling and cause accelerated differentiation of hematopoietic stem cells (Duncan, Rattis et al. 2005). One of the most widely used dominant negative constructs is the truncated MAML1 (Tu, Fang et al. 2005; Maillard, Tu et al. 2006; High, Zhang et al. 2007; Proweller, Wright et al. 2007; Santos, Sarmento et al. 2007), which only contains the Notch and CSL interaction domain, without the ability to bind to other co-activators (Maillard, Weng et al. 2004). MAML1, 2, and 3 have different levels of capability to interact with the intracellular domain of different Notch receptors (Wu, Sun et al. 2002). However, a dominant-negative form of MAML1 has the highest efficiency in blocking signals from all four Notch receptors and it has been shown to be a competent pan-notch inhibitor (Maillard, Weng et al. 2004). As a part of this thesis, an inducible, tissue-specific, dominant-negative MAML transgenic system is generated to inactivate Notch signaling in the endothelium.

1.3. Notch signaling in the vasculature

Considering that the Notch phenotype was first observed in Drosophila as the appearance of notched wings in a loss-of-function (LOF) mutant followed by its identification as a neurogenic gene (Wharton, Johansen et al. 1985), it is interesting that many of the LOF mouse mutants of the Notch signaling pathway display cardiovascular defects (reviewed in (Iso, Hamamori et al. 2003; Alva and Iruela-Arispe 2004)). Notch receptors Notch1, Notch2, Notch3, and Notch4 and ligands Jagged1, Jagged2, Dll1, and Dll4 are all expressed in developing vasculature (Villa, Walker et al. 2001; Varadkar, Kraman et al. 2008; Sorensen, Adams et al. 2009). However, upon closer examination, the pattern and timing of expression are variable within the group of Notch pathway genes, suggesting that Notch signaling plays multiple roles in the establishment of a stable vasculature (summarized in Table 1.3).

1.3.1. Notch in endothelial cell specification

Notch signaling has been shown, in various animal models, to be involved in endothelial specification in the dorsal aorta. In zebrafish development, blocking Notch signaling with GSI increases the endothelial population while decreasing the hematopoietic cell number (Lee, Vogeli et al. 2009), suggesting that Notch activation functions as a molecular switch between the two cell types, blocking endothelial differentiation in favor of hematopoietic lineages. In early avian development, Notch activation in the ventral mesoderm favors differentiation towards mural cell fate at the expense of the endothelial/hematopoietic lineages (Shin, Nagai et al. 2009). However, later in development, migration, integration and differentiation of somite-derived endothelial precursors into the dorsal aorta have all been shown to require Notch activation (Sato, Watanabe et al. 2008; Ohata, Tadokoro et al. 2009). These seemingly contradictory observations either represent the differences in molecular signaling between species or the ability of Notch signaling to regulate endothelial cell specification at different stages of differentiation.

In the mammalian system, there has been no detailed *in vivo* study of the role of Notch signaling in the specification of endothelial cells from precursor cells. *In vitro* ES cell differentiation studies have shown that Notch1 activation in ES cells blocks differentiation towards Flk-1 positive mesodermal progenitors (Schroeder, Meier-Stiegen et al. 2006). Activation of Notch4 in ES cell-derived Flk-1 positive mesodermal progenitor drives differentiation away from the hematopoietic fate and towards a cardiovascular fate (Chen, Stull et al. 2008). Both studies suggest a role for Notch signaling in the formation of endothelial cells in the mammalian system. However, in the LOF Notch mutants, the endothelial primary plexus is formed normally in the yolk sac (Alva and Iruela-Arispe 2004; Shawber and Kitajewski 2004). The main blood vessels, the dorsal aorta and the cardinal vein in the embryo proper, which are both established through the process of vasculogenesis, still contain endothelial cells. In the most severely affected Notch1/Notch4 double knockout mutant, although no observable lumen can be found in either the dorsal aorta or the cardinal vein, clusters of endothelial cells are found in the correct location (Krebs, Xue et al. 2000). It shows that the process of angioblast differentiation into endothelial cells is not affected during murine development.

1.3.1.1. Notch in endothelial arterial-venous specification

Nevertheless, Notch activation still has an important role in endothelial cell specification in mammalian vascular development. The first clue that Notch signaling is regulating arterial-venous differentiation comes from the gridlock (*grl)* mutant in zebrafish. The *grl* gene is the zebrafish homolog of the mammalian hey2 gene, a target of Notch signaling. Gridlock is expressed in the mesoderm prior to the formation of the dorsal aorta and axial vein. Upon the formation of the vessels, the expression of Gridlock in the vasculature is restricted to the dorsal aorta, not in the axial vein (Zhong, Rosenberg et al. 2000) and the *grl* mutant contains defects only in the arteries, not veins (Weinstein, Stemple et al. 1995). Another Notch pathway mutant *mindbomb* also showed decreased expression of the arterial marker

EphrinB2 in the developing dorsal aorta and ectopic expression of the venous marker *flt4* instead (Lawson, Scheer et al. 2001). The *grl* and *mindbomb* mutant phenotypes suggest that Notch signaling is required for arterial function of the newly formed dorsal aorta.

In mammalian development, the expression of Notch receptors, Notch1 and Notch4, and ligands, Jagged1, Dll1 and Dll4, has been localized mainly in the arterial system, not in veins (Villa, Walker et al. 2001). Notch activation during embryonic vascular development has been restricted to the arteries as well (Souilhol, Cormier et al. 2006; Del Monte, Grego-Bessa et al. 2007). With LOF and gain-of-function (GOF) mutants of the arterially-restricted Notch receptors and ligands, the role of Notch in arterial-venous differentiation during mammalian development becomes evident. Notch1 null mice exhibit embryonic lethality before E11.5. The dorsal aorta appears collapsed (Swiatek, Lindsell et al. 1994) and there is decreased expression of arterial markers (Fischer, Schumacher et al. 2004). Conversely, Transgenic mice expressing activated Notch1 (Shawber, Funahashi et al. 2007; Venkatesh, Park et al. 2008) or Notch4 (Krebs, Xue et al. 2000) receptor exhibit aberrant expression of arterial markers in the veins and arteriovenous malformation (AVM), where there is fusion between the dorsal aorta and the anterior cardinal vein. These studies show that the two Notch receptors expressed in embryonic arteries are essential for the arterial identity and proper arterial-venous specification during development.

Of the three Notch ligands expressed in embryonic arteries, each has different role in arterializations in vascular development. Dll4 heterozygous knock-in embryos die *in utero* at E10.5 (Duarte, Hirashima et al. 2004; Gale, Dominguez et al. 2004; Krebs, Shutter et al. 2004). $Dll4^{+/-}$ mutants exhibit a thinner dorsal aorta and an absence of internal carotid arteries while the venous plexus remains relatively normal (Gale, Dominguez et al. 2004). The arteries lack smooth muscle coverage and express reduced levels of arterial markers (Duarte, Hirashima et al. 2004; Gale, Dominguez et al. 2004). Interestingly, there is ectopic expression of venous marker EphB4 in the dorsal aorta (Duarte, Hirashima et al. 2004),

suggesting either that the venous specification is the default fate in the absence of arterial-driven signal or that Notch activation is actively suppressing venous fate. Conversely, overexpression of Dll4, either systemic or endothelial-specific, induces EphrinB2 in the anterior cardinal vein while down-regulation of EphB4 is observed (Trindade, Kumar et al. 2008). Due to the early lethality of the Dll4 mutant, arterializations in older embryos cannot be examined. Interestingly, the expression of another Delta-like ligand, Dll1, is induced in embryonic artery starting at E13.5 (Sorensen, Adams et al. 2009). Arteries in Dll1-/- mice also exhibit increased expression of the venous marker and decreased level of arterial markers (Sorensen, Adams et al. 2009), correlating with defects in arterialization even after most arteries are already established. The third arterial-restricted Notch ligand is Jagged1. Jagged1 expression is required for embryonic vascular development. However, unlike the Delta-like ligands, Jagged1 null embryos do not show reduced arterial marker in the dorsal aorta (High, Lu et al. 2008; Robert-Moreno, Guiu et al. 2008). Endothelial-specific ablation of Jagged1 fails to reduce the level of Notch1 activation in aortic endothelium (High, Lu et al. 2008), suggesting that Jagged1 is not involved in arterial-venous specification during vascular development. Jagged1 null mutants do exhibit other interesting vascular defects which will be discussed later.

Murine mutants of other Notch signaling pathway components, not surprisingly, also exhibit defects in arterial-venous specification. Mindbomb null mutants are not able to generate functional Notch ligands and recapitulate the vascular defects of Dll4 or Notch1 mutants (Koo, Lim et al. 2005). DNA-binding partner of intracellular Notch, CSL, is also required for arterial identity. Both systemic and endothelial-specific ablation of CSL leads to reduced arterial diameter with decreases in EphrinB2 expression and smooth muscle recruitment (Krebs, Shutter et al. 2004). Finally, combined deletion of Notch targets Hey1 and Hey2 exhibits the same phenotype of decreased arterial markers in arterial endothelium and reduced smooth muscle coverage (Fischer, Schumacher et al. 2004).

These studies suggest that proper arterialization of mammalian vessels requires signals from Dll4 (Dll1 later in development)-expressing cells to activate receptors Notch1 and/or Notch4. Receptor activation will result in CSL-dependent transcription activation of targets Hey1, Hey2 and EphrinB2.

1.3.2. Notch in angiogenesis and vascular remodeling

A predominant phenotype from most of the LOF Notch mutants is the disorganization of yolk sac vasculature (Gridley 2007; Roca and Adams 2007; Phng and Gerhardt 2009). Whereas the wildtype yolk sac has a system consisting of a large vitelline artery, smaller arteries and a network of capillaries at E9.5, the mutant vasculature exhibits a degenerating primary capillary plexus with vessels of uniform diameter. This complete lack of vascular remodeling points to defects in angiogenesis in the Notch LOF mutants.

Both GOF and LOF mutants of Notch1 and Notch4 show that the two receptors are essential in driving the process of embryonic angiogenesis, although expression of Notch1 can compensate for the loss of Notch4 (Krebs, Xue et al. 2000; Uyttendaele, Ho et al. 2001; Limbourg, Takeshita et al. 2005; Venkatesh, Park et al. 2008). Of all the Notch ligands, only Jagged1 and Dll4 are implicated in the process of angiogenesis, suggesting that Jagged1 and Dll4 activates Notch1 and Notch4 receptor to regulate vascular remodeling (Xue, Gao et al. 1999; Duarte, Hirashima et al. 2004; Gale, Dominguez et al. 2004; Krebs, Shutter et al. 2004; High, Lu et al. 2008). As expected, mutants with genomic inactivation of CSL in the endothelium also show defect in angiogenesis, as Notch activation of downstream targets requires CSL (Krebs, Shutter et al. 2004). Finally, while no angiogenic defect is observed in Hey1 or Hey2-null mutants, the combination of Hey1 and Hey2 inactivation shows both targets are important for embryonic angiogenesis (Fischer, Schumacher et al. 2004).

Angiogenic sprouting requires a sequence of highly coordinated endothelial activities, starting from the disruption of ECM around the formation of the new sprout to the final

stabilization of the nascent vessel. Notch activity appears to play a role in multiple steps of the angiogenic process.

1.3.2.1. Tip and stalk cell specification

More detailed studies of the function of Dll4 and Notch in angiogenesis are made with the neonatal retina model. Murine retina has no vasculature during embryogenesis. Soon after birth, the retinal vascular system starts to develop as a sprout from the optic disc and initially forms a primitive vascular plexus which is rapidly remodeled into large and small vessels (Uemura, Kusuhara et al. 2006). In retinal vasculature, Dll4 is mostly expressed in tip cells (Hellstrom, Phng et al. 2007) while Notch activity is strongest in the stalk cells (Hofmann and Luisa Iruela-Arispe 2007). When Notch signaling in endothelial cells is blocked by either GSI treatment or genetic deletion of one copy of Dll4, angiogenesis is affected and exhibits excessive tip cell formation and branching (Hellstrom, Phng et al. 2007; Suchting, Freitas et al. 2007). In zebrafish vascular development, GSI treatment or Dll4 protein knockdown also causes excessive vessel sprouting and branching in the intersomitic vessels (Leslie, Ariza-McNaughton et al. 2007). These studies suggest that Dll4 expression suppresses Notch activation in the tip cells and enables the expression of VEGFR-2. Conversely, in the stalk cells, Notch activation suppresses VEGFR-2 expression and decreasing the response to migratory signal of surrounding VEGF molecules. Notch activation also reduces the cell's ability to induce Dll4 expression through VEGFR-2 activation.

One recent study examines the role of Notch ligand Jagged1 in angiogenic sprouting and finds that Jagged1 has an opposite effect to angiogenesis as compared to Dll4. Endothelial-specific inactivation of Jagged1 blocks retinal angiogenesis (Benedito, Roca et al. 2009). Jagged1 is found to be excluded from the tip cells in wild type vasculature. In Jagged1-null endothelial cells, Dll4 expression is induced in both the tip and stalk cells and Notch signaling is activated aberrantly throughout the vasculature (Benedito, Roca et al.

2009). Over-activation of Notch signaling then leads to a decreased sensitivity to VEGF-induced sprouting. The expression and interplay of Notch ligands and receptors is coordinated in order to form a functional vascular system.

1.3.2.2. Notch in other endothelial functions

Notch has also been shown to affect angiogenesis through modulation of other endothelial behaviors. In addition to the specification of a tip cell, the extension of the new sprout needs controlled endothelial proliferation and migratory activity, which involves interaction between the endothelial cells and the ECM. Also, successful sprouting also requires anti-apoptotic signals in the absence of integrin-matrix interation (Brooks, Montgomery et al. 1994) and endothelial junction protein (Carmeliet, Lampugnani et al. 1999); both have been shown to be essential for endothelial survival. The role of Notch signaling in endothelial survival signaling will be reviewed in a later section.

Activation of Notch signaling in endothelial cells leads to cell cycle arrest *in vitro* (Noseda, Chang et al. 2004; Liu, Xiao et al. 2006; Harrington, Sainson et al. 2008) and in mouse models (Trindade, Kumar et al. 2008). On the other hand, inhibition of Notch signaling results in increased endothelial cell proliferation in sprouting assays *in vitro* (Sainson, Aoto et al. 2005), in mouse and zebrafish development *in vivo* (Hellstrom, Phng et al. 2007; Suchting, Freitas et al. 2007), in the adult mouse (Dou, Wang et al. 2008), and during tumor angiogenesis (Noguera-Troise, Daly et al. 2006; Ridgway, Zhang et al. 2006). In mouse, increased endothelial cell proliferation of both tip and stalk cells may contribute to increased vessel diameter and branching after GSI treatment (Hellstrom, Phng et al. 2007), after neutralization of Dll4 activity by soluble Dll4 ligand (Lobov, Renard et al. 2007) and in Dll4 heterozygous mutants (Suchting, Freitas et al. 2007).

Studies in endothelial cell cultures suggest that the inhibitory effect of Notch signaling on endothelial cell proliferation is mediated by the transcriptional regulation of downstream

targets of the NotchIC/CSL/MAML complex (Liu, Xiao et al. 2006). In endothelial cells, CSL-dependent Notch signaling regulates the expression of the cyclin-dependent kinase inhibitor $p21^{CIP1}$ (Noseda, Chang et al. 2004). $p21^{CIP1}$ expression is down-regulated by Notch1 and Notch4 activity, resulting in a reduction in the nuclear translocation of cyclinD and CDK4, in the down-regulation of Retinoblastoma protein phosphorylation, and, consequently, in cell cycle arrest (Noseda, Chang et al. 2004; Dou, Wang et al. 2008). Conversely, endothelial deletion of CSL in adult mice induced $p21^{CIP1}$ and endothelial cell proliferation (Dou, Wang et al. 2008). The Notch-induced cell cycle arrest may also be brought on by down-regulation of the minichromosome maintenance (MCM) proteins (Noseda, Niessen et al. 2005; Emuss, Lagos et al. 2009). These proteins are required as part of the DNA replication process during the S phase. As the level of endogenous Notch activation increases with endothelial cell-cell contact, Notch-induced inhibition of proliferation may be a mechanism to maintain homeostasis in an endothelial sheet (Noseda, Chang et al. 2004).

There is also some evidence that Notch signaling regulates the expression of ECM molecules. For example, there is increased transcription of fibronectin, laminin, and collagen in endothelial cells isolated from mouse embryos overexpressing Dll4 (Trindade, Kumar et al. 2008). As a result, these mutants show increased deposition of ECM around the dorsal aorta. Conversely, Dll4 heterozygous mouse embryos show decreased expression and irregular deposition of collagen IV and laminin (Benedito, Roca et al. 2009). Integrin expression is also regulated by Notch signaling in endothelial cells (Harrington, Sainson et al. 2008). Over-expression of the intracellular domain of Notch4 in endothelial cells results in a β1 integrin-mediated increase in adhesion to collagen, and these cells show a reduced sprouting response to VEGF both *in vitro* and *in vivo* (Leong, Hu et al. 2002). Together, these results illustrate that Notch can influence both matrix production and adhesive properties in the form of integrin receptor expression.

These studies showed that Notch is a multifaceted regulator of angiogenesis either in tumorgenesis or during development. The main role of Notch signaling in the vasculature lies in cell fate specification, both in vasculogenesis and angiogenesis. However, due to the early embryonic lethality of most Notch mutants, the role of Notch in the process of embryonic arteriogenesis has yet to be thoroughly investigated.

1.3.3. Notch signaling in smooth muscle cell development

The process of myogenesis is regulated by a small group of transcription regulators, including MyoD (myogenic differentiation antigen), Myogenin, myogenic factor 5 (Myf-5), MEF2 and the Myocardin-serum response factor (SRF) complex. While MyoD and Myogenin activity is sufficient for skeletal muscle differentiation, Myocardin is the main transcription regulator of smooth muscle differentiation (Long, Creemers et al. 2007). MEF2C is expressed in developing VSMC and is required for vascular development (Lin, Lu et al. 1998). *In vitro* experiments in the role of Notch signaling in smooth muscle differentiation generated two opposing results.

Activation of the Notch pathway by expression NotchIC or co-culturing with ligand-expressing cells is found to inhibit myogenic differentiation in C2C12 myoblastic cell line through MyoD or Myogenin (Shawber, Nofziger et al. 1996; Kuroda, Tani et al. 1999; Proweller, Pear et al. 2005). Hes1 transcription is rapidly induced by Notch activation in C2C12 cells, and this induction is correlated with an inhibition of MyoD-induced differentiation (Sasai, Kageyama et al. 1992). In addition to Hes1, Notch target Hey2 is also able to block myocardin-induced smooth muscle differentiation in 10T1/2 cells, blocking the binding of SRF to DNA by physically interacting with SRF (Doi, Iso et al. 2005). Activated forms of Notch inhibits the DNA binding of MEF2C and its cooperative activity with MyoD and myogenin to activate myogenesis by physical interaction (Wilson-Rawls, Molkentin et al. 1999). The interaction observed between NotchIC and MEF2C may be explained by the interaction

between MEF2C and Notch co-activation MAML1 (Shen, McElhinny et al. 2006). Notch may block MEF2C-induced myogenesis by pulling co-activator from the MEF2C trasactivation complex. In addition, Notch target Hey1 blocks MyoD-induced transcription of myogenin and MEF2C by binding to their promoters and hindering binding of MyoD (Buas, Kabak et al. 2010). Overall, Notch activation has been shown to inhibit MyoD or MEF2C-induced myogenesis.

In mesenchymal stem cells, however, contact with immobilized Notch ligand Jagged1, co-culture with Dll1 expressing cell, or expression of NotchIC is sufficient to induce Hes1 expression and induce smooth muscle differentiation (Kurpinski, Lam et al. 2010). In another co-culture system, Notch3 receptor on mural cells is activated by Jagged1 on endothelial cells and this interaction is required for the expression of mesenchymal markers in the mural cells (Liu, Kennard et al. 2009). In 10T1/2 cells and aortic smooth muscle cells, expression of intracellular domain of Notch1, Notch3 or co-culture with Jagged1 (but not Dll4) expressing cells induces expression of smooth muscle markers with CSL-dependent mechanism (Doi, Iso et al. 2005). Notch activation in endothelial cells has been shown to directly induce transcription of SMA (Noseda, Fu et al. 2006) and platelet-derived growth factor receptor (PDGFR)-β (Jin, Hansson et al. 2008), among up-regulation of other mesenchymal markers (Noseda, McLean et al. 2004). However, a feedback mechanism exists for Notch-induced SMA expression. Hey1 or Hey2 expression in smooth muscle cells can inhibit CSL binding to SMA-promoter and reduce the endogenous level of mesenchymal markers (Tang, Urs et al. 2008). This feedback mechanism or the differential signal required for smooth muscle/skeletal muscle differentiation may be partially responsible for the conflicting reports on the role of Notch activation in myogenesis.

In murine embryogenesis, the role of Notch signaling in vascular smooth muscle development is much less ambiguous. Lack of smooth muscle coverage is observed in multiple Notch pathway mutants, showing the requirement for Notch activation and

downstream signaling events in arteriogenesis. In Dll4 heterozygous knockout mutants, the dorsal aorta is constricted in diameter and showing reduced VSMC (Gale, Dominguez et al. 2004). In CSL-null mice, which lose all canonical Notch signaling capability, the expression of SMA is down-regulated (Krebs, Shutter et al. 2004). Genomic inactivation mutants of Hey2 showed thinner vessel wall in the ascending aorta, descending aorta and pulmonary artery (Sakata, Koibuchi et al. 2006), suggesting a VSMC defect. When both Hey1 and Hey2 are lost, there is a more apparent reduction of SM22-α positive cells around the dorsal aorta (Fischer, Schumacher et al. 2004). Finally, ligand modifier Mind bomb E3 ligase is also required for smooth muscle recruitment to the dorsal aorta (Koo, Lim et al. 2005). These observations point to an important role for Notch in VSMC development. However for most of the mutants general arterial-specification is altered, therefore the lack of smooth muscle may be secondary to arterial-venous defects.

Using tissue-specific targeting of Notch signaling, some recent studies have elucidated the role of Notch signaling in VSMC differentiation *in vivo*. Blockade of Notch signaling through expression of a dominant-negative form of MAML1 (dnMAML) in neural crest cells is achieved using either the Wnt1 or Pax3 promoter (High, Zhang et al. 2007). Blocking Notch signaling in the neural crest cells leads to lethality in late gestation or neonatally depending on the promoter used. Mortality is due to various cardiovascular malformations including the lack of smooth muscle coverage to the pharyngeal arch arteries. The expression of dnMAML blocks the transcription of Notch target genes Hey1, Hey2 and HeyL in the VSMC of pharyngeal arch arteries, without affecting the endothelium (High, Zhang et al. 2007). Notch blockage does not alter the migration of the neural crest cells but inhibits the ability to differentiate towards the VSMC fate. Interestingly, dnMAML expression in mature smooth muscle cells does not give the same cardiovascular defects (High, Zhang et al. 2007). However, in another study, Notch signaling is found to not only drive the differentiation process in neural crest progenitors, but also the expansion of mature VSMC. VSMC lacking

Notch2 by smooth muscle targeted gene inactivation leads to increased postnatal mortality in the first three weeks (Varadkar, Kraman et al. 2008). The mice have smaller aorta and pulmonary arteries and show fewer proliferating VSMC. Previously *in vitro* experiment shows that expression of Notch target Hey1 promotes VSMC proliferation by down-regulation of $p21^{CIP1}$ (Wang, Prince et al. 2003), which may be a possible mechanistic explanation for lack of cell growth in Notch2-null VSMC *in vivo*.

Interestingly, another study may shed light on the origin of the Notch activation in the neural crest-derived VSMC. When Notch ligand Jagged1 is inactivated specifically in the endothelium using a Tie2-cre/lox system, the mutants die *in utero* due to cardiovascular defects (High, Lu et al. 2008). When examined in detail, the pharyngeal arch arteries and the dorsal aorta rostral to the heart all exhibit a loss of SMA or SM22-α positive mural cells. While arterial-venous specification and endothelial Notch activation are not affected in the mutants, Notch activation in the peri-endothelial cells and smooth muscle differentiation are both reduced (High, Lu et al. 2008). This study, in combination with the neural crest studies, suggests that Jagged1 expression in endothelial cells can stimulate Notch receptor on the VSMC precursors to drive differentiation. One caveat of the study is the use of the Tie2 promoter for endothelial-specific inactivation of Jagged1. Tie2 expression has been observed in cell types other than endothelial cells; monocytes (De Palma, Murdoch et al. 2007), hematopoietic stem cells (Hsu, Ema et al. 2000), as well as endothelial progenitor cells (Nowak, Karrar et al. 2004) have been shown to express Tie2 on the cell surface. Therefore, the effect of Jagged1 inactivation may not be attributed solely to the endothelium.

Unexpectedly, in mutants with systemic Jagged1 inactivation, the dorsal aorta at the AGM (aorta-gonad-mesonephros) region does not exhibits reduced smooth muscle coverage (Robert-Moreno, Guiu et al. 2008), suggesting the Jagged1 induced smooth muscle differentiation observed by High and colleagues may be dependent on the vascular bed

examined, as VSMC of the AGM originate from the somites, not the neural crests (Wasteson, Johansson et al. 2008).

Mutation of the Notch3 receptor has been associated with a human disease, cerebral autosomal dominant arteriopathy with subcortical infarcts and leukoencephalopathy (CADASIL) (Joutel, Corpechot et al. 1996; Joutel, Corpechot et al. 1997), where cerebral vascular defects leads to stroke and dementia in patients. The arteriopathy is characterized by dismorphic intima due to VSMC degeneration (Ruchoux and Maurage 1997). The Notch3 mutation leads to an accumulation of the membrane-anchored extracellular domain of the receptor in VSMC (Joutel, Andreux et al. 2000) and this ectopic clustering of Notch3 receptors appears to be the cause of VSMC defects. However, the detailed mechanism of how Notch3 mutation leads to VSMC dysfunction is still under investigation. Interestingly, the maturation of arterial VSMC in mouse appears to require Notch3. In the absence of Notch3, the arterial smooth muscle cells are dysfunctional (Arboleda-Velasquez, Zhou et al. 2008). The arteries are enlarged with thinner vessel wall and disorganized tunica media. The arterial smooth muscle cells also appear to obtain a venous phenotype. As a result of these phenotypic defects, the Notch3-null mice are more susceptible to ischemic stroke when challenged (Arboleda-Velasquez, Zhou et al. 2008).

In avian development models, somitic cells or extraembryonic mesoderm requires Notch signaling to form the smooth muscle cells. Using a CSL-binding-promoter reporter to illustrate Notch activation, one study shows that Notch activated cells are preferentially found in the dorsal aorta (Sato, Watanabe et al. 2008). Activation of Notch signaling in the somites increased the ventral migration of somitic cells and incorporation into the dorsal aorta, while inhibition of Notch signaling hinders both processes. Notch activation also predisposes somitic cells towards a VSMC fate in the dorsal aorta (Sato, Watanabe et al. 2008). In later stage of development, the somite-derived dermomyotome can also contribute to the dorsal aorta and Notch activation drives the cells towards a mural cell fate as oppose to becoming

part of the dermis or skeletal muscle system (Ben-Yair and Kalcheim 2008). Interestingly, at the site of primitive hematopoiesis in the extraembryonic mesoderm, Notch activated cells are also biased to become VSMC (Shin, Nagai et al. 2009). These studies suggest that Notch activation drives smooth muscle differentiation in different vascular progenitors in avian development, both in the embryo proper or in the extraembryonic tissues.

Recently, a study in lung development yields interesting insight into arterial VSMC differentiation in the lung (Morimoto, Liu et al. 2010). Cell fate tracing reveals that the microvascular endothelium, the arterial endothelium and the arterial VSMC, but not bronchial VSMC, are all derived from progenitor cells that experienced Notch1 activation and are continuing to engage in Notch signaling at E14.5. While ablation of CSL in lung mesenchymal cells does not result in defects of lung function, there is a decrease in mesenchyme-derived arterial VSMC in the lung. However, EndMT may rescue the defect in VSMC differentiation and cause an overall normal phenotype (Morimoto, Liu et al. 2010).

Notch signaling is one of the pathways implicated in the process of EndMT during cardiac cushion formation (Noseda, McLean et al. 2004; Timmerman, Grego-Bessa et al. 2004). During cardiac development, the atrio-ventricular canal (AVC) is formed by the invasion of endothelial cell-derived mesenchyme into the cardiac jelly. The first step of EndMT is the loss of endothelial-to-endothelial junctions followed by the gain of mesenchymal phenotype. Notch activation in endothelial cells *in vitro* suppresses the expression of vascular endothelial cadherin (VE-cadherin), an important endothelial junctional protein and up-regulates mesenchymal markers (Noseda, McLean et al. 2004). In CSL-null or Notch1-null embryos, the cardiac jelly is devoid of mesenchymal cells (Timmerman, Grego-Bessa et al. 2004). Notch activation induces expression of the Snail family of transcription repressors (Timmerman, Grego-Bessa et al. 2004; Niessen, Fu et al. 2008) which in turn reduces the expression of endothelial junction proteins to initiates EndMT and increases migration of the transdifferentiated endothelial cells in AVC formation. Therefore, Notch is essential for the

initiation of EndMT in mammalian cardiac development. However, the role of Notch in EndMT in the developing mammalian vasculature has yet been examined.

Overall, studies involving Notch pathway mutant mice illustrate the importance of Notch activation in multiple processes during mammalian vascular development, as summarized in Table 1.3. Work done in this thesis will further delineate the role of Notch signaling in vascular smooth muscle development across all vascular beds *in vivo*.

Table 1.3. Vascular development processes affected in Notch pathway mutant mice

Vascular development process	Notch Receptor	Notch Ligand	Notch Target	Notch Co-activator/ modulator
Arterio-venous specification	Notch1 (Fischer, Schumacher et al. 2004; Venkatesh, Park et al. 2008) Notch4 (Shawber, Funahashi et al. 2007)	Dll1 (Sorensen, Adams et al. 2009) Dll4 (Duarte, Hirashima et al. 2004; Krebs, Shutter et al. 2004; Trindade, Kumar et al. 2008)	Hey1/Hey2 (Fischer, Schumacher et al. 2004)	CSL (Krebs, Shutter et al. 2004) Mindbomb (Koo, Lim et al. 2005)
Angiogenesis	Notch1 (Krebs, Xue et al. 2000; Limbourg, Takeshita et al. 2005) Notch4 (Krebs, Xue et al. 2000; Uyttendaele, Ho et al. 2001)	Jagged1 (Xue, Gao et al. 1999; Benedito, Roca et al. 2009) Dll4 (Duarte, Hirashima et al. 2004; Krebs, Shutter et al. 2004; Trindade, Kumar et al. 2008)	Hey1/Hey2 (Fischer, Schumacher et al. 2004)	CSL (Krebs, Shutter et al. 2004; Dou, Wang et al. 2008) Presenilin1 (Nakajima, Yuasa et al. 2003) Mindbomb (Koo, Lim et al. 2005)
Vascular smooth muscle cell development	Notch1 (Morimoto, Liu et al. 2010) Notch2 (Varadkar, Kraman et al. 2008) Notch3 (Domenga, Fardoux et al. 2004; Arboleda-Velasquez, Zhou et al. 2008)	Jagged1 (High, Lu et al. 2008) Dll4 (Gale, Dominguez et al. 2004)	Hey2 (Fischer, Schumacher et al. 2004; Sakata, Koibuchi et al. 2006) Hey1/Hey2 (Fischer, Schumacher et al. 2004)	CSL (Krebs, Shutter et al. 2004; Morimoto, Liu et al. 2010) Mindbomb (Koo, Lim et al. 2005)
Endothelial survival	Notch1 (Limbourg, Takeshita et al. 2005)	Dll4 (Trindade, Kumar et al. 2008)		Presenilin1 (Nakajima, Yuasa et al. 2003)

1.3.4. Notch and endothelial survival

There is conflicting evidence showing that Notch signaling promotes, blocks or has no effect towards endothelial apoptosis. During murine embryogenesis, over-expression of ligand Dll4 leads to vascular defects and increased expression of Notch targets (Trindade, Kumar et al. 2008). Despite the appearance of a dilated dorsal aorta, there is an increase in the proportion of apoptotic cells in the aortic endothelium. This study suggests that over-activation of Notch pathway leads to endothelial death. However, when Notch activation is inhibited by ablation of presenilin1, the catalytic unit of the γ-secretase complex, the capillary endothelium of the mutant embryo appears apoptotic (Nakajima, Yuasa et al. 2003). This observation, in contrast, shows that Notch activation is required for endothelial survival during embryogenesis. In addition, endothelial-specific genomic inactivation of receptor Notch1 also leads to aortic endothelial death (Limbourg, Takeshita et al. 2005), showing the discrepancy observed in the first two studies is not due to the difference in vascular bed examined. There is a possibility that the endothelial apoptosis observed is secondary to the disruption of the microenvironment. It could also represent the sensitivity of endothelial survival to the level of Notch activation during vascular development. Interestingly, genomic deletion of CSL in adult mouse does not lead to endothelial apoptosis (Dou, Wang et al. 2008), showing potential difference in the requirement for survival of Notch signaling in embryonic and adult endothelium.

In vitro experiments show the differential effect of Notch receptors on endothelial apoptosis. Multiple studies have shown that Notch4 has an anti-apoptotic effect on cultured endothelial cells. In both primary venous endothelial cells and a transformed microvascular endothelial cell-line, expression of activated Notch4 protects cells against lipopolysaccharide (LPS)-induced apoptosis (MacKenzie, Duriez et al. 2004). Conversely, reduction of Notch4 or Hes1 protein level by RNA interference (RNAi) leads to apoptosis in cultured primary venous endothelial cells (Quillard, Coupel et al. 2008). Interestingly, the same study also showed

decreased Notch4 expression in the endothelium in a transplant arteriosclerosis animal model, showing a possible mechanism for endothelium apoptosis observed in atherosclerotic plaques. Disruption in Notch ligand Dll4 by RNAi in endothelial cells also decreases the viable cell fraction under serum starvation compared to RNAi control cells (Patel, Li et al. 2005). Inhibition of Notch signaling by GSI shows a similar increase in serum starvation-induced apoptosis (Takeshita, Satoh et al. 2007). These studies show that endogenous homotypic endothelial Notch signaling *in vitro* plays a role in maintaining monolayer homeostasis by blocking apoptosis. However, Quillard and colleagues show that tumor necrosis factor (TNF) induces apoptosis in endothelial cells through activation of Notch2 receptor (Quillard, Devalliere et al. 2009). Activation of Notch2 in primary venous endothelial cells leads to apoptosis by suppressing the expression of anti-apoptotic protein Survivin. Since the basal expression of Notch2 is low in primary venous endothelial cells (Noseda, Chang et al. 2004; Quillard, Devalliere et al. 2009), Notch2 may not be the primary receptor required for maintenance of endothelial homeostasis. However, it may still play a role in TNF-stimulated endothelium.

The effect of Notch signaling on endothelial apoptosis is likely context-dependent. There is a lack of detailed studies on how Notch pathway can induce cell death or survival. In this thesis, I attempt to provide more insight into both the mechanism and context-dependent nature of the interplay between Notch and apoptosis.

1.4. Aims of the studies

Notch signaling is instrumental in the regulation of many vascular processes. From both the standpoint of a “basic” biologist who aims to understand the fundamental processes of living things or a clinical researcher who aims to discover novel therapeutics for human disorders, there is an interest in a more detailed examination on the role of Notch in the vasculature. Notch signaling plays an important role in cell fate decision in the establishment of a functional vasculature both during developmental processes and under pathological conditions through the regulation of arterial-venous specification and tip-stalk cell designation. The work described in this thesis examined the role of Notch in two processes that have not been under the same kind of scrutiny: embryonic arteriogenesis and endothelial apoptosis.

While the importance of smooth muscle cells in vascular stability during development and in the adult has been established, the characterization of VSMC precursors is still underway. Our lab has shown that Notch activation in cultured endothelial cells can induce EndMT, through both down-regulation of endothelial markers and up-regulation of smooth muscle markers (Noseda, McLean et al. 2004). While endothelial cells have been shown to give rise to VSMC in avian development, there is no study that directly shows the role of EndMT in mammalian arteriogenesis. Recently, several studies have been published that investigate the role of Notch signaling in mammalian smooth muscle development (reviewed by (Morrow, Guha et al. 2008)). The studies focus on neural crest-derived VSMC and show that Notch activation can facilitate VSMC differentiation and VSMC expansion. Using a binary inducible transgenic mouse system, we will examine whether EndMT occurs in mammalian vasculature and whether Notch activation can be a driving force in the process as observed in cell culture experiments.

Our lab and others have shown that Notch may be essential for the maintenance of endothelial homeostasis by regulating proliferation, tip cell formation and apoptosis. Notch

activation shows either pro-apoptotic or anti-apoptotic activities context-dependently. We have shown that Notch activation protects endothelial cells against LPS-induced apoptosis by two independent mechanisms (MacKenzie, Duriez et al. 2004). In this thesis, the downstream signaling involved in this protective effect will be examined. From our study of the EndMT process, the zinc-finger protein Slug is identified as a direct Notch target in endothelial cells (Niessen, Fu et al. 2008). Interestingly, in irradiated mouse bone marrow, Slug showed anti-apoptotic effects (Inoue, Seidel et al. 2002). Notch signaling may provide the pro-survival effect through the induction of Slug. In cancer cells, Notch activation often exerts anti-apoptotic activity through the activation of the PI3K signaling pathway. Thus, the role of PI3K is also examined in Notch-induced endothelial survival signaling. Finally, I have examined the context-dependent nature of Notch-induced survival by examining the outcome of different apoptotic stimuli.

Overall, two major hypotheses were tested in this thesis: (1) Endothelial cells can transdifferentiate into VSMC during murine artery development and the process is Notch-dependent; (2) Notch activation can protect endothelial cells against apoptosis by downstream signaling through Slug and/or PI3K.

Chapter 2. MATERIALS AND METHODS

2.1. Cell culture

The human dermal microvascular endothelial cell line HMEC-1 (HMEC), is a cell line transformed with SV40 large T antigen (Ades, Candal et al. 1992). HMEC was provided by the Centers for Disease Control and Prevention in Atlanta, GA. HMEC were cultured in MCDB 131 medium (Sigma-Aldrich, St. Louis, MO) supplemented with 10% heat-inactivated calf serum (CS) (HyClone, Logan, Utah), 2 mM Glutamine and 100 U each of penicillin and streptomycin (Gibco, Invitorgen, Carlsbad, CA). Human umbilical vein endothelial cells (HUVEC) were isolated as previously described (Karsan, Yee et al. 1997), and maintained in MCDB 131 medium supplemented with 10% heat-inactivated fetal bovine serum (FBS) (HyClone, Logan, Utah), 10% heat-inactivated CS, 20 ng/mL endothelial cell growth supplement (BD Bioscience, Bedford, MA), 16 U/mL heparin (Sigma-Aldrich, St. Louis, MO), 2 mM Glutamine and 100 U each of penicillin and steptomycin. Human aortic smooth muscle cells (HASMC) were purchased from Cascade Biologics (Invitrogen, Carlsbad, CA) and were cultured in Medium 231 supplemented with smooth muscle growth supplement (SMGS) (Cascade Biologics, Invitrogen, Carlsbad, CA) according to manufacturer's instructions. Both HUVEC and HASMC were used between passages 1 to 5. The retroviral producer cell line AmphoPheonix was obtained from Dr. Gary Nolan (Stanford University, Pal Alto, CA) and cultured in Dulbecco's modified Eagle's medium (DMEM, Sigma-Aldrich, St. Louis, MO) supplemented with 10% heat-inactivated CS, 2 mM glutamine and 100 U each of penicillin and streptomycin. All cells were maintained at 37°C in 5% CO_2.

2.1.1. Gene transfer

Human cells (HMEC, HUVEC and HASMC) were transduced using the retroviral vectors pLNCX, pLNC-Notch1IC, pLNC-Slug (Niessen, Fu et al. 2008), pLNC-dnAKT

(Sakoda, Gotoh et al. 2003), MSCV-IRES-YFP (MIY), MIY-Notch1IC (Noseda, McLean et al. 2004), MSCV-GFP and MSCV-dnMAML (Maillard, Weng et al. 2004) as previously described (Noseda, McLean et al. 2004). Briefly, constructs were transiently transfected into the retroviral packaging cell line AmphoPhoenix using *Trans*IT®-LT1 Transfection Reagent (Mirus Bio, Madison, WI). Retroviral supernatants were collected, filtered through a 0.45 μm filter, 8 μg/ml Polybrene (Sigma-Aldrich, St. Louis, MO) was added, and fresh medium was added back to the virus producing cells. The viral supernatant was then applied to target cells. This procedure was repeated twice over the next 48 hours.

The pLNCX transduced cells were then selected for Neomycin resistance using 300 mg/mL G418 (Invitrogen, Carlsbad, CA). The MSCV-GFP, MSC-dnMAML, and the MIY transduced cells were sorted by fluorescent activated cell sorting (FACS) for yellow fluorescent protein (YFP) or green fluorescent protein (GFP) using a FACS-440 flow-sorter (BD, Franklin Lakes, NJ). Stable polyclonal cells were obtained to avoid artifects due to retroviral integration sites. The pLNC-dnAKT construct was a generous gift from Dr. Issei Komuro, Chiba University Graduate School of Medicine, Japan. The MSCV-dnMAML construct was a gift from Dr. Warren Pear, University of Pennsylvania, Philadelphia, PA.

2.2. Transgenic mice

The Tie1tTA and tetOSLacZ mouse lines were generously provided by Dr. D. Dumont (Sunnybrook Health Sciences Centre, Toronto, ON) and were maintained on CD1 background as an outbred strain. The VEtTA mice were a gift from Dr. L. Benjamin (Harvard University, Boston, MA) and were maintained on FVB/NJ inbred background. All mouse lines were maintained as heterozygous transgenics. The tTA transgenics were identified with genotyping primers 5' - CTC ACT TTT GCC CTT TAG AA - 3' and 5' - GCT GTA CGC GGA CCC ACT TT - 3'. The tetOSLacZ heterozygous mice were identified with genotyping primers 5' – CTG GAT CAA ATC TGT CGA TCC TT - 3' and 5' – GCT GGA TGC GGC GTG CGG T - 3'.

The TetOSdnMAML mice were generated in collaboration with the BCCRC Transgenic Core (Vancouver, BC, Canada). The transgenic animals were generated by pronuclear injections of linearized DNA coding for tetOS promoter followed by cDNA of the dominant-negative Mastermind-like1-GFP fusion construct. The injected blastocysts were transplanted into pseudo pregnant females. Transgenic mice were identified with genotyping primers 5'- CAT GCC ATG GAT GGT GAG CAA GGG CGA G – 3' and 5' - CCA TCG ATT TAC TTG TAC AGC TCG TCC A – 3'. Germline transmission was obtained for 3 transgenic lines. However, only one line showed expression matching that of reporter gene activity when crossed with driver transgenic mice. That line was propagated as the TetOSdnMAML transgenic mouse line and was maintained on CD1 background as an outbred strain.

The VEtTA and Tie1tTA mice were also backcrossed to the C57BL/6J background. At the time of the experiment, both strains were in the fifth generation of C57BL/6J backcross.

All animal-related experiments are approved by and conform to the guidelines of the Animal Care Committee of the University of British Columbia (Vancouver, British Columbia)

2.2.1. Timed matings

Driver mouse (Tie1-tTA or VE-cadherin-tTA) were mated with responder mice (TetOSLacZ or TetOSdnMAML). The females were checked for vaginal plug in the morning. Noon of the day where plugs were observed was designated embryonic day 0.5 (E0.5). For tetracycline-treated embryos, plugged females were place on autoclaved water containing 50 mg/L tetracycline (Apotex Inc., North York, ON, Canada) at E0.5. The water bottle containing tetracycline was replaced daily. Tetracycline was withdrawn by replacing tetracycline-containing water with untreated water for the pregnant females at the specified days.

Staging of the embryos were done by identification of stage-specific landmarks. For E10.5 embryos, the prominent division between the telencephalic vesicle, the mesencephalic vesicle and the fourth ventricle, the presence of the hindlimb buds and the elongated forelimb, the absence of footplates in the limbs, the presence of nasal processes and the presence of both the first and the second branchial arches were all used to stage the embryos. For E12.5 embryos, the presence of angular footplates and visible “rays” at the location of future interdigital zones without the presence of digits were observed for both the forelimbs and hindlimbs. For E14.5 embryos, there were an absence of hair follicles at the site of future whiskers; in addition, the fingers were separated and there were deep indentations between the toes. Only embryos of the correct stages were used for further analysis.

2.3. Flow cytometry

Mouse embryos were dissected free of yolk sac tissue, minced and digested in a solution containing 1% BSA, 550 U/mL Collagenase Type II, 550 U/mL Collagenase Type IV, and 100 U/mL DNase I (Sigma-Aldrich, St. Louis, MO) in PBS for 15 minutes in a 37°C water bath. During digestion, the embryos were further broken down by repeated pipetting at 5 minute-intervals. Enzymatic reactions were inactivated by addition of DMEM with 5% CS. The embryonic cells were pelleted at 700 x G for 5 minutes at 4°C. The digested embryos were treated with red blood cell lysis buffer (0.8% NH_4Cl, 0.1mM EDTA) (Sigma-Aldrich, St. Louis, MO) and resuspended in DMEM with 5% CS. The single-cell suspensions were either analyzed for GFP expression or stained for with Phycoerythrin (PE)-conjugated rat anti-mouse CD31 monoclonal antibody (5 μg/mL) (BD Bioscience, San Jose, CA) or a rat anti-mouse PDGFR-β antibody (10 μg/mL) (eBioscience, San Diego, CA). Rat $IgG_{2a,\kappa}$ (BD Bioscience, San Jose, CA) was used as isotype control. Cells were incubated with antibodies for one hour on ice before analysis. For PDGFR-β, secondary antibody goat anti-rat Alexa Fluor 633 (1:200) (Invitrogen, Carlsbad, CA) was used for detection. All flow cytometry analysis was done with the EPIC Elite flow cytometer (Beckman Coulter, Brea, CA) and FCS Express (De Novo Software, Los Angeles, CA).

2.4. Immunofluorescence staining

For immunofluorescent staining of cultured cells, retroviral-transduced HMEC cells were plated at a density of 1.5 x 10^5 cells on a 4-well chamber slide (BD Biosciences, San Jose, CA). The cells were allowed to attach and grow until confluent. The cells were serum starved overnight and treated with DMSO (Sigma-Aldrich, St. Louis, MO) or LY294992 (Cell Signaling Technology, Danvers, MA) for the specified time. The cells were fixed in 4% paraformaldehyde (Sigma-Aldrich, St. Louis, MO), and blocked/permeablized in 4% FBS + 0.2% TritonX-100 (Sigma-Aldrich, St. Louis, MO) in PBS. Rabbit anti- Activated caspase 3 (BD Pharmingen, Franklin Lakes, NJ) was used at a dilution of 1:100 and the goat anti-rabbit Alexa594 conjugated secondary antibody was used at 1:200 (Molecular Probes, Invitrogen, Carlsbad, CA). The cells were counterstained with 4',6-diamidino-2-phenylindole (DAPI, 1 μg/mL) (Sigma-Aldrich, St. Louis, MO).

For staining of sorted embryonic cells, 2.0 x 10^4 cells were spotted onto a slide using the Cytospin2 centrifuge (Shandon, Thermo Fisher, Waltham, MA). The cells were dried onto the slides, fixed in 4% paraformaldehyde and blocked/permeablized in 4% FBS + 0.2% TritonX-100 in PBS. The cells were stained with rat anti-mouse CD31 monoclonal antibody (1:200) (BD Bioscience, San Jose, CA), and rabbit anti-human α-smooth muscle actin (1:100) (NeoMarkers, Thermo Fisher, Fremont, CA). The fluorochrome-conjugated secondary antibodies goat anti–rat Alexa Fluor 488 (Molecular Probe, Invitrogen, Carlsbad, CA) and goat anti–rabbit Alexa Fluor 594 (Molecular Probe, Invitrogen, Carlsbad, CA) were used, and nuclei were counterstained with DAPI.

Whole embryos were fixed in 2% paraformaldehyde in PBS (pH7.4) for 4 hours to overnight. Then the tissues were cryoprotected with overnight incubation in 30% sucrose (Sigma-Aldrich, St. Louis, MO), followed by 1 hour in Tissue-Tek® O.C.T. Compound (Opitimal Cutting Temperature; Sakura Finetek USA, Torrance, CA). The tissues were frozen

in O.C.T. compound at -80ºC and 10-µm-thick cryosections were made from frozen cryoblocks. The cryosections were blocked/permeablized with 4% goat serum + 0.2% TritonX-100 in PBS and stained with rat anti-mouse CD31 monoclonal antibody (1:200), rabbit anti-GFP antibody (1:300) (Molecular Probe, Invitrogen, Carlsbad, CA) and rabbit anti-human smooth muscle actin (1:100). The fluorochrome-conjugated secondary antibodies goat anti–rat Alexa Fluor 488 or Alexa Fluor 594 and goat anti–rabbit Alexa Fluor 488 or Alexa Fluor 594 were used, and nuclei were counterstained with DAPI.

Immunofluorescent staining was detected with an imaging microscope (Axioplan II; Carl Zeiss, Inc.), and images were captured with a digital camera (1350EX; QImaging, Surrey, BC, Canada).

2.4.1. Smooth muscle thickness quantification

Quantification of the smooth muscle thickness was done with the NIH *Image* software (Research Service Branch, National Institute of Health, Bethesda, MD) with additional user-defined algorithms. The algorithms were kindly provided by Dr. Alastair Kyle (BC Cancer Research Center, Vancouver, BC, Canada). Briefly, pixels with a value of 0 (white) were set to 1 and pixels with values of 255 (black) were set to 253. The lumen created by SMA staining was filled with black pixels (255) and the area outside of the SMA staining was set to be 254. For pixels that were between 1 and 253 and next to a 254 pixel (at the outer rim of the SMA staining), the distance between that pixel to the closest 255 pixel was recorded (the thickness of SMA staining at that point). Three thousand pixels were measured and the average SMA thickness was determined by calculating the mean for individual images. An example of the analysis is shown in Figure 2.1.

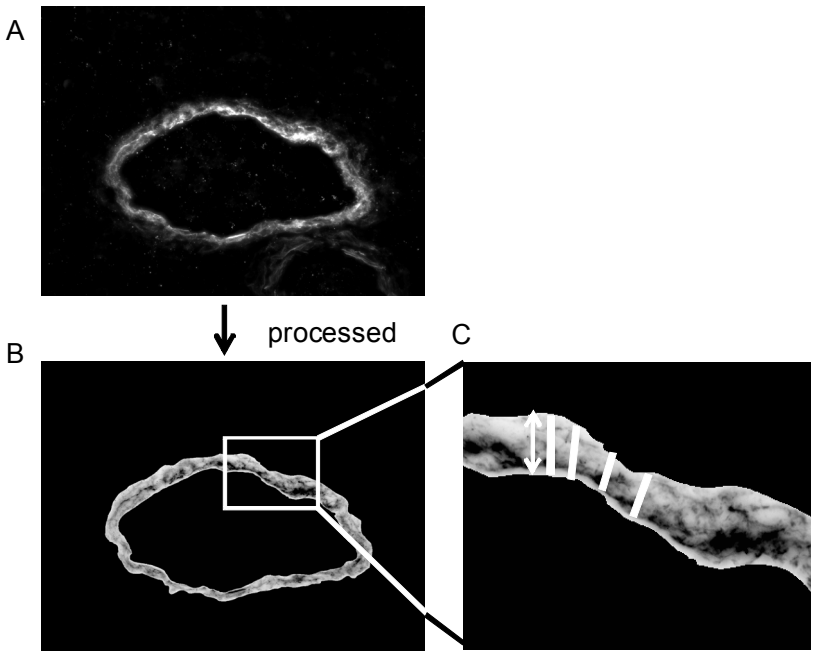

Figure 2.1. Smooth muscle thickness quantification. (A) Immunofluorescent image of a section of E12.5 descending aorta stained for α–smooth muscle actin (SMA). (B) The same image after undergoing processing to distinguish the stained region, the inner lumen and the area outside of the staining. (C) The shortest distance between a point on the outside rim of the staining to the inner lumen was tabulated for 2000 pixels along the staining (4 possible measurements are shown here). For this particular example, the SMA thickness is 17 ± 4 μm.

2.5. β-galactosidase detection

For wholemount X-gal staining, embryos were fixed in β-gal fixative solution (0.2% glutaraldehyde, 5 mM EGTA (Sigma-Aldrich, St. Louis, MO), 2 mM $MgCl_2$ (Sigma-Aldrich, St. Louis, MO) in phosphate buffered saline PBS pH7.4) for 10 minutes, then washed in β-gal wash solution (2 mM $MgCl_2$, 0.01% sodium deoxycholate (Sigma-Aldrich, St. Louis, MO), 0.02% NP-40 (Sigma-Aldrich, St. Louis, MO) in PBS pH7.4) three time for 15 minutes. Finally, the embryos were incubated with β-gal staining solution (1 mg/ml X-gal (Invitrogen, Carlsbad, CA), 5 mM potassium ferrocyanide (Sigma-Aldrich, St. Louis, MO), 5 mM potassium ferricyanide (Sigma-Aldrich, St. Louis, MO) in β-gal wash solution) for 2 hours at 37°C. The embryos were post-fixed in 2% paraformaldehyde and then embedded in OCT compound for cryosectioning.

For staining on tissue cryosections, the staining was carried out as described, except the sections were incubated with staining solution overnight at 37°C.

For staining for flow cytometry analysis, embryos were digested to single cell suspension as described. Cells were incubated with 0.5mM Fluorescein di-β-D-galactopyranoside (FDG) (Invitrogen, Carlsbad, CA) in 37°C waterbath for 2 minutes. Then enzymatic reaction was carried out on ice for 30 minutes before FACS analysis.

2.6. Apoptosis/survival Assays

Cells were serum-starved overnight with MCDB 131 + 2% CS and were treated with 100 μg/mL bacterial lipopolysaccharide (LPS) from *Escherichia coli* (Sigma-Aldrich, St. Louis, MO) and 25 μM of ALLN (N-Acetyl-L-leucyl-L-leucyl-L-norleucinal) (EMD Chemicals, Gibbstown, NJ) or 7.5 mM homocysteine (Sigma-Aldrich, St. Louis, MO) for the specified time, unless otherwise stated. Untreated cells were used as control for homocysteine treatment, while cells treated with 25 μM ALLN were used as controls for the LPS+ALLN treatment to examine the effect of LPS.

2.6.1. Annexin V binding assay

Medium from the plate with cells in suspension was collected and pooled with adherent cells trypsinized from the plate. The cells were washed twice with cold PBS and then resuspended in Binding Buffer (10 mM HEPES (Sigma-Aldrich, St. Louis, MO), pH 7.4; 140 mM NaCl (Sigma-Aldrich, St. Louis, MO); 2.5 mM $CaCl_2$ (Sigma-Aldrich, St. Louis, MO)) at a concentration of ~1 x 10^6 cells/ml. Two and a half micro-litres of PE-conjugated Annexin V (Invitrogen, Carlsbad, CA) were added to 1 x 10^5 cells and the cells were incubated for 15 minutes at room temperature. 400 μL of ice-cold Binding Buffer was added to the cells and the cells were analyzed by flow cytometry. The percentages of AnnexinV positive cells were determined.

2.6.2. Neutral Red uptake assay

HMEC were plated at the density of 3.0 x 10^4 cells per well in a 96-well plate. The cells were treated with LPS and ALLN or homocysteine as specified. The cells are incubated in MCDB 131 medium containing 2% CS and 0.0025% Neutral Red (Sigma-Aldrich, St. Louis, MO) for 4 hours under normal culture condition. After removing Neutral red-containing

medium carefully, cells were lysed and Neutral red was solubilized with 1% acetic acid (Sigma-Aldrich, St. Louis, MO) in 50% ethanol. The absorbance at 550 nm was quantified with Genios Microplate Reader (Tecan, Männedorf, Switzerland).

2.6.3. Activated caspase 3 detection

HMEC were plated at the density of 1.5 x 10^5 cells per well in a four-well chamber slide (BD Biosciences, San Jose, CA). The cells were treated with DMSO or 40 mm of LY294002 for 8 hours. Immunofluorescence staining for activated caspase 3 was performed as described in section 2.4. The percentage of cells with activated caspase 3 staining was determined by calculating the proportion of the nuclei (DAPI-positive) in the field with activated caspase 3 co-staining.

2.7. Immunoblotting

For immunoblotting, cells were lysed in RIPA buffer (PBS containing 1% NP-40 (Sigma-Aldrich, St. Louis, MO), 0.5% sodium deoxycholate, and 0.1% SDS (Sigma-Aldrich, St. Louis, MO)) with addition of fresh protease inhibitor cocktail (Roche Applied Science, Indianapolis, IN). Fifty mg of total protein, as measured using Bio-Rad DC Protein Assay System (Bio-Rad Laboratories, Hercules, CA), were analyzed by sodium dodecyl sulfate-polyacrylamide gel electrophoresis, transferred to nitrocellulose membranes (Bio-Rad Laboratories, Hercules, CA), and developed by enhanced chemiluminescence (PerkinElmer Life Sciences, Boston, MA). Membranes were probed using the following antibodies: 1:1000 rabbit anti-Slug (Cell Signaling Technology, Danvers MA), 1:1000 goat anti-Slug (clone G-18, Santa Cruz Biotechnology Inc., Santa Cruz, CA), 1:10000 mouse anti-Tubulin (Sigma-Aldrich, St. Louis, MO), 1:1000 rabbit anti-phospho-Akt (S473) (Cell Signaling Technology, Danvers MA), 1:5000 rabbit anti-Akt (Cell Signaling Technology, Danvers MA), 1:2000 goat anti-Notch1 (Santa Cruz Biotechnology Inc.), 1:1000 rabbit anti-human SMA, 1:1000 mouse anti-Myc-tag (Cell Signaling Technology, Danvers MA).

2.8. Real-time PCR

Total RNA was isolated from cells using TriZOL reagent (Invitrogen, Carlsbad, CA) according to manufacturer instruction. 2.5 μg of total RNA was treated with DNase I (Invitrogen, Carlsbad, CA) and was reverse transcribed by using the Superscript II kit with random primers (Invitrogen, Carlsbad, CA). Alternatively, Cells-to-cDNA™ II Kit (Ambion, Applied Biosystems, Austin, TX) was used to generate cDNA from 1 x 10^4 to 1 x 10^5 mouse embryonic cells according to manufacturer's instruction. For each PCR reaction 2.5 μl of the cDNA was used. Glyceraldehyde 3-phosphate dehydrogenase (GAPDH) was used as the loading control for comparison across samples. Real time quantitative RT-PCR was performed on The Applied Biosystems 7900HT Fast Real-Time PCR System by using the Power SYBR® Green PCR kit (Applied Biosystems, Foster City, CA). Primers are described in Table 2.1.

Table 2.1. Primers for quantitative RT-PCR

	Forward primer sequence 5'→ 3'	Reverse primer sequence 5'→ 3'
mouse CD31	AGCTAGCAAGAAGCAGGAAGGACA	TAAGGTGGCGATGACCACTCCAAT
mouse CD34	ATCATCTTCTGCTCCGAGTGCCAT	AGCAAACACTCAGGCCTAACCTCA
mouse cKit	TGCCAACCAAGACAGACAAGAGGA	AGGAGGATATTCCTGGCTGCCAAA
mouse Flk-1	AGGCCCATTGAGTCCAACTACACA	ATGTCTGCATGGTCCCATACTGGT
mouse MEF2D	GCTCCATGCAGTTCAGCAATCCAA	AGGCTCCATTAGCACTGTTGAGGT
mouse Msx2	TGAGGAAACACAAGACCAACCGGA	TGACCTGGGTCTCTGTAAGGTTCA
mouse SMA	ATTGTGCTGGACTCTGGAGATGGT	TGATGTCACGGACAATCTCACGCT
mouse Tal1	GTTCACCAACAACAACCGGGTGAA	AAGGCGGAGGATCTCATTCTTGCT
mouse Tie1	TGAACACTCAGACCCACAGCAACT	GCAGGTTGGCCAGCAATGTTAAGT
mouse Tie2	ACACTGTCCTCCCAACAGCTTCTT	TGATTCGATTGCCATCCAACGCAC
mouse Hey1	CACGCCACTATGCTCAATGT	TCTCCCTTCACCTCACTGCT

	Forward primer sequence 5'→ 3'	Reverse primer sequence 5'→ 3'
mouse Hey2	TTCTGTCTCTTTCGGCCACT	TTTGTCCCAGTGCTTGTCTG
mouse p53	AAAGGATGCCCATGCTACAGAGGA	AGGATTGTGTCTCAGCCCTGAAGT
mouse p21	GGAATTGGAGTCAGGCGCAGAT	GAAGAGACAACGGCACACTTTGCT
mouse Bax	ACAGCAATATGGAGCTGCAGAGGA	TGTCCAGCCCATGATGGTTCTGAT
mouse Lef1	TGGCATCCCTCATCCAGCTATTGT	TAGCGTGCACTCAGCTACGACATT
mouse Axin2	AAAGAAACTGGCAAGTGTCCACGC	GGCAAATTCGTCACTCGCCTTCTT
mouse MEF2C	ACTTCCTGGAGAAGCAGAAAGGCA	AACACGTTTCCTTCTTCAGCACGC
mouse CSL	TTGGTGTGTTCCTCAGCAAG	GCTCCCCACTGTTGTGAACT
mouse GAPDH	TGCAGTGGCAAAGTGGAGAT	TTTGCCGTGAGTGGAGTCATA
human Hey1	AGAGTGCGGACGAGAATGGAAACT	CGTCGGCGCTTCTCAATTATTCCT
human Slug	CCCTGAAGATGCATATTCGGAC	CTTCTCCCCCGTGTGAGTTCTA
human GAPDH	GGACCTGACCTGCCGTCTAGAA	GGTGTCGCTGTTGAAGTCAGAG

2.9. Statistical analysis

Results were expressed as means ± standard error of mean (SEM). Data were analyzed using a two-tailed Student's t-test or a paired Student's t-test using the GraphPad Prism statistical program.

Chapter 3. VASCULAR SMOOTH MUSCLE DIFFERENTIATION FROM TIE1^{+} PRECURSORS REQUIRES NOTCH

3.1. Introduction

VSMC play an important role in vascular homeostasis in the adult. During development, VSMC not only provide structural support for the nascent arteries, but are also involved in bidirectional signaling with the endothelium for the overall stability of the vasculature. However, the developmental origin of VSMC is still under investigation. Many embryonic tissues have been shown to be sources of VSMC during development [reviewed in (Gittenberger-de Groot, DeRuiter et al. 1999; Majesky 2007)]. Within a tissue, only a subset of cells has the ability to differentiate into VSMC. While cells from the mesoderm can migrate to the site of dorsal aorta formation during avian development, only a small percentage of mesoderm cells actually integrate as a part of the dorsal aorta (Sato, Watanabe et al. 2008), suggesting the existence of a local vascular progenitor cell within the tissue that is predisposed towards a vascular fate.

Studies have been done to isolate and culture such progenitor cells from mammalian sources, among these progenitors, mesoangioblasts (Minasi, Riminucci et al. 2002) and ES cell-derived cardiovascular progenitors (Yamashita, Itoh et al. 2000; Yang, Soonpaa et al. 2008) have both been shown to expand and differentiate into VSMC *ex vivo*. However, there is still a lack of direct *in vivo* evidence and *in situ* tracking of an immediate precursor cell that can differentiate into VSMC within the mammalian development system.

Anatomically, the endothelium is the most closely associated tissue to the VSMC, which makes it a prime candidate source of VSMC. Interestingly, the endothelium has been shown to be a possible source of VSMC through the process of EndMT in an avian developmental model (DeRuiter, Poelmann et al. 1997). In addition, we have previously observed EndMT in Notch-activated human endothelial cells (Noseda, McLean et al. 2004). However, there are

no studies examining whether the endothelium could be a source of smooth muscle progenitor cells during mammalian development.

Two reports have suggested that murine ES cells differentiate into VSMC via an endothelial intermediate (Ema, Faloon et al. 2003; Hill, Obrtlikova et al. 2010). However, the ES cell-derived endothelial cells expressed endothelial markers at a much lower level and mesenchymal markers at a much higher level compared to mature endothelial cells (Hill, Obrtlikova et al. 2010). Therefore, the isolation of endothelial cells from differentiating ES cells with endothelial markers such as CD31 (Ema, Faloon et al. 2003) or Tie1 (Marchetti, Gimond et al. 2002) may also result in enrichment of immature vascular precursors, in addition to mature endothelial cells. The close association between vascular precursor cells and endothelial cells makes it difficult to distinguish between precursor-derived VSMC and endothelial cell-derived VSMC.

Notch signaling is one of the evolutionarily conserved pathways implicated in the process of EndMT during cardiac cushion formation (Noseda, McLean et al. 2004). Disruption of Notch signaling during embryonic development leads to cardiac malformations as well as vascular defects (reviewed in (Phng and Gerhardt 2009)). A decrease in vascular smooth muscle coverage was observed in some Notch mutants, but the exact mechanism of the disruption and the cell type involved was not examined in detail. Using cell type specific targeting of Notch signaling, some recent studies have elucidated the role of Notch signaling in VSMC differentiation. Blockade of Notch signaling through expression of a dominant-negative form of MAML1 (dnMAML) in mouse embryonic neural crest cells leads to lethality in late gestation due to cardiovascular malformation (High, Zhang et al. 2007). There is a lack of smooth muscle coverage of the vessels where the VSMC has been shown to derive from a neural crest origin, such as the pharyngeal arch arteries (High, Zhang et al. 2007). In avian development models, enforced Notch activation in the somitic cells or extraembryonic mesoderm can be found to preferentially integrate into the smooth muscle layer of the dorsal

aorta or the arteries of the yolk sac (Ben-Yair and Kalcheim 2008; Sato, Watanabe et al. 2008; Shin, Nagai et al. 2009). These studies suggest that Notch signaling plays a role in VSMC differentiation from precursors that originate from either the neural crest or mesodermal sources. The effect of Notch signaling on VSMC differentiation from other sources is still not fully investigated.

To determine whether Notch-induced EndMT is involved in the development of VSMC in a mammalian system by promoting differentiation from local precursors, we have utilized a binary tetracycline-inducible transgenic system to inactivate Notch signaling in endothelial cells during murine vascular development. Surprisingly, the two endothelial promoters we used generated different phenotypes. Our findings indicate that mature endothelium is not a source of VSMC during murine development. We have also observed that the Tie1 promoter is active in a local precursor population that can give rise to VSMC in a Notch-dependent fashion. Our results suggest that Notch signaling is essential for the differentiation of VSMC from $Tie1^{+}/CD31^{+}/VE\text{-}cadherin^{-}$ precursor cells.

3.2. VSMC are derived from a Tie1^{+}CD31^{+}VE-cadherin^{-} precursor cell

To determine whether endothelial cells can transdifferentiate into VSMC in mammalian development, we used a tetracycline-inducible binary transgenic system to track the endothelial cells. This system requires crossing driver mice expressing the transcription activator (tTA) under an endothelial cell-specific promoter with responder mice expressing a transgene under the tTA-activated tetOS promoter (Figure 3.1). We employed two different endothelial drivers, Tie1-tTA (Tie1tTA)(Sarao and Dumont 1998) and VE-cadherin-tTA (VEtTA)(Sun, Phung et al. 2005), to drive the expression of the β-galactosidase reporter. Tie1 is an orphan receptor tyrosine kinase involved in the regulation of the Tie2/Angiopoietin pathway and is expressed on the surface of endothelial cells (Partanen, Armstrong et al. 1992; Puri, Partanen et al. 1999) and immature hematopoietic cells (Rodewald and Sato 1996). VE-cadherin is an endothelial-specific junctional protein involved, as the name suggests, in the formation of the homotypic adherens junction between endothelial cells (Lampugnani, Corada et al. 1995). Both promoters are widely used for endothelial-specific expression of transgenes (Mukai, Rikitake et al. 2006; Rao, Lobov et al. 2007; Reiss, Droste et al. 2007; Lohela, Helotera et al. 2008; Wolfram, Diaconu et al. 2009).

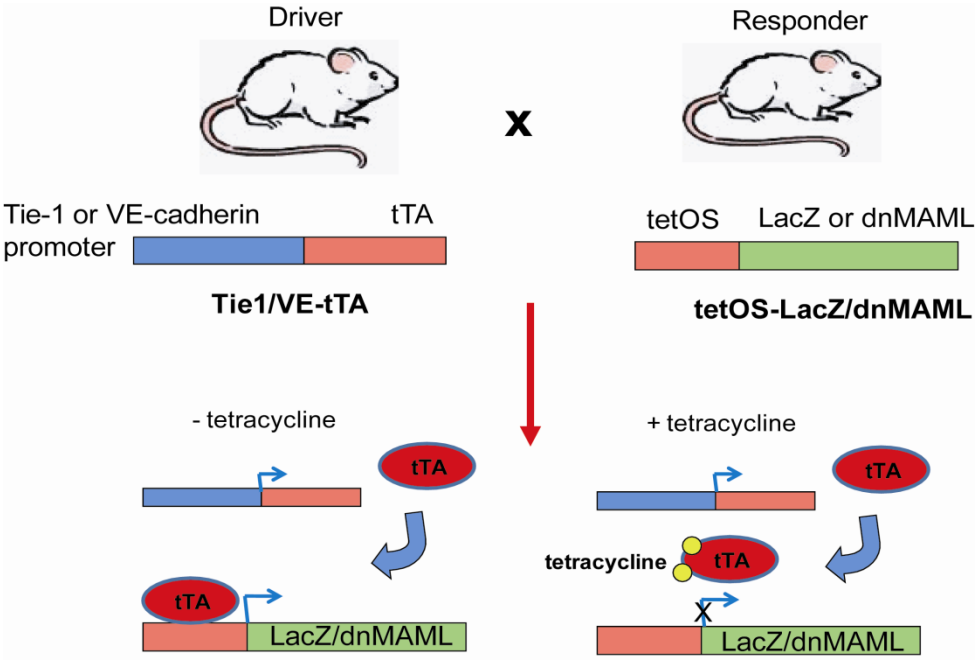

Figure 3.1. The tetracycline-inducible, endothelial-specific transgenic system. This system requires crossing driver mice expressing tTA transcription activator under either the Tie1 (Tie1tTA) or the VE-cadherin (VE-tTA) promoter with responder mice expressing a transgene under the tTA-activated tetOS promoter. The two responder lines drive the expression of β-galactosidase reporter (tetOS-LacZ) or dnMAML (tetOS-dnMAML), an inhibitor of Notch signaling. Treatment of mice with tetracycline suppresses the expression of the transgenes, while tetracycline withdrawal induces endothelial expression of the transgenes.

Both promoters were active in the embryonic vasculature at the stages when VSMC development occurs as demonstrated by wholemount X-gal staining (Figure 3.2A-D) (Takahashi, Imanaka et al. 1996). We confirmed that this system is capable of marking endothelial cell-derived mesenchymal cells, by showing β-galactosidase activity in the cardiac cushion mesenchyme of the atrio-ventricular canal at E10.5 (Figure 3.2E and F).

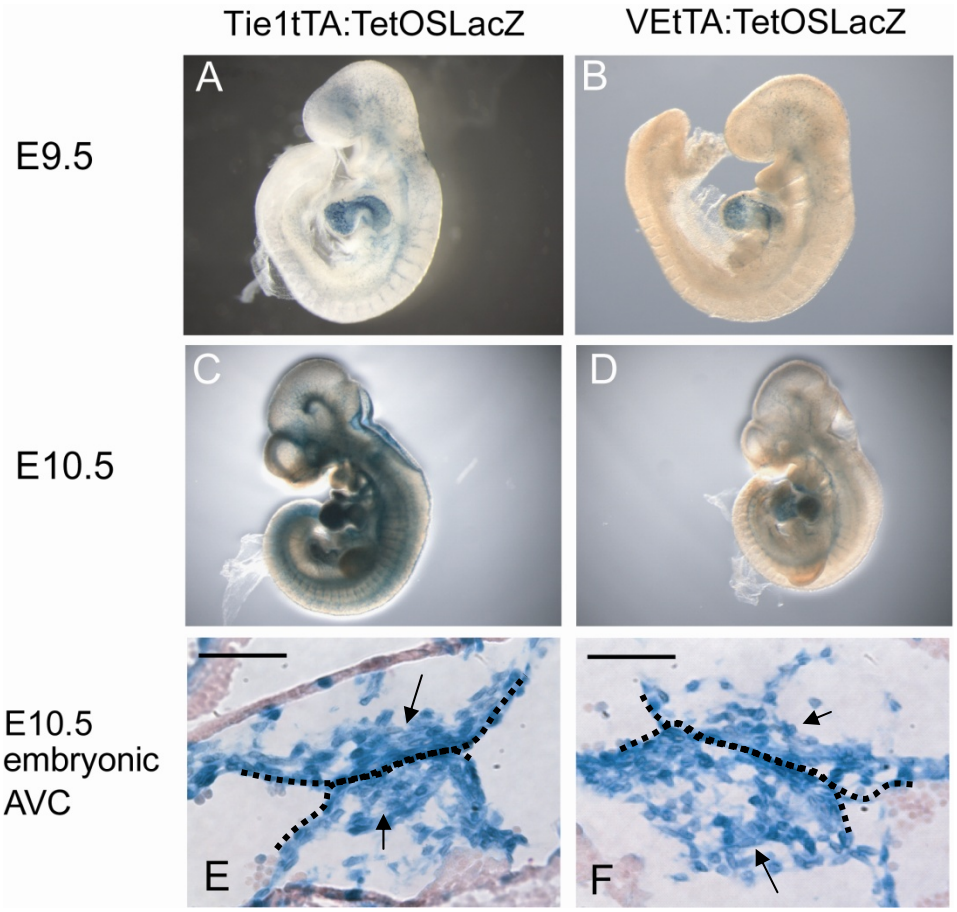

Figure 3.2. Endothelial expression of β-galactosidase reporter. (A-D) Both the Tie1 and VE-cadherin promoters drove reporter β-galactosidase expression, as detected by wholemount X-gal staining, in the developing heart and vasculature at E9.5 (A and B) and E10.5 (C and D). The endocardial cells (dashed lines) and endothelial-derived mesenchymal cells (arrows) in the atrio-ventricular canal (AVC) are labeled with β-galactosidase activity (E and F, bar = 50 μm).

We next examined the descending aorta at E12.5 to determine whether endothelial cells were a source of VSMC. VE-cadherin promoter driven β-gal activity was detected in the endothelial cells and some luminal cells, which may be endothelial cell-derived hematopoietic cells, but not in the surrounding peri-endothelial cells (Figure 3.3B). In contrast, the Tie1 promoter drove the expression of β-gal not only in endothelial cells, but also in the surrounding VSMC, which was verified by co-staining for α-smooth muscle actin (SMA) and β-gal activity (Figure 3.3A). This phenomenon was not restricted to the descending aorta, but was observed in all vascular beds examined (Figure 3.3 C to N), even though VSMC from the different arteries have been suggested to arise from different developmental sources (Majesky 2007). To rule out ectopic promoter activity from transgene insertion sites, endogenous Tie1 promoter activity was examined in embryos that were heterozygous for genomic LacZ knock-in at the Tie1 locus. At E10.5, β-gal activity was observed in the peri-endothelial cells of developing arteries of the knock-in mice (Figure 3.4 A and B).

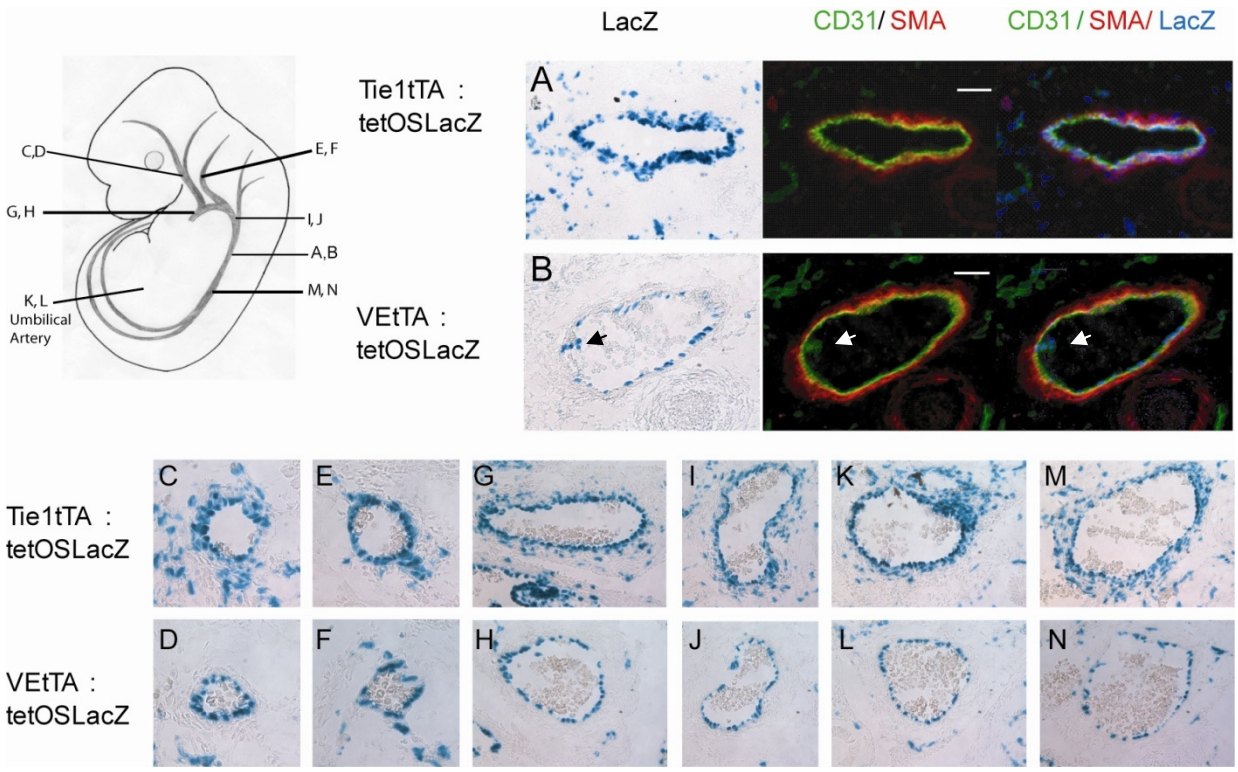

Figure 3.3. The Tie1 promoter, but not the VE-cadherin (VE) promoter, is active in peri-endothelial cells. (A-B) β-gal activity in the descending aorta of E12.5 embryos was detected by X-gal staining. In Tie1tTA:tetOSLacZ (Tie1LacZ) embryos, β-galactosidase activity overlaps with both CD31 staining and SMA staining (A); VEtTA:tetOSLacZ (VELacZ) embryos show only endothelial and hematopoietic (arrow) β-galactosidase activity (B). The same observations are made in carotid arteries (C and D), vertebral arteries (E and F), different segments of the descending aorta (G vs. H, I vs. J and M vs. N) and the umbilical arteries (K and L).SMA: α–smooth muscle actin.

Since a close family member of Tie1, Tie2 is expressed on vascular progenitor cells and Tie1 can regulate Tie2 activity, Tie1 may also be expressed on precursor cells in addition to mature endothelial cells (Zengin, Chalajour et al. 2006; Foubert, Matrone et al. 2008). Using the Tie1 and VE-cadherin promoters, one may finally be able to discern between the role of precursor cells and the endothelium in VSMC differentiation. These findings suggested that Tie1 can be used to mark a subpopulation of VSMC or a VE-cadherin$^-$ precursor cell that is capable of VSMC differentiation. Further, we conclude that mature endothelial cells are not an embryonic source of VSMC.

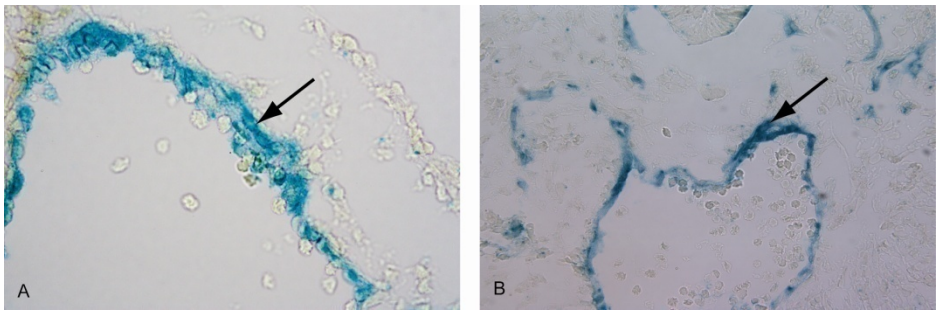

Figure 3.4. Endogenous Tie1 promoter shows activity in peri-endothelial cells. β-gal activity in E10.5 Tie1 LacZ knock-in embryos was detected by X-gal staining. β-gal activity was observed in the thin layer of peri-endothelial cells (arrow) of the umbilical artery (A) and the abdominal aorta (B).

We subsequently attempted to isolate and further characterize the Tie1$^+$ vascular cells that we identified in the embryonic vasculature. Cells positive for β-gal activity from the E10.5 Tie1tTA:TetOSLacZ or VEtTA:TetOSLacZ embryos were sorted using Fluorescein-based fluorescent β-gal substrate FDG (Figure 3.5A-C). At E10.5, VSMC development of the dorsal aorta is still in progress and VSMC development is initiating in other smaller arteries in the embryo (Takahashi, Imanaka et al. 1996). Therefore, while mature VSMC may be present at E10.5, there should still be a population of undifferentitated VSMC precursor cells.

As expected, examination of marker transcripts in E10.5 Tie1$^+$ and VE-cadherin$^+$ embryonic cells by quantitative reverse-transcription polymerase chain reaction (qRT-PCR) revealed an enrichment of endothelial markers (CD31, CD34, Flk-1, Tie1, Tie2 and VE-cadherin) compared to the whole unsorted embryo (Figure 3.5D). When comparing the Tie1$^+$ to the VE-cadherin$^+$ population, a similar level of endothelial markers expression was seen, suggesting the same level of enrichment for endothelial cells (Figure 3.5E). In addition, in the Tie1$^+$ population, enrichment of the mesenchymal progenitor marker muscle segment homeobox (Msx)2 and SMA was also observed (Figure 3.5E). A similar marker expression profile has been described for mesoangioblasts (Minasi, Riminucci et al. 2002), which are embryo-derived mesodermal progenitors that can differentiate into smooth muscle cells *in vitro*.

To determine the source of the increased level of mesenchymal markers in the Tie1$^+$ cells, the sorted cells were cytospun onto a slide and marker expression of individual cells was examined by Immunofluorescence. The majority of the sorted cells from E10.5 Tie1tTA:TetOSLacZ embryos showed expression of the endothelial marker CD31, which may represent the mature endothelial cells (Figure 3.5F). There were also cells expressing the mesenchymal marker SMA and cells that showed co-expression of both CD31 and SMA, which may represent the undifferentiated precursor cells (Ferreira, Gerecht et al. 2007) (Figure 3.5F). This finding suggests that the Tie1$^+$ population contains a precursor cell type that shares characteristics with progenitors capable of differentiating into VSMC.

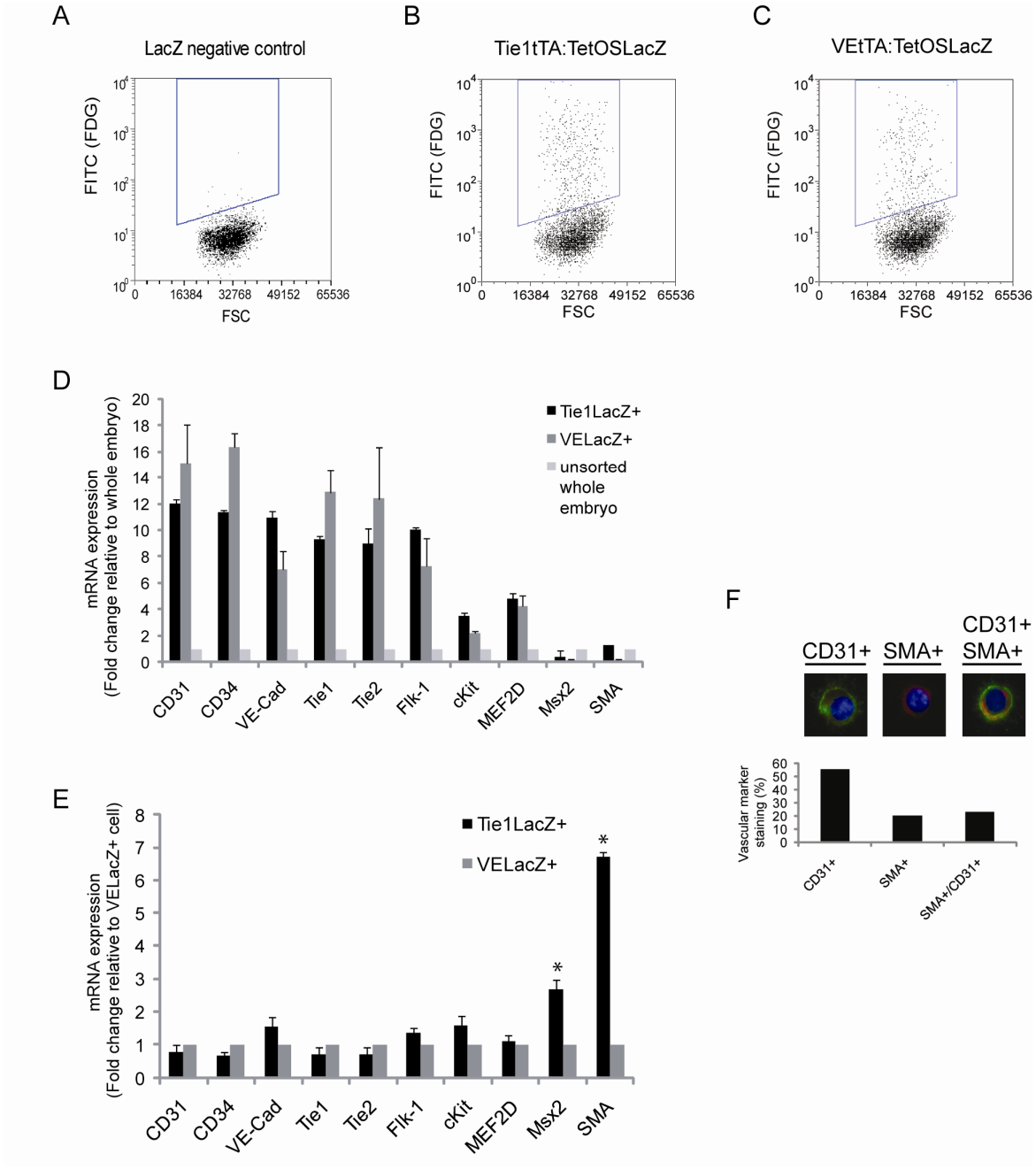

Figure 3.5. Tie1-positive cells show characteristics of VSMC precursor cells. (A-C) E10.5 Tie1LacZ (B) and VELacZ (C) embryos were digested into single cells. Cells positive for β-galactosidase activity were isolated by fluorescence activated cell sorting (FACS). (D)Endothelial markers were enriched from both sorted population by qRT-PCR analysis compared to whole embryo control. (E) Tie1LacZ+ population expresses the same level of endothelial markers compared to VELacZ+ population, with additional mesenchymal marker expression (n = 3, **P* < 0.05). Data presented as mean±SEM. (F) Tie1LacZ+ cells from E10.5 embryos (4 embryos pooled) showed expression of CD31 alone (green), SMA alone (red) and a population of cells co-expressing CD31 and SMA. DAPI counterstain is shown in blue. P-value was determined by Student's t-test.

Co-expression of CD31 and SMA in the $Tie1^+$ cells suggests that the potential precursor cells may express CD31. Interestingly, a $CD31^+$ population negative for β-gal activity was observed with flow cytometry analysis in the VEtTA:TetOSLacZ embryos i.e. VE-cadherin-negative (Figure 3.6A). The $VELacZ^-/CD31^+$ cells also expressed mesenchymal markers Msx2 and SMA, but had low expression of endothelial markers compared to $VELacZ^+/CD31^+$ endothelial cells (Figure 3.6B). Analysis of the $Tie1^+$ embryonic cells suggests that Tie1 promoter activity may be used to enrich a potential VSMC precursor cells that can give rise to smooth muscle cells in all embryonic arteries examined, while VE-cadherin promoter activity marked a mature endothelial population incapable of transdifferentiating into VSMC.

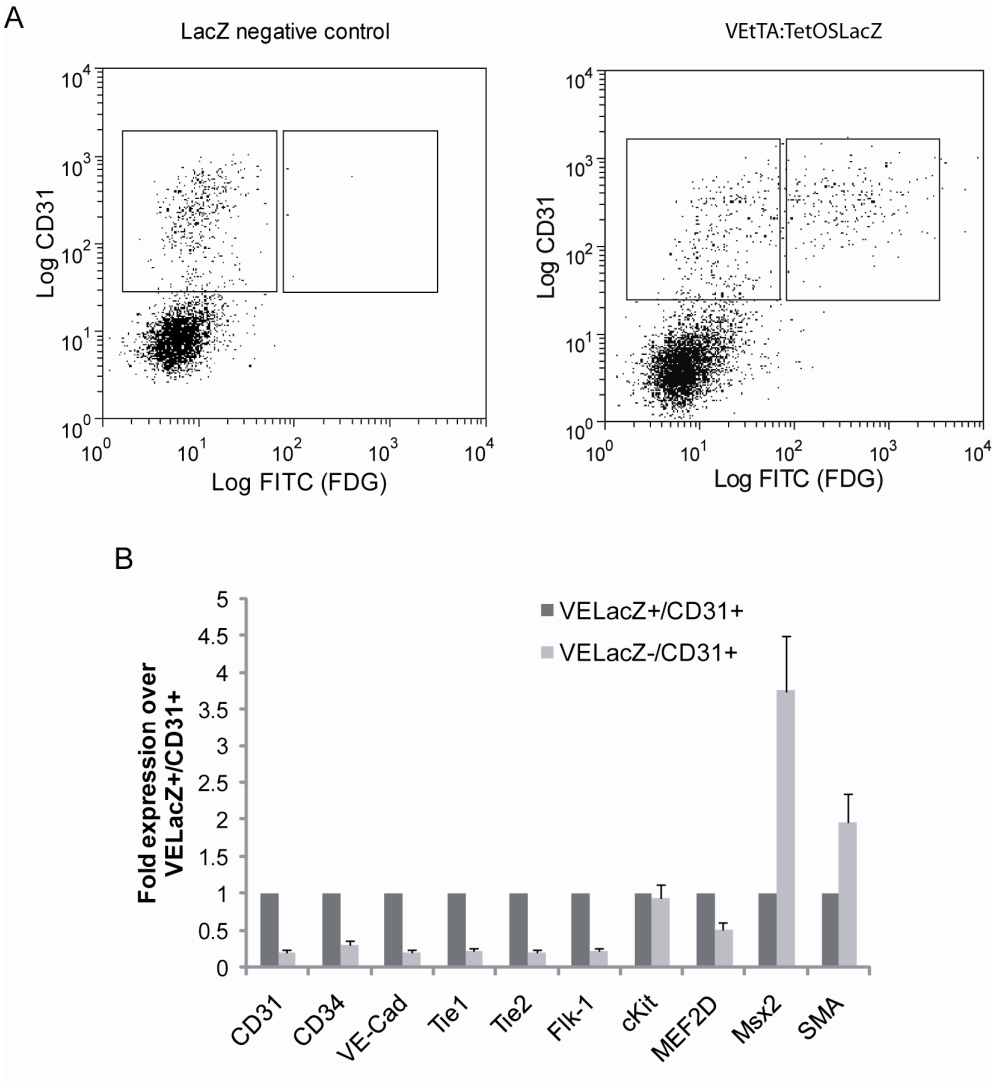

Figure 3.6. Precursor cells are enriched in the LacZ-/CD31+ population in VEtTA:TetOSLacZ embryos. CD31+ cells were sorted according to β-galactosidase activity (FITC) from VEtTA:TetOSLacZ E10.5 embryos (A). VELacZ-/CD31+ cells expressed mesenchymal progenitor markers Msx2 and SMA, while having low expression of endothelial markers (B) (n = 2).

3.3. A tissue-specific, inducible transgenic model for Notch inhibition

To investigate the effect of Notch signaling on Tie1^{+} cells *in vivo*, we used the tetracycline-inducible, binary transgenic system to express an N-terminal dominant-negative mutant of Mastermind-like 1, dnMAML, which retains the Notch and CSL binding domains of MAML1, but lacks co-activator-binding capability (Weng, Nam et al. 2003), under the control of Tie1 promoter (Figure 3.1). In human endothelial cell culture, expression of a constitutively active form of Notch, NotchIC, induced the direct Notch mesenchymal target genes Slug (Niessen, Fu et al. 2008) and SMA (Noseda, Fu et al. 2006). Co-expression with the dnMAML construct successfully blocked induction of both Notch targets (Figure 3.7).

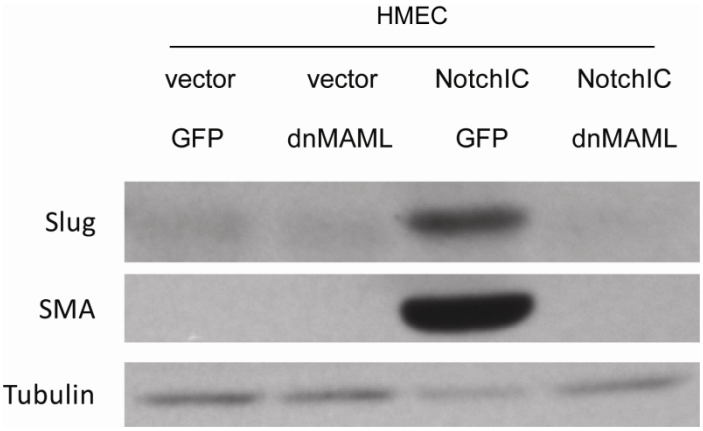

Fiugre 3.7. Expression of dnMAML blocks Notch-induced target expression. Human microvascular endothelial cells (HMEC) were transduced with activated Notch (NotchIC) and dnMAML. Expression of Notch targets Slug and SMA were detected with immunoblotting. NotchIC expression in HMEC induced Slug and SMA, while co-expression of dnMAML blocked the induction.

We established the tetracycline-inducible system (TetOS-dnMAML) to bypass the cardiac defects and the embryonic lethality induced by endothelial-specific inhibition of Notch signaling (Limbourg, Takeshita et al. 2005) and to examine VSMC development in embryos ranging from mid (E10.5) to late (E14.5) gestation. The VEtTA mice were also analyzed to exclude effects due to blockade of Notch signaling in the mature endothelium. When dnMAML was expressed constitutively in the endothelium, the embryo died *in utero* at E11.5, with visible defects and developmental delay at E10.5 regardless of which promoter was used (Figure 3.8A-D). The cardiac defect-induced lethality was in agreement with previous studies done in murine embryos with Tie2-promoter-driven genomic inaction of Notch1 (Limbourg, Takeshita et al. 2005).

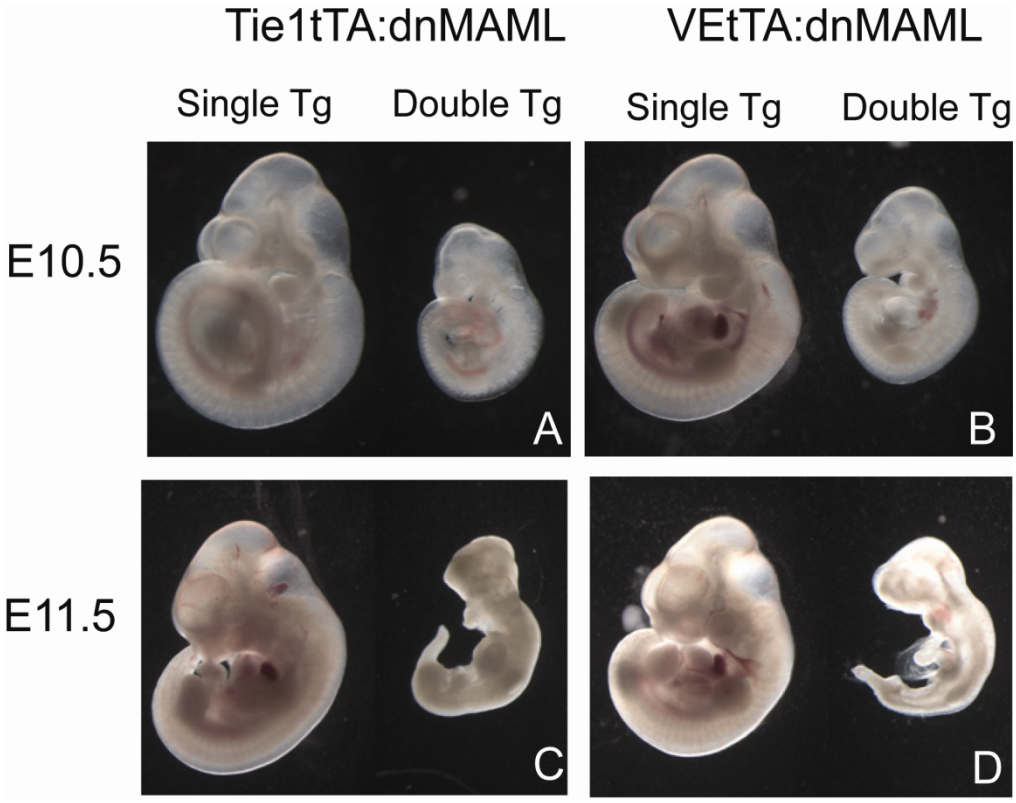

Figure 3.8. Inhibition of Notch in developing endothelium causes embryonic lethality. (A-B) Developmental delay was observed in both Tie1 and VE-cadherin (VE) promoter driven expression of dnMAML at E10.5. Single Tg: single transgenic control littermate; Double Tg: double transgenic mutant. (C-D) Only necrotic double transgenic embryos were obtained at E11.5.

Addition of tetracycline to the drinking water of the mice enabled delay of dnMAML expression, which is fused to green fluorescent protein (GFP) for detection, to bypass embryonic lethality, and withdrawal of tetracycline induced the expression of dnMAML and down-regulated the expression of the Notch target gene Hey2 in embryonic endothelial cells within the first 24 hours (Figure 3.9A-B). The rapid induction of dnMAML after tetracycline withdrawal enabled precise timing of Notch inhibition unique to this transgenic system. Recent studies have suggested that MAML may interact with other transcription regulators to modify transcription of their target genes (McElhinny, Li et al. 2008). In the present transgenic system, expression of the dnMAML construct did not affect signaling through MEF2C, p53 and β-catenin as demonstrated by the transcript level of their respective targets (Figure 3.9B). Overall, the transgenic system provided an inducible method of blocking Notch signaling.

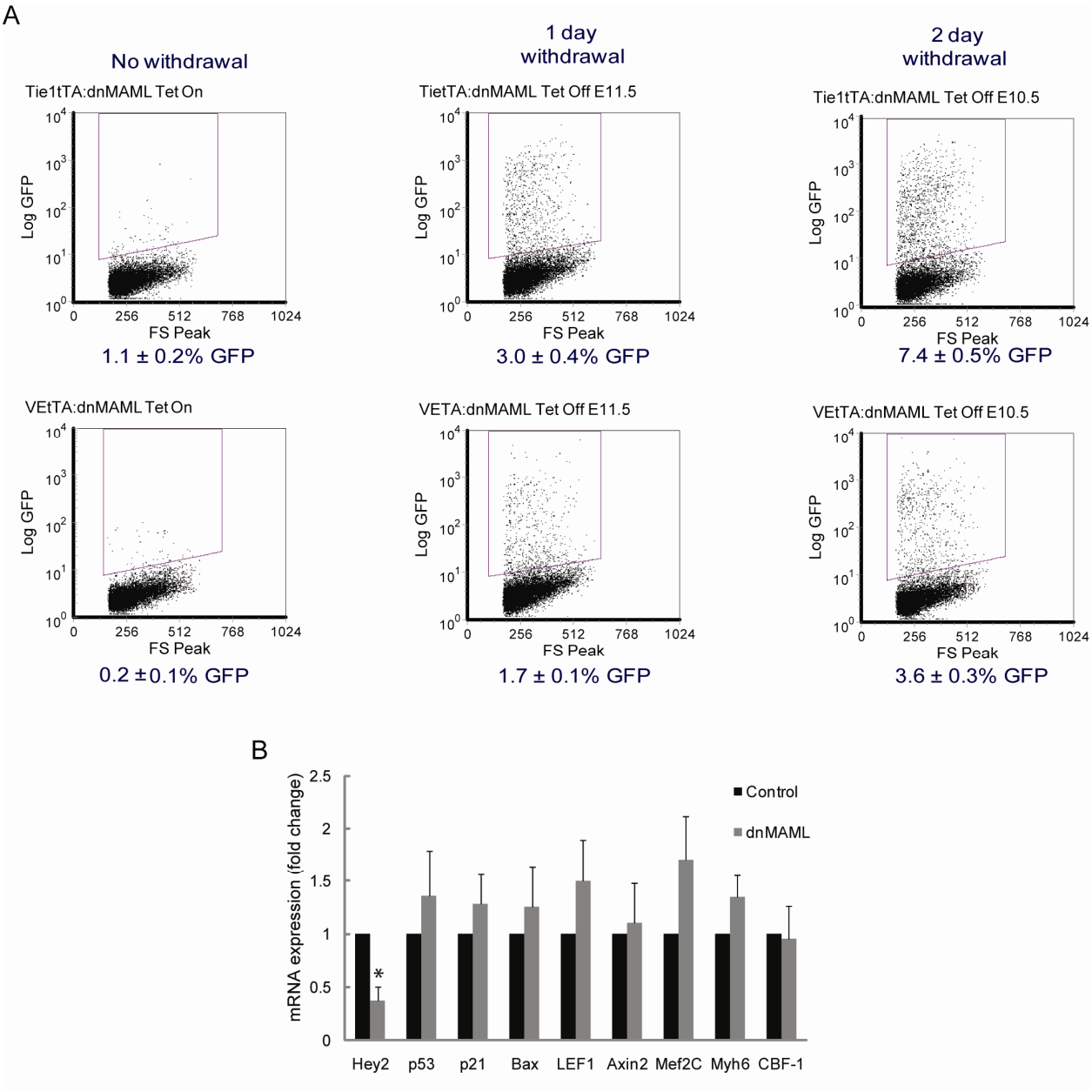

Figure 3.9. Expression of dominant-negative Mastermind-like1 in endothelial cells leads to blockade of Notch signaling. (A) One day after withdrawing tetracycline, there was observable expression of dnMAML-GFP fusion protein with both Tie1 and VE-cadherin promoters, with a further increase after two days. (B) Endothelial cells from E10.5 Tie1:dnMAML double transgenic embryos showed decreased level of Notch target Hey2 compared to wildtype embryos, while transcript levels of targets for other possible MAML binding partners (p53, β-catenin, or MEF2C) remained unaltered. * *P* = 0.01. P-value was determined by Student's t-test.

3.4. Blockade of Notch signaling in Tie1-positive precursors leads to hemorrhage localized to newly-forming vasculature

To examine the effect of blocking Notch in Tie1^{+} vascular precursors on embryonic arteriogenesis, embryos were treated with tetracycline starting at E0.5. The removal of tetracycline treatment and the induction of dnMAML expression at E10.5 for two days led to localized hemorrhages in both the forebrain and hindbrain region in the Tie1tTA:dnMAML double transgenic embryos (Figure 3.10C). However, VEtTA:dnMAML double transgenic embryos undergoing the same treatment did not show gross morphological defects (Figure 3.10D). Interestingly, when dnMAML was induced at E11.5 for two days in the Tie1tTA:dnMAML embryos, the E13.5 embryos displayed hemorrhage covering, in addition to the forebrain and hindbrain, the midbrain and the tip of the tail. When we examined the E14.5 Tie1tTA:dnMAML embryos after inducing dnMAML at E12.5, the hemorrhagic lesions were located at the tip of the snout and the interdigital zone of the forelimbs and hindlimbs. In contrast, the hindbrain appeared normal at this time point (Figure 3.10E and G). The pattern of hemorrhage was consistent across different litters of embryos at the same stages with the same schedule of tetracycline treatment, suggesting that the defects are specific and local. The hemorrhagic regions corresponded to areas undergoing significant morphological remodeling at the time of Notch blockade (Kaufman MH, 1992). Once the remodeling was complete, Tie1 promoter-driven dnMAML expression no longer caused hemorrhages in that location. The changes in the location of the hemorrhage demonstrate that the requirement for Notch signaling is both spatially and temporally regulated during embryonic vascular development. At all stages examined, there were no hemorrhagic defects in the VEtTA:dnMAML embryos with two-day induction of dnMAML (Figure 3.10F and H and Table 3.1).

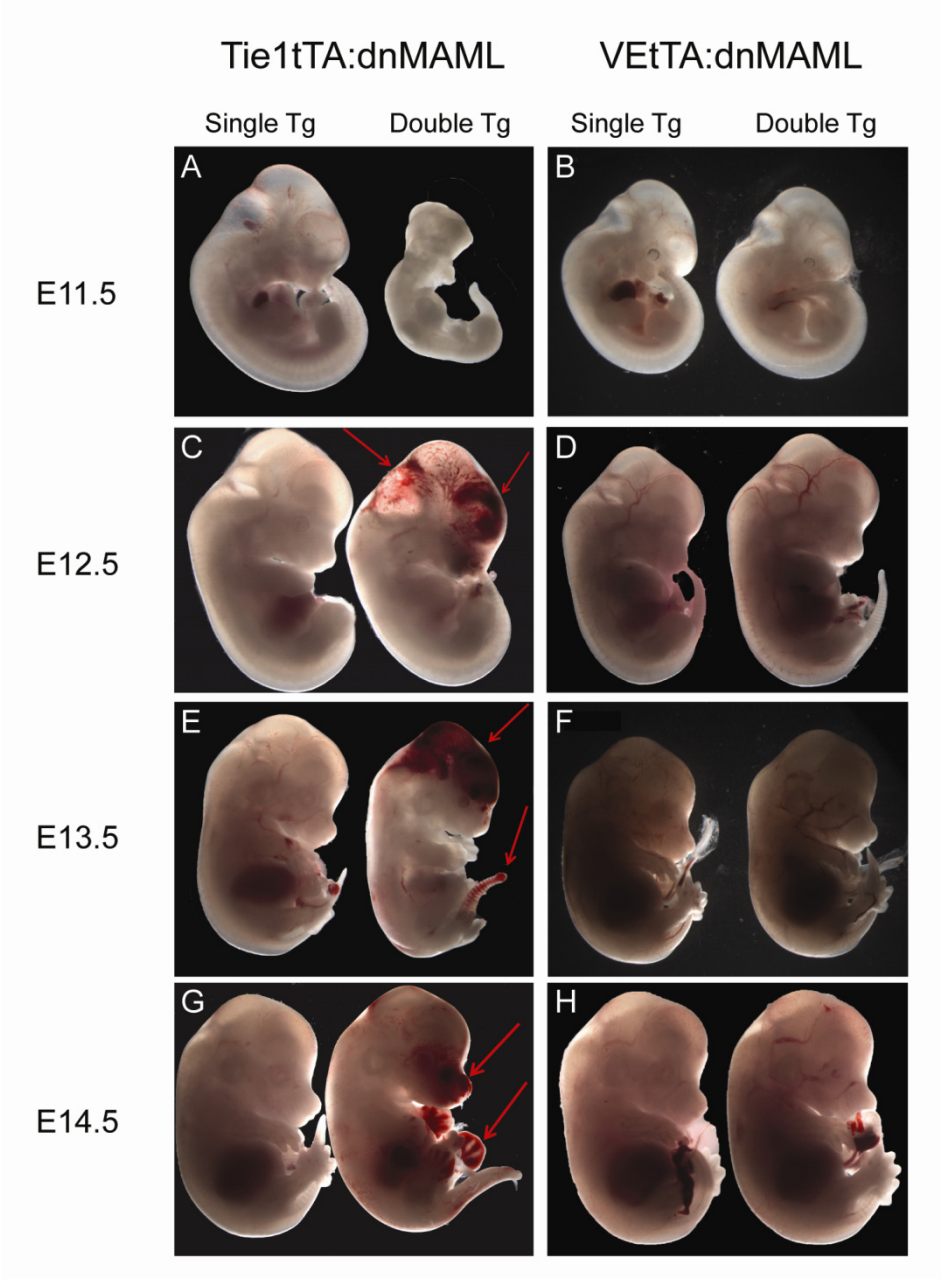

Figure 3.10. Blocking Notch signaling in Tie1-positive cells leads to localized hemorrhaging. (A-H) Wholemount micrographs of embryos with dnMAML expression for 2 days prior to dissection. At E11.5, Tie1tTA:dnMAML embryos were necrotic, with visible developmental delay(A); whereas the VEtTA:dnMAML embryos were not hemorrhagic(B). At E12.5 Tie1tTA:dnMAML embryos showed hemorrhages localized in the forebrain region with sporadic hemorrhages in the hindbrain (C, red arrow indicates location of hemorrhages). At E13.5, there were widespread hemorrhages in both the forebrain and the hind brain with additional hemorrhagic lesions at the midbrain and the tip of the tail (E). At E14.5, the embryos displayed hemorrhaging in the tip of the snout and the interdigital zone of the developing limbs (G). At all the time points examined, there were no gross morphological defects in the VEtTA:dnMAML embryos.

Table 3.1.. Summary of embryo phenotypes

Genotype	Embryo stage	TET withdraw	Gross morphology
Tie1tTA:dnMAML	E9.5	n/a	developmentally delayed, beating heart, n = 4
Tie1tTA:dnMAML	E10.5	n/a	developmentally delayed, hemorrhagic, n = 8
Tie1tTA:dnMAML	E11.5	n/a	necrotic, n = 3
Tie1tTA:dnMAML	E12.5	E11.5	normal, GFP positive, n = 10
Tie1tTA:dnMAML	E14.5	E13.5	normal, GFP positive, n = 5
Tie1tTA:dnMAML	E11.5	E9.5	necrotic, n = 3
Tie1tTA:dnMAML	E12.5	E10.5	hemorrhage in the head region, beating heart, n = 17
Tie1tTA:dnMAML	E13.5	E11.5	hemorrhage in the head and tail, n = 4
Tie1tTA:dnMAML	E14.5	E12.5	necrotic, hemorrhage in the facial region, limb and tail, n =12
VEtTA:dnMAML	E9.5	n/a	developmentally delayed, beating heart, n = 3
VEtTA:dnMAML	E10.5	n/a	developmentally delayed, beating heart, n = 4
VEtTA:dnMAML	E11.5	n/a	necrotic, n = 3
VEtTA:dnMAML	E11.5	E9.5	normal, GFP positive, n = 2
VEtTA:dnMAML	E12.5	E10.5	normal, GFP positive, n = 8
VEtTA:dnMAML	E13.5	E11.5	normal, GFP positive, n = 3
VEtTA:dnMAML	E14.5	E12.5	normal, GFP positive, n = 4

TET = tetracycline

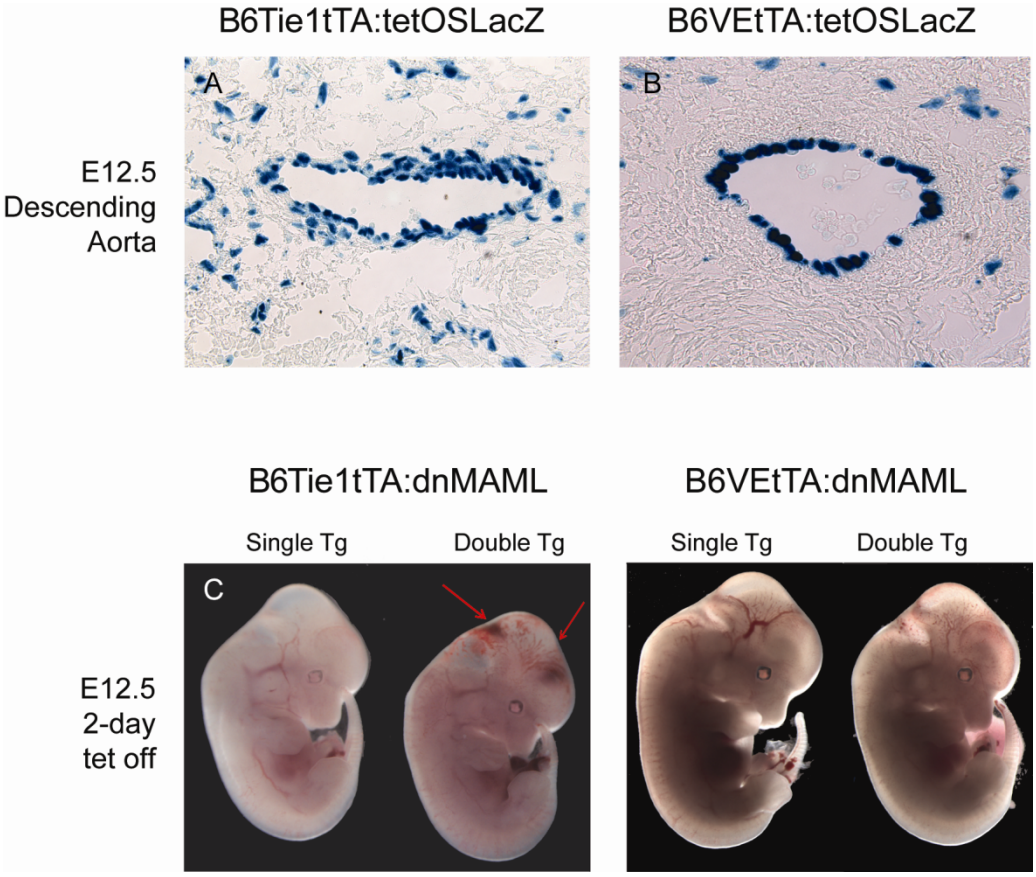

Figure 3.11. Tie1tTA and VEtTA transgenic mice in C57BL/6J background behave similarly to the original albino strains. (A-B) β-gal activity in the descending aorta of E12.5 embryos was detected by X-gal staining. In B6Tie1tTA:tetOSLacZ embryos, β-galactosidase activity was detected in both the endothelium and the peri-endothelial cells (A); B6VEtTA:tetOSLacZ embryos showed only endothelial β-galactosidase activity (B). At E12.5 B6Tie1tTA:dnMAML embryos showed hemorrhages localized in the forebrain region with sporadic hemorrhages in the hindbrain (C, red arrow indicates location of hemorrhages). B6VEtTA:dnMAML embryos did not have hemorrhagic lesions. The B6 strain transgenics showed similar phenotype as the transgenics of albino background strains.

The two driver transgenic mice, Tie1tTA and VEtTA, were derived from and maintained in different background strains. To eliminate strain-dependent difference in phenotypes, we backcrossed both Tie1tTA and VEtTA transgenic mice into the C57BL/6J (B6) background. After five generations of backcrossing, the promoter activity of both transgenics was examined by crossing with the β-gal reporter mouse. Peri-endothelial β-gal acitivity was observed with the B6-Tie1tTA driver, but not the B6-VEtTA driver mouse (Figure 3.11A and B), showing that the phenotypic discrepancies between the Tie1 or VE-cadherin-promoter-driven transgenic mice are independent of the strain difference. Similarly, the hemorrhagic phenotype was obtained when B6Tie1tTA was used to drive dnMAML expression, but not in B6VEtTA:dnMAML embryos (Figure 3.11C and D). Therefore, the strain difference between the two driver transgenic mice did not cause the differences in phenotype observed.

To further study the discrepancies of phenotype obtained by the two endothelial promoters, we examined the expression of the dnMAML-GFP fusion protein by flow cytometry in both Tie1tTA:dnMAML and VEtTA:dnMAML E12.5 embryos after two days of tetracycline withdrawal. For both strains of transgenic embryos, close to 90% of the CD31 positive endothelial cells expressed dnMAML-GFP after two days of induction (Figure 3.12B and C). Furthermore, the mean GFP fluorescence intensities for the two strains were comparable (Figure 3.12C), showing equal expression level of dnMAML-GFP with both promoters. Immunofluorescence analysis of the descending aorta for both strains also showed co-localization of CD31 and GFP in the endothelium (Figure 3.13). Interestingly, several $CD31^+$ cells co-expressing dnMAML-GFP were observed in the peri-endothelial layers in the aorta, potentially representing the Tie1+CD31+ precursor cells isolated from Tie1tTA:LacZ embryos. The CD31 staining in these peri-endothelial cells appeared dimmer compared to the staining in the endothelium, suggesting they are not part of the mature endothelium (Figure 3.13). Blockade of Notch signaling in endothelial cells alone, as shown

by the VEtTA:dnMAML embryos, was not sufficient to generate the hemorrhagic phenotype observed. This suggested that the hemorrhagic defect is due to blockade of Notch signaling in a $Tie1^{+}CD31^{+}VE\text{-}cadherin^{-}$ population.

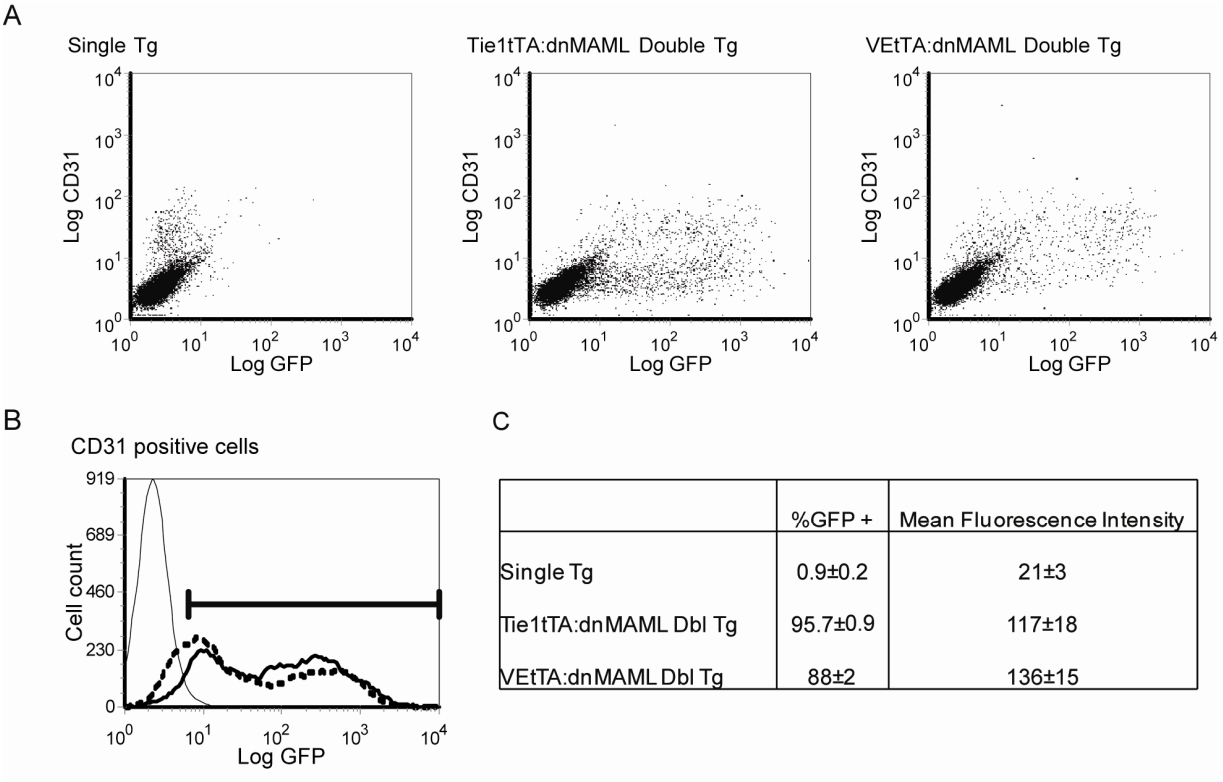

Figure 3.12. Expression of the dnMAML construct is comparable between Tie1tTA:dnMAML and VEtTA:dnMAML embryos. E12.5 Tie1tTA:dnMAML and VEtTA:dnMAML embryos were digested into single cells and stained for the endothelial marker CD31. GFP and CD31 expression was analysed by flow cytometry(A) . Approximately 90% of the endothelial cells (CD31 positive) expressed dnMAML-GFP fusion protein two days after tetracycline withdrawal (B). The mean fluorescence intensity of GFP was 117 unit and 136 unit for Tie1 (solid) and VE-driven (dashed) expression respectively (C). Results shown are mean ± SEM.

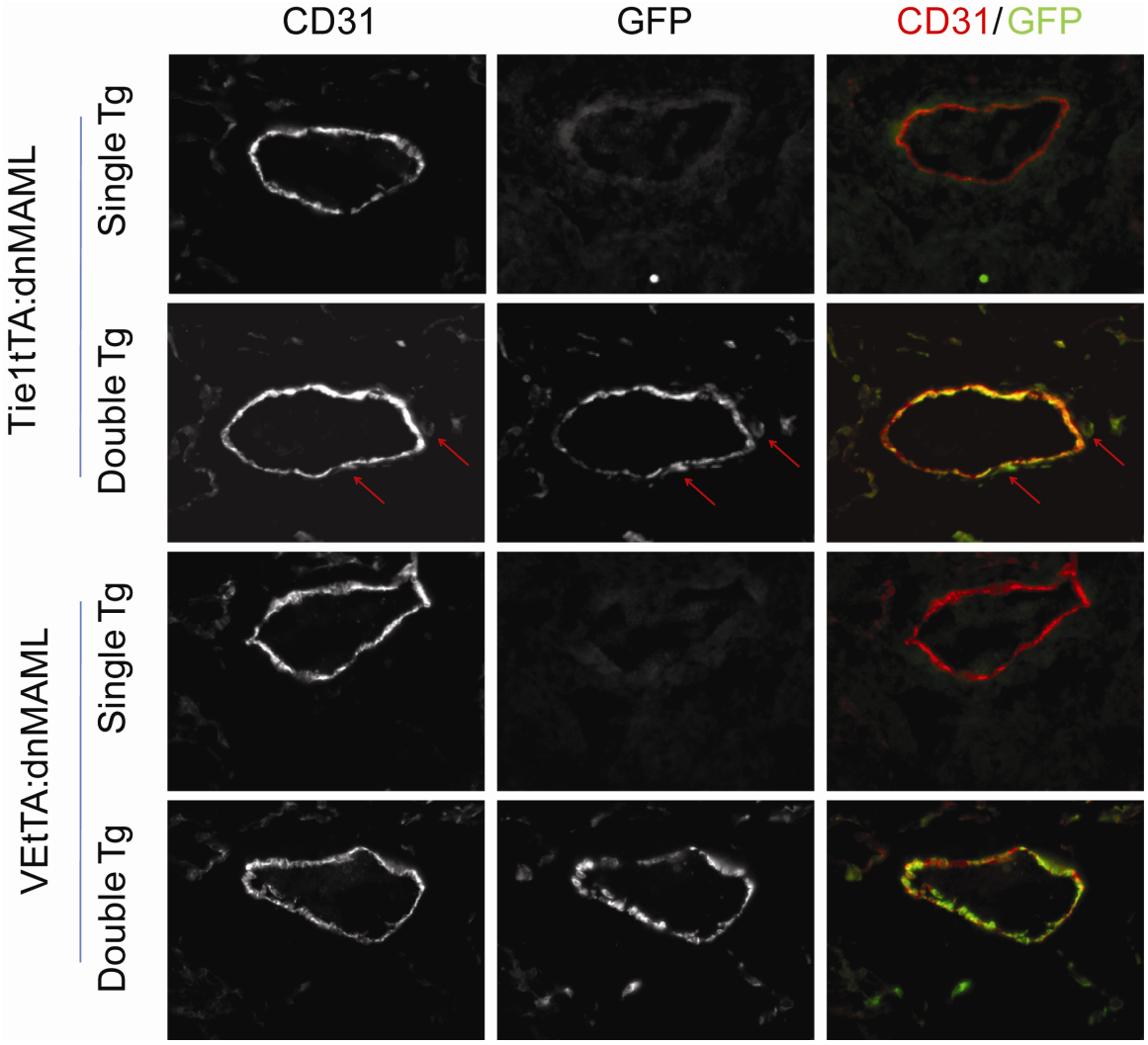

Figure 3.13. Tie1 promoter drives dnMAML expression in endothelial cells and CD31^{dim} perivascular cells. VEtTA:dnMAML double transgenic E12.5 embryos with 2-day induction of dnMAML shows correspondence of GFP expression and CD31 staining in the endothelial cells of the descending aorta. In Tie1tTA:dnMAML double transgenic embryos of the same stage, dnMAML-GFP expression is detected in both the endothelial cells and in perivascular cells (red arrows). These GFP-positive cells also show expression of CD31 that is lower than that of the endothelial cells.

3.5. Notch signaling is required for differentiation of Tie1-positive precursors into vascular smooth muscle cells

Occurrence of hemorrhage often suggests defects in structural integrity of vessels. Since the Tie1^{+}VE-cadherin^{-} vascular cells represent a potential VSMC precursor cell, we examined smooth muscle coverage around the arteries by staining for SMA in the Tie1tTA:dnMAML double transgenic embryos. E12.5 embryos with two day induction of dnMAML were sectioned and the thickness of the SMA staining around the carotid arteries and descending aorta were quantified using the NIH *image* software. In both the descending aorta and carotid arteries, there were decreases in the thickness of VSMC in the double transgenic embryos compared to single transgenic littermates (Figure 3.14A to H). The vertebral artery in the Tie1tTA:dnMAML mutants appeared collapsed with no VSMC around the vessel. In the VEtTA:dnMAML double transgenic embryos, however, no difference was observed in smooth muscle coverage of the arteries (Figure 3.14I to P), suggesting that the effect was solely due to the blockade of Notch signal in the Tie1^{+} VE-cadherin^{-} population, not due to a paracrine effect or heterotypic signaling from the endothelium to the VSMC.

Figure 3.14. Blockade of Notch signaling in Tie1-positive precursor cells impedes vascular smooth muscle differentiation *in vivo*. (A-F) SMA expression in E12.5 embryonic arteries in Tie1tTA:dnMAML mice. In the descending aorta (A and B), vertebral arteries (C and D), and carotid arteries (E and F), there was a reduction of SMA staining in double transgenic embryos (Double Tg) compared to single transgenic littermates (Single Tg). When the thickness of the SMA staining was quantified, the difference was shown to be statistically significant (P = 0.009 for the descending aorta and P < 0.0001 for the carotid artery) (G and H). (I-N) SMA expression was analyzed for E12.5 embryonic arteries in VEtTA:dnMAML mice and showed no significant difference in VSMC thickness between Double Tg and Single Tg (P = 0.67 for the descending aorta and P = 0.10 for the carotid artery). Bar = 50 μm. P-value was determined by Student's t-test.

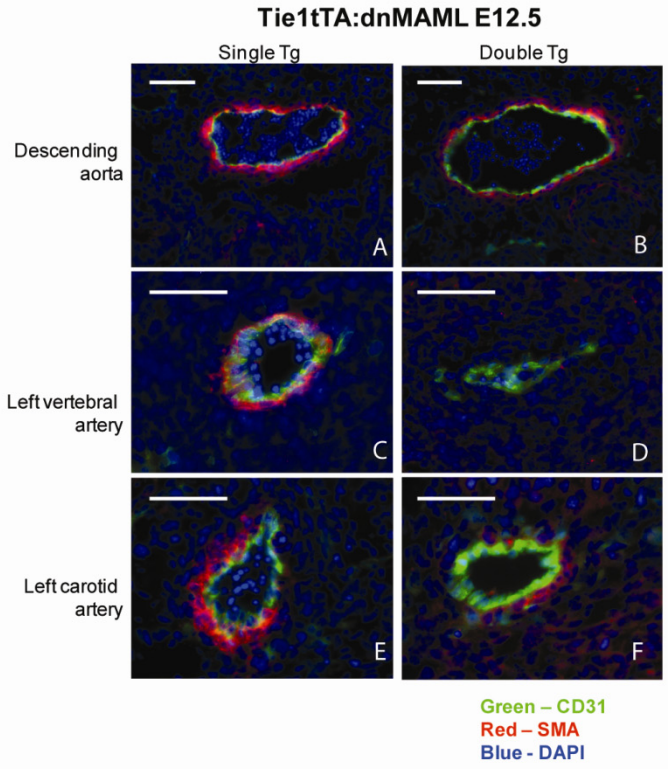
Tie1tTA:dnMAML E12.5
Single Tg
Double Tg
Descending aorta
Left vertebral artery
Left carotid artery
A
B
C
D
E
F
Green – CD31
Red – SMA
Blue - DAPI

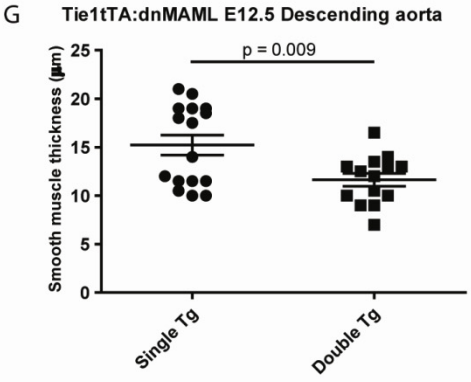
G
Tie1tTA:dnMAML E12.5 Descending aorta
p = 0.009
Smooth muscle thickness (μm)
25
20
15
10
5
0
Single Tg
Double Tg

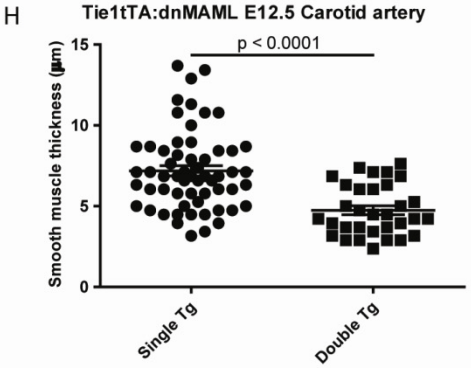
H
Tie1tTA:dnMAML E12.5 Carotid artery
p < 0.0001
Smooth muscle thickness (μm)
15
10
5
0
Single Tg
Double Tg

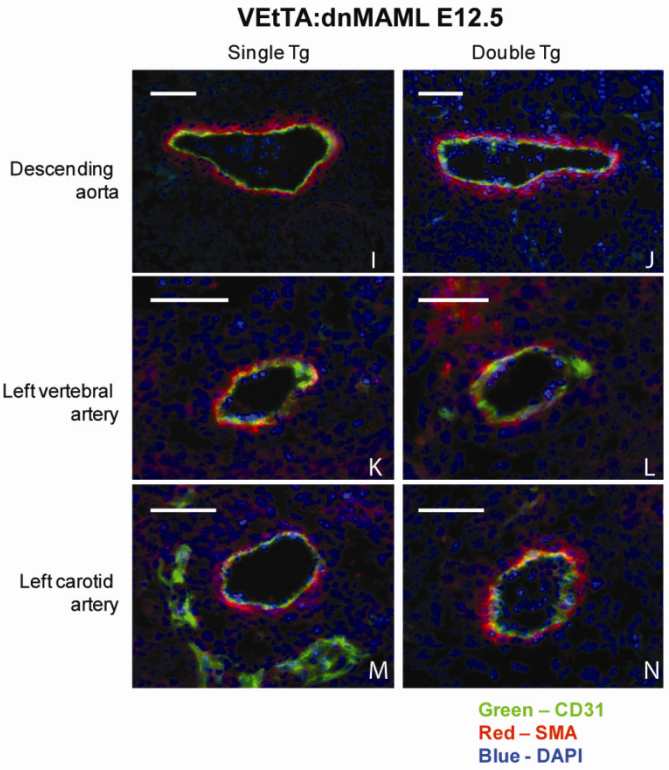
VEtTA:dnMAML E12.5
Single Tg
Double Tg
Descending aorta
Left vertebral artery
Left carotid artery
I
J
K
L
M
N
Green – CD31
Red – SMA
Blue - DAPI

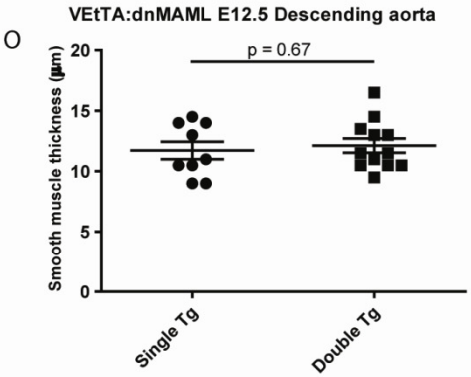
O
VEtTA:dnMAML E12.5 Descending aorta
p = 0.67
Smooth muscle thickness (μm)
20
15
10
5
0
Single Tg
Double Tg

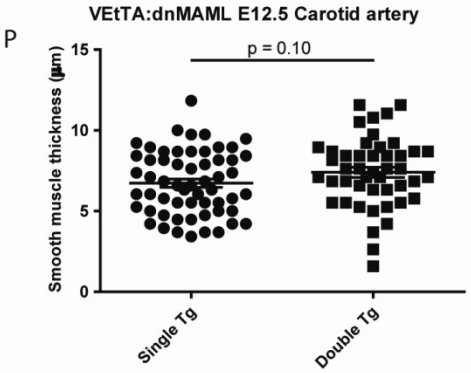
P
VEtTA:dnMAML E12.5 Carotid artery
p = 0.10
Smooth muscle thickness (μm)
15
10
5
0
Single Tg
Double Tg

We also examined the overall percentage of VSMC by surface PDGFR-β staining in E10.5 embryos after one day dnMAML induction. At E10.5, PDGFR-β expression has been described to be expressed mainly in endocardial cells and the peri-aortic mesenchyme (Shinbrot, Peters et al. 1994). In the Tie1tTA:dnMAML double transgenic embryos there was a significant decrease in the amount of PDGFR-β^+ cells compared to littermate controls (Figure 3.15).

Moreover, High et al. showed that when dnMAML was expressed in smooth muscle cells with the SM22-α promoter, there were no defects in smooth muscle cells of the developing aorta observed (High, Zhang et al. 2007). All together, our findings and observations by High and colleagues suggest that Notch activation is required in the Tie1+ precursor cells, but not in mature endothelial cells or mature VSMC, for VSMC development during murine embryogenesis.

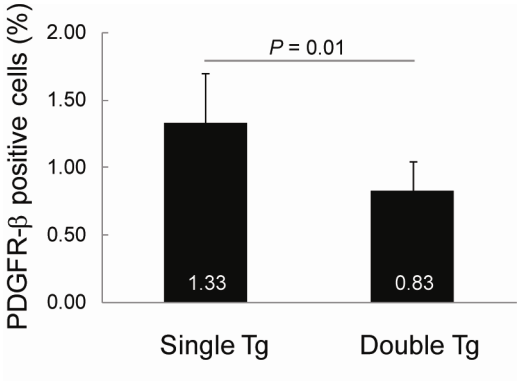

Figure 3.15. Expression of dnMAML in E10.5 embryos decreases the percentage of PDGFR-β positive cells. E10.5 Tie1tTA:dnMAML murine embryos were digested into single cells. Percentage of PDGFR-β positive cells were determined by flow cytometry. Result presented as mean ± SEM of 7 embryos. P-value was determined by Student's t-test.

3.6 Notch activation is not required in Tie1+ precursors after VSMC fate is acquired

When dnMAML expression was induced at different time points during development in the Tie1tTA:dnMAML mutant embryos, the pattern of hemorrhagic regions was altered (Figure 3.10). To determine whether VSMC coverage of the same vessels was affected by blocking Notch in $Tie1^+$ precursors at a later time point, we examined the descending aorta in E14.5 Tie1tTA:dnMAML embryos with two day induction of dnMAML. Interestingly, we did not observe a difference in the VSMC coverage, although robust dnMAML-GFP expression was detected in the endothelium (Figure 3.16A and B). However, in the E14.5 descending aorta, no peri-endothelial expression of dnMAML-GFP was observed, suggesting either a decrease in the $Tie1^+$VE-$cadherin^-$ population or the lack of involvement of this population in VSMC formation in the descending aorta at E14.5.

At E12.5, when dnMAML was induced in these embryos, there are already multiple layers of VSMC investing the descending aorta (Figure 3.14A and I). We speculated that blocking Notch in Tie1+ cells does not affect the smooth muscle coverage of arteries that contained VSMC prior to induction of dnMAML expression. This further demonstrates that the $Tie1^+$ population contains local VSMC precursors necessary for the *de novo* formation of VSMC, but not necessary for further VSMC expansion of more mature arteries. This would also suggest that Notch signaling was involved in the differentiation of nascent VSMC in newly established arteries.

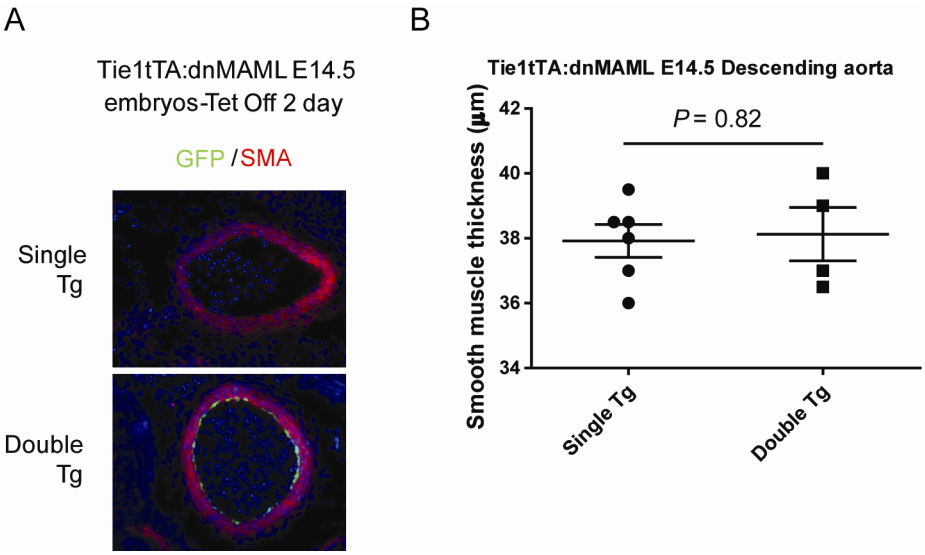

Figure 3.16. Blocking Notch signaling in Tie1^{+} precursor cells does not affect VSMC coverage of already established arteries. (A) Tie1 promoter driven expression of dnMAML-GFP for two days did not decrease SMA staining in E14.5 descending aorta. (B) Quantification of smooth muscle thickness showed no difference between the single transgenic controls and the double transgenic embryos. P-value was determined by Student's t-test.

Different regions of the same vessel may also mature at different times during development. We therefore examined smooth muscle coverage along the entire length of the carotid artery to determine whether Notch blockade had differential effects on smooth muscle generation depending on the distance away from the aortic arch. While both the proximal and distal halves of the carotid artery in Tie1tTA:dnMAML embryos showed significantly less smooth muscle coverage compared to littermate controls (Figure 3.17C to E), the decrease in VSMC in the distal region of the carotid artery was much more pronounced (Figure 3.17F). This finding suggests that as the embryo grows, the distal region of the artery is undergoing active remodeling, and blocking Notch signaling in Tie1^{+} precursor cells had a more apparent effect on VSMC development. The results also suggest that the Tie1+ cells represent local VSMC precursors and that there is minimal migration of the precursors along the same vessel in the rostro-caudal axis. Moreover, once the artery stabilizes, the requirement for Notch signaling in these precursor cells is reduced or eliminated. Taken together, these data illustrate the presence of a Tie1^{+} VE-cadherin^{-} VSMC precursor that requires Notch signaling for VSMC differentiation.

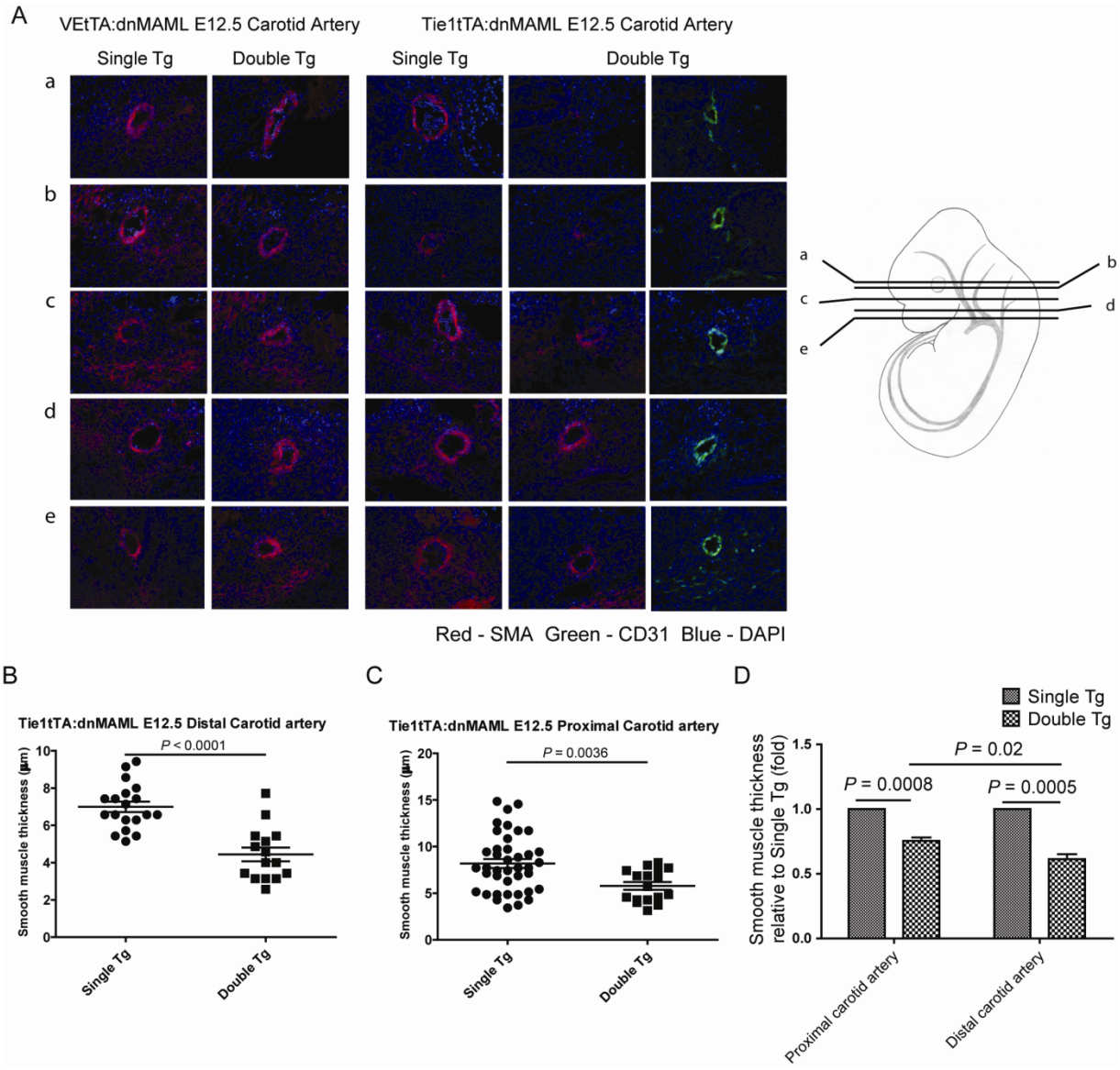

Figure 3.17. Effect of Notch blockade is more evident in distal portion of carotid artery compared to region proximal to the aorta. (A) Smooth muscle actin staining was used to determine smooth muscle thickness around carotid arteries at different locations. SMA Immunofluorescence staining of representative carotid sections showed a more apparent decrease in smooth muscle coverage at distal end of the carotid artery. (B and C) Student t-test was performed on the carotid smooth muscle thickness between the single transgenic controls (Single Tg) and the double transgenic mutant (Double Tg) embryos. (D) The difference is greater in the distal carotid compared to the proximal carotid. P-value was determined by Student's t-test.

3.7. Discussion

VSMC can be derived from different embryonic tissues during development (Majesky 2007). Previous studies on the developmental origins of VSMC often focused on tissue defined population of progenitor cells, such as the neural crest cells (Jiang, Rowitch et al. 2000) and the somites (Pouget, Pottin et al. 2008). In this study, we have shown that during mouse vascular development, there is a $Tie1^+$ precursor population that can give rise to VSMC in a variety of different arterial beds, including ones that were previously identified as neural crest or somite-derived. Whether this Tie1-promoter active progenitor represents a common subpopulation within the previously described VSMC origins is still under investigation. Other vascular progenitor cells, such as the mesoangioblasts (Minasi, Riminucci et al. 2002) and the ESC-derived $Flk\text{-}1^+$ cells (Yang, Soonpaa et al. 2008), have been isolated and cultured with *in vitro* techniques. However, a direct visualization of the progenitor cell fate during normal vascular development using Flk1-cre knock-in mouse shows that $Flk1^+$ progenitor cells can give rise to cardiac and skeletal muscle, but not VSMC (Motoike, Markham et al. 2003). A vascular progenitor can also be isolated from differentiating ES cells by selecting for cells with Tie1-promoter activity (Marchetti, Gimond et al. 2002). This finding strengthens our observation that Tie1 is a marker that can be used to purify VSMC precursor cells. Thus, this study shows for the first time the presence of an immediate vascular precursor that can differentiate into smooth muscle cells *in vivo* during mammalian embryogenesis.

Many signaling pathways have been implicated in smooth muscle development (Yoshida and Owens 2005) and there have been several recent studies looking at the role of Notch signaling in VSMC phenotype (reviewed by (Morrow, Guha et al. 2008)). By *in vitro* experiments, it has been shown that Notch signaling can up-regulate transcription of mesenchymal markers, SMA (Noseda, Fu et al. 2006) and PDGFR-β (Jin, Hansson et al. 2008), and can drive mesenchymal transdifferentiation (Noseda, McLean et al. 2004). The

effect of Notch signaling in VSMC of the neural crest origin (High, Zhang et al. 2007) and the somitic origin during development (Ben-Yair and Kalcheim 2008; Sato, Watanabe et al. 2008; Shin, Nagai et al. 2009) has been studied using mammalian and avian models, respectively. In the avian dorsal aorta development models, somitic cells expressing activated Notch receptor are found to preferentially integrate into the dorsal aorta as both endothelial cells and VSMC. In this study, we have seen that Notch signaling is required in the differentiation of VSMC precursor cells that can give rise to VSMC of different embryonic arteries in a mammalian system. The $Tie1^{+}$ precursor likely represents an immediate precursor predisposed for VSMC fate, regardless of where the cells originally migrated from (Figure 3.18). The tissue-specific requirement for Notch in VSMC differentiation shown in previous studies may simply be reflecting the effect of Notch activation on this distinct $Tie1^{+}$ population. We also observed that sustained Notch activation is not necessary for further maturation of the vessel. Interestingly, Proweller and colleagues also showed that Notch activity is not required for maintenance of embryonic VSMC (Proweller, Wright et al. 2007). Taken together, the findings suggest that arteriogenesis in embryonic vasculature involves first a Notch-dependent differentiation of local $Tie1^{+}$ VE-$Cadherin^{-}$ precursor cells into VSMC, followed by the expansion of VSMC, which may be Notch-independent.

Failure of local progenitors to differentiate into VSMC also provides insight into the process of embryonic vascular development as the pattern of defects caused by the expression of dnMAML corresponds to sites of active arteriogenesis. Our results suggest that the differentiation of VSMC in the thoracic dorsal aorta is initiated prior to E10.5 as induction of dnMAML expression at E10.5 did not completely deplete, but only reduced, VSMC in descending aorta at E12.5. For the region of carotid artery distal to the aorta, however, dnMAML expression at E10.5 severely reduced the smooth muscle coverage of the vessel at E12.5, revealing that VSMC development occurs first in the thoracic region of the embryo,

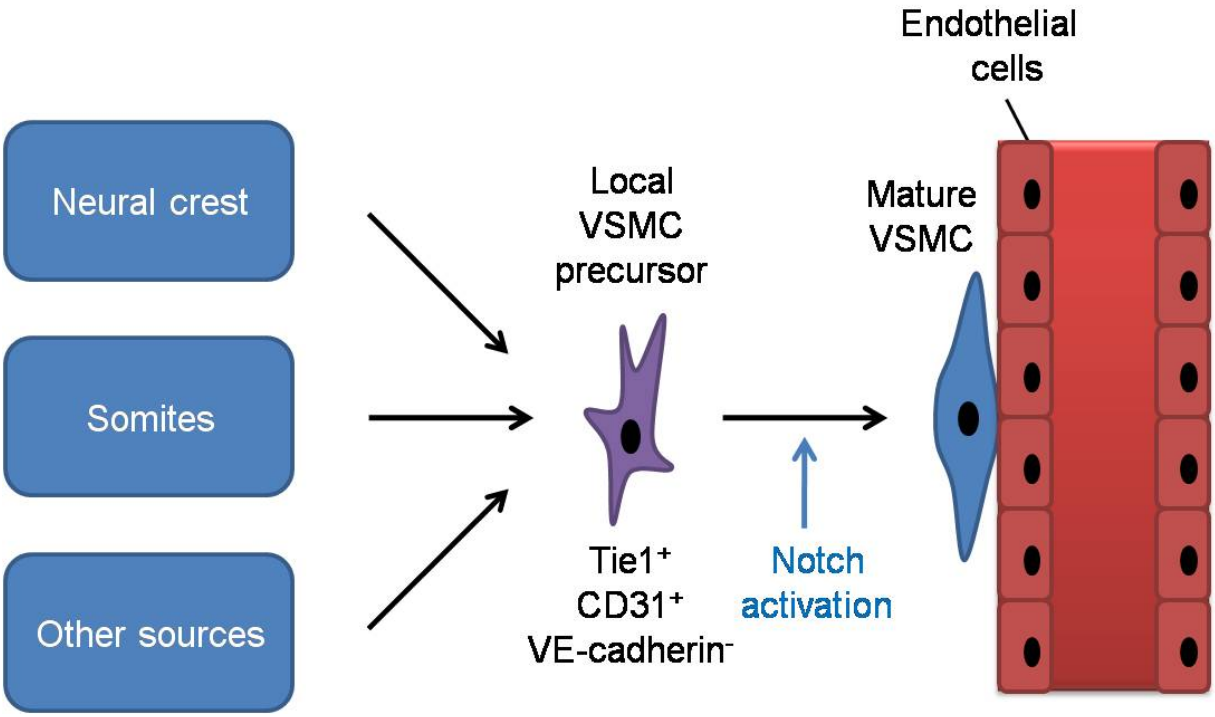

Figure 3.18. Proposed role of Notch activation in embryonic arteriogenesis. The Tie1+ CD31+ VE-cadherin- population contains a local common vascular smooth muscle cell (VSMC) precursor. Notch activation is required for the differentiation of the precursor cells into mature VSMC at the onset of arteriogenesis of nascent arteries. Once the artery is invested with VSMC, Notch activation in the precursor is no longer required.

then progresses cranially and caudally towards the extremities. This is also demonstrated by the later onset of hemorrhaging in the tail when Notch blockade is induced at E11.5. The same conclusion was drawn by Takahashi and colleagues (Takahashi, Imanaka et al. 1996) when they examined the expression of SMA during murine embryogenesis. They did not observe SMA expression around the vertebral arteries until E11.5, which supports our observation that VSMC differentiation of the vertebral artery is completely disrupted at E12.5 by Notch blockade initiated at E10.5. Using the Tie1tTA:dnMAML transgenic system, we can potentially map out the process of embryonic arteriogenesis in embryos of all stages.

Chapter 4. NOTCH ACTIVATION PROMOTES ENDOTHELIAL SURVIVAL THROUGH A PI3K-SLUG AXIS

4.1. Introduction

Vascular homeostasis in the adult requires active maintenance by a balance of signals that leads to a non-proliferative, non-angiogenic, and non-apoptotic endothelial monolayer. Apoptosis is a form of death in which the cell participates in its own demise. It is a tightly regulated process that maintains the homeostasis of a biological system. Many injurious stimuli are present in the bloodstream, to which endothelial cells, the cells lining the inside of blood vessels, are constantly being exposed. Therefore, the endothelium must develop mechanisms to ensure its resistance to apoptotic agents without disturbing the homeostatic state.

Endothelial apoptosis is associated with the initiation and progression of atherosclerosis (Alvarez, Gips et al. 1997; Tricot, Mallat et al. 2000) and attributed to the complication of sepsis (Bannerman and Goldblum 2003), among other cardiovascular diseases (Stefanec 2000). In atherosclerosis, plaques develop containing cholesterol deposits, leukocytes, platelets and smooth muscle cells, leading to the narrowing of vessels. Apoptotic endothelial cells have been observed in patients suffering from atherosclerosis (Alvarez, Gips et al. 1997; Tricot, Mallat et al. 2000). Platelets and leukocytes have increased adherence to apoptotic endothelial cells which may contribute to the progression of plaque formation (Bombeli, Schwartz et al. 1999; Schwartz, Karsan et al. 1999). *In vitro* experiments have also shown that apoptotic endothelial cells stimulate the survival and proliferation of VSMC, leading to intimal thickening and growth of plaque (Raymond, Desormeaux et al. 2004; Sakao, Taraseviciene-Stewart et al. 2007). One of the risk factors for atherosclerosis is hyperhomocysteinemia, where patients experience an elevated plasma concentration of total homocysteine (Clarke, Daly et al. 1991; McCully 1996). Homocysteine is a metabolic product

in the conversion between methionine and cysteine. Serum homocysteine levels can be increased through genetic mutation of enzymes in the homocysteine metabolic pathway or dietary deficiency of vitamin B's required for homocysteine metabolism. Homocysteine stimulation has been shown to cause endothelial apoptosis both *in vitro* and *in vivo* (Zhang, Cai et al. 2001; Hossain, van Thienen et al. 2003; Wilson and Lentz 2005).

Another human disease that is associated with endothelial death is sepsis. Sepsis is a systemic inflammatory disorder whose complications include systemic vascular collapse, multi-organ failure and acute respiratory distress (Bannerman and Goldblum 2003). LPS, present on gram-negative bacteria, has been shown to induce sepsis (Parrillo 1993). LPS stimulation induces endothelial apoptosis *in vitro* and *in viv*o (Haimovitz-Friedman, Cordon-Cardo et al. 1997; Bannerman and Goldblum 2003). Endothelial apoptosis leads to detachment of cells from the vessel, activation of coagulant, and increase in vascular permeability. These endothelial defects may exacerbate the sepsis syndrome, especially in the lung, where respiratory distress can be caused by edema. Inhibition of endothelial apoptosis has been shown to reduce the level of acute lung injury in LPS-challenged animals (Kawasaki, Kuwano et al. 2000). Induction of endothelial survival signaling, therefore, may protect against the effect of these injurious chemicals in the bloodstream and halt the progression of some cardiovascular diseases. Several signaling pathways have been implicated in the precise balance of survival and apoptosis in endothelial cells. Results from our lab and others have illustrated that Notch signaling plays a very important role in endothelial biology (MacKenzie, Duriez et al. 2004; Karsan 2005; Noseda, Niessen et al. 2005).

Our lab has previously shown that activation of Notch1 and Notch4 can protect endothelial cells against LPS-induced apoptosis (MacKenzie, Duriez et al. 2004). The Notch-induced pro-survival effect is partially mediated though the induction of Bcl-2 and the maintenance of mitochondrial membrane integrity (MacKenzie, Duriez et al. 2004). However,

other mechanisms are involved in Notch-induced survival signaling. This section of the thesis focuses on the analysis of Notch-induced survival signaling, presents evidence that the survival function is context-dependent, and provides a possible mechanism to explain the context-dependent activity of the Notch pathway in apoptosis.

4.2. Notch protects against LPS, but not homocysteine,-induced apoptosis

The conflicting observations on the effects of Notch activation in endothelial apoptosis *in vivo*, as discussed in section 1.3.4, suggest a context-dependent role for Notch in the induction of survival signals. To further examine the effect of Notch activation on endothelial survival, a human dermal microvascular endothelial cell line, HMEC, was treated with two different apoptotic stimuli known to affect endothelial cell function in the context of cardiovascular disorder. HMEC transduced with the constitutively active Notch construct or empty vector control were both stimulated with LPS and ALLN (N-Acetyl-L-leucyl-L-leucyl-L-norleucinal, a proteasome inhibitor) or homocysteine for 16 hours under serum-starved conditions. ALLN treatment blocks LPS-induced cell survival signals via inhibition of NFκB activation thereby revealing LPS-induced apoptosis (Zen, Karsan et al. 1998). Cell survival was monitored by neutral red uptake and was quantified as a percentage of the untreated cells. Notch activation in HMEC led to a higher proportion of live cells when stimulated with LPS and ALLN compared to control cells, but decreased cell survival when treated with homocysteine (Figure 4.1A). As neutral red uptake quantifies live cells, the increase in cell number could be caused by cell proliferation rather than survival. To confirm that apoptosis is affected in Notch activated cells, LPS or homocysteine-induced apoptosis was examined by the Annexin V binding assay. Fluorescent dye-conjugated annexin V binds to phosphatidylserine on the surface of early apoptotic cells, which enables quantification of apoptosis by flow cytometry (Koopman, Reutelingsperger et al. 1994; Vermes, Haanen et al. 1995). Upon LPS treatment, Notch activated cells showed a marked decrease in the apoptotic population compared to the vector control cells (Figure 4.1B), while Notch activation exacerbated the apoptotic effect of homocysteine (Figure 4.1C). Thus, in endothelial cells, Notch activation can act either as an anti-apoptotic factor or a pro-apoptotic factor depending on the stimulus, possibly through interaction with other pathways.

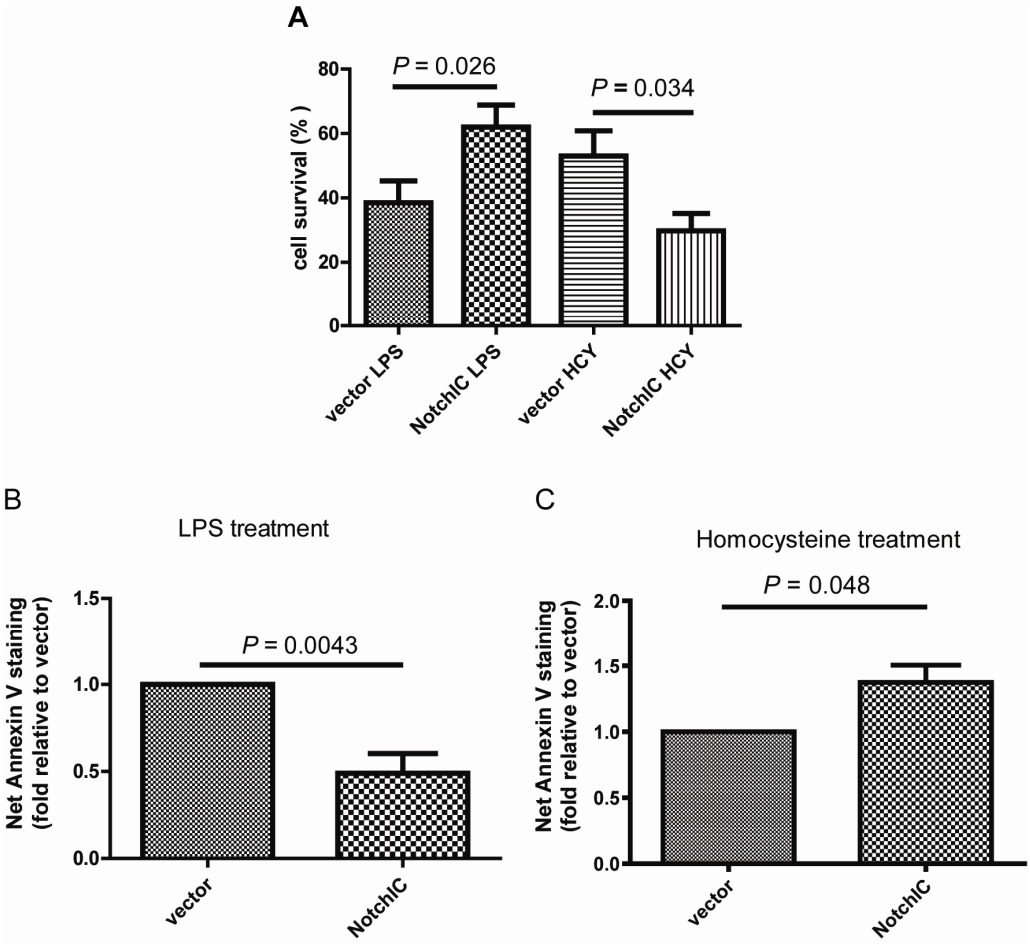

Figure 4.1. Notch activation protects endothelial cells against LPS-induced apoptosis while enhancing homocysteine-induced apoptosis. (A) Endothelial cells transduced with vector control or activated Notch (NotchIC) were treated with 100 μg/mL LPS and 25 μM of ALLN (n = 10) or 7.5 mM homocysteine (n = 7) for 16 hours. Cell survival was determined by neutral red uptake. NotchIC cells showed higher level of survival when treated with LPS, but lower level of survival when treated with homocysteine, compared to vector control cells. (B and C) The difference observed in cell survival is due to the effect of Notch activation on apoptosis as determined by the Annexin V binding assay. NotchIC and vector control HMEC were treated with 100 μg/mL LPS and 25 μM of ALLN (n = 5) or 7.5 mM homocysteine (n = 4) for 8 hours. Results shown are mean ± SEM. P-value was determined by Student's t-test.

4.3 Notch signaling activates the PI3K pathway through a secreted factor

In endothelial cells, homocysteine and LPS have the ability to activate some of the same apoptotic pathways (see Table 1.2). However, while LPS can also stimulate anti-apoptotic signaling through activation of the PI3K pathway (Wong, Hull et al. 2004), homocysteine interferes with PI3K signaling in endothelial cells (Suhara, Fukuo et al. 2004). To examine whether Notch activation can interact with the PI3K pathway in endothelial cells, two different types of human endothelial cells were examined. Since some signaling pathways may be altered in transformed cell lines such as HMEC, primary human umbilical vein endothelial cells (HUVEC) were used alongside HMEC to verify the findings. Both HMEC and HUVEC expressing NotchIC exhibited higher PI3K activity as shown by increased phosphorylation of its downstream effector Akt (Figure 4.2A).

Since PI3K signaling is downstream of many growth factor receptors, we examined whether Notch activates PI3K through a cell-autonomous mechanism or through a secreted factor. Low-serum containing medium conditioned by NotchIC expressing HMEC or vector control HMEC was applied to parental HMEC. Only the medium conditioned with Notch activated HMEC was able to stimulate PI3K in the parental HMEC (Figure 4.2B). Densitometry was used to quantify the ratio between phosphorylated and total amount of Akt (Figure 4.2C). Statistical analysis showed a significant induction of Akt phosphorylation by medium conditioned with NotchIC-expressing HMEC. The phosphorylation of Akt was detected in the first 5 minutes after application of the medium (Figure 4.2B). This rapid response implicates a direct activation of PI3K, rather than a secondary effect through other pathways, supporting the presence of a secreted factor induced by Notch. The identity of the secreted factor remains under investigation.

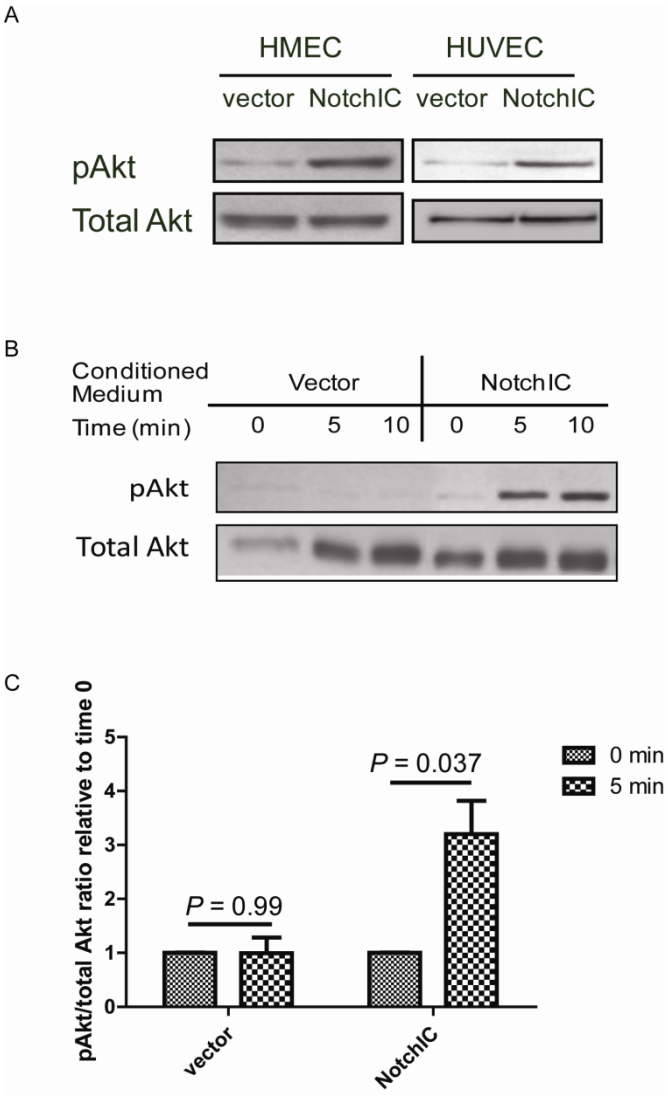

Figure 4.2. Notch activation in endothelial cells leads to activation of PI3K signaling through a secreted factor. (A) Endothelial cells (HMEC or HUVEC) transduced with activated Notch (NotchIC) showed an increased level of Akt phosphorylation (pAkt) by immunoblotting with phospho-specific antibody, indicative of increased PI3K activity. (B) Medium conditioned by Notch activated cells or vector control cells was applied onto parental HMEC cells. Conditioned medium from Notch activated cells induced Akt phosphorylation while vector control conditioned medium did not. (C) The level of Akt phosphorylation was quantified by densitometry and the ratio of phosphorylated to total Akt was determined. Results shown are mean ± SEM of 4 experiments. P-value was determined by Student's t-test.

4.4. PI3K activity is essential for survival of Notch-activated endothelial cells

In many Notch-dependent cancer cell lines, the Notch pathway induces oncogenesis through the activation of PI3K which provides important cell survival signals in cancer cell lines (Mungamuri, Yang et al. 2006; Calzavara, Chiaramonte et al. 2008; Meurette, Stylianou et al. 2009). To examine the role of PI3K activation in Notch-activated endothelium, NotchIC-expressing endothelial cells were treated with a reversible chemical inhibitor of PI3K, LY294002. Following treatment with LY294002, there was an observable increase in cell death in NotchIC-expressing endothelial cells, but not in vector control cells. Immunofluorescence staining for activated effector Caspase 3 was used to determine the percentage of apoptotic cells in vector control or Notch-activated cells treated with LY294002. While there were few (around 10%) apoptotic cells in either untreated vector control endothelial cells, NotchIC-expressing cells, or LY294002-treated control cells, there was a marked increase of apoptosis in Notch-activated endothelial cells treated with the PI3K inhibitor (Figure 4.3A, B). Induction of apoptosis by PI3K pathway inhibition in Notch-activated cells was verified with another PI3K inhibitor, wortmannin, since inhibitor specificity may be a concern. Treatment with both LY294002 and wortmannin showed increased apoptosis in Notch-activated cells by the Annexin V binding assay (Figure 4.3C). Wortmannin is less stable when diluted to working concentration at physiological pH (Holleran, Egorin et al. 2003), which may explain the reduced effect of wortmannin-induced apoptosis compared to LY294002 treatment in NotchIC cells (Figure 4.3C).

These results showed that PI3K activity is essential for survival of endothelial cells when Notch is activated. This requirement for PI3K was not observed in endothelial cells transduced with the empty vector, suggesting that Notch activation leads to induction of parallel pro-apoptotic pathways as well as a PI3K survival pathway. The opposing pathways

are balanced in Notch-activated cells, and the inhibition of PI3K tips the scales towards the apoptotic signals.

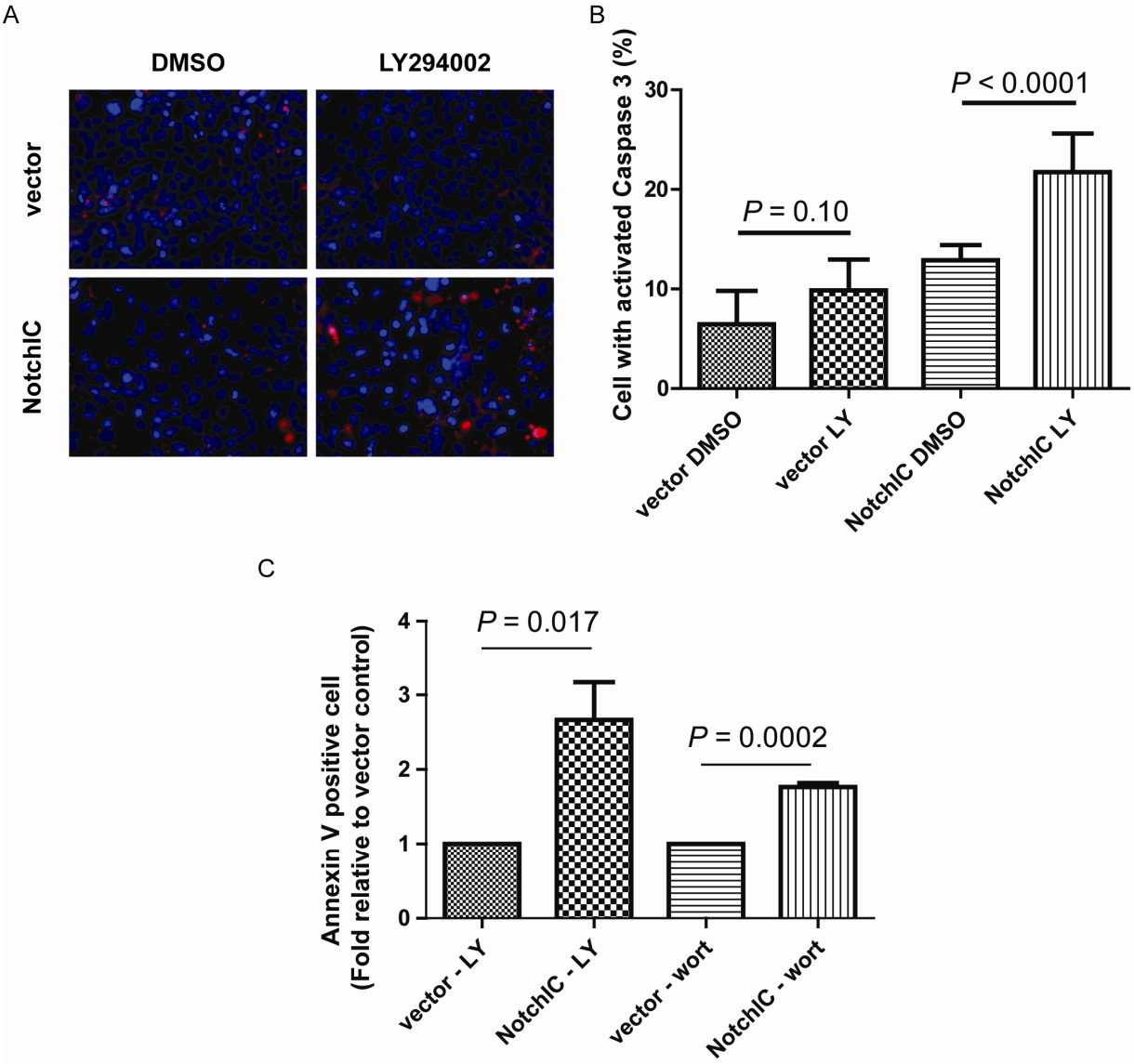

Figure 4.3. PI3K pathway activity is necessary for the survival of Notch-activated endothelial cells. (A and B) HMEC transduced with vector control or NotchIC were treated with DMSO or 40μm PI3K inhibitor LY294002 for 8 hours. Apoptotic cells were quantified (n = 3) by immunofluorescence staining with antibody against activated caspase 3 (red) and counterstained with DAPI (blue). (C) HMEC transduced with vector control or NotchIC were treated with DMSO (vehicle), 40 μm LY294002 (LY) or 1 μM wortmannin (wort) for 16 hours. Percentage of apoptotic cells was determined by Annexin V binding. Results shown are mean ± SEM of 4 experiments. P-value was determined by the Student's t-test.

4.5. PI3K activity is required for Notch-induced Slug expression

We have shown that PI3K activity is required for endothelial survival when Notch is activated. Previous work from our lab has suggested that the expression of a direct transcriptional target of Notch, Slug, is also important for cell survival in Notch-activated endothelial cells (Niessen, Fu et al. 2008). To determine whether there is a link between the expression of Slug and PI3K activity, we evaluated the expression of Slug in Notch activated cells with and without PI3K inhibition. In HMEC, there was no observable basal level of Slug protein expression and Notch activation up-regulated Slug as previously observed (Niessen, Fu et al. 2008). Treatment with LY294002 decreased Notch-induced Slug expression (Figure 4.4A,B). Our lab has previously shown that Notch activation induces Slug through CSL-dependent transcriptional activation (Niessen, Fu et al. 2008). An additional level of regulation is shown here as Notch activates PI3K, which is in turn required for Slug expression. Since Slug expression is required for endothelial survival in Notch activated cells, the apoptosis induced by inhibition of PI3K observed may be through down-regulation of Slug. These data show that Notch activation induces a PI3K-Slug signaling axis important for endothelial survival.

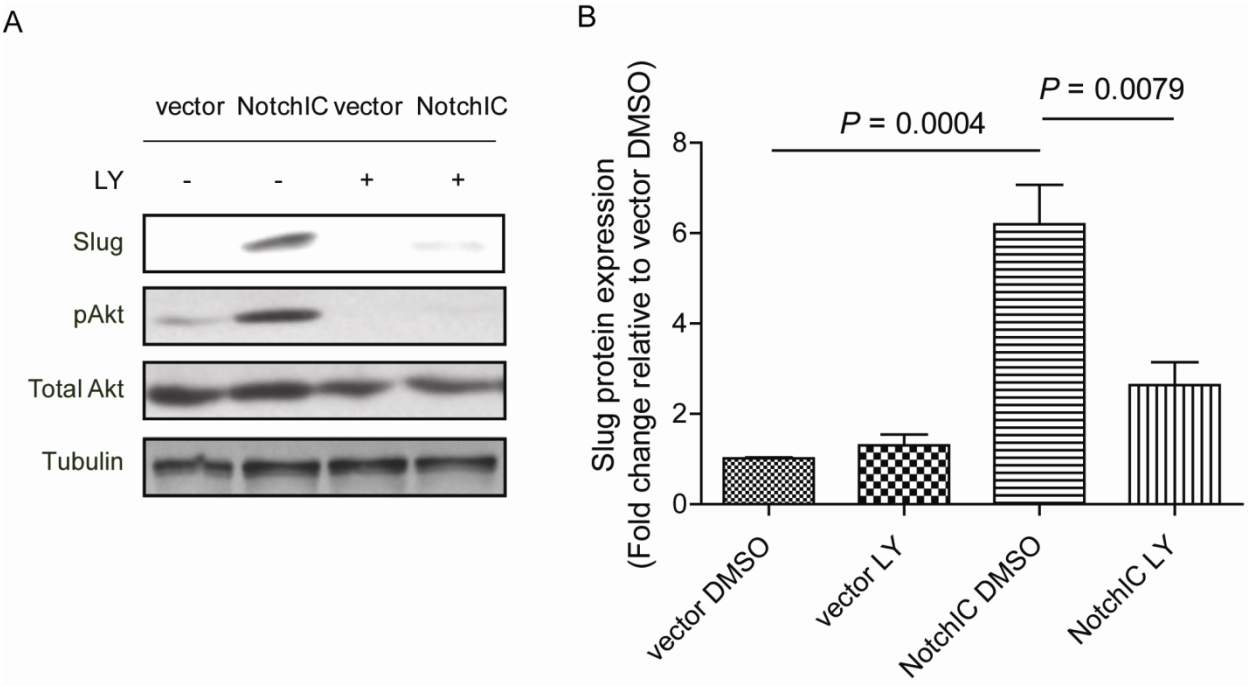

Figure 4.4. PI3K activity is required for Notch-induced Slug expression. (A) HMEC transduced with NotchIC showed induction of Slug expression by immunoblotting. The expression of Slug was down-regulated by inhibition of PI3K with 40 μM of LY294002 (LY) for 4 hours. (B) The level of Slug expression was quantified by densitometry and the ratio of Slug to Tubulin was determined. Results shown are mean ± SEM of 5 experiments. P-value was determined by Student's t-test.

The most studied downstream effector of the PI3K pathway is Akt, which is required for many of the previously described functions of PI3K. To determine whether PI3K modulates Slug expression through Akt, a kinase-dead Akt dominant-negative mutant (dnAKT) with three amino acid replacements (K179M, T308A, S473A) was used to inhibit Akt-dependent signaling (Sakoda, Gotoh et al. 2003). Expression of dnAKT did not decrease Notch-induced Slug expression (Figure 4.5A). In addition, treatment with the Akt inhibitor triciribine, which inhibits all three AKT family members, also did not reduce Slug expression in NotchIC-expressing cells (Figure 4.5B), suggesting that PI3K regulates Slug expression through an Akt-independent mechanism. High concentrations of LY294002 are also known to inhibit signaling through mTOR (mammalian target of rapamycin) (Brunn, Williams et al. 1996). To confirm that the effect of LY294002 treatment was not through inhibition of mTOR, NotchIC-expressing HMEC were treated with rapamycin, a chemical inhibitor of mTOR. Rapamycin did not inhibit Notch-induced Slug expression (Figure 4.5C). However, rapamycin only inhibits mTOR signaling through the raptor-mTOR complex without blocking signaling through the rictor-mTOR complex (Sarbassov, Ali et al. 2004). Therefore, we could not definitively conclude that Slug expression is not regulated by mTOR activity.

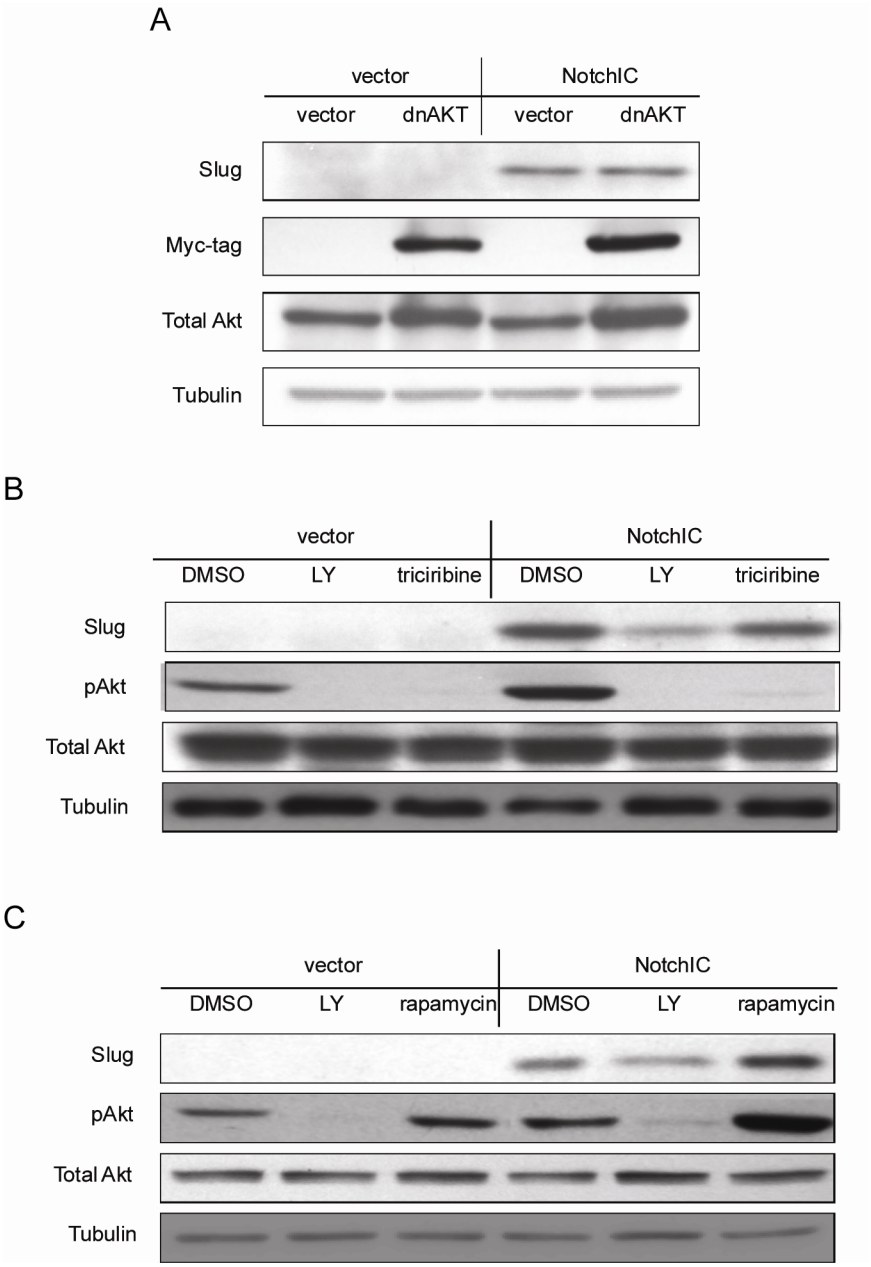

Figure 4.5. Akt or mTOR activity is not required for Notch-induced Slug expression. (A) Co-transduction of a dominant-negative form of Akt (dnAKT) (myc-tagged) with NotchIC did not down-regulate Notch-induced Slug protein as detected by immunoblotting. (B) Inhibition of Akt (25 μM triciribine) or (C) mTOR (1 μM rapamycin) did not alter Notch-induced Slug protein expression. The expression of Slug was down-regulated by inhibition of PI3K with 40 μM of LY294002 (LY) for 4 hours.

To further examine the mechanism of PI3K-dependent Slug expression, mRNA was isolated from HMEC transduced with either NotchIC or empty vector and treated with either LY294002 or DMSO vehicle. Transcript level of Slug was quantified using qRT-PCR. Notch activation up-regulated expression of its direct targets Hey1 and Slug in endothelial cells, confirming previous observations (Figure 4.6A). Interestingly, both basal and Notch-induced Slug transcripts were reduced by PI3K inhibition (Figure 4.6B). This decrease was not caused by a generalized inhibition of Notch-dependent transcription, as the mRNA level of Hey1 was not affected by PI3K inhibition (Figure 4.6C). This finding suggests that PI3K is able to regulate Slug transcription via a Notch-independent mechanism or that PI3K activity regulates Slug transcript stability. Further experiments are required to distinguish between the two mechanisms.

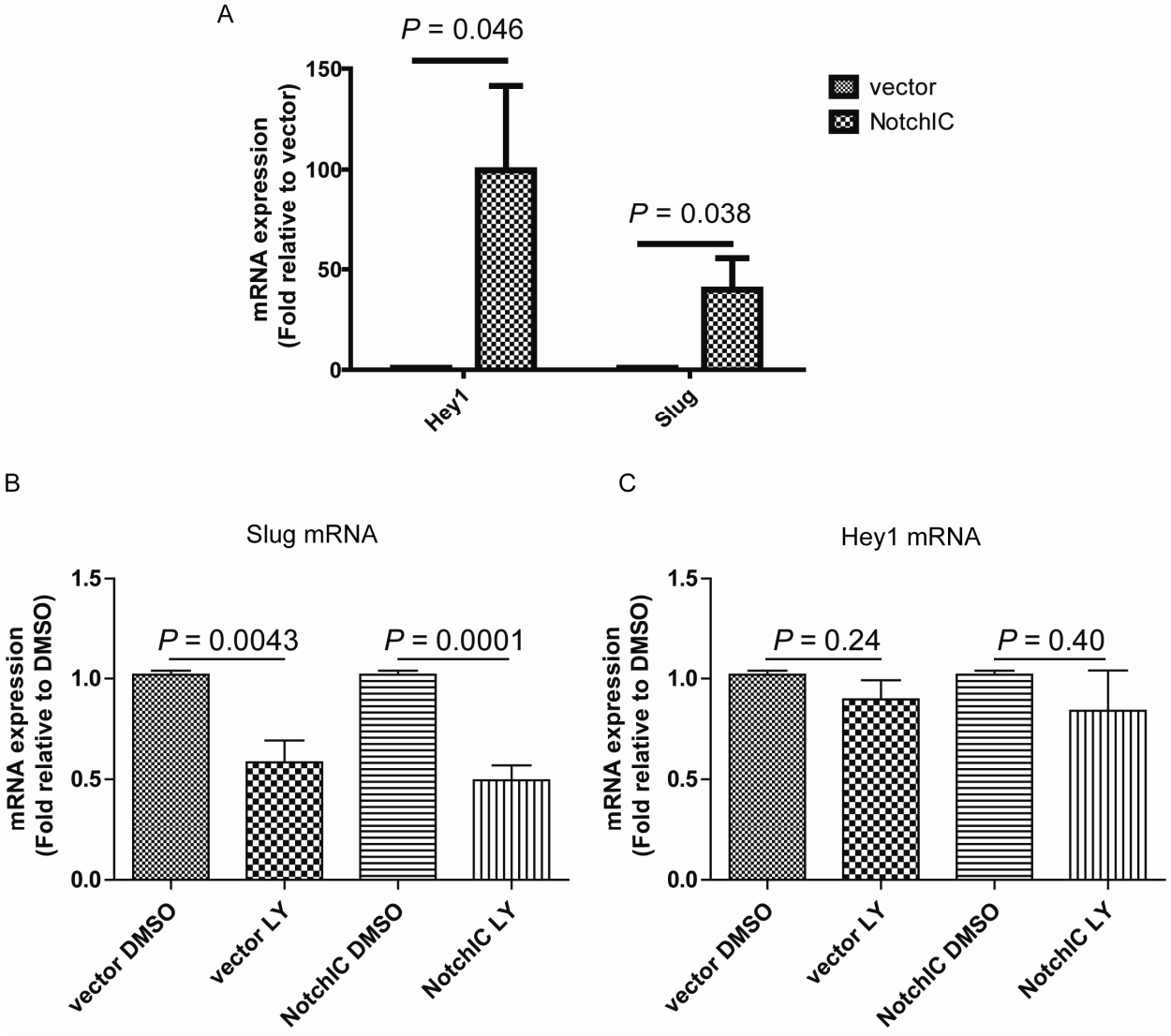

Figure 4.6. PI3K inhibition decreases both basal and Notch-induced Slug transcript level. (A) NotchIC expression in HMEC up-regulated mRNA level of both Hey1 and Slug. (B) Both endogenous and Notch-induced Slug transcription was reduced by PI3K inhibition. HMEC transduced with NotchIC or vector control were treated with 40 μM of LY294002 or DMSO vehicle for 4 hours. The mRNA for Slug (B) and Hey1 (C) were quantified by quantitative RT-PCR. Results shown are mean ± SEM of 5 experiments. P-value was determined by Student's t-test.

4.6. Slug protects endothelial cells against LPS-induced apoptosis

In other cell types, Slug has been shown to be an anti-apoptotic factor, protecting against DNA-damage-induced cell death (Wu, Heinrichs et al. 2005; Kurrey, Jalgaonkar et al. 2009). The requirement for Slug expression for cell survival in Notch activated endothelium suggests that Slug also has anti-apoptotic function in endothelial cells. To investigate the possibility that Notch imparts its protective activity against LPS stimulation through Slug, Slug transduced HMEC were treated with LPS and ALLN or homocysteine. Slug expression in HMEC led to a higher proportion of live cells when the cells were stimulated with LPS and ALLN, but cell survival was unchanged compared to control when cells were treated with homocysteine (Figure 4.7A). To confirm that apoptosis is affected in Slug-expressing cells, LPS or homocysteine-induced apoptosis was examined by the Annexin V binding assay. Upon LPS treatment, Slug-expressing cells showed a marked decrease in the apoptotic population compared to the vector control (Figure 4.7B), while Slug again did not inhibit homocysteine-induced apoptosis in HMEC (Figure 4.7C). The ability of Slug to convey an anti-apoptotic effect against LPS stimulation showed that Slug may be the downstream effector for Notch-induced protection. Slug did not offer the same protection against homocysteine-induced apoptosis, but unlike Notch, Slug did not exacerbate the effect of homocysteine treatment. The lack of Slug-induced protection against homocysteine treatment may indicate that the downstream signaling from Slug does not interfere with homocysteine-induced apoptotic signal; alternatively, homocysteine treatment may inhibit the pro-survival activity of Slug. This finding also shows that Slug does not induce parallel apoptotic pathways.

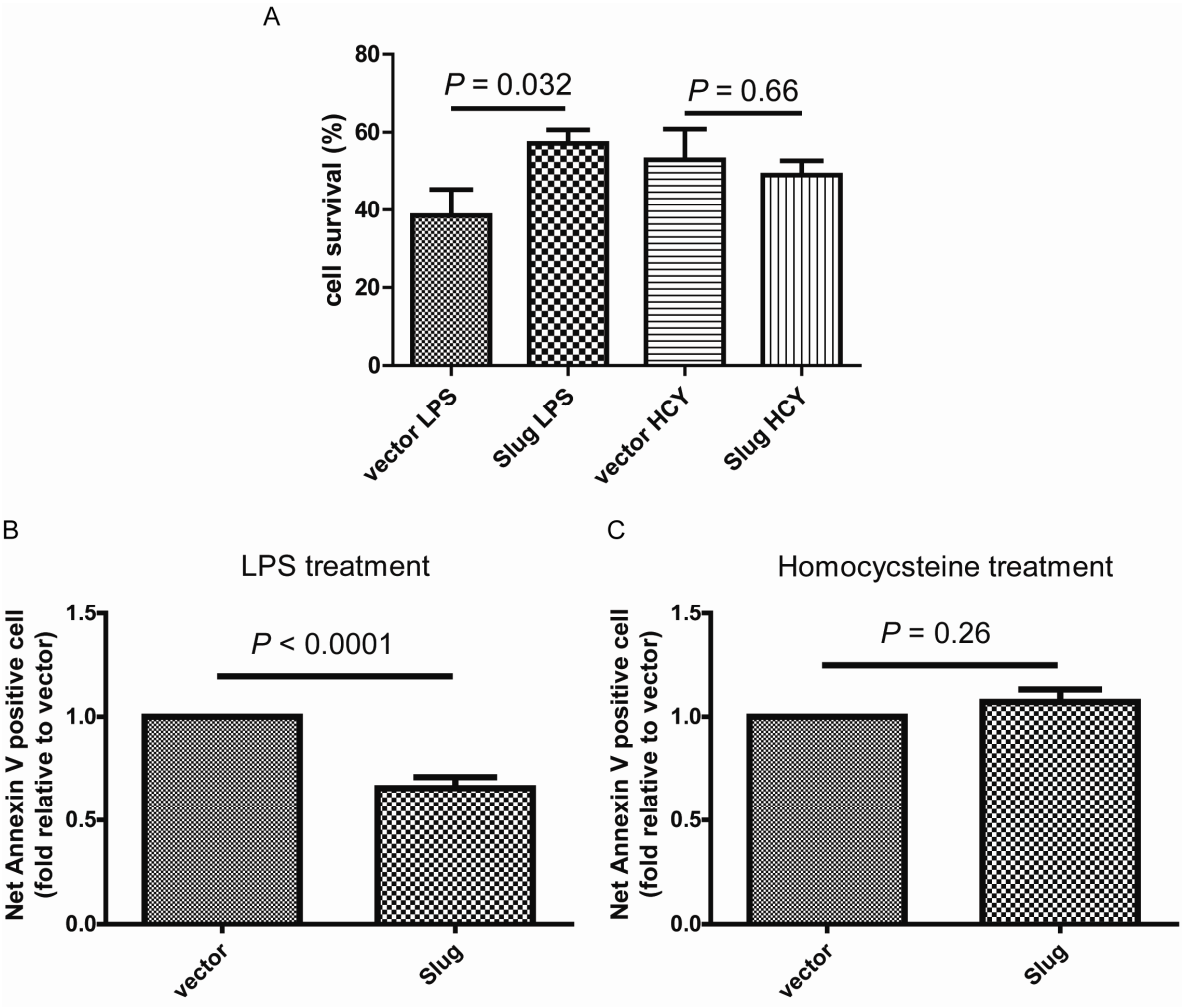

Figure 4.7. Slug protects endothelial cells against LPS-induced apoptosis while exhibiting no effect on homocysteine-induced apoptosis. (A) Endothelial cells transduced with vector control or Slug were treated with 100 μg/mL LPS and 25 μM of ALLN (n = 4) or 7.5 mM homocysteine (n = 4) for 16 hours. Cell survival was determined by neutral red uptake. Slug cells showed higher level of survival when treated with LPS compared to vector control cells. (B and C) The difference observed in cell survival was due to the effect of Slug expression on apoptosis as determined by Annexin V binding. Slug and vector control HMEC were treated with 100 μg/mL LPS and 25 μM of ALLN (n = 4) or 7.5 mM homocysteine (n = 3) for 8 hours. Results shown are mean ± SEM. P-value was determined by Student's t-test.

4.7. Homocysteine induces apoptosis in Notch-activated cells by regulating PI3K and Slug

Since both PI3K activity and Slug expression were important for the survival of Notch-activated cells, we hypothesized that homocysteine may interfere with either PI3K or Slug to induce an apoptotic phenotype in endothelial cells expressing NotchIC. Homocysteine treatment in Notch-activated cells reduced Akt phosphorylation, suggesting a decrease in PI3K activity (Figure 4.8A). Notch-induced Slug expression was also down-regulated by homocysteine treatment (Figure 4.8A). This result suggests that homocysteine stimulation leads to increased cell death in Notch-activated cells by blocking essential anti-apoptotic signals. On the other hand, LPS treatment of NotchIC-expressing HMEC did not change Slug protein expression (Figure 4.8A). These findings suggest that LPS stimulation may be able to enhance the endothelial survival signal through the PI3K-Slug axis in Notch activated cells, leading to increased cell survival compared to control cells. Homocysteine treatment, however, inhibits Notch-induced survival signaling by blocking PI3K activation and Slug expression, thereby amplifying Notch-induced apoptotic signals.

Interestingly, homocysteine treatment also down-regulated Slug protein expression when Slug was expressed from an expression vector using a heterologous promoter (Figure 4.8B). This shows that homocysteine did not decrease Slug expression through transcription regulation or modulation of mRNA stability, since the mammalian expression construct did not include the endogenous Slug promoter or the 5' and 3' UTR region. Homocysteine may regulate Slug protein expression through modification of Slug protein stability thereby inhibiting Slug-induced anti-apoptotic activity.

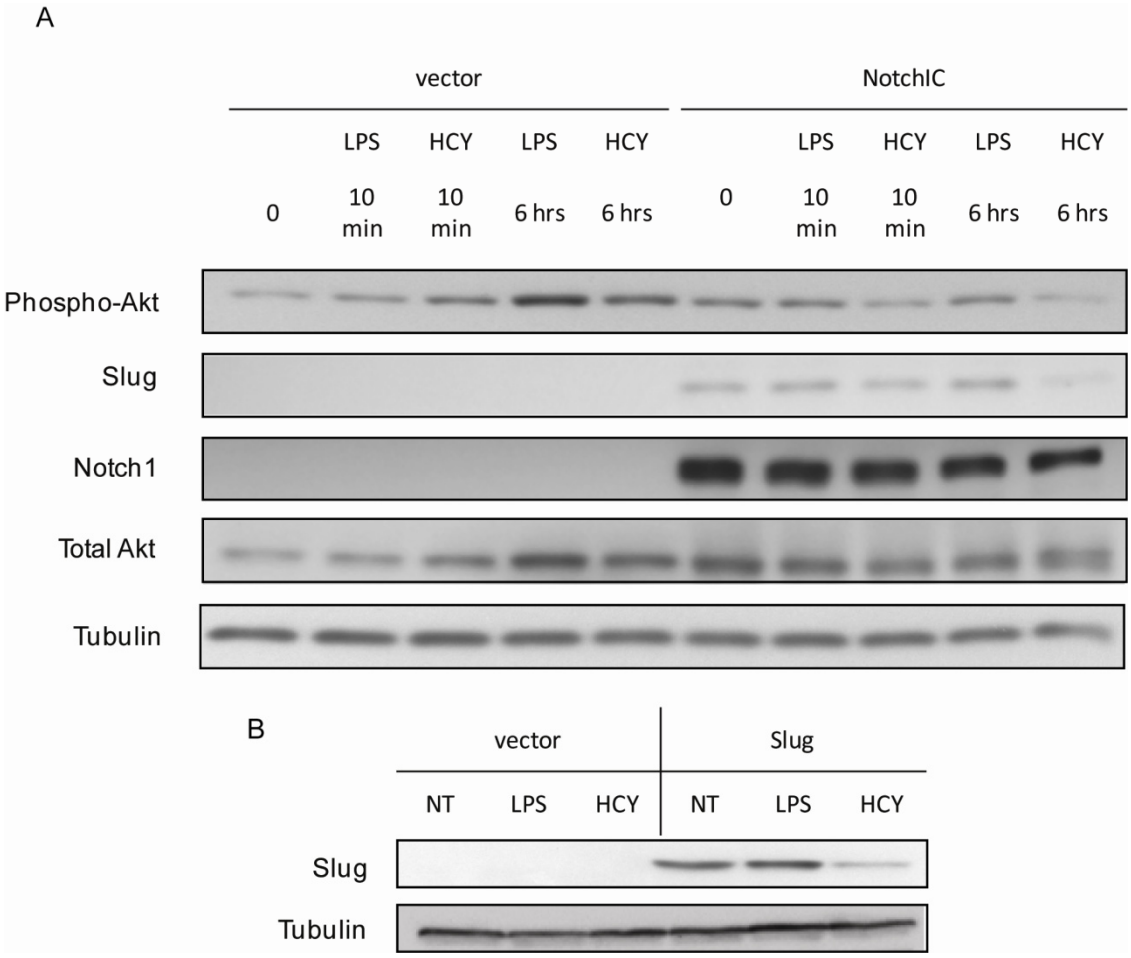

Figure 4.8. Homocysteine blocks Notch-induced PI3K activation and Slug expression. (A) HMEC transduced with NotchIC or empty vector were treated with LPS or homocysteine (HCY) for the indicated time. The level of Akt phosphorylation and Slug expression was detected with immunoblotting. Notch1IC expression was also confirmed with immunoblotting. (B) HMEC transduced with flag-tagged Slug or empty vector were treated with LPS or HCY for 8 hours. The level of Slug expression was detected by immunoblotting.

4.8. Discussion

This study presents a mechanism for the Notch-induced endothelial survival observed upon LPS-stimulation: the Notch-PI3K-Slug signaling axis (Figure 4.9). In this study, treatment of Notch-activated endothelial cells with the apoptotic agents, LPS or homocysteine resulted in a differential effect. The context-dependent effect of Notch depended on the interaction with the PI3K signaling pathway and the expression of Slug (Figure 4.9). *In vivo* studies have also shown a context-dependent effect of Notch signaling in endothelial survival (Nakajima, Yuasa et al. 2003; Limbourg, Takeshita et al. 2005; Dou, Wang et al. 2008; Trindade, Kumar et al. 2008). Whether the differential effect of Notch activation *in vivo* is dependent on the status of PI3K signaling still needs to be examined.

4.8.1. Possible candidates for a Notch-induced pro-apoptotic signal

Our lab has previously shown that Notch activation leads to a decrease of $p21^{CIP1}$ expression in endothelial cells (Noseda, Chang et al. 2004). In addition to the well-studied role as the inhibitor of cyclin-dependent kinases, $p21^{CIP1}$ also acts as an anti-apoptotic factor in endothelial cells under serum-starvation (Bruhl, Heeschen et al. 2004; Mattiussi, Turrini et al. 2004). Although the downstream signals for $p21^{CIP1}$ mediated protective activity are still unknown, Notch may still be inducing endothelial apoptosis through down-regulation of $p21^{CIP1}$.

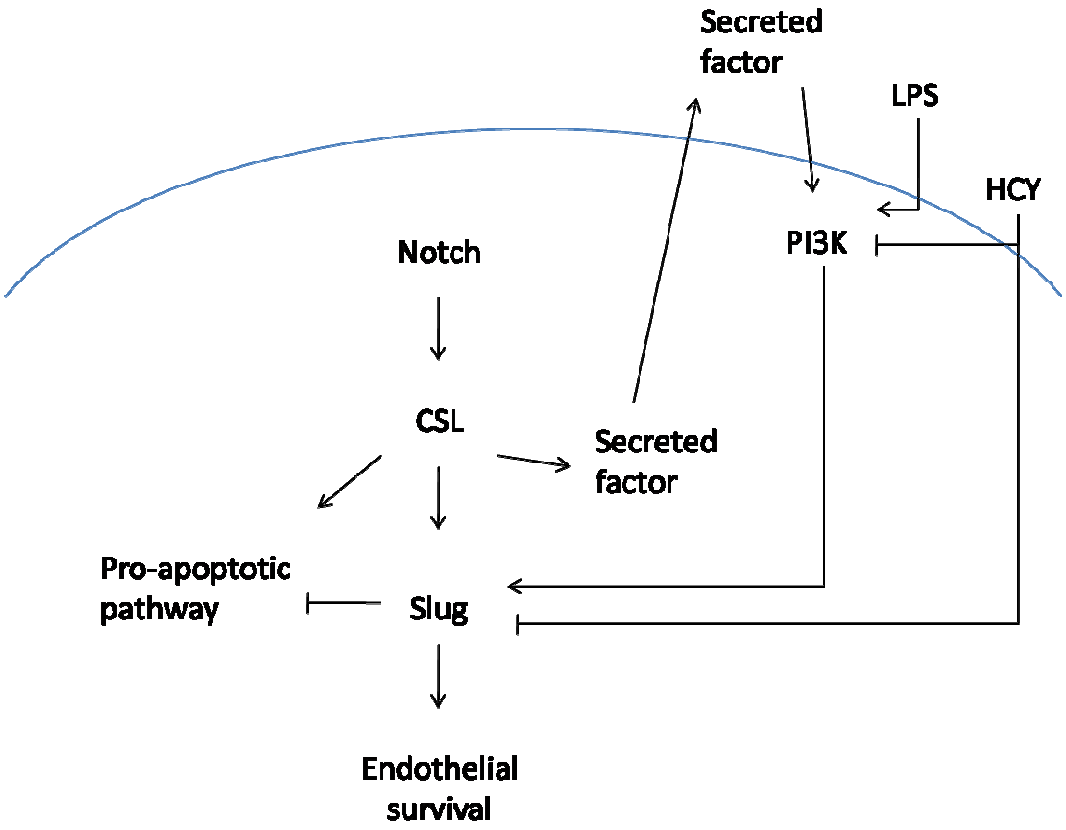

Figure 4.9. Model of Notch-induced survival signaling. Notch activates both pro- and anti-apoptotic signaling pathways. The anti-apoptotic pathway depends on PI3K activity and Slug expression. Notch regulates anti-apoptotic protein Slug by two mechanisms: direct transcription activation via CSL and through activation of PI3K. Notch activates PI3K through a secreted factor yet to be identified. Inhibition of PI3K leads to down-regulation of Slug expression, which in turn tips the balance of death and survival signals towards apoptosis. Notch activation reduces LPS-induced apoptosis through up-regulation of Slug; homocysteine, on the other hand, down-regulates PI3K activation and Slug expression to block Notch-induced survival signals.

Notch signaling in endothelial cells is known to interact with other pathways, most notably the TGF-β signaling pathway. Work from our lab has demonstrated synergistic interaction between Notch and TGF-β signaling through up-regulation of Smad3 (mothers against decapentaplegic homolog 3) (Fu, Chang et al. 2009). TGF-β signal can induce apoptosis in endothelial cells in a context-dependent mechanism (Tsukada, Eguchi et al. 1995; Pollman, Naumovski et al. 1999; Lu, Patel et al. 2009). Therefore, Notch-induced TGF-β signaling activity may drive the pro-apoptotic signaling observed in endothelial cells.

4.8.2. Possible mechanisms of Slug down-regulation by PI3K inhibition

One recent study links PI3K activity to transcriptional regulation of Slug. Saegusa and colleagues showed that activation of Akt leads to increased nuclear β-catenin, which in turn activates transcription of Slug (Saegusa, Hashimura et al. 2009). NF-κB activity has also been shown to induce Slug transcription during frog development (Zhang, Carl et al. 2006). PI3K activity can lead to activation of NF-κB (Sizemore, Leung et al. 1999). However, both of the pathways require Akt activation. There is currently no study that shows the regulation of Slug transcription by a PI3K-dependent Akt-independent pathway.

Our lab and others have shown that Slug is an unstable protein with a half-life of around 2 hours and is subjected to proteasomal degradation (Vernon and LaBonne 2006; Wang, Wang et al. 2009). Although a close family member Snail is phosphorylated by glycogen synthase kinase (GSK)-3β (which is inhibited by PI3K signaling) and targeted for proteosomal degradation through phosphorylation (Zhou, Deng et al. 2004), Slug is not a substrate of GSK-3β (Vernon and LaBonne 2006). Slug is, however, identified as a binding partner for a F-box protein Partner of paired (Ppa) in frog neural crest cells and Ppa can recruit E3 ubiquitin-ligase to Slug, leading to its degradation (Vernon and LaBonne 2006). Interestingly, a human homolog of Ppa, F-box and leucine-rich repeat protein 14 (FBXL14), has recently been shown to induce proteasome degradation of Snail (Vinas-Castells, Beltran

et al. 2010). However, the degradation of Slug by FBXL14 was not examined and there is no established connection between Ppa or FBXL14 and PI3K signaling.

PI3K may also act through p53 to regulate expression of Slug. The tumor-supressor p53 has been shown to regulate Slug expression by two opposing mechanisms. p53 can bind to the Slug promoter and activate Slug transcription (Wu, Heinrichs et al. 2005). However, p53 also negatively regulate Slug protein stability. Mdm2 (mouse double minute 2) is an E3 ubiquitin ligase, a p53 transcriptional target, and a substrate for Akt kinase activity (Ogawara, Kishishita et al. 2002). Mdm2 is phosphorylated by Akt, which enables interaction between Mdm2 and p53. Mdm2 then facilitates the ubiquitination and proteasomal degradation of p53 (Fuchs, Adler et al. 1998). A recent study showed that Slug is also ubiquinated by Mdm2 and degraded by the proteasome (Wang, Wang et al. 2009). Therefore, p53 activity can lead to down-regulation of Slug protein expression by induction of Mdm2, which can also be regulated by PI3K.

A closer examination is required to elucidate the effect of PI3K inhibition and homocysteine treatment on these pathways to determine the mechanism of Slug transcript and protein regulation in endothelial cells.

Chapter 5. SUMMARY, PERSPECTIVES, AND FUTURE DIRECTIONS

5.1. Notch in arteriogenesis

Data presented in Chapter 3 of this thesis suggests the presence of a $Tie1^{+}CD31^{+}VE\text{-}cadherin^{-}$ vascular smooth muscle precursor cell during embryonic vascular development. Using the transgenic mouse system that we generated, we also showed that Notch activation is required for the differentiation into VSMC from this $Tie1^{+}$ precursor cell. While the focus of vascular smooth muscle development research has been on the heterogeneity of the tissue of origin (Gittenberger-de Groot, DeRuiter et al. 1999; Majesky 2007), little is known about the population of immediate precursors that are predisposed for differentiation within every vascular bed. This is the first *in situ* observation of an immediate vascular smooth muscle precursor cell in mammalian vascular development. We have also demonstrated that mature endothelial cells cannot be a source of VSMC in mammalian embryonic vasculature.

Using a dnMAML transgenic mouse model, we showed that the requirement for Notch signaling in the $Tie1^{+}$ vascular precursors depends on the maturity of the vessel. When Notch was blocked at the onset of vascular smooth muscle development, the vascular precursors fail to differentiate, causing a reduction or the complete absence of vascular smooth muscle coverage around the vessel. However, blocking Notch in the precursor population did not affect the growth of the smooth muscle layer around the more mature vessels when the vessel already contained differentiated smooth muscle cells prior to the indction of dnMAML. This suggests that development of the VSMC during embryonic arteriogenesis has at least two phases: one where smooth muscle cells are generated *de novo* from vascular precursor cells, followed by the second phase where the smooth muscle layer grows through the proliferation of existing cells (Varadkar, Kraman et al. 2008). We have shown that Notch is

required for phase one of vascular smooth muscle development, and Varadkar and colleague also showed a possible role of Notch in vascular smooth muscle expansion during embryogenesis (Varadkar, Kraman et al. 2008).

5.1.1. Establishment of a new tool: tetOSdnMAML transgenic mouse

When the work presented in this thesis began, exploration of the role of Notch signaling in the field of mammalian vascular development had also just begun (Iso, Hamamori et al. 2003). The vascular phenotype of Notch1 null mutant mice demonstrated the requirement for Notch signaling in embryonic vascular remodeling and heart development (Swiatek, Lindsell et al. 1994). Similar phenotypes were recapitulated in other Notch pathway mutants (Xue, Gao et al. 1999; Krebs, Xue et al. 2000; Fischer, Schumacher et al. 2004; Gale, Dominguez et al. 2004; Krebs, Shutter et al. 2004). Endothelial-specific inactivation of Notch pathway components, using the Tie2 promoter, which is now known not to be specific to endothelial cells, confirmed the importance of Notch signaling in the vascular cell type during embryogenesis (Krebs, Shutter et al. 2004; Limbourg, Takeshita et al. 2005; High, Lu et al. 2008). However, due to early embryonic lethality of the Notch mutants at mid-gestation, the role of the Notch signaling pathway in the development of VSMC remained to be examined. To bypass the lethality caused by the cardiac development defects, we generated a tetracycline-inducible, tissue-specific transgenic mouse that expresses a pan-Notch signaling inhibitor, dnMAML. Through titration of the tetracycline treatment, Notch signaling can be blocked within one day of tetracycline withdrawal. The level of responsiveness of our transgenic system can only be rivaled by exogenous treatments such as GSI, which cannot be applied in a tissue-specific fashion. In addition, the tetracycline-inducible system provides a reversible system for Notch inhibition. Unlike the inducible Cre-Lox system, where genomic DNA is irreversibly excised (Zhang, Riesterer et al. 1996), temporal regulation of dnMAML

expression can be achieved by the addition or withdrawal of tetracycline from the drinking water. However, further optimization of the system is required for the efficient suppression of dnMAML. Overall, the tetOS-dnMAML transgenic mouse provides an opportunity to study the role of Notch signaling in a specific cell type at a defined time.

5.1.2. Characterization of the VSMC precursor

While the studies described in Chapter 3 of this thesis provide strong evidence for the presence of the $Tie1^+$ $CD31^+$ VE-$cadherin^-$ VSMC precursor cells, a direct demonstration of this population's ability to differentiate into VSMC is still lacking. Alternatively, the Tie1 promoter activity can be marking a subset of mature VSMC within all vascular beds, although the hemorrhagic defects and VSMC differentiation defects observed in the Tie1dnMAMLembryos cannot be explained by the blockade of Notch in a subset of VSMC. To further characterize the $Tie1^+CD31^+$VE-$cadherin^-$ VSMC precursor and dissect the mechanism of VSMC development, the cells will be isolated from mouse embryos and cultured *ex vivo*. In order to separate the precursor cells from contaminating mature endothelial cells and VSMC, single cell clones will be established and we will determine the ability of the clonal cells to differentiate into VSMC. Since the precursors express typical markers of the endothelial cells, the ability of the $Tie1^+CD31^+$VE-$cadherin^-$ precursor cells to differentiate into mature endothelial cells will also be examined. Clonal precursor cells may be examined for their capability to differentiate into other cell types. Once this VSMC precursor cell can be established *ex vivo*, different cytokines and chemical inhibitors can be used to examine the role of different signaling pathways in the differentiation and/or maintenance of vascular smooth muscle precursors.

High and colleagues provided the first evidence for the role of Notch in mammalian vascular smooth muscle development during the course of this study. Using the same

dnMAML construct in a different transgenic system, they showed that blocking Notch in the neural crest cells inhibits smooth muscle differentiation in the pharyngeal arch arteries (High, Zhang et al. 2007). Here, we show the presence of $Tie1^{+}$ cell-derived VSMC in neural crest-derived vessels such as the carotid artery and the aortic arch, as well as in other vascular beds. Therefore, by blocking Notch in all neural crest-derived tissue, Notch activation in the Tie1+ precursor may also be inhibited. We have shown that by blocking Notch in the Tie1+ precursor cell alone, without affecting other neural crest-derived cells, smooth muscle differentiation in the carotid arteries is blocked. It is possible that the smooth muscle phenotype of the neural crest-specific Notch inhibition is a result of blocking Notch in the Tie1+ VSMC precursors within the neural crest-derived population. Although the Tie1tTA:LacZ reporter embryos showed peri-endothelial staining in all arteries examined, and the hemorrhagic defects were observed in multiple vascular beds in the Tie1tTA:dnMAML embryos (suggesting the existence of a common VSMC precursors in different arteries) there is still no direct evidence for the existence of this precursor cell. To demonstrate that the Tie1+ population contains a common VSMC precursor, we will attempt to isolate Tie1+CD31+VE-cadherin- cells from different embryonic arteries. Using microdissection, different arteries undergoing the initiation of arteriogenesis can be isolated from Tie1tTA:tetOSLacZ embryos. If a common Tie1+ VSMC precursor cell exists, then we can isolate single cell colonies capable of differentiating into mature VSMC from different vascular beds. The presence of a common local VSMC precursor will not contradict the previously observed mosaic nature of VSMC. The precursors may still originate from different embryonic tissues, therefore may be regulated by different signaling pathways and require different mechanisms prior to arriving at their final arterial destinations.

5.1.3. Clinical implication of Notch-induced VSMC differentiation

Blocking Notch signaling in the endothelium for two days does not affect smooth muscle development, showing that Notch activation in the endothelium is not necessary for providing any paracrine signals for the differentiation, proliferation or survival of embryonic VSMC. However, expression of the Notch ligand Jagged1 in the endothelium is required for vascular smooth muscle differentiation from neural crest progenitors (High, Lu et al. 2008). Endothelial cells may be driving vascular smooth muscle development through heterotypic signaling by providing the necessary ligands for Notch receptors on the vascular precursor cells. The human disorder, Alagille syndrome, is an autosomal dominant arteriodysplastic syndrome with multiple organ system involvement caused by mutations of the *Jagged1* gene. Patients with Alagille syndrome suffer from increased incidence of intracranial bleeding, which contributes to the mortality of the disorder (Emerick, Rand et al. 1999). One can speculate that the expression of Jagged1 in the endothelium is required for stabilization of the brain vasculature through ensuring mural cell coverage of the vessels. However, the mural cells of the brain have not been closely examined to show whether vascular smooth muscle defects may play a role in the hemorrhaging observed.

Moreover, missense mutations in the *Notch1* gene have been associated with patients with thoracic aortic aneurysms (McKellar, Tester et al. 2007). Thoracic aortic aneurysms have previously been associated with mutations in the TGFβ receptors (Pannu, Fadulu et al. 2005), which are known to regulate VSMC differentiation and phenotypes (Bobik 2006). While the molecular and cellular implication of the *Notch1* mutations are yet to be determined, it is possible that Notch-dependent VSMC differentiation/maturation plays a role in the development of aortic aneurysm. It would be interesting to examine the effect of these Notch1 mutations on VSMC phenotype.

In the adult, VSMC differentiation is involved in intimal thickening observed in atherosclerosis and arterial stenosis, although the origin of the VSMC precursors is still a subject of much debate (van Oostrom, Fledderus et al. 2009; Orlandi and Bennett 2010). Bone-marrow-derived intimal VSMC was observed after arterial injury in murine atherosclerosis model (Sata, Saiura et al. 2002), while a contribution from resident precursors was also demonstrated in neointima formation (Bentzon, Weile et al. 2006; Torsney, Mandal et al. 2007). Whether this resident VSMC precursor is Tie1-positive or shares any properties with the Tie1+ precursor described in this thesis is yet to be determined. Several studies have characterized the expression of components of the Notch signaling pathway following vascular injury. Hedgehog-induced Notch1 expression increases in intimal VSMC after vascular injury (Morrow, Cullen et al. 2009). Expressions of Notch1, Notch3, Jagged1 and Hey1 were also observed in bone marrow-derived cells in the neointima of injured vessels (Doi, Iso et al. 2009). Intimal hyperplasia after vascular injury was significantly reduced in Hey2 knock-out mice, suggesting a functional role of the Notch target gene in neointimal formation (Sakata, Xiang et al. 2004). However, the exact role of Notch activity during injury-induced intimal thickening requires further investigation. The dnMAML mouse model established in this thesis may be used to examine the potential role of the Notch signaling pathway in VSMC differentiation during neointimal formation.

5.1.4. Possible involvement of other cell types in arteriogenesis

One caveat for the experiments using the Tie1tTA animal is the lack of specificity of the promoter. Expression of Tie1 is not restricted to the endothelium and the vascular precursor cells. Using a similar Tie1 promoter, Gustafsson and colleagues show that the Tie1 promoter is also active in around ten percent of hematopoietic cells and in several areas of the adult brain (Gustafsson, Brakebusch et al. 2001). Therefore, the phenotype and lethality observed

in the Tie1tTA:dnMAML embryos may have resulted from Notch inhibition in multiple cell types. Neverthelesss, the spatial and temporal specificities of the hemorrhagic phenotype in Tie1tTA:dnMAML embryos suggests that the effect is local and not caused by systemic defects such as abnormal platelet development. Using the VEtTA transgenic mouse, we show that the hemorrhagic phenotype is not caused by blocking Notch in the endothelium.

In this thesis, we demonstrated a defect in VSMC development when Notch activation is blocked in $Tie1^+$ cells. However, we could not prove that the effect is cell-autonomous. We also have to consider any possible paracrine effects that dysregulated hematopoietic cells (due to blockade of Notch) may have on the vascular phenotypes. Due to limitations of the *in vivo* system used, we cannot isolate the cellular source of the VSMC defect. A more detailed examination on the expression pattern of dnMAML in other cell types is necessary before we can attribute the phenotype to the smooth muscle differentiation defect. Alternatively, VSMC precursor cells expressing dnMAML may be isolated from the Tie1tTA:dnMAML embryos prior to arteriogenesis and the ability of the precursor to differentiate toward VSMC fate can be examined.

5.2. Notch and survival signalling

In Chapter 4 of this thesis, the mechanism of Notch-induced endothelial survival signaling was examined. Surprisingly, we found that Notch activation can have conflicting effects on endothelial apoptosis that are dependent on the apoptotic stimulus. To understand this observation, we further probed the downstream mechanisms of Notch-induced cell survival. Notch activation in endothelial cells leads to the release of a secreted factor, which in turn activates PI3K. In Notch-activated endothelial cells, but not in control cells, PI3K activity is required for cell survival, revealing the presence of parallel apoptotic signals induced by Notch. PI3K activation imparts an endothelial cell survival effect in Notch activated cells by the induction of the anti-apoptotic protein Slug. Combined with previous data from our lab, we have shown that Notch regulates the expression of Slug through two mechanisms: direct transcriptional activation (Niessen, Fu et al. 2008) and additional transcriptional regulation through Notch-induced activation of PI3K.

5.2.1. Mechanisms for Notch-induced PI3K activation

Notch can interact with other signaling pathways through PI3K. For example, Notch activates mTOR through PI3K signaling, and mTOR expression is able to down-regulate p53 protein expression (Mungamuri, Yang et al. 2006), thus providing a link between two major survival/apoptosis pathways. Therefore, by understanding the mechanism of Notch-induced PI3K activation, we can further our knowledge of the regulation of endothelial cell survival by Notch activation, which may be extended to other cell types such as cancer cells.

The activation of PI3K signaling by Notch activation has been observed in various other normal or cancer cell lines (Ciofani and Zuniga-Pflucker 2005; Mungamuri, Yang et al. 2006; Gude, Emmanuel et al. 2008; Wang, Li et al. 2010) and likely involves Notch-induced transcriptional activation (Liu, Xiao et al. 2006). However, a non-canonical Notch signaling

(not through transcriptional activation with CSL/MAML complex) has also been suggested to regulate phosphorylation of Akt through the mTOR-rictor complex (Perumalsamy, Nagala et al. 2009). Recent studies have shown that Notch can activate Akt via the down-regulation of PTEN (Palomero, Sulis et al. 2007; Eliasz, Liang et al. 2010), although in the case of T-cell acute lymphoblastic leukemia (T-ALL), Notch activation imparts oncogenicity through other pathways in addition to PI3K pathway regulation (Medyouf, Gao et al. 2010). Induction of growth factor receptors, which signal through the PI3K pathway, by Notch has also been implicated in the oncogenic activity of Notch (Eliasz, Liang et al. 2010).

In this study, we showed that Notch induces PI3K through a secreted factor. The same mechanism of PI3K activation has been observed in mammary epithelial cells (Meurette, Stylianou et al. 2009). The medium conditioned by mammary epithelial cells expressing NotchIC induced Akt phosphorylation in parental cells, while the conditioned medium from the vector control cells did not activate PI3K (Meurette, Stylianou et al. 2009). The identity of the Notch-induced secreted factor will be investigated. Our lab has performed a microarray analysis on Notch-activated endothelial cells; therefore a candidate gene approach to identify the secreted factor is possible. However, an upregulation of the mRNA may not always translate into an upregulation of protein, thus a global protein analysis on differentiatial level of secreted proteins between NotchIC-transduced or vector control-transduced endothelial cell will be preferable towards identifying the factor.

5.2.3. Homocysteine and Slug expression

Regulation of Slug expression by homocysteine treatment may play a role in embryonic heart development. Maternal hyperhomocysteinemia has been shown to be a risk factor for congenital heart defects in human (Verkleij-Hagoort, Bliek et al. 2007). In animal models, hyperhomocysteinemia can cause cardiac defects in the neural crest-derived outflow tract,

which develops into the pulmonary artery and the aortic arch (Boot, Steegers-Theunissen et al. 2003). Interestingly, Slug expression is found to be important for proper formation of neural crest-derived tissues in frog development (LaBonne and Bronner-Fraser 2000). However, while Slug expression is present during cardiac outflow tract development, Slug is not essential for mammalian cardiac development because of the functional redundancy of a close family member Snail (Niessen, Fu et al. 2008). In the present study, we have shown that homocysteine treatment down-regulates the expression of Slug. It will be interesting to see whether the effect of homocysteine on cardiac development can be explained, at least partially, by the loss of Slug and/or Snail expression.

5.2.4. Alternative methods of Notch activation

One caveat of the study is the strength of Notch activation by the NotchIC construct. NotchIC is considered a strong constitutive activator of the Notch pathway. Expression of NotchIC in endothelial cells not only affects the survival signaling pathway, but also inhibits endothelial proliferation (Noseda, Chang et al. 2004) and induces mesenchymal transdifferentiation (Noseda, McLean et al. 2004). It may become difficult to distinguish between the primary effects of Notch activation and the secondary effects brought on by the Notch-induced changes in the endothelial cells. Two possible alternative methods of Notch activation may offer a weaker, therefore, more physiologically relevant level of Notch activity. Inducible systems of Notch activation are available which will enable a regulated level and timing of the Notch signals. NotchIC has been fused to the ligand binding domain of the estrogen receptor (NotchIC-ER) providing a tamoxifen-induced nuclear translocation of NotchIC and transcription activation of Notch targets (Jeffries and Capobianco 2000). Also, a tetracycline inducible system, similar to the one used in our transgenic mouse, can also be used to induce expression of NotchIC in a more controlled way. Notch signaling can also be activated by co-culturing with ligand-expressing cells. *In vivo*, Jagged1 and Dll4 are the two

main ligands activating the Notch signaling pathway in the vasculature. Our lab has shown that co-culture with Notch ligand-expressing cells can recapitulate the effects of NotchIC on endothelial cells, albeit to a lesser degree (Noseda, Chang et al. 2004; Noseda, McLean et al. 2004). To confirm the observations obtained by NotchIC expression in the endothelial cells, experiments can be conducted with using endothelial cell lines co-cultured with Jagged1- or Dll4-expressing cells.

In conclusion, the studies presented in this thesis have identified a role for Notch signaling in VSMC development and endothelial survival signaling. Importantly, we have identified a common vascular smooth muscle precursor cell and showed that Notch activation is required for its differentiation. Our finding also provides a possible mechanism for the stimulus-dependent activity of Notch-mediated cell survival.

Together with our other studies (see Appendix C), our data shows that Notch activation plays a role in maintaining the quiescent adult endothelial monolayer, by suppressing angiogenic sprouting, inhibiting endothelial proliferation and promoting endothelial survival. However, during development, the Notch signaling pathway appears to be important for cell type specification, partially by promoting mesenchymal differentiation.

BIBLIOGRAPHY

Adams, J. M. (2003). "Ways of dying: multiple pathways to apoptosis." Genes Dev **17**(20): 2481-95.

Adams, R. H., G. A. Wilkinson, et al. (1999). "Roles of ephrinB ligands and EphB receptors in cardiovascular development: demarcation of arterial/venous domains, vascular morphogenesis, and sprouting angiogenesis." Genes Dev **13**(3): 295-306.

Ades, E. W., F. J. Candal, et al. (1992). "HMEC-1: establishment of an immortalized human microvascular endothelial cell line." J Invest Dermatol **99**(6): 683-90.

Alva, J. A. and M. L. Iruela-Arispe (2004). "Notch signaling in vascular morphogenesis." Curr Opin Hematol **11**(4): 278-83.

Alvarez, R. J., S. J. Gips, et al. (1997). "17beta-estradiol inhibits apoptosis of endothelial cells." Biochem Biophys Res Commun **237**(2): 372-81.

Arboleda-Velasquez, J. F., Z. Zhou, et al. (2008). "Linking Notch signaling to ischemic stroke." Proc Natl Acad Sci U S A **105**(12): 4856-61.

Arciniegas, E., M. G. Frid, et al. (2007). "Perspectives on endothelial-to-mesenchymal transition: potential contribution to vascular remodeling in chronic pulmonary hypertension." Am J Physiol Lung Cell Mol Physiol **293**(1): L1-8.

Arciniegas, E., C. Y. Neves, et al. (2005). "Endothelial-mesenchymal transition occurs during embryonic pulmonary artery development." Endothelium **12**(4): 193-200.

Artavanis-Tsakonas, S., M. D. Rand, et al. (1999). "Notch signaling: cell fate control and signal integration in development." Science **284**(5415): 770-6.

Aste-Amezaga, M., N. Zhang, et al. (2010). "Characterization of Notch1 antibodies that inhibit signaling of both normal and mutated Notch1 receptors." PLoS One **5**(2): e9094.

Bannerman, D. D. and S. E. Goldblum (2003). "Mechanisms of bacterial lipopolysaccharide-induced endothelial apoptosis." Am J Physiol Lung Cell Mol Physiol **284**(6): L899-914.

Bannerman, D. D., J. C. Tupper, et al. (2001). "A constitutive cytoprotective pathway protects endothelial cells from lipopolysaccharide-induced apoptosis." J Biol Chem **276**(18): 14924-32.

Baron, M., H. Aslam, et al. (2002). "Multiple levels of Notch signal regulation (review)." Mol Membr Biol **19**(1): 27-38.

Ben-Yair, R. and C. Kalcheim (2008). "Notch and bone morphogenetic protein differentially act on dermomyotome cells to generate endothelium, smooth, and striated muscle." J Cell Biol **180**(3): 607-18.

Benedito, R., C. Roca, et al. (2009). "The notch ligands Dll4 and Jagged1 have opposing effects on angiogenesis." Cell **137**(6): 1124-35.

Bentzon, J. F., C. Weile, et al. (2006). "Smooth muscle cells in atherosclerosis originate from the local vessel wall and not circulating progenitor cells in ApoE knockout mice." Arterioscler Thromb Vasc Biol **26**(12): 2696-702.

Blaumueller, C. M., H. Qi, et al. (1997). "Intracellular cleavage of Notch leads to a heterodimeric receptor on the plasma membrane." Cell **90**(2): 281-91.

Bobik, A. (2006). "Transforming growth factor-betas and vascular disorders." Arterioscler Thromb Vasc Biol **26**(8): 1712-20.

Bombeli, T., B. R. Schwartz, et al. (1999). "Endothelial cells undergoing apoptosis become proadhesive for nonactivated platelets." Blood **93**(11): 3831-8.

Boot, M. J., R. P. Steegers-Theunissen, et al. (2003). "Folic acid and homocysteine affect neural crest and neuroepithelial cell outgrowth and differentiation in vitro." Dev Dyn **227**(2): 301-8.

Bray, S. (1998). "Notch signalling in Drosophila: three ways to use a pathway." Semin Cell Dev Biol **9**(6): 591-7.

Brooks, P. C., A. M. Montgomery, et al. (1994). "Integrin alpha v beta 3 antagonists promote tumor regression by inducing apoptosis of angiogenic blood vessels." Cell **79**(7): 1157-64.
Brou, C., F. Logeat, et al. (2000). "A novel proteolytic cleavage involved in Notch signaling: the role of the disintegrin-metalloprotease TACE." Mol Cell **5**(2): 207-16.
Bruckner, K., L. Perez, et al. (2000). "Glycosyltransferase activity of Fringe modulates Notch-Delta interactions." Nature **406**(6794): 411-5.
Bruhl, T., C. Heeschen, et al. (2004). "p21Cip1 levels differentially regulate turnover of mature endothelial cells, endothelial progenitor cells, and in vivo neovascularization." Circ Res **94**(5): 686-92.
Brunn, G. J., J. Williams, et al. (1996). "Direct inhibition of the signaling functions of the mammalian target of rapamycin by the phosphoinositide 3-kinase inhibitors, wortmannin and LY294002." EMBO J **15**(19): 5256-67.
Buas, M. F., S. Kabak, et al. (2010). "The Notch effector Hey1 associates with myogenic target genes to repress myogenesis." J Biol Chem **285**(2): 1249-58.
Calzavara, E., R. Chiaramonte, et al. (2008). "Reciprocal regulation of Notch and PI3K/Akt signalling in T-ALL cells in vitro." J Cell Biochem **103**(5): 1405-12.
Carmeliet, P. (2000). "Mechanisms of angiogenesis and arteriogenesis." Nat Med **6**(4): 389-95.
Carmeliet, P. (2003). "Angiogenesis in health and disease." Nat Med **9**(6): 653-60.
Carmeliet, P., M. G. Lampugnani, et al. (1999). "Targeted deficiency or cytosolic truncation of the VE-cadherin gene in mice impairs VEGF-mediated endothelial survival and angiogenesis." Cell **98**(2): 147-57.
Chen, V. C., R. Stull, et al. (2008). "Notch signaling respecifies the hemangioblast to a cardiac fate." Nat Biotechnol **26**(10): 1169-78.
Cines, D. B., E. S. Pollak, et al. (1998). "Endothelial cells in physiology and in the pathophysiology of vascular disorders." Blood **91**(10): 3527-61.
Ciofani, M. and J. C. Zuniga-Pflucker (2005). "Notch promotes survival of pre-T cells at the beta-selection checkpoint by regulating cellular metabolism." Nat Immunol **6**(9): 881-8.
Ciruna, B. and J. Rossant (2001). "FGF signaling regulates mesoderm cell fate specification and morphogenetic movement at the primitive streak." Dev Cell **1**(1): 37-49.
Clarke, R., L. Daly, et al. (1991). "Hyperhomocysteinemia: an independent risk factor for vascular disease." N Engl J Med **324**(17): 1149-55.
Coffin, J. D., J. Harrison, et al. (1991). "Angioblast differentiation and morphogenesis of the vascular endothelium in the mouse embryo." Dev Biol **148**(1): 51-62.
Coffin, J. D. and T. J. Poole (1988). "Embryonic vascular development: immunohistochemical identification of the origin and subsequent morphogenesis of the major vessel primordia in quail embryos." Development **102**(4): 735-48.
Colville-Nash, P. R. and D. L. Scott (1992). "Angiogenesis and rheumatoid arthritis: pathogenic and therapeutic implications." Ann Rheum Dis **51**(7): 919-25.
Cordes, R., K. Schuster-Gossler, et al. (2004). "Specification of vertebral identity is coupled to Notch signalling and the segmentation clock." Development **131**(6): 1221-33.
Coultas, L., K. Chawengsaksophak, et al. (2005). "Endothelial cells and VEGF in vascular development." Nature **438**(7070): 937-45.
Cox, C. M. and T. J. Poole (2000). "Angioblast differentiation is influenced by the local environment: FGF-2 induces angioblasts and patterns vessel formation in the quail embryo." Dev Dyn **218**(2): 371-82.
Darland, D. C. and P. A. D'Amore (2001). "TGF beta is required for the formation of capillary-like structures in three-dimensional cocultures of 10T1/2 and endothelial cells." Angiogenesis **4**(1): 11-20.
De Palma, M., C. Murdoch, et al. (2007). "Tie2-expressing monocytes: regulation of tumor angiogenesis and therapeutic implications." Trends Immunol **28**(12): 519-24.

De Strooper, B., W. Annaert, et al. (1999). "A presenilin-1-dependent gamma-secretase-like protease mediates release of Notch intracellular domain." Nature **398**(6727): 518-22.
Deissler, H., G. K. Lang, et al. (2006). "TGFbeta induces transdifferentiation of iBREC to alphaSMA-expressing cells." Int J Mol Med **18**(4): 577-82.
Del Monte, G., J. Grego-Bessa, et al. (2007). "Monitoring Notch1 activity in development: evidence for a feedback regulatory loop." Dev Dyn **236**(9): 2594-614.
DeRuiter, M. C., R. E. Poelmann, et al. (1997). "Embryonic endothelial cells transdifferentiate into mesenchymal cells expressing smooth muscle actins in vivo and in vitro." Circ Res **80**(4): 444-51.
Dettman, R. W., W. Denetclaw, Jr., et al. (1998). "Common epicardial origin of coronary vascular smooth muscle, perivascular fibroblasts, and intermyocardial fibroblasts in the avian heart." Dev Biol **193**(2): 169-81.
Doi, H., T. Iso, et al. (2009). "Notch signaling regulates the differentiation of bone marrow-derived cells into smooth muscle-like cells during arterial lesion formation." Biochem Biophys Res Commun **381**(4): 654-9.
Doi, H., T. Iso, et al. (2005). "HERP1 inhibits myocardin-induced vascular smooth muscle cell differentiation by interfering with SRF binding to CArG box." Arteriosclerosis Thrombosis and Vascular Biology **25**(11): 2328-2334.
Domenga, V., P. Fardoux, et al. (2004). "Notch3 is required for arterial identity and maturation of vascular smooth muscle cells." Genes Dev **18**(22): 2730-5.
Dontu, G., K. W. Jackson, et al. (2004). "Role of Notch signaling in cell-fate determination of human mammary stem/progenitor cells." Breast Cancer Res **6**(6): R605-15.
Dou, G. R., Y. C. Wang, et al. (2008). "RBP-J, the transcription factor downstream of Notch receptors, is essential for the maintenance of vascular homeostasis in adult mice." FASEB J **22**(5): 1606-17.
Dou, S., X. Zeng, et al. (1994). "The recombination signal sequence-binding protein RBP-2N functions as a transcriptional repressor." Mol Cell Biol **14**(5): 3310-9.
Drake, C. J., J. E. Hungerford, et al. (1998). "Morphogenesis of the first blood vessels." Ann N Y Acad Sci **857**: 155-79.
Duarte, A., M. Hirashima, et al. (2004). "Dosage-sensitive requirement for mouse Dll4 in artery development." Genes Dev **18**(20): 2474-8.
Duncan, A. W., F. M. Rattis, et al. (2005). "Integration of Notch and Wnt signaling in hematopoietic stem cell maintenance." Nat Immunol **6**(3): 314-22.
Eliasz, S., S. Liang, et al. (2010). "Notch-1 stimulates survival of lung adenocarcinoma cells during hypoxia by activating the IGF-1R pathway." Oncogene.
Ema, M., P. Faloon, et al. (2003). "Combinatorial effects of Flk1 and Tal1 on vascular and hematopoietic development in the mouse." Genes Dev **17**(3): 380-93.
Emerick, K. M., E. B. Rand, et al. (1999). "Features of Alagille syndrome in 92 patients: frequency and relation to prognosis." Hepatology **29**(3): 822-9.
Emuss, V., D. Lagos, et al. (2009). "KSHV manipulates Notch signaling by DLL4 and JAG1 to alter cell cycle genes in lymphatic endothelia." PLoS Pathog **5**(10): e1000616.
Esner, M., S. M. Meilhac, et al. (2006). "Smooth muscle of the dorsal aorta shares a common clonal origin with skeletal muscle of the myotome." Development **133**(4): 737-49.
Espinosa, L., J. Ingles-Esteve, et al. (2003). "Phosphorylation by glycogen synthase kinase-3 beta down-regulates Notch activity, a link for Notch and Wnt pathways." J Biol Chem **278**(34): 32227-35.
Ferguson, J. E., 3rd, R. W. Kelley, et al. (2005). "Mechanisms of endothelial differentiation in embryonic vasculogenesis." Arterioscler Thromb Vasc Biol **25**(11): 2246-54.

Ferreira, L. S., S. Gerecht, et al. (2007). "Vascular progenitor cells isolated from human embryonic stem cells give rise to endothelial and smooth muscle like cells and form vascular networks in vivo." Circ Res **101**(3): 286-94.
Fischer, A., N. Schumacher, et al. (2004). "The Notch target genes Hey1 and Hey2 are required for embryonic vascular development." Genes Dev **18**(8): 901-11.
Flamme, I., T. Frolich, et al. (1997). "Molecular mechanisms of vasculogenesis and embryonic angiogenesis." J Cell Physiol **173**(2): 206-10.
Folkman, J. (1984). "What is the role of endothelial cells in angiogenesis?" Lab Invest **51**(6): 601-4.
Foubert, P., G. Matrone, et al. (2008). "Coadministration of endothelial and smooth muscle progenitor cells enhances the efficiency of proangiogenic cell-based therapy." Circ Res **103**(7): 751-60.
Fryer, C. J., E. Lamar, et al. (2002). "Mastermind mediates chromatin-specific transcription and turnover of the Notch enhancer complex." Genes Dev **16**(11): 1397-411.
Fryer, C. J., J. B. White, et al. (2004). "Mastermind recruits CycC:CDK8 to phosphorylate the Notch ICD and coordinate activation with turnover." Mol Cell **16**(4): 509-20.
Fu, Y., A. Chang, et al. (2009). "Differential regulation of TGFbeta signaling pathways by notch in human endothelial cells." J Biol Chem.
Fuchs, S. Y., V. Adler, et al. (1998). "Mdm2 association with p53 targets its ubiquitination." Oncogene **17**(19): 2543-7.
Gale, N. W., M. G. Dominguez, et al. (2004). "Haploinsufficiency of delta-like 4 ligand results in embryonic lethality due to major defects in arterial and vascular development." Proc Natl Acad Sci U S A **101**(45): 15949-54.
Gazave, E., P. Lapebie, et al. (2009). "Origin and evolution of the Notch signalling pathway: an overview from eukaryotic genomes." BMC Evol Biol **9**: 249.
Geling, A., H. Steiner, et al. (2002). "A gamma-secretase inhibitor blocks Notch signaling in vivo and causes a severe neurogenic phenotype in zebrafish." EMBO Rep **3**(7): 688-94.
Gerhardt, H., M. Golding, et al. (2003). "VEGF guides angiogenic sprouting utilizing endothelial tip cell filopodia." J Cell Biol **161**(6): 1163-77.
Gerhart, J. (1999). "1998 Warkany lecture: signaling pathways in development." Teratology **60**(4): 226-39.
Gittenberger-de Groot, A. C., M. C. DeRuiter, et al. (1999). "Smooth muscle cell origin and its relation to heterogeneity in development and disease." Arterioscler Thromb Vasc Biol **19**(7): 1589-94.
Gittenberger-de Groot, A. C., M. P. Vrancken Peeters, et al. (1998). "Epicardium-derived cells contribute a novel population to the myocardial wall and the atrioventricular cushions." Circ Res **82**(10): 1043-52.
Goutte, C., M. Tsunozaki, et al. (2002). "APH-1 is a multipass membrane protein essential for the Notch signaling pathway in Caenorhabditis elegans embryos." Proc Natl Acad Sci U S A **99**(2): 775-9.
Gridley, T. (2007). "Notch signaling in vascular development and physiology." Development **134**(15): 2709-18.
Gude, N. A., G. Emmanuel, et al. (2008). "Activation of Notch-mediated protective signaling in the myocardium." Circ Res **102**(9): 1025-35.
Gupta-Rossi, N., E. Six, et al. (2004). "Monoubiquitination and endocytosis direct gamma-secretase cleavage of activated Notch receptor." J Cell Biol **166**(1): 73-83.
Gustafsson, E., C. Brakebusch, et al. (2001). "Tie-1-directed expression of Cre recombinase in endothelial cells of embryoid bodies and transgenic mice." J Cell Sci **114**(Pt 4): 671-6.
Haar, J. L. and G. A. Ackerman (1971). "A phase and electron microscopic study of vasculogenesis and erythropoiesis in the yolk sac of the mouse." Anat Rec **170**(2): 199-223.
Haimovitz-Friedman, A., C. Cordon-Cardo, et al. (1997). "Lipopolysaccharide induces disseminated endothelial apoptosis requiring ceramide generation." J Exp Med **186**(11): 1831-41.

Hanahan, D. and J. Folkman (1996). "Patterns and emerging mechanisms of the angiogenic switch during tumorigenesis." Cell **86**(3): 353-64.
Harrington, L. S., R. C. Sainson, et al. (2008). "Regulation of multiple angiogenic pathways by Dll4 and Notch in human umbilical vein endothelial cells." Microvasc Res **75**(2): 144-54.
Hellstrom, M., L. K. Phng, et al. (2007). "Dll4 signalling through Notch1 regulates formation of tip cells during angiogenesis." Nature **445**(7129): 776-80.
Herzog, Y., C. Kalcheim, et al. (2001). "Differential expression of neuropilin-1 and neuropilin-2 in arteries and veins." Mech Dev **109**(1): 115-9.
High, F. A., M. M. Lu, et al. (2008). "Endothelial expression of the Notch ligand Jagged1 is required for vascular smooth muscle development." Proc Natl Acad Sci U S A **105**(6): 1955-9.
High, F. A., M. Zhang, et al. (2007). "An essential role for Notch in neural crest during cardiovascular development and smooth muscle differentiation." J Clin Invest **117**(2): 353-63.
Hill, K. L., P. Obrtlikova, et al. (2010). "Human embryonic stem cell-derived vascular progenitor cells capable of endothelial and smooth muscle cell function." Exp Hematol **38**(3): 246-257 e1.
Hobson, B. and J. Denekamp (1984). "Endothelial proliferation in tumours and normal tissues: continuous labelling studies." Br J Cancer **49**(4): 405-13.
Hoey, T., W. C. Yen, et al. (2009). "DLL4 blockade inhibits tumor growth and reduces tumor-initiating cell frequency." Cell Stem Cell **5**(2): 168-77.
Hofmann, J. J. and M. Luisa Iruela-Arispe (2007). "Notch expression patterns in the retina: An eye on receptor-ligand distribution during angiogenesis." Gene Expr Patterns **7**(4): 461-70.
Holleran, J. L., M. J. Egorin, et al. (2003). "Use of high-performance liquid chromatography to characterize the rapid decomposition of wortmannin in tissue culture media." Anal Biochem **323**(1): 19-25.
Hossain, G. S., J. V. van Thienen, et al. (2003). "TDAG51 is induced by homocysteine, promotes detachment-mediated programmed cell death, and contributes to the cevelopment of atherosclerosis in hyperhomocysteinemia." J Biol Chem **278**(32): 30317-27.
Hsieh, J. J., S. Zhou, et al. (1999). "CIR, a corepressor linking the DNA binding factor CBF1 to the histone deacetylase complex." Proc Natl Acad Sci U S A **96**(1): 23-8.
Hsu, H. C., H. Ema, et al. (2000). "Hematopoietic stem cells express Tie-2 receptor in the murine fetal liver." Blood **96**(12): 3757-62.
Hu, Y., Y. Ye, et al. (2002). "Nicastrin is required for gamma-secretase cleavage of the Drosophila Notch receptor." Dev Cell **2**(1): 69-78.
Huang, K. T., L. Kuo, et al. (1998). "Lipopolysaccharide activates endothelial nitric oxide synthase through protein tyrosine kinase." Biochem Biophys Res Commun **245**(1): 33-7.
Hungerford, J. E. and C. D. Little (1999). "Developmental biology of the vascular smooth muscle cell: building a multilayered vessel wall." J Vasc Res **36**(1): 2-27.
Hungerford, J. E., G. K. Owens, et al. (1996). "Development of the aortic vessel wall as defined by vascular smooth muscle and extracellular matrix markers." Dev Biol **178**(2): 375-92.
Hurlbut, G. D., M. W. Kankel, et al. (2007). "Crossing paths with Notch in the hyper-network." Curr Opin Cell Biol **19**(2): 166-75.
Inoue, A., M. G. Seidel, et al. (2002). "Slug, a highly conserved zinc finger transcriptional repressor, protects hematopoietic progenitor cells from radiation-induced apoptosis in vivo." Cancer Cell **2**(4): 279-88.
Iso, T., Y. Hamamori, et al. (2003). "Notch signaling in vascular development." Arterioscler Thromb Vasc Biol **23**(4): 543-53.
Iso, T., V. Sartorelli, et al. (2001). "HERP, a new primary target of Notch regulated by ligand binding." Mol Cell Biol **21**(17): 6071-9.
Itoh, M., C. H. Kim, et al. (2003). "Mind bomb is a ubiquitin ligase that is essential for efficient activation of Notch signaling by Delta." Dev Cell **4**(1): 67-82.

Jeffries, S. and A. J. Capobianco (2000). "Neoplastic transformation by Notch requires nuclear localization." Mol Cell Biol **20**(11): 3928-41.
Jeffries, S., D. J. Robbins, et al. (2002). "Characterization of a high-molecular-weight Notch complex in the nucleus of Notch(ic)-transformed RKE cells and in a human T-cell leukemia cell line." Mol Cell Biol **22**(11): 3927-41.
Jiang, X., D. H. Rowitch, et al. (2000). "Fate of the mammalian cardiac neural crest." Development **127**(8): 1607-16.
Jin, S., E. M. Hansson, et al. (2008). "Notch signaling regulates platelet-derived growth factor receptor-beta expression in vascular smooth muscle cells." Circ Res **102**(12): 1483-91.
Joutel, A., F. Andreux, et al. (2000). "The ectodomain of the Notch3 receptor accumulates within the cerebrovasculature of CADASIL patients." J Clin Invest **105**(5): 597-605.
Joutel, A., C. Corpechot, et al. (1996). "Notch3 mutations in CADASIL, a hereditary adult-onset condition causing stroke and dementia." Nature **383**(6602): 707-10.
Joutel, A., C. Corpechot, et al. (1997). "Notch3 mutations in cerebral autosomal dominant arteriopathy with subcortical infarcts and leukoencephalopathy (CADASIL), a mendelian condition causing stroke and vascular dementia." Ann N Y Acad Sci **826**: 213-7.
Kao, H. Y., P. Ordentlich, et al. (1998). "A histone deacetylase corepressor complex regulates the Notch signal transduction pathway." Genes Dev **12**(15): 2269-77.
Karsan, A. (2005). "The role of notch in modeling and maintaining the vasculature." Can J Physiol Pharmacol **83**(1): 14-23.
Karsan, A., E. Yee, et al. (1997). "Fibroblast growth factor-2 inhibits endothelial cell apoptosis by Bcl-2-dependent and independent mechanisms." Am J Pathol **151**(6): 1775-84.
Kattman, S. J., T. L. Huber, et al. (2006). "Multipotent flk-1+ cardiovascular progenitor cells give rise to the cardiomyocyte, endothelial, and vascular smooth muscle lineages." Dev Cell **11**(5): 723-32.
Kaufman, MH (1992). The Atlas of Mouse Development. Oxford, UK: Academic Press. p145,157,177.
Kawasaki, M., K. Kuwano, et al. (2000). "Protection from lethal apoptosis in lipopolysaccharide-induced acute lung injury in mice by a caspase inhibitor." Am J Pathol **157**(2): 597-603.
Kerr, J. F., A. H. Wyllie, et al. (1972). "Apoptosis: a basic biological phenomenon with wide-ranging implications in tissue kinetics." Br J Cancer **26**(4): 239-57.
Kimberly, W. T., M. J. LaVoie, et al. (2003). "Gamma-secretase is a membrane protein complex comprised of presenilin, nicastrin, Aph-1, and Pen-2." Proc Natl Acad Sci U S A **100**(11): 6382-7.
Kirby, M. L., T. F. Gale, et al. (1983). "Neural crest cells contribute to normal aorticopulmonary septation." Science **220**(4601): 1059-61.
Kitao, A., Y. Sato, et al. (2009). "Endothelial to mesenchymal transition via transforming growth factor-beta1/Smad activation is associated with portal venous stenosis in idiopathic portal hypertension." Am J Pathol **175**(2): 616-26.
Koblizek, T. I., C. Weiss, et al. (1998). "Angiopoietin-1 induces sprouting angiogenesis in vitro." Curr Biol **8**(9): 529-32.
Koo, B. K., H. S. Lim, et al. (2005). "Mind bomb 1 is essential for generating functional Notch ligands to activate Notch." Development **132**(15): 3459-70.
Koopman, G., C. P. Reutelingsperger, et al. (1994). "Annexin V for flow cytometric detection of phosphatidylserine expression on B cells undergoing apoptosis." Blood **84**(5): 1415-20.
Kopan, R., J. S. Nye, et al. (1994). "The intracellular domain of mouse Notch: a constitutively activated repressor of myogenesis directed at the basic helix-loop-helix region of MyoD." Development **120**(9): 2385-96.
Krebs, L. T., J. R. Shutter, et al. (2004). "Haploinsufficient lethality and formation of arteriovenous malformations in Notch pathway mutants." Genes Dev **18**(20): 2469-73.

Krebs, L. T., Y. Xue, et al. (2000). "Notch signaling is essential for vascular morphogenesis in mice." Genes Dev **14**(11): 1343-52.
Kuroda, K., S. Tani, et al. (1999). "Delta-induced Notch signaling mediated by RBP-J inhibits MyoD expression and myogenesis." J Biol Chem **274**(11): 7238-44.
Kurooka, H. and T. Honjo (2000). "Functional interaction between the mouse notch1 intracellular region and histone acetyltransferases PCAF and GCN5." J Biol Chem **275**(22): 17211-20.
Kurpinski, K., H. Lam, et al. (2010). "TGF-beta and Notch Signaling Mediate Stem Cell Differentiation into Smooth Muscle Cells." Stem Cells.
Kurrey, N. K., S. P. Jalgaonkar, et al. (2009). "Snail and slug mediate radioresistance and chemoresistance by antagonizing p53-mediated apoptosis and acquiring a stem-like phenotype in ovarian cancer cells." Stem Cells **27**(9): 2059-68.
LaBonne, C. and M. Bronner-Fraser (2000). "Snail-related transcriptional repressors are required in Xenopus for both the induction of the neural crest and its subsequent migration." Dev Biol **221**(1): 195-205.
Lampugnani, M. G., M. Corada, et al. (1995). "The molecular organization of endothelial cell to cell junctions: differential association of plakoglobin, beta-catenin, and alpha-catenin with vascular endothelial cadherin (VE-cadherin)." J Cell Biol **129**(1): 203-17.
Lawson, N. D., N. Scheer, et al. (2001). "Notch signaling is required for arterial-venous differentiation during embryonic vascular development." Development **128**(19): 3675-83.
Le Lievre, C. S. and N. M. Le Douarin (1975). "Mesenchymal derivatives of the neural crest: analysis of chimaeric quail and chick embryos." J Embryol Exp Morphol **34**(1): 125-54.
Lee, C. Y., K. M. Vogeli, et al. (2009). "Notch signaling functions as a cell-fate switch between the endothelial and hematopoietic lineages." Curr Biol **19**(19): 1616-22.
Lee, S., T. T. Chen, et al. (2007). "Autocrine VEGF signaling is required for vascular homeostasis." Cell **130**(4): 691-703.
Lee, S. J., K. M. Kim, et al. (2005). "Nitric oxide inhibition of homocysteine-induced human endothelial cell apoptosis by down-regulation of p53-dependent Noxa expression through the formation of S-nitrosohomocysteine." J Biol Chem **280**(7): 5781-8.
Leong, K. G., X. Hu, et al. (2002). "Activated Notch4 inhibits angiogenesis: role of beta 1-integrin activation." Mol Cell Biol **22**(8): 2830-41.
Leslie, J. D., L. Ariza-McNaughton, et al. (2007). "Endothelial signalling by the Notch ligand Delta-like 4 restricts angiogenesis." Development **134**(5): 839-44.
Li, D. Y., L. K. Sorensen, et al. (1999). "Defective angiogenesis in mice lacking endoglin." Science **284**(5419): 1534-7.
Li, J., F. Chen, et al. (2000). "Neural crest expression of Cre recombinase directed by the proximal Pax3 promoter in transgenic mice." Genesis **26**(2): 162-4.
Limbourg, F. P., K. Takeshita, et al. (2005). "Essential role of endothelial Notch1 in angiogenesis." Circulation **111**(14): 1826-32.
Lin, Q., J. Lu, et al. (1998). "Requirement of the MADS-box transcription factor MEF2C for vascular development." Development **125**(22): 4565-74.
Liu, H., S. Kennard, et al. (2009). "NOTCH3 expression is induced in mural cells through an autoregulatory loop that requires endothelial-expressed JAGGED1." Circ Res **104**(4): 466-75.
Liu, W., S. A. Ahmad, et al. (2000). "Endothelial cell survival and apoptosis in the tumor vasculature." Apoptosis **5**(4): 323-8.
Liu, Z. J., M. Xiao, et al. (2006). "Notch1 signaling promotes primary melanoma progression by activating mitogen-activated protein kinase/phosphatidylinositol 3-kinase-Akt pathways and up-regulating N-cadherin expression." Cancer Res **66**(8): 4182-90.
Liu, Z. J., M. Xiao, et al. (2006). "Inhibition of endothelial cell proliferation by Notch1 signaling is mediated by repressing MAPK and PI3K/Akt pathways and requires MAML1." FASEB J **20**(7): 1009-11.

Lobov, I. B., R. A. Renard, et al. (2007). "Delta-like ligand 4 (Dll4) is induced by VEGF as a negative regulator of angiogenic sprouting." Proc Natl Acad Sci U S A **104**(9): 3219-24.
Logeat, F., C. Bessia, et al. (1998). "The Notch1 receptor is cleaved constitutively by a furin-like convertase." Proc Natl Acad Sci U S A **95**(14): 8108-12.
Lohela, M., H. Helotera, et al. (2008). "Transgenic induction of vascular endothelial growth factor-C is strongly angiogenic in mouse embryos but leads to persistent lymphatic hyperplasia in adult tissues." Am J Pathol **173**(6): 1891-901.
Long, X., E. E. Creemers, et al. (2007). "Myocardin is a bifunctional switch for smooth versus skeletal muscle differentiation." Proc Natl Acad Sci U S A **104**(42): 16570-5.
Lopez-Schier, H. and D. St Johnston (2002). "Drosophila nicastrin is essential for the intramembranous cleavage of notch." Dev Cell **2**(1): 79-89.
Lu, Q., B. Patel, et al. (2009). "Transforming growth factor-beta1 causes pulmonary microvascular endothelial cell apoptosis via ALK5." Am J Physiol Lung Cell Mol Physiol **296**(5): L825-38.
MacKenzie, F., P. Duriez, et al. (2004). "Notch4-induced inhibition of endothelial sprouting requires the ankyrin repeats and involves signaling through RBP-Jkappa." Blood **104**(6): 1760-8.
MacKenzie, F., P. Duriez, et al. (2004). "Notch4 inhibits endothelial apoptosis via RBP-Jkappa-dependent and -independent pathways." J Biol Chem **279**(12): 11657-63.
Maillard, I., L. Tu, et al. (2006). "The requirement for Notch signaling at the beta-selection checkpoint in vivo is absolute and independent of the pre-T cell receptor." J Exp Med **203**(10): 2239-45.
Maillard, I., A. P. Weng, et al. (2004). "Mastermind critically regulates Notch-mediated lymphoid cell fate decisions." Blood **104**(6): 1696-702.
Majesky, M. W. (2007). "Developmental basis of vascular smooth muscle diversity." Arterioscler Thromb Vasc Biol **27**(6): 1248-58.
Marchetti, S., C. Gimond, et al. (2002). "Endothelial cells genetically selected from differentiating mouse embryonic stem cells incorporate at sites of neovascularization in vivo." J Cell Sci **115**(Pt 10): 2075-85.
Mattiussi, S., P. Turrini, et al. (2004). "p21(Waf1/Cip1/Sdi1) mediates shear stress-dependent antiapoptotic function." Cardiovasc Res **61**(4): 693-704.
McCully, K. S. (1996). "Homocysteine and vascular disease." Nat Med **2**(4): 386-9.
McElhinny, A. S., J. L. Li, et al. (2008). "Mastermind-like transcriptional co-activators: emerging roles in regulating cross talk among multiple signaling pathways." Oncogene **27**(38): 5138-47.
McGill, M. A., S. E. Dho, et al. (2009). "Numb regulates post-endocytic trafficking and degradation of Notch1." J Biol Chem **284**(39): 26427-38.
McKellar, S. H., D. J. Tester, et al. (2007). "Novel NOTCH1 mutations in patients with bicuspid aortic valve disease and thoracic aortic aneurysms." J Thorac Cardiovasc Surg **134**(2): 290-6.
Medyouf, H., X. Gao, et al. (2010). "Acute T-cell leukemias remain dependent on Notch signaling despite PTEN and INK4A/ARF loss." Blood **115**(6): 1175-84.
Meurette, O., S. Stylianou, et al. (2009). "Notch activation induces Akt signaling via an autocrine loop to prevent apoptosis in breast epithelial cells." Cancer Res **69**(12): 5015-22.
Mikawa, T. and R. G. Gourdie (1996). "Pericardial mesoderm generates a population of coronary smooth muscle cells migrating into the heart along with ingrowth of the epicardial organ." Dev Biol **174**(2): 221-32.
Milano, J., J. McKay, et al. (2004). "Modulation of notch processing by gamma-secretase inhibitors causes intestinal goblet cell metaplasia and induction of genes known to specify gut secretory lineage differentiation." Toxicol Sci **82**(1): 341-58.
Minasi, M. G., M. Riminucci, et al. (2002). "The meso-angioblast: a multipotent, self-renewing cell that originates from the dorsal aorta and differentiates into most mesodermal tissues." Development **129**(11): 2773-83.
Morel, V., R. Le Borgne, et al. (2003). "Snail is required for Delta endocytosis and Notch-dependent activation of single-minded expression." Dev Genes Evol **213**(2): 65-72.

Morimoto, M., Z. Liu, et al. (2010). "Canonical Notch signaling in the developing lung is required for determination of arterial smooth muscle cells and selection of Clara versus ciliated cell fate." J Cell Sci **123**(Pt 2): 213-24.
Morrow, D., J. P. Cullen, et al. (2009). "Sonic Hedgehog induces Notch target gene expression in vascular smooth muscle cells via VEGF-A." Arterioscler Thromb Vasc Biol **29**(7): 1112-8.
Morrow, D., S. Guha, et al. (2008). "Notch and vascular smooth muscle cell phenotype." Circ Res **103**(12): 1370-82.
Motoike, T., D. W. Markham, et al. (2003). "Evidence for novel fate of Flk1+ progenitor: contribution to muscle lineage." Genesis **35**(3): 153-9.
Mukai, Y., Y. Rikitake, et al. (2006). "Decreased vascular lesion formation in mice with inducible endothelial-specific expression of protein kinase Akt." J Clin Invest **116**(2): 334-43.
Mungamuri, S. K., X. Yang, et al. (2006). "Survival signaling by Notch1: mammalian target of rapamycin (mTOR)-dependent inhibition of p53." Cancer Res **66**(9): 4715-24.
Munshi, N., A. Z. Fernandis, et al. (2002). "Lipopolysaccharide-induced apoptosis of endothelial cells and its inhibition by vascular endothelial growth factor." J Immunol **168**(11): 5860-6.
Nakajima, M., S. Yuasa, et al. (2003). "Abnormal blood vessel development in mice lacking presenilin-1." Mech Dev **120**(6): 657-67.
Niessen, K., Y. Fu, et al. (2008). "Slug is a direct Notch target required for initiation of cardiac cushion cellularization." J Cell Biol **182**(2): 315-25.
Noguera-Troise, I., C. Daly, et al. (2006). "Blockade of Dll4 inhibits tumour growth by promoting non-productive angiogenesis." Nature **444**(7122): 1032-7.
Noseda, M., L. Chang, et al. (2004). "Notch activation induces endothelial cell cycle arrest and participates in contact inhibition: role of p21Cip1 repression." Mol Cell Biol **24**(20): 8813-22.
Noseda, M., Y. Fu, et al. (2006). "Smooth Muscle alpha-actin is a direct target of Notch/CSL." Circ Res **98**(12): 1468-70.
Noseda, M., G. McLean, et al. (2004). "Notch activation results in phenotypic and functional changes consistent with endothelial-to-mesenchymal transformation." Circ Res **94**(7): 910-7.
Noseda, M., K. Niessen, et al. (2005). "Notch-dependent cell cycle arrest is associated with downregulation of minichromosome maintenance proteins." Circ Res **97**(2): 102-4.
Nowak, G., A. Karrar, et al. (2004). "Expression of vascular endothelial growth factor receptor-2 or Tie-2 on peripheral blood cells defines functionally competent cell populations capable of reendothelialization." Circulation **110**(24): 3699-707.
Oberg, C., J. Li, et al. (2001). "The Notch intracellular domain is ubiquitinated and negatively regulated by the mammalian Sel-10 homolog." J Biol Chem **276**(38): 35847-53.
Ogawara, Y., S. Kishishita, et al. (2002). "Akt enhances Mdm2-mediated ubiquitination and degradation of p53." J Biol Chem **277**(24): 21843-50.
Ohata, E., R. Tadokoro, et al. (2009). "Notch signal is sufficient to direct an endothelial conversion from non-endothelial somitic cells conveyed to the aortic region by CXCR4." Dev Biol **335**(1): 33-42.
Okajima, T. and K. D. Irvine (2002). "Regulation of notch signaling by o-linked fucose." Cell **111**(6): 893-904.
Okamura, Y. and Y. Saga (2008). "Pofut1 is required for the proper localization of the Notch receptor during mouse development." Mech Dev **125**(8): 663-73.
Orlandi, A. and M. Bennett (2010). "Progenitor cell-derived smooth muscle cells in vascular disease." Biochem Pharmacol **79**(12): 1706-13.
Oswald, F., B. Tauber, et al. (2001). "p300 acts as a transcriptional coactivator for mammalian Notch-1." Mol Cell Biol **21**(22): 7761-74.
Owens, G. K., M. S. Kumar, et al. (2004). "Molecular regulation of vascular smooth muscle cell differentiation in development and disease." Physiol Rev **84**(3): 767-801.

Palomero, T., M. L. Sulis, et al. (2007). "Mutational loss of PTEN induces resistance to NOTCH1 inhibition in T-cell leukemia." Nat Med **13**(10): 1203-10.
Panin, V. M., V. Papayannopoulos, et al. (1997). "Fringe modulates Notch-ligand interactions." Nature **387**(6636): 908-12.
Pannu, H., V. T. Fadulu, et al. (2005). "Mutations in transforming growth factor-beta receptor type II cause familial thoracic aortic aneurysms and dissections." Circulation **112**(4): 513-20.
Pardali, E. and P. ten Dijke (2009). "Transforming growth factor-beta signaling and tumor angiogenesis." Front Biosci **14**: 4848-61.
Pardanaud, L., D. Luton, et al. (1996). "Two distinct endothelial lineages in ontogeny, one of them related to hemopoiesis." Development **122**(5): 1363-71.
Parks, A. L., K. M. Klueg, et al. (2000). "Ligand endocytosis drives receptor dissociation and activation in the Notch pathway." Development **127**(7): 1373-85.
Parrillo, J. E. (1993). "Pathogenetic mechanisms of septic shock." N Engl J Med **328**(20): 1471-7.
Partanen, J., E. Armstrong, et al. (1992). "A novel endothelial cell surface receptor tyrosine kinase with extracellular epidermal growth factor homology domains." Mol Cell Biol **12**(4): 1698-707.
Patel, N. S., J. L. Li, et al. (2005). "Up-regulation of delta-like 4 ligand in human tumor vasculature and the role of basal expression in endothelial cell function." Cancer Res **65**(19): 8690-7.
Perez-Pomares, J. M., D. Macias, et al. (1998). "The origin of the subepicardial mesenchyme in the avian embryo: an immunohistochemical and quail-chick chimera study." Dev Biol **200**(1): 57-68.
Perumalsamy, L. R., M. Nagala, et al. (2009). "A hierarchical cascade activated by non-canonical Notch signaling and the mTOR-Rictor complex regulates neglect-induced death in mammalian cells." Cell Death Differ **16**(6): 879-89.
Phng, L. K. and H. Gerhardt (2009). "Angiogenesis: a team effort coordinated by notch." Dev Cell **16**(2): 196-208.
Pires-daSilva, A. and R. J. Sommer (2003). "The evolution of signalling pathways in animal development." Nat Rev Genet **4**(1): 39-49.
Pollman, M. J., L. Naumovski, et al. (1999). "Vascular cell apoptosis: cell type-specific modulation by transforming growth factor-beta1 in endothelial cells versus smooth muscle cells." Circulation **99**(15): 2019-26.
Poole, T. J. and J. D. Coffin (1989). "Vasculogenesis and angiogenesis: two distinct morphogenetic mechanisms establish embryonic vascular pattern." J Exp Zool **251**(2): 224-31.
Pouget, C., R. Gautier, et al. (2006). "Somite-derived cells replace ventral aortic hemangioblasts and provide aortic smooth muscle cells of the trunk." Development **133**(6): 1013-22.
Pouget, C., K. Pottin, et al. (2008). "Sclerotomal origin of vascular smooth muscle cells and pericytes in the embryo." Dev Biol **315**(2): 437-47.
Pratt, E. B., J. S. Wentzell, et al. (2010). "The cell giveth and the cell taketh away: An overview of Notch pathway activation by endocytic trafficking of ligands and receptors." Acta Histochem.
Proweller, A., W. S. Pear, et al. (2005). "Notch signaling represses myocardin-induced smooth muscle cell differentiation." J Biol Chem **280**(10): 8994-9004.
Proweller, A., A. C. Wright, et al. (2007). "Notch signaling in vascular smooth muscle cells is required to pattern the cerebral vasculature." Proc Natl Acad Sci U S A **104**(41): 16275-80.
Puri, M. C., J. Partanen, et al. (1999). "Interaction of the TEK and TIE receptor tyrosine kinases during cardiovascular development." Development **126**(20): 4569-80.
Quillard, T., S. Coupel, et al. (2008). "Impaired Notch4 activity elicits endothelial cell activation and apoptosis: implication for transplant arteriosclerosis." Arterioscler Thromb Vasc Biol **28**(12): 2258-65.
Quillard, T., J. Devalliere, et al. (2009). "Notch2 signaling sensitizes endothelial cells to apoptosis by negatively regulating the key protective molecule survivin." PLoS One **4**(12): e8244.

Rand, M. D., L. M. Grimm, et al. (2000). "Calcium depletion dissociates and activates heterodimeric notch receptors." Mol Cell Biol **20**(5): 1825-35.
Rao, S., I. B. Lobov, et al. (2007). "Obligatory participation of macrophages in an angiopoietin 2-mediated cell death switch." Development **134**(24): 4449-58.
Ray, W. J., M. Yao, et al. (1999). "Cell surface presenilin-1 participates in the gamma-secretase-like proteolysis of Notch." J Biol Chem **274**(51): 36801-7.
Raymond, M. A., A. Desormeaux, et al. (2004). "Apoptosis of endothelial cells triggers a caspase-dependent anti-apoptotic paracrine loop active on VSMC." FASEB J **18**(6): 705-7.
Rebay, I., R. J. Fleming, et al. (1991). "Specific EGF repeats of Notch mediate interactions with Delta and Serrate: implications for Notch as a multifunctional receptor." Cell **67**(4): 687-99.
Reiss, Y., J. Droste, et al. (2007). "Angiopoietin-2 impairs revascularization after limb ischemia." Circ Res **101**(1): 88-96.
Reynolds, L. P., S. D. Killilea, et al. (1992). "Angiogenesis in the female reproductive system." FASEB J **6**(3): 886-92.
Ridgway, J., G. Zhang, et al. (2006). "Inhibition of Dll4 signalling inhibits tumour growth by deregulating angiogenesis." Nature **444**(7122): 1083-7.
Robert-Moreno, A., J. Guiu, et al. (2008). "Impaired embryonic haematopoiesis yet normal arterial development in the absence of the Notch ligand Jagged1." EMBO J **27**(13): 1886-95.
Roca, C. and R. H. Adams (2007). "Regulation of vascular morphogenesis by Notch signaling." Genes Dev **21**(20): 2511-24.
Rodewald, H. R. and T. N. Sato (1996). "Tie1, a receptor tyrosine kinase essential for vascular endothelial cell integrity, is not critical for the development of hematopoietic cells." Oncogene **12**(2): 397-404.
Rooke, J., D. Pan, et al. (1996). "KUZ, a conserved metalloprotease-disintegrin protein with two roles in Drosophila neurogenesis." Science **273**(5279): 1227-31.
Ruchoux, M. M. and C. A. Maurage (1997). "CADASIL: Cerebral autosomal dominant arteriopathy with subcortical infarcts and leukoencephalopathy." J Neuropathol Exp Neurol **56**(9): 947-64.
Saegusa, M., M. Hashimura, et al. (2009). "Requirement of the Akt/beta-catenin pathway for uterine carcinosarcoma genesis, modulating E-cadherin expression through the transactivation of slug." Am J Pathol **174**(6): 2107-15.
Sainson, R. C., J. Aoto, et al. (2005). "Cell-autonomous notch signaling regulates endothelial cell branching and proliferation during vascular tubulogenesis." FASEB J **19**(8): 1027-9.
Sakao, S., L. Taraseviciene-Stewart, et al. (2007). "VEGF-R blockade causes endothelial cell apoptosis, expansion of surviving CD34+ precursor cells and transdifferentiation to smooth muscle-like and neuronal-like cells." FASEB J **21**(13): 3640-52.
Sakata, Y., N. Koibuchi, et al. (2006). "The spectrum of cardiovascular anomalies in CHF1/Hey2 deficient mice reveals roles in endocardial cushion, myocardial and vascular maturation." J Mol Cell Cardiol **40**(2): 267-73.
Sakata, Y., F. Xiang, et al. (2004). "Transcription factor CHF1/Hey2 regulates neointimal formation in vivo and vascular smooth muscle proliferation and migration in vitro." Arterioscler Thromb Vasc Biol **24**(11): 2069-74.
Sakoda, H., Y. Gotoh, et al. (2003). "Differing roles of Akt and serum- and glucocorticoid-regulated kinase in glucose metabolism, DNA synthesis, and oncogenic activity." J Biol Chem **278**(28): 25802-7.
Santos, M. A., L. M. Sarmento, et al. (2007). "Notch1 engagement by Delta-like-1 promotes differentiation of B lymphocytes to antibody-secreting cells." Proc Natl Acad Sci U S A **104**(39): 15454-9.
Sarao, R. and D. J. Dumont (1998). "Conditional transgene expression in endothelial cells." Transgenic Res **7**(6): 421-7.

Sarbassov, D. D., S. M. Ali, et al. (2004). "Rictor, a novel binding partner of mTOR, defines a rapamycin-insensitive and raptor-independent pathway that regulates the cytoskeleton." Curr Biol **14**(14): 1296-302.
Sasai, Y., R. Kageyama, et al. (1992). "Two mammalian helix-loop-helix factors structurally related to Drosophila hairy and Enhancer of split." Genes Dev **6**(12B): 2620-34.
Sasamura, T., H. O. Ishikawa, et al. (2007). "The O-fucosyltransferase O-fut1 is an extracellular component that is essential for the constitutive endocytic trafficking of Notch in Drosophila." Development **134**(7): 1347-56.
Sata, M., A. Saiura, et al. (2002). "Hematopoietic stem cells differentiate into vascular cells that participate in the pathogenesis of atherosclerosis." Nat Med **8**(4): 403-9.
Sato, Y., T. Watanabe, et al. (2008). "Notch mediates the segmental specification of angioblasts in somites and their directed migration toward the dorsal aorta in avian embryos." Dev Cell **14**(6): 890-901.
Schroeder, T., F. Meier-Stiegen, et al. (2006). "Activated Notch1 alters differentiation of embryonic stem cells into mesodermal cell lineages at multiple stages of development." Mech Dev **123**(7): 570-9.
Schroeter, E. H., J. A. Kisslinger, et al. (1998). "Notch-1 signalling requires ligand-induced proteolytic release of intracellular domain." Nature **393**(6683): 382-6.
Schwartz, B. R., A. Karsan, et al. (1999). "A novel beta 1 integrin-dependent mechanism of leukocyte adherence to apoptotic cells." J Immunol **162**(8): 4842-8.
Schwartz, S. M. and E. P. Benditt (1977). "Aortic endothelial cell replication. I. Effects of age and hypertension in the rat." Circ Res **41**(2): 248-55.
Shawber, C., D. Nofziger, et al. (1996). "Notch signaling inhibits muscle cell differentiation through a CBF1-independent pathway." Development **122**(12): 3765-73.
Shawber, C. J., I. Das, et al. (2003). "Notch signaling in primary endothelial cells." Ann N Y Acad Sci **995**: 162-70.
Shawber, C. J., Y. Funahashi, et al. (2007). "Notch alters VEGF responsiveness in human and murine endothelial cells by direct regulation of VEGFR-3 expression." J Clin Invest **117**(11): 3369-82.
Shawber, C. J. and J. Kitajewski (2004). "Notch function in the vasculature: insights from zebrafish, mouse and man." Bioessays **26**(3): 225-34.
Shen, H., A. S. McElhinny, et al. (2006). "The Notch coactivator, MAML1, functions as a novel coactivator for MEF2C-mediated transcription and is required for normal myogenesis." Genes Dev **20**(6): 675-88.
Shin, M., H. Nagai, et al. (2009). "Notch mediates Wnt and BMP signals in the early separation of smooth muscle progenitors and blood/endothelial common progenitors." Development **136**(4): 595-603.
Shinbrot, E., K. G. Peters, et al. (1994). "Expression of the platelet-derived growth factor beta receptor during organogenesis and tissue differentiation in the mouse embryo." Dev Dyn **199**(3): 169-75.
Sizemore, N., S. Leung, et al. (1999). "Activation of phosphatidylinositol 3-kinase in response to interleukin-1 leads to phosphorylation and activation of the NF-kappaB p65/RelA subunit." Mol Cell Biol **19**(7): 4798-805.
Sorensen, I., R. H. Adams, et al. (2009). "DLL1-mediated Notch activation regulates endothelial identity in mouse fetal arteries." Blood **113**(22): 5680-8.
Souilhol, C., S. Cormier, et al. (2006). "Nas transgenic mouse line allows visualization of Notch pathway activity in vivo." Genesis **44**(6): 277-86.
Stefanec, T. (2000). "Endothelial apoptosis: could it have a role in the pathogenesis and treatment of disease?" Chest **117**(3): 841-54.
Stifani, S., C. M. Blaumueller, et al. (1992). "Human homologs of a Drosophila Enhancer of split gene product define a novel family of nuclear proteins." Nat Genet **2**(4): 343.

Suchting, S., C. Freitas, et al. (2007). "The Notch ligand Delta-like 4 negatively regulates endothelial tip cell formation and vessel branching." Proc Natl Acad Sci U S A **104**(9): 3225-30.
Suhara, T., K. Fukuo, et al. (2004). "Homocysteine enhances endothelial apoptosis via upregulation of Fas-mediated pathways." Hypertension **43**(6): 1208-13.
Sun, J. F., T. Phung, et al. (2005). "Microvascular patterning is controlled by fine-tuning the Akt signal." Proc Natl Acad Sci U S A **102**(1): 128-33.
Swiatek, P. J., C. E. Lindsell, et al. (1994). "Notch1 is essential for postimplantation development in mice." Genes Dev **8**(6): 707-19.
Takahashi, Y., T. Imanaka, et al. (1996). "Spatial and temporal pattern of smooth muscle cell differentiation during development of the vascular system in the mouse embryo." Anat Embryol (Berl) **194**(5): 515-26.
Takeshita, K., M. Satoh, et al. (2007). "Critical role of endothelial Notch1 signaling in postnatal angiogenesis." Circ Res **100**(1): 70-8.
Tamura, K., Y. Taniguchi, et al. (1995). "Physical interaction between a novel domain of the receptor Notch and the transcription factor RBP-J kappa/Su(H)." Curr Biol **5**(12): 1416-23.
Tang, Y., S. Urs, et al. (2008). "Hairy-related transcription factors inhibit Notch-induced smooth muscle alpha-actin expression by interfering with Notch intracellular domain/CBF-1 complex interaction with the CBF-1-binding site." Circ Res **102**(6): 661-8.
Thornberry, N. A. and Y. Lazebnik (1998). "Caspases: enemies within." Science **281**(5381): 1312-6.
Timmerman, L. A., J. Grego-Bessa, et al. (2004). "Notch promotes epithelial-mesenchymal transition during cardiac development and oncogenic transformation." Genes Dev **18**(1): 99-115.
Torsney, E., K. Mandal, et al. (2007). "Characterisation of progenitor cells in human atherosclerotic vessels." Atherosclerosis **191**(2): 259-64.
Tricot, O., Z. Mallat, et al. (2000). "Relation between endothelial cell apoptosis and blood flow direction in human atherosclerotic plaques." Circulation **101**(21): 2450-3.
Trindade, A., S. R. Kumar, et al. (2008). "Overexpression of delta-like 4 induces arterialization and attenuates vessel formation in developing mouse embryos." Blood **112**(5): 1720-9.
Tsukada, T., K. Eguchi, et al. (1995). "Transforming growth factor beta 1 induces apoptotic cell death in cultured human umbilical vein endothelial cells with down-regulated expression of bcl-2." Biochem Biophys Res Commun **210**(3): 1076-82.
Tu, L., T. C. Fang, et al. (2005). "Notch signaling is an important regulator of type 2 immunity." J Exp Med **202**(8): 1037-42.
Tun, T., Y. Hamaguchi, et al. (1994). "Recognition sequence of a highly conserved DNA binding protein RBP-J kappa." Nucleic Acids Res **22**(6): 965-71.
Tyagi, N., A. V. Ovechkin, et al. (2006). "Mitochondrial mechanism of microvascular endothelial cells apoptosis in hyperhomocysteinemia." J Cell Biochem **98**(5): 1150-62.
Uemura, A., S. Kusuhara, et al. (2006). "Angiogenesis in the mouse retina: a model system for experimental manipulation." Exp Cell Res **312**(5): 676-83.
Uyttendaele, H., J. Ho, et al. (2001). "Vascular patterning defects associated with expression of activated Notch4 in embryonic endothelium." Proc Natl Acad Sci U S A **98**(10): 5643-8.
Vaccari, T., H. Lu, et al. (2008). "Endosomal entry regulates Notch receptor activation in Drosophila melanogaster." J Cell Biol **180**(4): 755-62.
van Oostrom, O., J. O. Fledderus, et al. (2009). "Smooth muscle progenitor cells: friend or foe in vascular disease?" Curr Stem Cell Res Ther **4**(2): 131-40.
Varadkar, P., M. Kraman, et al. (2008). "Notch2 is required for the proliferation of cardiac neural crest-derived smooth muscle cells." Dev Dyn **237**(4): 1144-52.
Venkatesh, D. A., K. S. Park, et al. (2008). "Cardiovascular and hematopoietic defects associated with Notch1 activation in embryonic Tie2-expressing populations." Circ Res **103**(4): 423-31.

Verkleij-Hagoort, A., J. Bliek, et al. (2007). "Hyperhomocysteinemia and MTHFR polymorphisms in association with orofacial clefts and congenital heart defects: a meta-analysis." Am J Med Genet A **143A**(9): 952-60.
Vermes, I., C. Haanen, et al. (1995). "A novel assay for apoptosis. Flow cytometric detection of phosphatidylserine expression on early apoptotic cells using fluorescein labelled Annexin V." J Immunol Methods **184**(1): 39-51.
Vernon, A. E. and C. LaBonne (2006). "Slug stability is dynamically regulated during neural crest development by the F-box protein Ppa." Development **133**(17): 3359-70.
Villa, N., L. Walker, et al. (2001). "Vascular expression of Notch pathway receptors and ligands is restricted to arterial vessels." Mech Dev **108**(1-2): 161-4.
Vinas-Castells, R., M. Beltran, et al. (2010). "The hypoxia-controlled FBXL14 ubiquitin ligase targets SNAIL1 for proteasome degradation." J Biol Chem **285**(6): 3794-805.
Vogeli, K. M., S. W. Jin, et al. (2006). "A common progenitor for haematopoietic and endothelial lineages in the zebrafish gastrula." Nature **443**(7109): 337-9.
Waltzer, L., F. Logeat, et al. (1994). "The human J kappa recombination signal sequence binding protein (RBP-J kappa) targets the Epstein-Barr virus EBNA2 protein to its DNA responsive elements." EMBO J **13**(23): 5633-8.
Wang, H. L., I. O. Akinci, et al. (2007). "The intrinsic apoptotic pathway is required for lipopolysaccharide-induced lung endothelial cell death." J Immunol **179**(3): 1834-41.
Wang, H. U., Z. F. Chen, et al. (1998). "Molecular distinction and angiogenic interaction between embryonic arteries and veins revealed by ephrin-B2 and its receptor Eph-B4." Cell **93**(5): 741-53.
Wang, S. P., W. L. Wang, et al. (2009). "p53 controls cancer cell invasion by inducing the MDM2-mediated degradation of Slug." Nat Cell Biol **11**(6): 694-704.
Wang, W., C. Z. Prince, et al. (2003). "HRT1 modulates vascular smooth muscle cell proliferation and apoptosis." Biochem Biophys Res Commun **308**(3): 596-601.
Wang, Z., Y. Li, et al. (2010). "Down-regulation of Notch-1 and Jagged-1 inhibits prostate cancer cell growth, migration and invasion, and induces apoptosis via inactivation of Akt, mTOR, and NF-kappaB signaling pathways." J Cell Biochem **109**(4): 726-36.
Wasteson, P., B. R. Johansson, et al. (2008). "Developmental origin of smooth muscle cells in the descending aorta in mice." Development **135**(10): 1823-32.
Weinstein, B. M., D. L. Stemple, et al. (1995). "Gridlock, a localized heritable vascular patterning defect in the zebrafish." Nat Med **1**(11): 1143-7.
Weng, A. P., Y. Nam, et al. (2003). "Growth suppression of pre-T acute lymphoblastic leukemia cells by inhibition of notch signaling." Mol Cell Biol **23**(2): 655-64.
Wharton, K. A., K. M. Johansen, et al. (1985). "Nucleotide sequence from the neurogenic locus notch implies a gene product that shares homology with proteins containing EGF-like repeats." Cell **43**(3 Pt 2): 567-81.
Wheatley, S. C., C. M. Isacke, et al. (1993). "Restricted expression of the hyaluronan receptor, CD44, during postimplantation mouse embryogenesis suggests key roles in tissue formation and patterning." Development **119**(2): 295-306.
Wiegreffe, C., B. Christ, et al. (2009). "Remodeling of aortic smooth muscle during avian embryonic development." Dev Dyn **238**(3): 624-31.
Wilson-Rawls, J., J. D. Molkentin, et al. (1999). "Activated notch inhibits myogenic activity of the MADS-Box transcription factor myocyte enhancer factor 2C." Mol Cell Biol **19**(4): 2853-62.
Wilson, K. M. and S. R. Lentz (2005). "Mechanisms of the atherogenic effects of elevated homocysteine in experimental models." Semin Vasc Med **5**(2): 163-71.
Wilting, J. and J. Becker (2006). "Two endothelial cell lines derived from the somite." Anat Embryol (Berl) **211 Suppl 1**: 57-63.

Wolfram, J. A., D. Diaconu, et al. (2009). "Keratinocyte but not endothelial cell-specific overexpression of Tie2 leads to the development of psoriasis." Am J Pathol **174**(4): 1443-58.
Wong, F., C. Hull, et al. (2004). "Lipopolysaccharide initiates a TRAF6-mediated endothelial survival signal." Blood **103**(12): 4520-6.
Wong, G. T., D. Manfra, et al. (2004). "Chronic treatment with the gamma-secretase inhibitor LY-411,575 inhibits beta-amyloid peptide production and alters lymphopoiesis and intestinal cell differentiation." J Biol Chem **279**(13): 12876-82.
Wu, G., S. Lyapina, et al. (2001). "SEL-10 is an inhibitor of notch signaling that targets notch for ubiquitin-mediated protein degradation." Mol Cell Biol **21**(21): 7403-15.
Wu, L., T. Sun, et al. (2002). "Identification of a family of mastermind-like transcriptional coactivators for mammalian notch receptors." Mol Cell Biol **22**(21): 7688-700.
Wu, W. S., S. Heinrichs, et al. (2005). "Slug antagonizes p53-mediated apoptosis of hematopoietic progenitors by repressing puma." Cell **123**(4): 641-53.
Xue, Y., X. Gao, et al. (1999). "Embryonic lethality and vascular defects in mice lacking the Notch ligand Jagged1." Hum Mol Genet **8**(5): 723-30.
Yamashita, J., H. Itoh, et al. (2000). "Flk1-positive cells derived from embryonic stem cells serve as vascular progenitors." Nature **408**(6808): 92-6.
Yang, L., M. H. Soonpaa, et al. (2008). "Human cardiovascular progenitor cells develop from a KDR+ embryonic-stem-cell-derived population." Nature **453**(7194): 524-8.
Yoshida, T. and G. K. Owens (2005). "Molecular determinants of vascular smooth muscle cell diversity." Circ Res **96**(3): 280-91.
You, L. R., F. J. Lin, et al. (2005). "Suppression of Notch signalling by the COUP-TFII transcription factor regulates vein identity." Nature **435**(7038): 98-104.
Zen, K., A. Karsan, et al. (1998). "Lipopolysaccharide-induced NF-kappaB activation in human endothelial cells involves degradation of IkappaBalpha but not IkappaBbeta." Exp Cell Res **243**(2): 425-33.
Zengin, E., F. Chalajour, et al. (2006). "Vascular wall resident progenitor cells: a source for postnatal vasculogenesis." Development **133**(8): 1543-51.
Zhang, C., Y. Cai, et al. (2001). "Homocysteine induces programmed cell death in human vascular endothelial cells through activation of the unfolded protein response." J Biol Chem **276**(38): 35867-74.
Zhang, C., T. F. Carl, et al. (2006). "An NF-kappaB and slug regulatory loop active in early vertebrate mesoderm." PLoS One **1**: e106.
Zhang, Y., C. Riesterer, et al. (1996). "Inducible site-directed recombination in mouse embryonic stem cells." Nucleic Acids Res **24**(4): 543-8.
Zhong, T. P., M. Rosenberg, et al. (2000). "gridlock, an HLH gene required for assembly of the aorta in zebrafish." Science **287**(5459): 1820-4.
Zhou, B. P., J. Deng, et al. (2004). "Dual regulation of Snail by GSK-3beta-mediated phosphorylation in control of epithelial-mesenchymal transition." Nat Cell Biol **6**(10): 931-40.

APPENDICES

Appendix A. Ethics approvals

The following are the animal care certificates, human ethical approvals and biohazard approvals required during the work shown in this thesis.

THE UNIVERSITY OF BRITISH COLUMBIA

ANIMAL CARE CERTIFICATE

Application Number: A06-0137

Investigator or Course Director: Aly Karsan

Department: Pathology & Laboratory Medicine

Animals:

Mice Tie1-tTA x TetOS:nlsLacZ 40

Start Date: **July 1, 2006** **Approval Date:** **June 23, 2009**

Funding Sources:

Funding Agency: Heart and Stroke Foundation of British Columbia and Yukon
Funding Title: Molecular mechanisms of endothelial survival/apoptosis

Unfunded title: N/A

The Animal Care Committee has examined and approved the use of animals for the above experimental project.

This certificate is valid for one year from the above start or approval date (whichever is later) provided there is no change in the experimental procedures. Annual review is required by the CCAC and some granting agencies.

A copy of this certificate must be displayed in your animal facility.

Office of Research Services and Administration
102, 6190 Agronomy Road, Vancouver, BC V6T 1Z3
Phone: 604-827-5111 Fax: 604-822-5093

THE UNIVERSITY OF BRITISH COLUMBIA

ANIMAL CARE CERTIFICATE

Application Number: A07-0717

Investigator or Course Director: Aly Karsan

Department: Pathology & Laboratory Medicine

Animals:

Mice Rosa 101
Mice C57Bl/6J 253
Mice VE-tTA 266
Mice Top-NotchIC 248
Mice ScL-CRE-ERT 303
Mice eNOS-/- 65
Mice Tie1-tTA 266
Mice Notch1tm2Rko/GridJ 101
Mice VE-CRE 10
Mice SM22-rtTA 200
Mice TekCRE 10
Mice TetOS-dnMAML-GFP 266
Mice Rosa-YFP 121
Mice TetOS-LacZ 218

Start Date: **December 14, 2007** **Approval Date:** **March 26, 2009**

Funding Sources:

Funding Agency: Canadian Institutes of Health Research (CIHR)
Funding Title: Endothelial to mesenchymal transformation

Funding Agency: Heart and Stroke Foundation of British Columbia and Yukon
Funding Title: Dissecting gene regulatory networks in cardiac cushion development

Funding Agency: Canadian Institutes of Health Research (CIHR)
Funding Title: Endothelial to mesenchymal transformation

Funding Agency: Genome British Columbia
Funding Title: Dissecting gene regulatory networks in mammalian organogenesis

Funding Agency:	Genome Canada
Funding Title:	Dissecting gene regulatory networks in mammalian organogenesis
Unfunded title:	N/A

The Animal Care Committee has examined and approved the use of animals for the above experimental project.

This certificate is valid for one year from the above start or approval date (whichever is later) provided there is no change in the experimental procedures. Annual review is required by the CCAC and some granting agencies.

A copy of this certificate must be displayed in your animal facility.

Office of Research Services and Administration
102, 6190 Agronomy Road, Vancouver, BC V6T 1Z3
Phone: 604-827-5111 Fax: 604-822-5093

UBC-Providence Health Care Research Institute
Office of Research Services
11th Floor Hornby Site - SPH
c/o 1081 Burrard St.
Vancouver, BC V6Z 1Y6
Tel: (604) 806-8567
Fax: (604) 806-8568

ETHICS CERTIFICATE OF EXPEDITED APPROVAL: ANNUAL RENEWAL

PRINCIPAL INVESTIGATOR:	DEPARTMENT:	UBC-PHC REB NUMBER:
Aly Karsan	PHCRI	H03-50104

INSTITUTION(S) WHERE RESEARCH WILL BE CARRIED OUT:

Institution	Site
BC Cancer Agency	Vancouver BCCA
Children's and Women's Health Centre of BC (incl. Sunny Hill)	Women's Health Research Institute
Providence Health Care	St. Paul's Hospital

Other locations where the research will be conducted:
N/A

CO-INVESTIGATOR(S):
N/A

SPONSORING AGENCIES:
Heart and Stroke Foundation of Canada - "Molecular Mechanims of Endothelial Survival/Apoptosis"

PROJECT TITLE:
Molecular Mechanims of Endothelial Survival/Apoptosis

EXPIRY DATE OF THIS APPROVAL: March 26, 2011

APPROVAL DATE: March 26, 2010

CERTIFICATION:

1. The membership of the UBC-PHC REB complies with the membership requirements for research ethics boards defined in Part C Division 5 of the Food and Drug Regulations of Canada.
2. The UBC-PHC REB carries out its functions in a manner fully consistent with Good Clinical Practices.
3. The UBC-PHC REB has reviewed and approved the research project named on this Certificate of Approval including any associated consent form and taken the action noted above. This research project is to be conducted by the principal investigator named above at the specified research site(s). This review of the UBC-PHC REB have been documented in writing.

The UBC-PHC Research Ethics Board Chair or Associate Chair, has reviewed the documentation for the above named project. The research study, as presented in the documentation, was found to be acceptable on ethical grounds for research involving human subjects and was approved for renewal.

Approval of the UBC-PHC Research Ethics Board or Associate Chair, verified by the signature of one of the following:

Dr. Kuo-Hsing Kuo,
Chair

Dr. J. Kernahan,
Associate Chair

Dr. I. Fedoroff,
Associate Chair

The University of British Columbia

Biohazard Approval Certificate

PROTOCOL NUMBER: **B06-0065**

INVESTIGATOR OR COURSE DIRECTOR: Aly Karsan

DEPARTMENT: **Pathology & Laboratory Medicine**

PROJECT OR COURSE TITLE: **Molecular Mechanisms of Endothelial Survival/Apoptosis**

APPROVAL DATE: **September 2, 2009** START DATE: **June 29, 2006**

APPROVED CONTAINMENT LEVEL: **2**

UNFUNDED TITLE: **N/A**

The Principal Investigator/Course Director is responsible for ensuring that all research or course work involving biological hazards is conducted in accordance with the University of British Columbia Policies and Procedures, Biosafety Practices and Public Health Agency of Canada guidelines.

This certificate is valid for one year from the above start or approval date (whichever is later) provided there are no changes. Annual review is required.

A copy of this certificate must be displayed in your facility.

Office of Research Services
102, 6190 Agronomy Road, Vancouver, V6T 1Z3
Phone: 604-827-5111 FAX: 604-822-5093

The University of British Columbia

Biohazard Approval Certificate

PROTOCOL NUMBER: **B06-0124**

INVESTIGATOR OR COURSE DIRECTOR: Aly Karsan

DEPARTMENT: **Pathology & Laboratory Medicine**

PROJECT OR COURSE TITLE: **Endothelial-to-mesenchymal transformation**

APPROVAL DATE: **September 2, 2009** START DATE: **June 29, 2006**

APPROVED CONTAINMENT LEVEL: **2**

UNFUNDED TITLE: **N/A**

The Principal Investigator/Course Director is responsible for ensuring that all research or course work involving biological hazards is conducted in accordance with the University of British Columbia Policies and Procedures, Biosafety Practices and Public Health Agency of Canada guidelines.

This certificate is valid for one year from the above start or approval date (whichever is later) provided there are no changes. Annual review is required.

A copy of this certificate must be displayed in your facility.

Office of Research Services
102, 6190 Agronomy Road, Vancouver, V6T 1Z3
Phone: 604-827-5111 FAX: 604-822-5093

Appendix B. List of publications

The following is a list of publications achieved during my graduate school career. Publications listed here are results of collaborative work with other members of the lab examining the role of Notch in endothelial-mesenchymal transdifferentiation and endothelial cell cycle regulation. Each publication is summarized here and my contribution to the publication is also listed.

Noseda M*, McLean G*, Niessen K, **Chang L**, Pollet I, Montpetit R, Shahidi R, Dorovini-Zis K, Li L, Beckstead B, Durand RE, Hoodless PA, Karsan A. (2004) Notch activation results in phenotypic and functional changes consistent with endothelial-to-mesenchymal transformation. *Circ Res*. 94, 910-917

- This peer-reviewed article is among the first to demonstrate *in vitro* Notch-induced endothelial-to-mesenchymal transdifferentiation, a process examined *in vivo* in Chapter 3 of this thesis
- I was involved in generating the endothelial cell lines used in this study and in the generation of the following data:
  - Figure 2. Notch activation induces mesenchymal transdifferentiation of endothelial cells from different vascular beds.
  - Figure 5B. Jagged1 induces EMT.
  - Supplemental Figure 1. Notch activation induced EMT in endothelial cells from different vascular beds

Noseda M, **Chang L**, McLean G, Grim JE, Clurman BE, Smith LL, Karsan A. (2004) Notch Activation Induces Endothelial Cell Cycle Arrest and Participates in Contact Inhibition: Role of $p21^{Cip1}$ Repression. *Mol Cell Biol*. 24, 8813-8822

- This peer-reviewed article shows a role of Notch in endothelial contact-inhibition.
- I was involved in generating the endothelial cell lines used in this study and in the generation of the following data:
  - Figure 5A. Tamoxifen-induced nuclear translocation of the Notch4IC-ER fusion protein.
  - Figure 6B. Notch inhibits serum-induced cdk4-kinase activity.
  - Figure 7A. Expression of p21 rescues the reduction of cdk4 nuclear localization.
  - Figure 8C. Notch inhibition reduces endothelial contact inhibition of proliferation.

Fu Y, Chang A, **Chang L**, Niessen K, Eapen S, Setiadi A, Karsan A. (2009) Differential regulation of transforming growth factor beta signaling pathways by Notch in human endothelial cells. *J Biol Chem.* 284(29):19452-62.

- This peer-reviewed article demonstrated a mechanism for direct interaction between the Notch and TGF-β signaling pathways in endothelial cells, which are both implicated in endothelial-to-mesenchymal transdifferentiation.
- I was involved in generating the following data:
  Figure 4. Inhibition of Notch reduces Smad3 expression in the developing heart.

Niessen K, Fu Y, **Chang L**, Hoodless PA, McFadden D, Karsan A. (2008) Slug is a direct Notch target required for initiation of cardiac cushion cellularization. *J Cell Biol*. 182(2):315-25.

- This peer-reviewed article demonstrates that Slug is a direct target for Notch and the role of Slug in endothelial-to-mesenchymal transdifferentiation during heart development. Chapter 4 of this thesis discussed an additional function for Notch-induced Slug expression.
- I was involved in the unpublished data using the transgenic system I generated as described in this thesis.

Noseda M, Fu Y, Niessen K, Wong F, **Chang L**, McLean G, Karsan A. (2006) Smooth Muscle alpha-actin is a direct target of Notch/CSL. *Circ Res*. 98(12), 1468-1470

- This peer-reviewed article shows that SMA is a direct target of Notch/CSL transcription regulation.
- I was involved in generating the endothelial, fibroblast, and vascular smooth muscle cell lines used in this study and in the generation of the following data:
  Supplemental Figure 1. Notch induces transcript level of SMA

MacKenzie F, Duriez P, Larrivee B, **Chang L**, Pollet I, Wong F, Yip C, Karsan A. (2004) Notch4-induced inhibition of endothelial sprouting requires the ankyrin repeats and involves signaling through RBP-Jkappa. *Blood* 104, 1760-1768

- This peer-reviewed article shows Notch-induced inhibition of angiogenesis is CSL-dependent and is partially through regulation of endothelial migration.
- I was involved in generating a Notch mutant construct used in this study.

Noseda M, Niessen K, McLean G, **Chang L**, Karsan A. (2005) Notch-dependent cell cycle arrest is associated with downregulation of minichromosome maintenance proteins. *Circ Res.* 97(2), 102-104.

- This peer-reviewed article demonstrated another mechanism for Notch-induced endothelial growth inhibition.
- I was involved in generating the endothelial, fibroblast, and vascular smooth muscle cell lines used in this study.

Appendix C. Previously published material

The following is a compilation of the peer-reviewed publications listed in Appendix B:

Notch Activation Results in Phenotypic and Functional Changes Consistent With Endothelial-to-Mesenchymal Transformation

Michela Noseda, Graeme McLean, Kyle Niessen, Linda Chang, Ingrid Pollet, Rachel Montpetit, Réza Shahidi, Katerina Dorovini-Zis, Linheng Li, Benjamin Beckstead, Ralph E. Durand, Pamela A. Hoodless and Aly Karsan

Circ. Res. 2004;94;910-917; originally published online Feb 26, 2004;
DOI: 10.1161/01.RES.0000124300.76171.C9
Circulation Research is published by the American Heart Association. 7272 Greenville Avenue, Dallas, TX 72514
 Print ISSN: 0009-7330. Online ISSN: 1524-4571

Notch Activation Results in Phenotypic and Functional Changes Consistent With Endothelial-to-Mesenchymal Transformation

Michela Noseda,* Graeme McLean,* Kyle Niessen, Linda Chang, Ingrid Pollet, Rachel Montpetit, Réza Shahidi, Katerina Dorovini-Zis, Linheng Li, Benjamin Beckstead, Ralph E. Durand, Pamela A. Hoodless, Aly Karsan

Abstract—Various studies have identified a critical role for Notch signaling in cardiovascular development. In this and other systems, Notch receptors and ligands are expressed in regions that undergo epithelial-to-mesenchymal transformation. However, there is no direct evidence that Notch activation can induce mesenchymal transdifferentiation. In this study we show that Notch activation in endothelial cells results in morphological, phenotypic, and functional changes consistent with mesenchymal transformation. These changes include downregulation of endothelial markers (vascular endothelial [VE]-cadherin, Tie1, Tie2, platelet-endothelial cell adhesion molecule-1, and endothelial NO synthase), upregulation of mesenchymal markers (α-smooth muscle actin, fibronectin, and platelet-derived growth factor receptors), and migration toward platelet-derived growth factor-BB. Notch-induced endothelial-to-mesenchymal transformation does not seem to require external regulation and is restricted to cells expressing activated Notch. Jagged1 stimulation of endothelial cells induces a similar mesenchymal transformation, and Jagged1, Notch1, and Notch4 are expressed in the ventricular outflow tract during stages of endocardial cushion formation. This is the first evidence that Jagged1-Notch interactions induce endothelial-to-mesenchymal transformation, and our findings suggest that Notch signaling may be required for proper endocardial cushion differentiation and/or vascular smooth muscle cell development. **(*Circ Res*. 2004;94:910-917.)**

Key Words: endothelial-to-mesenchymal transformation ■ Notch ■ Jagged1 ■ endocardial cushion

The Notch signaling pathway plays a critical role during development. Four mammalian Notch receptors (Notch1 through 4) and 5 Notch ligands (Delta-like [Dll]-1, Dll3, Dll4, Jagged1, and Jagged2) have been identified. Notch receptor-ligand interaction results in a series of proteolytic cleavages of the Notch receptor, producing a C-terminal intracellular fragment (NotchIC) that translocates to the nucleus. In the nucleus, NotchIC binds to the transcriptional repressor CBF1/RBP-Jκ, thereby derepressing or coactivating the expression of various lineage-specific genes.[1]

Perturbation of the Notch pathway has been implicated in the pathogenesis of various cardiovascular diseases in humans.[2] Of interest, patients with Jagged1 mutations (Alagille syndrome) display congenital cardiovascular anomalies that seem to be secondary to faulty endocardial cushion formation.[3–6] In the mouse, Notch1-deficient embryos demonstrate severe vascular developmental defects, which are exacerbated in Notch1/Notch4 double-mutant embryos.[7] Constitutive activation of Notch4 also causes defects in vascular remodeling.[8,9] Mice that are rendered null for Jagged1 die from hemorrhage early during embryogenesis, whereas mice that are doubly heterozygous for a Jagged1-null allele and a Notch2 hypomorphic allele exhibit cardiac anomalies similar to those seen in Alagille syndrome.[10,11] Genes that lie downstream of Notch activation, such as the basic helix-loop-helix factor, HRT2/HEY2, have also been implicated in cardiovascular development.[12,13]

Notch receptors and their ligands have been localized to the vasculature.[14] Notch receptors have also been observed in the endocardium, and the Notch ligand Jagged1 is present on endocardial and periendocardial cells of the cardiac cushions.[15,16] The endocardial cushion is a specialized embryonic

Original received November 3, 2003; revision received February 6, 2004; accepted February 16, 2004.

From the Department of Pathology and Laboratory Medicine (M.N., I.P., A.K.) and Experimental Medicine Program (G.M., K.N., L.C., A.K.), University of British Columbia; Department of Medical Biophysics (M.N., G.M., K.N., L.C., I.P., R.E.D., A.K.), Terry Fox Research Laboratories (R.M., P.A.H.), and Department of Pathology and Laboratory Medicine (A.K.), British Columbia Cancer Agency; and Department of Pathology (R.S., K.D.-Z.), Division of Neuropathology, University of British Columbia and Vancouver Hospital and Health Sciences Centre, Vancouver, British Columbia, Canada; Stem Cell Research Laboratory (L.L.), Stowers Institute for Medical Research, Kansas City, Mo; and Department of Bioengineering (B.B.), University of Washington, Seattle, Wash.

*Both authors contributed equally to this study.

Correspondence to Aly Karsan, Department of Pathology and Laboratory Medicine and Experimental Medicine Program, University of British Columbia, Vancouver, BC V6T 2B5, Canada. E-mail akarsan@bccrc.ca

Circulation Research **is available at http://www.circresaha.org** **DOI: 10.1161/01.RES.0000124300.76171.C9**

tissue that gives rise to the cardiac valves and membranous septa. A critical event in cardiac cushion formation is a differentiation process referred to as endothelial-to-mesenchymal transformation (EMT), which is a specific form of epithelial-to-mesenchymal transformation.[17,18] In the cardiovascular system of the adult, mesenchymal cells derived from the transformation of a subset of cardiac valve endothelial cells may also be necessary for maintenance of the leaflet architecture.[19] Furthermore, EMT may play a role in the development of neointimal lesions in transplant atherosclerosis and restenosis.[20]

Intercellular signaling between Notch receptors and ligands is critical for cell fate determination by influencing cell proliferation, differentiation, and apoptosis.[21] Notch members and their ligands are expressed in various regions that undergo EMT in order for development to proceed appropriately.[22,23] Our studies demonstrate that Notch activation in endothelial cells promotes mesenchymal transformation and suggest that Jagged1-Notch interactions may participate in endocardial cushion formation by inducing EMT.

Materials and Methods

Cell Culture and Reagents

The HMEC-1 microvascular endothelial cell line, hereafter referred to as HMEC, was provided by the Centers for Disease Control and Prevention (Atlanta, Ga) and cultured as previously described.[9] Human umbilical vein endothelial cells (HUVECs) were isolated and cultured as previously described.[24] Human aortic endothelial cells (HAECs) were purchased and cultured in supplemented endothelial growth media (Clonetics). Ovine endocardial cells (OECs) were isolated from sheep cardiac ventricles by treatment with collagenase (45 minutes at 37°C). DiI-acetylated LDL uptake and expression of endothelial markers (vascular endothelial [VE]-cadherin and platelet-endothelial cell adhesion molecule [PECAM-1]) were confirmed. OECs were maintained in Waymouth's media (Gibco) with 10% FBS and antibiotics.

Gene Transfer

Endothelial cells were transduced using the retroviral vector MSCV-IRES-YFP (MIY) (gift from R.K. Humphries, British Columbia Cancer Agency, Vancouver, BC). cDNA constructs encoding the C-terminal HA-tagged Notch4 intracellular domain, Notch1 intracellular domain (gift of S. Artavanis-Tsakonas, Harvard Medical School, Charlestown, Mass), and full-length Jagged1 were cloned into MIY. Endothelial cells were transduced as previously described.[25]

Transmission Electron Microscopy

Endothelial cultures were processed as previously described.[26] Briefly, cultures were washed with M199, fixed in 2.5% glutaraldehyde/2% paraformaldehyde in 0.2 mol/L sodium cacodylate buffer for 1 hour, post-fixed in 1% OsO_4 for 1 hour, stained en bloc with uranyl magnesium acetate, dehydrated, and embedded in Epon-Araldite. Blocks cut from the embedded cultures were reembedded for cross-sectioning. Thin sections were stained with uranyl acetate and lead citrate and viewed on a Zeiss EM 10 microscope.

Immunoblotting

Cells were lysed, and 50 μg of total protein was analyzed by SDS-PAGE. The monoclonal antibody against the HA epitope was purchased from BAbCo, and anti–VE-cadherin, anti–PECAM-1, anti-Tie1, and anti-Tie2 antibodies were all from Santa Cruz Biotechnology. Anti-endothelial NO synthase (eNOS/NOS type III) and anti-fibronectin antibodies were purchased from Transduction Laboratories, and anti–α-smooth muscle actin (SMA) antibody was obtained from Cymbus Biotechnology (Hampshire, UK). Anti-phospho-Smad2 and anti-total-Smad2 antibodies (gift from N. Khalil, University of British Columbia, Vancouver, BC) were manufactured by UBI.

Migration Assay

The ability of endothelial cells to migrate toward platelet-derived growth factor (PDGF)-BB (20 ng/mL) was measured by a modified Boyden chamber assay as previously described.[9]

Immunocytochemistry

Cells were fixed in 4% paraformaldehyde and blocked/permeablized in 4% FCS/0.2% Triton X-100/PBS. Secondary antibodies were Alexa 594-conjugated. To quantitate the proportion of SMA-positive cells, at least five high-power fields (comprising at least 200 cells) were evaluated, and the proportion of SMA-positive cells expressed were as a percentage of the total number of DAPI-stained nuclei in each field.

Flow Cytometry

Cells were trypsinized, washed in PBS, and fixed in 4% paraformaldehyde. Cells were blocked/permeabilized, stained with anti-SMA antibody, and analyzed on an EPICS ELITE-ESP flow cytometer (Beckman Coulter).

Luciferase Assays

Endothelial cells were transfected by electroporation (1.5×10^6 cells) with 1 to 5 μg of plasmid DNA as previously described.[27] Forty-eight hours after transfection, dual-luciferase reporter assays were performed according to manufacturer's recommendations (Promega Corporation). The CBF1-dependent reporter, 4xCBF1wt-LUC, was a gift from S.D. Hayward (Johns Hopkins School of Medicine, Baltimore, Md).[28] The SMA promoter-reporter construct encompassing a 5.4-kb region comprising -2555 to $+2813$ of the rat SMA gene was a gift from F. Dandre and G.K. Owens (University of Virginia, Charlottesville, Va). Transfections were normalized by transfecting cells with 50 ng of the *Renilla* luciferase plasmid pRL-CMV (Promega).

In Situ Hybridization

The murine Jagged1 probe was a gift from S.E. Egan (Hospital for Sick Children, Toronto, Ontario), and the Notch1 and Notch4 probes were a gift from J. Rossant (Samuel Lunenfeld Research Institute, Toronto, Ontario). For whole-mount in situ hybridization, embryonic hearts were fixed overnight at 4°C in 4% paraformaldehyde in PBS, dehydrated in methanol, and stored at -20°C. For hybridizations, embryonic hearts were processed as described.[29]

Reverse Transcriptase–Polymerase Chain Reaction

Total RNA was isolated using TRIzol Reagent (Invitrogen), DNase-treated, and reverse-transcribed to cDNA, followed by polymerase chain reaction (PCR) (see the online data supplement for primers and annealing conditions, available at http://circres.ahajournals.org). A control reaction, omitting reverse transcriptase (RT), was performed for each RNA sample to verify the absence of genomic DNA.

Results

Activated Notch Induces Endothelial-to-Mesenchymal Transformation

During the course of a previous study, we noted that HMECs expressing Notch4IC (HMEC-Notch4IC) lost the characteristic cobblestone morphology of confluent endothelial cells.[9] As seen in Figure 1A, HMEC-Notch4IC formed multilayered cultures suggesting loss of endothelial phenotype and potential transformation to mesenchymal cells. Transmission electron microscopy confirmed that HMEC-Notch4IC failed to form monolayers and proper cell-to-cell junctions and

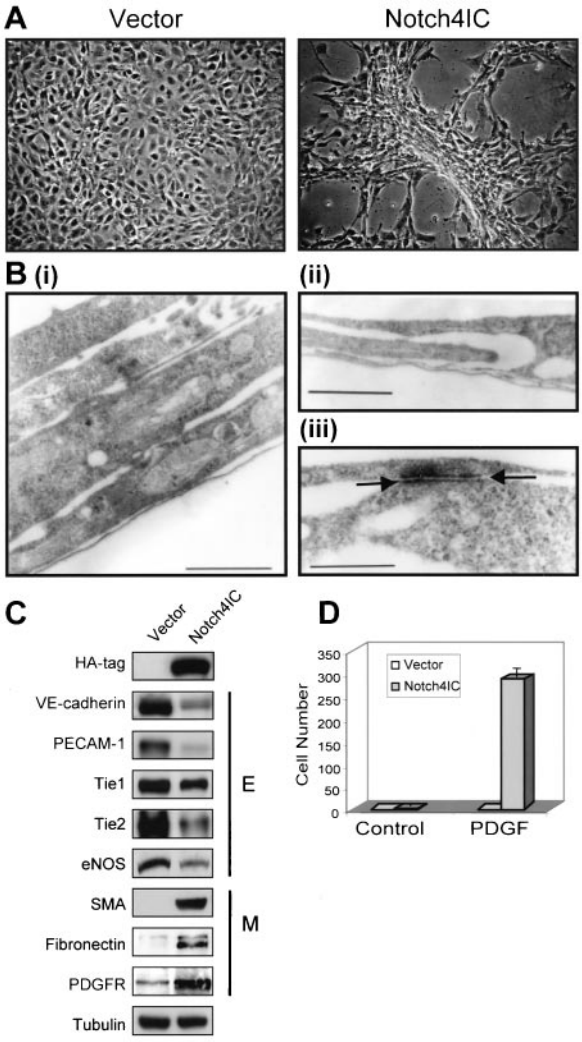

Figure 1. Activated Notch4 induces EMT. A, Phase-contrast micrographs of HMECs transduced with either the empty vector or Notch4IC. B, Transmission electron micrographs of cultures in A. HMEC-Notch4IC are arrayed in overlapping cell layers (i, magnification ×51 000, bar=1 μm) with no evidence of intercellular junctions between adjacent cells (ii, magnification ×18 000, bar=2 μm). HMEC-vector (iii, magnification ×61 000, bar=0.75 μm) cells are focally apposed and form junctional complexes (arrows). C, Immunoblots probed for endothelial (E) and mesenchymal (M) markers on cell lysates harvested from HMEC-vector or HMEC-Notch4IC. D, Migration of HMECs transduced with either the empty vector or Notch4IC toward medium (control) or 20 ng/mL PDGF-BB was measured using a modified Boyden chamber assay. Results are mean±SD of 3 independent experiments.

showed marked overlapping with infrequent, rudimentary cell contacts (Figures 1B, panel i, and 1B, panel ii). In contrast, HMEC-vector cells retained their capacity to form junctions (Figure 1B, panel iii).

VE-cadherin is a cell adhesion molecule that is localized to the interendothelial region and is required for the formation of adherens junctions.[30] Immunoblotting for VE-cadherin demonstrated significant downregulation of this critical junctional molecule, suggesting mesenchymal transformation (Figure 1C). Furthermore, we noted a reduction in expression, to varying degrees, of several other endothelial-specific proteins (PECAM-1, Tie1, Tie2, and endothelial NOS) (Figure 1C). In addition to the loss of endothelial phenotype, EMT implies the acquisition of mesenchymal markers.[19,31–35] To determine whether Notch4-activated cells upregulate mesenchymal proteins, we examined expression of SMA, fibronectin, and PDGF receptors in HMEC-Notch4IC. Immunoblotting shows induction of all three proteins in HMEC-Notch4IC (Figure 1C).

PDGF is a known chemotactic factor for mesenchymal cells, and in particular, PDGF-BB plays a role in recruitment of mesenchymal cells during vascular development.[35,36] Hence, we examined the chemotactic response of HMEC-Notch4IC or HMEC-vector to PDGF-BB. HMEC-Notch4IC was able to migrate toward PDGF-BB in a modified Boyden chamber assay, whereas vector-transduced cells did not (Figure 1D). Thus, Notch4 activation in endothelial cells induces morphological, phenotypic, and functional changes observed during EMT.

Several studies have shown that aortic endothelium can differentiate into mesenchymal-like cells in vitro.[31,37] More recent work has demonstrated that HUVECs also retain the potential to differentiate into mesenchymal cells.[19,38] In addition to Notch4, Notch1 is also expressed in endothelial cells.[14] Hence, we transduced HMECs, HAECs, and HUVECs with Notch4IC, Notch1IC, or empty vector. Our data demonstrated that activated Notch1, as well as Notch4, had the potential to induce EMT in endothelial cells from different vascular beds, as determined by morphological, immunophenotypic, and functional criteria (online Figure 1 and data not shown). Because of the critical requirement for EMT during cardiac cushion formation, we determined whether activated Notch was also able to induce EMT in cardiac endothelial cells. OECs were transduced with the empty vector, Notch4IC, or Notch1IC. OECs also underwent a morphological transformation, as witnessed by loss of uniform cell shape, loss of intercellular contacts, cellular polarization, formation of filopodia (Figure 2A), and the induction of SMA (Figure 2B). Downregulation of endocardial proteins such as PECAM-1 was also confirmed (data not shown).

To determine the efficiency of Notch-induced EMT in different endothelial types, we quantitated SMA-positive cells by immunofluorescent staining 10 to 14 days after transduction. HAECs and OECs demonstrated the greatest capacity to undergo Notch-induced EMT (Figure 2C). Interestingly, in all endothelial types, Notch1 showed greater efficacy in inducing EMT. Taken together, these results indicate that activated Notch is able to induce mesenchymal transformation in endothelial cells from various vascular beds and suggest that different Notch members may play similar functional roles in EMT.

Notch-Induced EMT Is Restricted to Cells Expressing Activated Notch

Activated Notch may induce EMT in conjunction with activation of other signaling molecules. In this regard, transforming growth factor-β (TGF-β) has been suggested to play an important role in EMT in the endocardial cushion, as well as in ovine and human valvular and bovine aortic endothelial

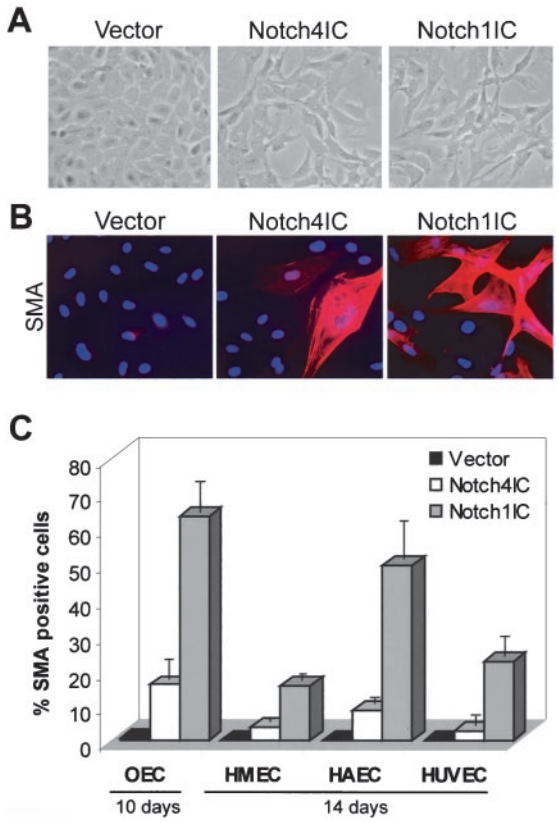

Figure 2. Activated Notch4 and Notch1 induce transdifferentiation of endothelial cells from various vascular beds. OECs were transduced with the empty vector, Notch4IC, or Notch1IC and analyzed by phase-contrast microscopy (A) or immunofluorescence for SMA expression (B) 10 days after transduction. C, Endothelial cells from various sources were transduced with empty vector, Notch4IC, or Notch1IC. At 10 days (OECs) or 14 days (HMECs, HAECs, or HUVECs) after transduction, the proportion of SMA-positive cells was assayed and expressed as a percentage of the total cell number (mean±SD). Results are representative of 3 independent experiments.

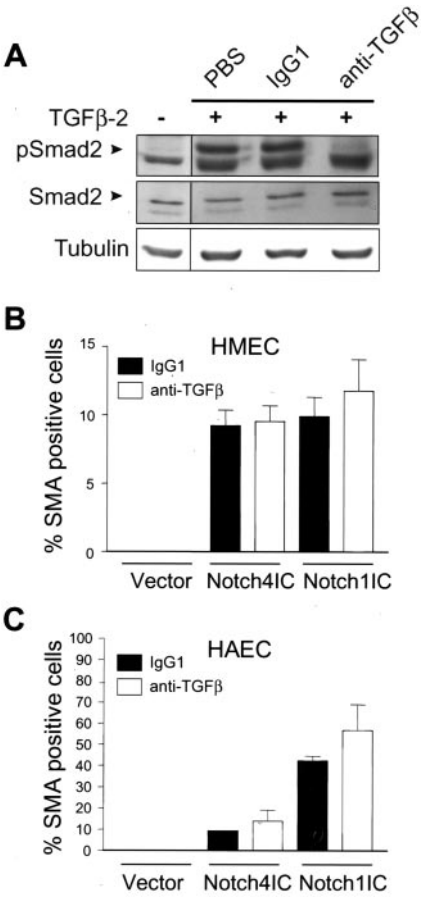

Figure 3. TGF-β is not required for Notch-induced EMT. HMECs and HAECs were treated with either 10 μg/mL control IgG1 or a pan–anti-TGF-β neutralizing antibody during transduction with the empty vector, Notch4IC, or Notch1IC. Subsequently, medium was changed daily with the addition of fresh IgG1 (10 μg/mL) or pan-anti–TGF-β antibody (10 μg/mL). Total cell lysates were probed with an anti–phospho-Smad2 antibody and tubulin (A). HMECs (B) and HAECs (C) were analyzed by immunofluorescence for the expression of SMA-positive cells (mean±SD), enumerated 14 days after transduction, as described in Materials and Methods. Results are representative of 2 independent experiments.

cells.[19,31,39] Primary human endothelial cells transduced with Notch4IC or Notch1IC showed variable levels of TGF-β expression with no consistent increase induced by Notch activation, although HMEC-Notch4IC did show increased TGF-β_2 secretion (data not shown). To determine whether TGF-β stimulation was sufficient to induce EMT, we treated HMECs and HAECs with recombinant TGF-β_1 or TGF-β_2 (5 ng/mL) for up to 28 days. Consistent with studies performed on human vascular endothelial cells, treatment of HMECs and HAECs with exogenous TGF-β_1 or TGF-β_2 did not induce morphological changes of EMT or expression of SMA (data not shown).[19] Furthermore, inhibition of TGF-β activity with a pan-anti–TGF-β–neutralizing antibody did not inhibit or reduce the Notch4IC- or Notch1IC-induced morphological changes or SMA expression in either HMECs or HAECs despite the ability of this antibody to inhibit phosphorylation of Smad2 (Figure 3).

To determine whether NotchIC-transduced endothelial cells secrete other soluble factors that are capable of inducing phenotypic changes, we added 3-day conditioned medium from HMEC-vector and HMEC-Notch4IC to parental HMECs or primary HAECs. We did not observe morphological changes or SMA expression in HMECs or HAECs treated daily with conditioned medium from Notch4IC-transduced HMECs over a 28-day period (data not shown). The above findings suggest that Notch-induced mesenchymal transformation does not depend on paracrine factors and is likely restricted to cells expressing activated Notch.

To confirm that Notch-induced mesenchymal transformation occurs only in cells expressing activated Notch, HMECs were infected with a retroviral vector (MIY) that contains yellow fluorescence protein (YFP) linked to the transgene through an internal ribosomal entry site. Only the YFP-positive (Notch4IC-expressing) cells expressed SMA, as determined by flow cytometry (Figure 4A). This finding was confirmed by high-purity cell sorting of YFP-positive and YFP-negative subpopulations of both Notch4IC- and vector-transduced cells. Immunoblotting of the sorted populations showed downregulation of endothelial-specific proteins and

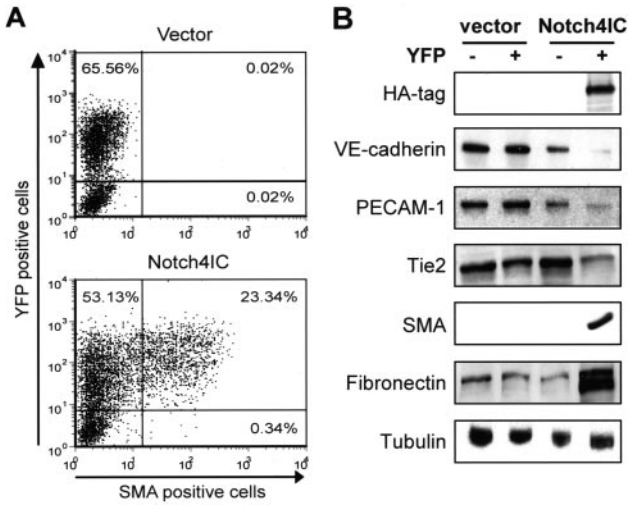

Figure 4. Notch-induced mesenchymal transformation is cell autonomous. A, HMECs were transduced with the empty vector or Notch4IC and analyzed by flow cytometry for YFP and SMA expression after 21 days. Results are representative of 3 independent experiments. B, HMECs were transduced with the empty vector or Notch4IC and sorted into YFP-positive and YFP-negative populations. The sorted cells were then analyzed by immunoblotting for the expression of endothelial and mesenchymal markers. Results are representative of 2 experiments.

upregulation of mesenchymal markers only in YFP-positive HMEC-Notch4IC (Figure 4B). Studies using Notch1IC-expressing HUVECs similarly demonstrated that only YFP-positive (Notch1IC-expressing) HUVECs expressed SMA (online Figure 2). Thus, only endothelial cells that express activated Notch undergo EMT, and external factors do not seem to be required for this process in vitro. However, additional studies assessing the role of TGF-β family members will be required to understand the interaction of this pathway with Notch signaling during EMT.

Jagged1 Induces EMT

The Notch ligand, Jagged1, is expressed on endothelial and smooth muscle cells during development and in the adult.[14] Jagged1 mutations are associated with congenital cardiac anomalies that may be secondary to defective endocardial cushion development.[3–6] To determine whether Jagged1-Notch interactions can induce EMT, we expressed wild-type Jagged1 in HMECs (HMEC-Jagged1). HMEC-Jagged1 or HMEC-vector were cocultured with parental HMECs, and expression of endothelial markers was analyzed by immunoblotting. In cocultures with HMEC-Jagged1, VE-cadherin, PECAM-1 and Tie2 were downregulated and fibronectin was upregulated (Figure 5A). We verified that Jagged1-Notch interactions induced SMA expression by immunofluorescent staining (Figure 5B). To confirm activation of the Notch pathway by Jagged1, HMEC-Jagged1 cocultures and HMEC-vector cocultures were transiently transfected with a CBF1-dependent promoter-luciferase construct. HMEC-Jagged1 cocultures demonstrated 4.5-fold higher CBF1-luciferase activity compared with HMEC-vector cocultures, demonstrating that enforced expression of Jagged1 activates CBF1-dependent Notch signaling (Figure 5C). The presence of a

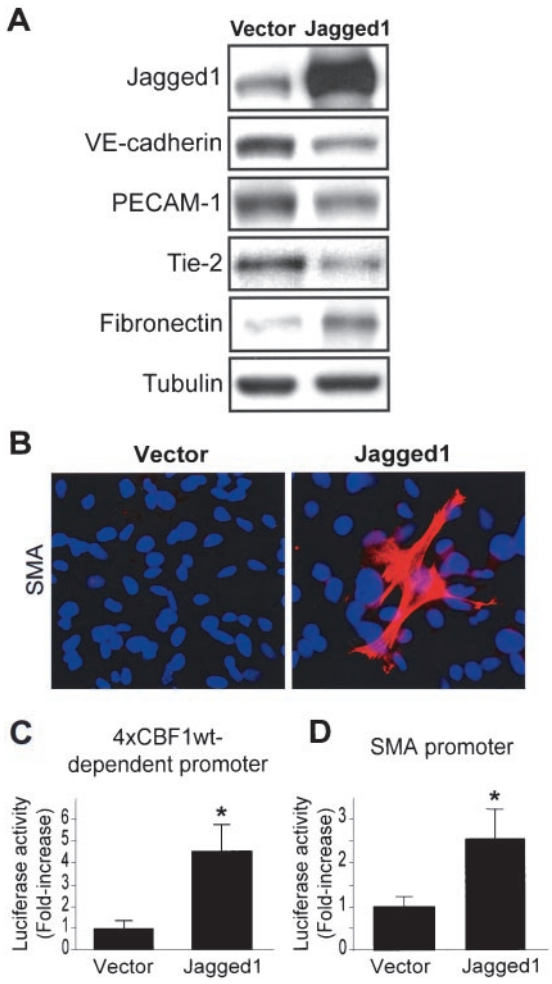

Figure 5. Jagged1 induces EMT. A, HMEC-vector or HMEC-Jagged1 cocultures were examined for expression of endothelial and mesenchymal markers by immunoblotting. B, Expression of SMA was tested by immunofluorescence. HMEC-vector or HMEC-Jagged1 cocultures were transiently cotransfected with a constitutively active *Renilla* luciferase plasmid and a CBF1-dependent promoter-luciferase construct (C) or an SMA promoter-luciferase construct (D), and relative luciferase activity was determined, as described in Materials and Methods. The graphs show a single experiment done in triplicate and are representative of 3 independent experiments (mean±SD). *$P<0.05$.

conserved consensus CBF-1 binding site that is located 64 to 59 nucleotides upstream of the cap site in the SMA promoter suggests that activation of Notch may directly induce SMA transcription. Promoter-luciferase assays using Notch4IC- or Notch1IC-transduced HMECs demonstrated a Notch-dependent increase in SMA promoter activity that was confirmed by induction of SMA mRNA by RT-PCR (data not shown). Examination of HMEC-Jagged1 cocultures also demonstrated a 2.5-fold increase in SMA promoter-luciferase activity over HMEC vector, indicating that Jagged1-Notch interactions are capable of upregulating SMA expression (Figure 5D). These results do not prove a direct transcriptional regulation of SMA by putative Notch-CBF1 complexes but suggest that increased expression of SMA may be attributable to induction of transcription. Taken together, our results support the hypothesis that Jagged1-Notch interac-

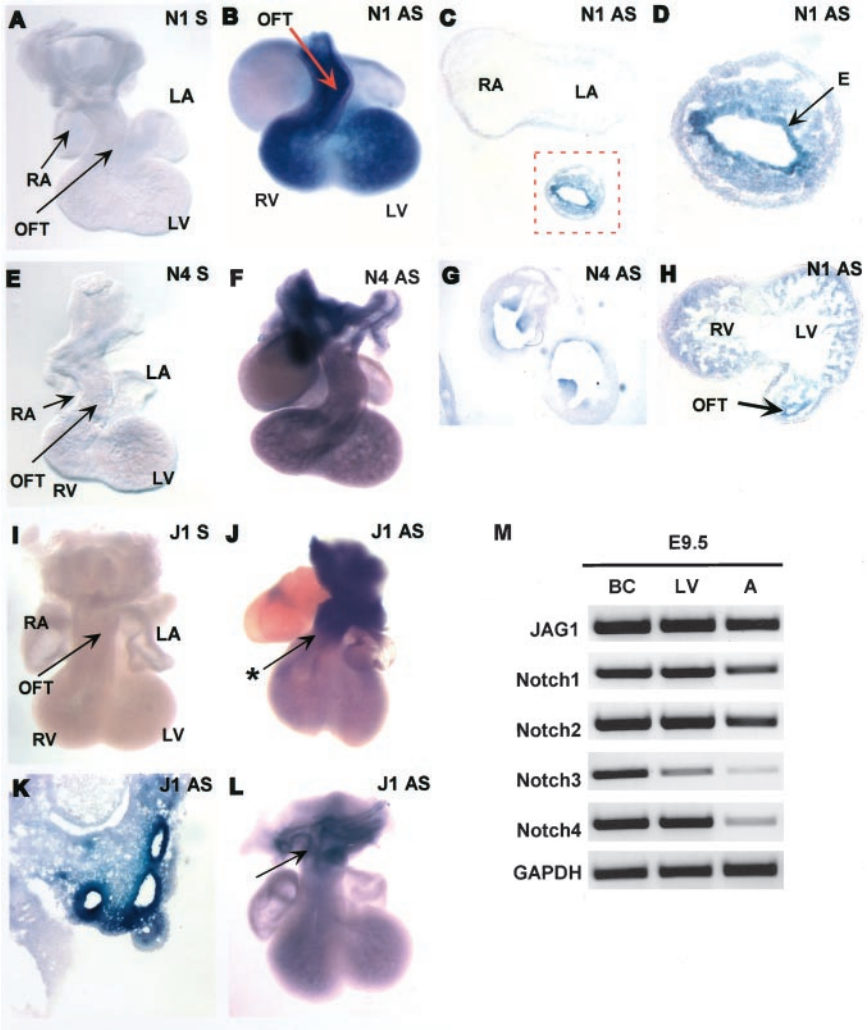

Figure 6. Notch1, Notch4, and Jagged1 are expressed during heart development. Expression of Notch1 mRNA was examined by whole-mount in situ hybridization of E10.5 mouse hearts using sense (A) and anti-sense (B through D and H) RNA probes. Cross sections of an E10.5 heart hybridized for Notch1 expression at the level of the atria (C and D) and ventricles (H) are shown. The region outlined in red in C is shown enlarged in D. The arrow in H points to expression of Notch1 in the endothelial lining of the outflow tract. Notch4 expression was examined in E10.5 hearts using sense (E) and anti-sense (F and G) RNA probes. Notch4 expression is also shown in cross sections from the outflow tract of E11.5 mouse hearts (G). Jagged1 expression (I through L) is shown in both E10.5 (I through K) and E11.5 (L) mouse hearts. The Jagged1 sense control is shown at E11.5 (I). Cross section of an E10.5 heart showing Jagged1 expression is shown in K. The asterisk in panel J indicates the point in the outflow tract where the aorta and pulmonary arteries have begun to separate. M, Semiquantitative RT-PCR was used to examine the expression of Jagged1 and Notch 1 to 4 in E9.5 hearts. E9.5 hearts were dissected and divided into 3 regions, the atria, the left ventricle, and the bulbus cordis, which included the outflow tract and the right ventricle. RA indicates right atria; LA, left atria; RV, right ventricle; LV, left ventricle; OFT, outflow tract; BC, bulbus cordis; N1, Notch1 probe; N4, Notch4 probe; J1, Jagged1 probe; S, sense probe; AS, anti-sense probe; and E, endothelium.

tions contribute to the transdifferentiation of endothelial cells to a mesenchymal phenotype.

Notch1, Notch4, and Jagged1 Are Expressed in the Early Developing Heart

Because our data demonstrate that in vitro Jagged1-Notch interactions induce EMT, we sought to determine whether Notch1, Notch4, and Jagged1 were expressed in areas where EMT is occurring in the developing heart. EMT begins at approximately embryonic day (E) 9.5 in the atrioventricular endocardial cushions and at E10.5 in the ventricular outflow tract.[40] At E10.5, Notch1 is expressed throughout the ventricles in the forming trabeculae (Figure 6H). Low-level expression is also observed in the inner endocardial layer of the atria (Figure 6C and data not shown). The highest level of Notch1 expression is present in the endothelium of the outflow tract at the time when EMT is commencing in this region (Figures 6C, 6D, and 6H). Notch4 exhibits low levels of expression throughout the heart at E10.5 (Figure 6F) and is selectively observed in regions of presumptive valve leaflet development in the outflow tract at E11.5 (Figure 6G).

Jagged1 expression can be detected as early as E9.5 in the bulbus cordis of the developing heart (data not shown), the region of the heart that will form the right ventricle and the outflow tract. By E10.5, Jagged1 expression can be detected throughout the heart, including the atria and ventricles, with significantly higher levels observed in the outflow tract (Figure 6J). In the outflow tract, expression is observed in both the endothelial cells and in the surrounding mesenchyme, with notably higher expression in the anterior portion of the outflow tract (Figure 6K). A clear boundary between high expression and low expression is seen at the region of the outflow tract where separation of the pulmonary artery and the aorta begins. Expression of Jagged1 in the outflow tract is maintained at E11.5 (Figure 6L). To examine expression of Notch receptors and ligands earlier in cardiac development, RT-PCR was performed on mouse hearts harvested at E9.5 and separated into atria, ventricles, and bulbus cordis (outflow tract). As seen in Figure 6M, Jagged1 and all four Notch receptors are strongly expressed in the bulbus cordis.

Discussion

Our findings demonstrate that expression of activated Notch1 or Notch4 in endothelial cells causes transdifferentiation to a mesenchymal phenotype and implicate Jagged1-Notch interactions in promoting EMT. One role for Notch-mediated EMT may occur during endocardial cushion formation. Endocardial cushion development is a key process in the

formation of the valves and membranous septum, which partitions the heart tube into an atrium and ventricle and the common ventricular outflow tract into dorsal aorta and pulmonary artery.[17,18] Given that Notch receptors and the ligand Jagged1 are expressed in regions of the heart where EMT is required for proper development, the results described herein support a role for Jagged1-Notch interactions in promoting mesenchymal transformation during cardiac cushion formation and subsequent valvuloseptal development.[15,16] Interestingly, ≈70% of patients affected by Alagille syndrome, a disorder with pleiotropic developmental abnormalities, have mutations in the Jagged1 gene.[3–6] The most frequent cardiac anomaly in these patients is peripheral pulmonic stenosis. However, abnormalities that implicate defective endocardial cushion development are also described.[3–6] In particular, a recent study reported that 13% of patients with Alagille syndrome are affected by tetralogy of Fallot.[5] Furthermore, mutations of Jagged1 are associated with defects of cardiac cushion development independent of the other developmental anomalies reported by Alagille.[6,41] We speculate that defective Notch activation and consequent attenuation of EMT may play a role in the pathogenesis of atrioventricular defects associated with Jagged1 mutations.

There is accumulating evidence that endothelial cells can transdifferentiate into smooth muscle cells during developmental and pathological processes.[42] Labeling studies in quail embryos showed that injected endothelial cells integrate into the dorsal aorta and become subendothelial mesenchymal cells expressing SMA.[43] Several groups have shown that Flk1+ (vascular endothelial growth factor receptor-2) cells derived from embryonic stem cells can differentiate into endothelial cells and subsequently into smooth muscle cells with loss of Flk1 expression.[44–46] Smooth muscle cells derived from endothelial cells have been shown to incorporate into sites of neovascularization in the adult.[46,47] Endothelial to smooth muscle cell transdifferentiation is not restricted to embryonic cells, because several groups have shown that adult endothelial cells can differentiate into smooth muscle cells.[31,37,38]

Other studies have observed that neointimal smooth muscle cells in atherosclerosis and restenosis seem to arise from endothelial cells.[20,31,48] Notch receptors and Jagged1 are expressed in both endothelial and periendothelial cells, and a marked increase in expression of Jagged1 and Jagged2 and Notch2 through 4 has been described in the regenerating endothelium after balloon injury of the rat carotid artery.[49] Mature vascular endothelium can give rise to smooth muscle cells via EMT using a mechanism that requires cell-cell contact.[31] This is in line with our findings showing that Jagged1-Notch interactions on adjacent cells induce EMT. It is tempting to speculate that Notch activation may play a role in smooth muscle formation in neointimal growth or during vascular development.

In mammals, members of the TGF-β superfamily as well as various extracellular matrix proteins seem to play an important role in EMT during endocardial cushion formation.[18,50] However, both TGF-β–dependent and TGF-β–independent events are involved, and TGF-β does not induce SMA in microvascular endothelial cells and umbilical vein endothelium.[19,51] In our in vitro system, Notch-mediated EMT is restricted to cells expressing activated Notch, and TGF-β_1 and -β_2 do not seem to be essential for Notch-mediated transformation. However, additional investigation is required to verify whether other members of the TGF-β superfamily are involved and whether EMT requires crosstalk between the Notch and TGF-β pathways in vivo. Nevertheless, our data indicate a potential role for the Notch pathway in endocardial cushion development and possibly in vascular smooth muscle development and neointimal formation.

Acknowledgments

This research was supported by grants to A.K. from the Heart and Stroke Foundation of British Columbia and the Yukon and to A.K. and P.H. from the National Cancer Institute of Canada with funds from the Canadian Cancer Society and the Terry Fox Foundation. M.N. was supported by a fellowship from Fondazione Italiana per la Ricerca sul Cancro, a fellowship from the Canadian Institutes of Health Research, and a Research Trainee Award from the Michael Smith Foundation for Health Research. G.M. was supported by a Research Trainee Award from the Michael Smith Foundation for Health Research. P.H. is a Scholar of the Canadian Institutes of Health Research and the Michael Smith Foundation for Health Research. A.K. is a Clinician-Scientist of the Canadian Institutes of Health Research and a Scholar of the Michael Smith Foundation for Health Research. We thank Denise McDougal for assistance with flow cytometry and cell sorting.

References

1. Bray S, Furriols M. Notch pathway: making sense of suppressor of hairless. *Curr Biol*. 2001;11:R217–R221.
2. Joutel A, Tournier-Lasserve E. Notch signalling pathway and human diseases. *Semin Cell Dev Biol*. 1998;9:619–625.
3. Li L, Krantz ID, Deng Y, Genin A, Banta AB, Collins CC, Qi M, Trask BJ, Kuo WL, Cochran J, Costa T, Pierpont ME, Rand EB, Piccoli DA, Hood L, Spinner NB. Alagille syndrome is caused by mutations in human Jagged1, which encodes a ligand for Notch1. *Nat Genet*. 1997;16:243–251.
4. Oda T, Elkahloun AG, Pike BL, Okajima K, Krantz ID, Genin A, Piccoli DA, Meltzer PS, Spinner NB, Collins FS, Chandrasekharappa SC. Mutations in the human Jagged1 gene are responsible for Alagille syndrome. *Nat Genet*. 1997;16:235–242.
5. McElhinney DB, Krantz ID, Bason L, Piccoli DA, Emerick KM, Spinner NB, Goldmuntz E. Analysis of cardiovascular phenotype and genotype-phenotype correlation in individuals with a JAG1 mutation and/or Alagille syndrome. *Circulation*. 2002;106:2567–2574.
6. Eldadah ZA, Hamosh A, Biery NJ, Montgomery RA, Duke M, Elkins R, Dietz HC. Familial tetralogy of Fallot caused by mutation in the jagged1 gene. *Hum Mol Genet*. 2001;10:163–169.
7. Krebs LT, Xue Y, Norton CR, Shutter JR, Maguire M, Sundberg JP, Gallahan D, Closson V, Kitajewski J, Callahan R, Smith GH, Stark KL, Gridley T. Notch signaling is essential for vascular morphogenesis in mice. *Genes Dev*. 2000;14:1343–1352.
8. Uyttendaele H, Ho J, Rossant J, Kitajewski J. Vascular patterning defects associated with expression of activated Notch4 in embryonic endothelium. *Proc Natl Acad Sci U S A*. 2001;98:5643–5648.
9. Leong KG, Hu X, Li L, Noseda M, Larrivee B, Hull C, Hood L, Wong F, Karsan A. Activated Notch4 inhibits angiogenesis: role of ß$_1$-integrin activation. *Mol Cell Biol*. 2002;22:2830–2841.
10. Xue Y, Gao X, Lindsell CE, Norton CR, Chang B, Hicks C, Gendron-Maguire M, Rand EB, Weinmaster G, Gridley T. Embryonic lethality and vascular defects in mice lacking the Notch ligand Jagged1. *Hum Mol Genet*. 1999;8:723–730.
11. McCright B, Lozier J, Gridley T. A mouse model of Alagille syndrome: Notch2 as a genetic modifier of Jag1 haploinsufficiency. *Development*. 2002;129:1075–1082.
12. Sakata Y, Kamei CN, Nakagami H, Bronson R, Liao JK, Chin MT. Ventricular septal defect and cardiomyopathy in mice lacking the transcription factor CHF1/Hey2. *Proc Natl Acad Sci U S A*. 2002;99:16197–16202.

13. Donovan J, Kordylewska A, Jan YN, Utset MF. Tetralogy of Fallot and other congenital heart defects in Hey2 mutant mice. *Curr Biol*. 2002;12: 1605–1610.
14. Iso T, Hamamori Y, Kedes L. Notch signaling in vascular development. *Arterioscler Thromb Vasc Biol*. 2003;23:543–553.
15. Loomes KM, Taichman DB, Glover CL, Williams PT, Markowitz JE, Piccoli DA, Baldwin HS, Oakey RJ. Characterization of Notch receptor expression in the developing mammalian heart and liver. *Am J Med Genet*. 2002;112:181–189.
16. Loomes KM, Underkoffler LA, Morabito J, Gottlieb S, Piccoli DA, Spinner NB, Baldwin HS, Oakey RJ. The expression of Jagged1 in the developing mammalian heart correlates with cardiovascular disease in Alagille syndrome. *Hum Mol Gen*. 1999;8:2443–2449.
17. Icardo JM, Manasek FJ. *Cardiogenesis: Development, Mechanisms and Embryology*. 2nd ed. New York, NY: Raven Press; 1992.
18. Eisenberg LM, Markwald RR. Molecular regulation of atrioventricular valvuloseptal morphogenesis. *Circ Res*. 1995;77:1–6.
19. Paranya G, Vineberg S, Dvorin E, Kaushal S, Roth SJ, Rabkin E, Schoen FJ, Bischoff J. Aortic valve endothelial cells undergo transforming growth factor-ß–mediated and non-transforming growth factor-ß-mediated transdifferentiation in vitro. *Am J Pathol*. 2001;159:1335–1343.
20. Beranek JT. Vascular endothelium-derived cells containing smooth muscle actin are present in restenosis. *Lab Invest*. 1995;72:771.
21. Artavanis-Tsakonas S, Rand MD, Lake RJ. Notch signaling: cell fate control and signal integration in development. *Science*. 1999;284: 770–776.
22. Weinmaster G, Roberts VJ, Lemke G. A homolog of *Drosophila* Notch expressed during mammalian development. *Development*. 1991;113: 199–205.
23. Valsecchi C, Ghezzi C, Ballabio A, Rugarli EI. JAGGED2: a putative Notch ligand expressed in the apical ectodermal ridge and in sites of epithelial-mesenchymal interactions. *Mech Dev*. 1997;69:203–207.
24. Karsan A, Yee E, Poirier GG, Zhou P, Craig R, Harlan JM. Fibroblast growth factor-2 inhibits endothelial cell apoptosis by Bcl-2-dependent and independent mechanisms. *Am J Pathol*. 1997;151:1775–1784.
25. Karsan A, Yee E, Harlan JM. Endothelial cell death induced by tumor necrosis factor-α is inhibited by the Bcl-2 family member, A1. *J Biol Chem*. 1996;271:27201–27204.
26. Dorovini-Zis K, Prameya R, Bowman PD. Culture and characterization of microvascular endothelial cells derived from human brain. *Lab Invest*. 1991;64:425–436.
27. Ear T, Giguere P, Fleury A, Stankova J, Payet MD, Dupuis G. High efficiency transient transfection of genes in human umbilical vein endothelial cells by electroporation. *J Immunol Methods*. 2001;257:41–49.
28. Hsieh JJ, Henkel T, Salmon P, Robey E, Peterson MG, Hayward SD. Truncated mammalian Notch1 activates CBF1/RBPJk-repressed genes by a mechanism resembling that of Epstein-Barr virus EBNA2. *Mol Cell Biol*. 1996;16:952–959.
29. Hoodless PA, Pye M, Chazaud C, Labbe E, Attisano L, Rossant J, Wrana JL. FoxH1 (Fast) functions to specify the anterior primitive streak in the mouse. *Genes Dev*. 2001;15:1257–1271.
30. Dejana E. Endothelial adherens junctions: implications in the control of vascular permeability and angiogenesis. *J Clin Invest*. 1997;100:S7–S10.
31. Frid MG, Kale VA, Stenmark KR. Mature vascular endothelium can give rise to smooth muscle cells via endothelial-mesenchymal transdifferentiation: in vitro analysis. *Circ Res*. 2002;90:1189–1196.
32. Nakajima Y, Mironov V, Yamagishi T, Nakamura H, Markwald RR. Expression of smooth muscle α-actin in mesenchymal cells during formation of avian endocardial cushion tissue: a role for transforming growth factor $ß_3$. *Dev Dyn*. 1997;209:296–309.
33. Icardo JM, Manasek FJ. An indirect immunofluorescence study of the distribution of fibronectin during the formation of the cushion tissue mesenchyme in the embryonic heart. *Dev Biol*. 1984;101:336–345.
34. Ffrench-Constant C, Hynes RO. Patterns of fibronectin gene expression and splicing during cell migration in chicken embryos. *Development*. 1988;104:369–382.
35. Ataliotis P, Mercola M. Distribution and functions of platelet-derived growth factors and their receptors during embryogenesis. *Int Rev Cytol*. 1997;172:95–127.
36. Hellstrom M, Kalen M, Lindahl P, Abramsson A, Betsholtz C. Role of PDGF-B and PDGFR-ß in recruitment of vascular smooth muscle cells and pericytes during embryonic blood vessel formation in the mouse. *Development*. 1999;126:3047–3055.
37. Arciniegas E, Sutton AB, Allen TD, Schor AM. Transforming growth factor $ß_1$ promotes the differentiation of endothelial cells into smooth muscle-like cells in vitro. *J Cell Sci*. 1992;103:521–529.
38. Ishisaki A, Hayashi H, Li AJ, Imamura T. Human umbilical vein endothelium-derived cells retain potential to differentiate into smooth muscle-like cells. *J Biol Chem*. 2003;278:1303–1309.
39. Boyer AS, Ayerinskas II, Vincent EB, McKinney LA, Weeks DL, Runyan RB. TGF$ß_2$ and TGF$ß_3$ have separate and sequential activities during epithelial-mesenchymal cell transformation in the embryonic heart. *Dev Biol*. 1999;208:530–545.
40. Camenisch TD, Molin DG, Person A, Runyan RB, Gittenberger-de Groot AC, McDonald JA, Klewer SE. Temporal and distinct TGFß ligand requirements during mouse and avian endocardial cushion morphogenesis. *Dev Biol*. 2002;248:170–181.
41. Krantz ID, Smith R, Colliton RP, Tinkel H, Zackai EH, Piccoli DA, Goldmuntz E, Spinner NB. Jagged1 mutations in patients ascertained with isolated congenital heart defects. *Am J Med Genet*. 1999;84:56–60.
42. Drake CJ, Hungerford JE, Little CD. Morphogenesis of the first blood vessels. *Ann N Y Acad Sci*. 1998;857:155–179.
43. DeRuiter MC, Poelmann RE, VanMunsteren JC, Mironov V, Markwald RR, Gittenberger-de Groot AC. Embryonic endothelial cells transdifferentiate into mesenchymal cells expressing smooth muscle actins in vivo and in vitro. *Circ Res*. 1997;80:444–451.
44. Ema M, Faloon P, Zhang WJ, Hirashima M, Reid T, Stanford WL, Orkin S, Choi K, Rossant J. Combinatorial effects of Flk1 and Tal1 on vascular and hematopoietic development in the mouse. *Genes Dev*. 2003;17: 380–393.
45. Yamashita J, Itoh H, Hirashima M, Ogawa M, Nishikawa S, Yurugi T, Naito M, Nakao K. Flk1-positive cells derived from embryonic stem cells serve as vascular progenitors. *Nature*. 2000;408:92–96.
46. Marchetti S, Gimond C, Iljin K, Bourcier C, Alitalo K, Pouyssegur J, Pages G. Endothelial cells genetically selected from differentiating mouse embryonic stem cells incorporate at sites of neovascularization in vivo. *J Cell Sci*. 2002;115:2075–2085.
47. Yurugi-Kobayashi T, Itoh H, Yamashita J, Yamahara K, Hirai H, Kobayashi T, Ogawa M, Nishikawa S, Nakao K. Effective contribution of transplanted vascular progenitor cells derived from embryonic stem cells to adult neovascularization in proper differentiation stage. *Blood*. 2003; 101:2675–2678.
48. Majesky MW, Schwartz SM. An origin for smooth muscle cells from endothelium? *Circ Res*. 1997;80:601–603.
49. Lindner V, Booth C, Prudovsky I, Small D, Maciag T, Liaw L. Members of the Jagged/Notch gene families are expressed in injured arteries and regulate cell phenotype via alterations in cell matrix and cell-cell interaction. *Am J Pathol*. 2001;159:875–883.
50. Nakajima Y, Yamagishi T, Hokari S, Nakamura H. Mechanisms involved in valvuloseptal endocardial cushion formation in early cardiogenesis: roles of transforming growth factor (TGF)-ß and bone morphogenetic protein (BMP). *Anat Rec*. 2000;258:119–127.
51. Boyer AS, Erickson CP, Runyan RB. Epithelial-mesenchymal transformation in the embryonic heart is mediated through distinct pertussis toxin-sensitive and TGFß signal transduction mechanisms. *Dev Dyn*. 1999;214:81–91.

Supplementary data

Material and methods

PCR primers and conditions were as follows: Notch1 sense 5' GGC CAC CTC TTC ACT GCT TC 3', anti-sense 5' CCG GAA CTT CTT GGT CTC CA 3' (60°C, 35 cycles); Notch2 sense 5' AAC TGG AGA GTC CAA GAA ACG 3', anti-sense 5' TGG TAG ACC AAG TCT GTG ATG AT 3'(53°C, 35 cycles); Notch3 sense 5' CAC CTT GGC CCC CTA AG 3', anti-sense 5' TGG AAT GCA GTG AAG TGA GG 3' (60°C, 35 cycles); Notch4 sense 5' CAA GCT CCC GTA GTC CTA CTT C 3', anti-sense 5' GGC AGG TGC CCC CAT T 3'(53°C, 35 cycles); Jagged1 sense 5' AAT GGA GAC TCC TTC ACC TGT 3', anti-sense 5' CGT CCA TTC AGG CAC TGG 3' (53°C, 35 cycles); GAPDH. (sense 5' GCA TGG CCT TCC GTG T 3', anti-sense 5' GGG CCG AGT TGG GAT AGG 3' (53°C, 25 cycles).

Supplementary data, Figure 1

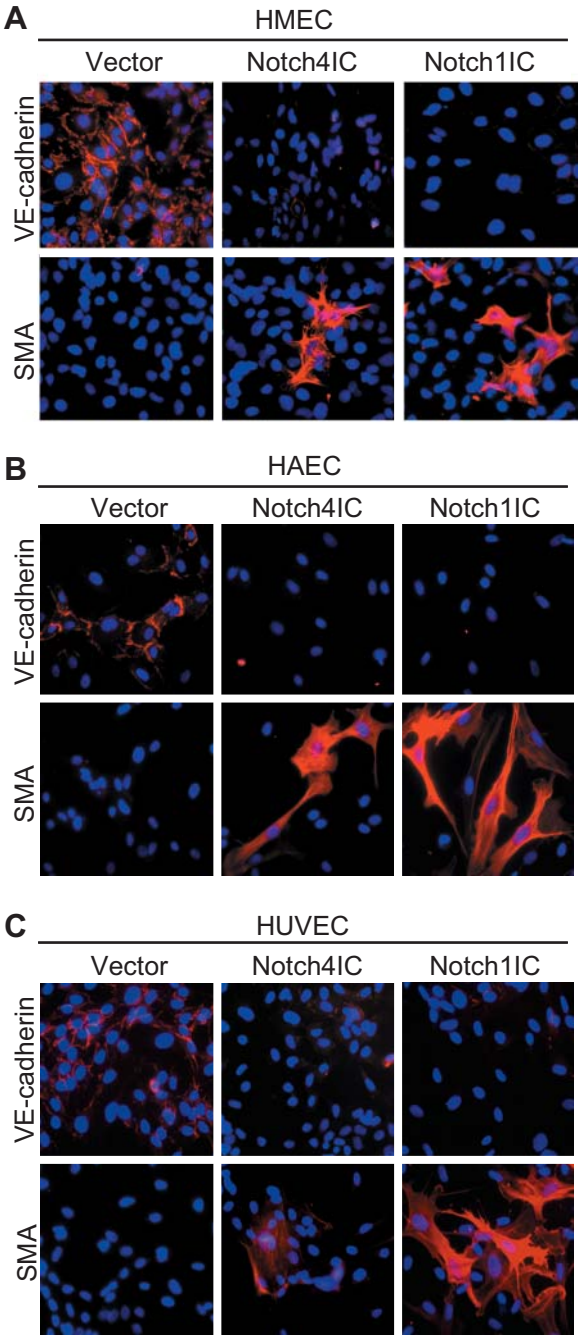

HMEC (A), HAEC (B) and HUVEC (C) were transduced with the empty vector, Notch4IC or Notch1IC and analyzed by immunofluorescence for VE-cadherin and SMA expression 14 days after transduction. Cell nuclei were counter-stained with DAPI. Results are representative of 3 independent experiments done in triplicate.

Supplementary data, Figure 2

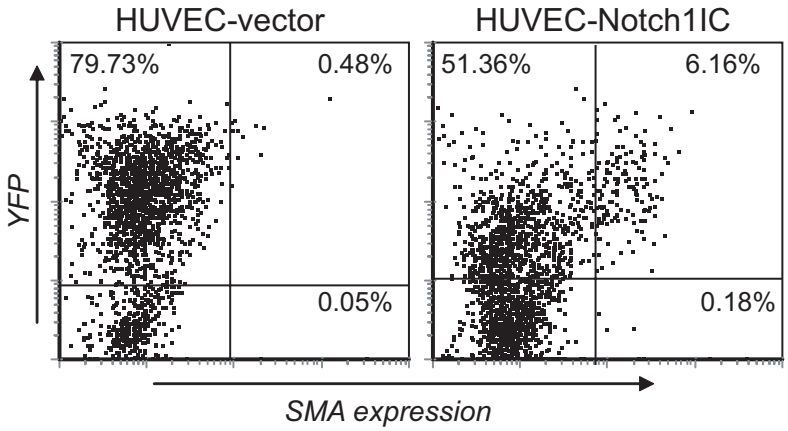

HUVEC were transduced with the empty vector or Notch1IC and analyzed by flow cytometry for YFP and SMA expression. Cells were analyzed 14 days after transduction.Percentage of cells in quadrants is indicated .

MOLECULAR AND CELLULAR BIOLOGY, Oct. 2004, p. 8813–8822 Vol. 24, No. 20
0270-7306/04/$08.00+0 DOI: 10.1128/MCB.24.20.8813–8822.2004

Notch Activation Induces Endothelial Cell Cycle Arrest and Participates in Contact Inhibition: Role of $p21^{Cip1}$ Repression†

Michela Noseda,[1,2] Linda Chang,[1,3] Graeme McLean,[1,3] Jonathan E. Grim,[4] Bruce E. Clurman,[4] Laura L. Smith,[4] and Aly Karsan[1,2,3,5]*

Department of Medical Biophysics[1] and Department of Pathology and Laboratory Medicine,[5] British Columbia Cancer Agency, and Experimental Medicine Program[3] and Department of Pathology and Laboratory Medicine,[2] University of British Columbia, Vancouver, British Columbia, Canada, and Basic Sciences, Human Biology and Clinical Divisions, Fred Hutchinson Cancer Research Center, Seattle, Washington[4]

Received 11 January 2004/Returned for modification 4 March 2004/Accepted 19 July 2004

Although previous studies demonstrate that appropriate Notch signaling is required during angiogenesis and in vascular homeostasis, the mechanisms by which Notch regulates vascular function remain to be elucidated. Here, we show that activation of the Notch pathway by the ligand Jagged1 reduces the proliferation of endothelial cells. Notch activation inhibits proliferation of endothelial cells in a cell-autonomous manner by inhibiting phosphorylation of the retinoblastoma protein (Rb). During cell cycle entry, $p21^{Cip1}$ is upregulated in endothelial cells. Activated Notch inhibits mitogen-induced upregulation of $p21^{Cip1}$ and delays cyclin D-cdk4-mediated Rb phosphorylation. Notch-dependent repression of $p21^{Cip1}$ prevents nuclear localization of cyclin D and cdk4. The necessity of $p21^{Cip1}$ for nuclear translocation of cyclin D-cdk4 and S-phase entry in endothelial cells was demonstrated by targeted downregulation of $p21^{Cip1}$ by using RNA interference. We further demonstrate that when endothelial cells reach confluence, Notch is activated and $p21^{Cip1}$ is downregulated. Inhibition of the Notch pathway at confluence prevents $p21^{Cip1}$ downregulation and induces Rb phosphorylation. We suggest that Notch activation contributes to contact inhibition of endothelial cells, in part through repression of $p21^{Cip1}$ expression.

The Notch pathway is a highly conserved intercellular signaling mechanism that is activated by interactions of transmembrane ligands of the Jagged (Jagged1 and Jagged2) and Delta (Delta-like 1 [Dll-1], Dll3, and Dll4) families with Notch receptors (Notch1 to -4) expressed on adjacent cells (1). Notch receptors and their ligands have been localized to the vascular endothelium and supporting cells in both the embryo and the adult (12, 20, 27, 34, 35, 37, 41).

Several studies demonstrate that perturbation of the Notch pathway affects vascular development. Mice lacking the Notch ligand Jagged1 die at embryonic day 11.5, exhibiting defects in vascular remodeling. Similar defects are observed in Notch1 null mice (15, 43). Mice that are rendered null for both Notch1 and Notch4 die earlier and show a more severe vascular phenotype than Notch1 null mutants (15). Mice deficient in presenilin-1, which is involved in the cleavage and activation of Notch, show perinatal lethality with a complex phenotype, including abnormal blood vessel development and intracranial hemorrhage (22, 31). Interestingly, vascular defects observed when constitutively active Notch4 is expressed selectively in endothelial cells are also consistent with altered vascular remodeling (17, 40). Hence, mutations inhibiting the Notch pathway, as well as a sustained activation of Notch, similarly affect vascular development, suggesting that there is a requirement for fine temporal and spatial regulation of Notch signaling. Despite the preponderance of evidence implicating Notch signaling in vascular development, the mechanisms by which Notch exerts its effects on the vasculature remain to be elucidated.

In other systems, Notch signaling determines cell fate by influencing cell proliferation, differentiation, and apoptosis, but the specific effects of Notch activation are related to the cell type and context (1, 38). Activation of the pathway results from engagement of Notch by ligand, which triggers a series of proteolytic cleavages resulting in release of the intracellular portion (NotchIC) from its membrane tether and subsequent nuclear translocation (1). In the nucleus, binding of NotchIC to the transcription factor CBF1 (RBP-Jκ) upregulates expression of target genes of the HES (hairy/enhancer of split) and HRT (hairy-related transcription factor) basic helix-loop-helix family of proteins (1, 12).

In the quiescent vasculature of the adult, it is estimated that only 0.01% of cells are actively proliferating (8, 11). In contrast, during angiogenesis, elongation of the new sprout depends on the proliferation of endothelial cells (8, 11). It has been suggested that Notch activation is absent in vessels at the early stages of angiogenesis when endothelial cells are proliferating but that Notch is reactivated when endothelial cells stop proliferating and vessels begin to stabilize (9, 39). Notch activation can stimulate or inhibit proliferation by modulating

* Corresponding author. Mailing address: British Columbia Cancer Research Centre, 601 West 10th Ave., Vancouver, British Columbia, Canada V5Z 1L3. Phone: (604) 877-6248. Fax: (604) 877-6002. E-mail: akarsan@bccrc.ca.

† Supplemental material for this article may be found at http://mcb.asm.org/.

cell cycle regulation in a cell type-specific and context-dependent manner (2, 13, 26, 28, 36, 42).

Cell cycle transitions are controlled by cyclin-dependent kinase complexes, which are comprised of regulatory (cyclin) and catalytic (serine-threonine kinase and cdk) subunits (32). Synthesis of D-type cyclins and assembly with their catalytic partners (cdk4 and cdk6) depends upon mitogenic stimulation. Mitogen-dependent nuclear accumulation of cyclin D-dependent kinases initiates the phosphorylation and inhibition of the retinoblastoma gene product (Rb) (32). Rb phosphorylation results in conformational changes that release transcription factors of the E2F family, histone deacetylases, and chromosomal remodeling complexes, thereby promoting expression of target genes necessary for progression towards S phase, including cyclin E and cyclin A (32).

In this report we examine the hypothesis that the Notch pathway is involved in regulation of endothelial cell proliferation. We have previously seen that activated Notch4 does not affect proliferation of simian virus 40 (SV40) large T antigen-transformed endothelial cells (17). Given that SV40 T antigen is able to bind Rb and inhibit its antiproliferative function, we investigated the role of Notch signaling in cell cycle regulation of primary human endothelial cells that express functional Rb. Our results show that Notch activation induces cell cycle arrest in primary endothelial cells via a mechanism that inhibits Rb phosphorylation. Inhibition of Rb phosphorylation is effected by Notch-mediated $p21^{Cip1}$ repression, which reduces cyclin D-cdk4 nuclear targeting and thus Rb phosphorylation activity. Further, endothelial cell-cell contact activates Notch and reduces $p21^{Cip1}$ expression, suggesting that activation of the Notch pathway participates in contact inhibition of endothelial cells.

MATERIALS AND METHODS

Cell culture. The human microvascular endothelial cell line HMEC-1 was provided by the Centers for Disease Control and Prevention (Atlanta, Ga.) (17). Human umbilical vein endothelial cells (HUVEC) were isolated and cultured as previously described (14). Primary human microvascular endothelial cells (HMVEC) and human aortic endothelial cells (HAEC) were purchased from Clonetics and cultured according to manufacturer's instructions. HMEC-1 lines and HUVEC were cultured in MCDB medium (Sigma, St. Louis, Mo.) containing, respectively, 10 or 20% heat-inactivated fetal calf serum (HyClone, Logan, Utah). Cells were incubated for 24 to 48 h in MCDB containing 0.2% serum to synchronize them in G_0. To activate the fusion protein Notch4IC-estrogen receptor (Notch4IC-ER), cells were treated with 250 nM 4-hydroxytamoxifen (4-OHT). In cell synchronization experiments, 4-OHT was added 8 h prior to serum addition. The presenilin inhibitor *N*-[*N*-(3,5-difluorophenacetyl)]-L-alanyl-3-amino-1-methyl-5phenyl-1,3-dihydro-benzo[e](1,4)diazepin-2-one (DFP-AA), was purchased from Calbiochem.

Plasmids and gene transfer. Constructs encoding the C-terminal HA-tagged Notch4IC (17), Notch1IC, and Jagged1 cDNA (a gift of L. Li) were subcloned into the retroviral vector MSCV-IRES-YFP (MIY) (a gift of R. K. Humphries). For the Notch4IC-ER fusion protein, cDNA encoding Notch4IC was subcloned in frame N terminal to the binding domain of the mutated estrogen receptor encoded in the retroviral vector pBabe-hb-ER (a gift of M. McMahon). Endothelial cells were transduced as previously described with the following modifications (17): FuGENE 6 transfection reagent (Roche Diagnostic Corporation, Indianapolis, Ind.) was used for transient transfections of the Ampho Phoenix packaging cell lines, and multiple rounds of infections were performed. pBabe-hb-ER alone was used as a control in experiments based on the inducible system. Expression of Notch4IC, Notch1IC, and Notch4IC-ER fusion protein was confirmed by immunoblotting or immunofluorescence staining after each series of transductions (see Fig. S1 in the supplemental material). cDNA encoding human $p21^{Cip1}$ was obtained from the American Type Culture Collection and subcloned into MIY.

Luciferase assays. The p21-luc construct was obtained by excising the fragment encoding the proximal 2.4-kb region of the human p21 promoter from p53R-green fluorescent protein (a gift from G. Li) (5, 45) and subcloning it into pGL3 Basic vector (Promega Corporation, Madison, Wis.). HA-tagged Notch4IC and Notch1IC were subcloned into pcDNA3 (Invitrogen). For normalization, cells were cotransfected with the *Renilla* luciferase plasmid pRL-CMV (Promega). Endothelial cells were transfected with SuperFect transfection reagent (Qiagen) according to the manufacturer's recommendations. Dual-luciferase reporter assays (Promega) were performed 48 h after transfection.

RNA interference. Retroviral delivery of interfering short-hairpin RNA (siRNA) constructs was accomplished as previously described (7). Briefly, PCR was used to generate an H1 short-hairpin RNA cassette, which was inserted into the unique NheI site in the downstream U3 region of the pBabePuro vector. The siRNAs targeting $p21^{Cip1}$ and $p27^{Kip1}$ correspond to nucleotides 431 to 452 (5′-AGACCAGCATGACAGATTTCTA-3′) and 245 to 264 (5′-GCAGCTTGC CCGAGTTCTAC-3′) of each mRNA, respectively.

Reverse transcription-PCR (RT-PCR). Total RNA was isolated by using TRIzol reagent (Invitrogen, Carlsbad, Calif.) and was DNase treated. A control reaction omitting reverse transcriptase was performed in each experiment. PCR was performed with the following primers: Notch1, 5′-CACTGTGGGCGGGT CC-3′ and 5′-GTTGTATTGGTTCGGCACCAT-3′; Notch2, 5′-CCCAATGGG CAAGAAGTCTA-3′ and 5′-CACAATGTGGTGGTGGGATA-3′; Notch3, 5′-TGAGACGCTCGTCAGTTCTT-3′ and 5′-TGGAATGCAGTGAAGTGAG G-3′; Notch4, 5′-TAGGGCTCCCCAGCTCTC-3′ and 5′-GGCAGGTGCCCC CATT-3′; Jagged1, 5′-CTATGATGAGGGGGATGCt-3′ and 5′-CGTCCATT CAGGCACTGG-3′; and Dll4, 5′-GCATTGTTTACATTGCATCCTG-3′ and 5′-CAAGGGCGTGCGCGTCAAAGTA-3′.

Flow cytometry. For cell cycle analysis, exponentially growing cells were labeled with 5 μg of Hoechst 33342 (Sigma) per ml for 30 min, trypsinized, and analyzed by flow cytometry as previously described (17). For analysis of bromodeoxyuridine (BrdU) incorporation versus DNA content, cells were labeled with 10 μM BrdU for 2 h, fixed in 70% ethanol, and treated as previously described (17). Samples were run on an EPICS ELITE-ESP flow cytometer (Beckman Coulter), and data were analyzed by using FCS Express V2 (De Novo Software, Thornhill, Ontario, Canada). Cells were sorted on a FACS 440 instrument (Becton Dickinson).

Immunoblotting. Cells were lysed in radioimmunoprecipitation assay buffer (1% NP-40, 0.5% sodium deoxycholate, 0.1% sodium dodecyl sulfate [SDS]), with addition of fresh protease inhibitor cocktail (Sigma), 0.5 mM phenylmethylsulfonyl fluoride, and phosphatase inhibitors (0.5 mM sodium orthovanadate and 30 mM sodium fluoride). Proteins were quantitated by the D_C protein assay (Bio-Rad Laboratories, Hercules, Calif.). Fifty micrograms of protein was separated by SDS-polyacrylamide gel electrophoresis, and transferred to nitrocellulose membranes (Bio-Rad Laboratories) and developed by enhanced chemiluminescence (PerkinElmer Life Science, Boston, Mass.). The mouse monoclonal antibody against the HA epitope was purchased from BAbCo (Richmond, Calif.). Anti-ER, anti-cdk4, anti-cyclin D, anti-p21, anti-p15, anti-p16, and anti-cyclin A antibodies were all obtained from Santa Cruz Biotechnology, Inc (Santa Cruz, Calif.). Anti-p27 antibody was purchased from Transduction Laboratories, anti-Rb (clone G3-245) antibody was purchased from BD Bioscience (Bedford, Mass.), and anti-alpha-tubulin was from Sigma.

cdk4 kinase assay. Cells were treated as described in Results. Lysates from exponentially growing untreated endothelial cells were used as a positive control. Cells were lysed in HEB (50 mM HEPES [pH 7.5], 0.1% Tween, 150 mM NaCl, 1 mM EDTA, 2.5 mM EGTA, 10% glycerol, 1 mM dithiothreitol) containing protease inhibitors and phosphatase inhibitors as described above (with addition of 10 mM glycerolphosphate). Six hundred micrograms of total protein was precleared with protein-G Sepharose beads (Sigma) and incubated with anti-cdk4 antibody (Santa Cruz Biotechnology). Incubation without primary antibody was performed as a negative control. cdk4 complexes were incubated with protein G-Sepharose beads for 30 min. After three washes in HEB and two washes in kinase buffer (20 mM HEPES [pH 7.5], 20 mM $MgCl_2$, 0.1% β-mercaptoethanol), the beads were suspended in kinase buffer containing Rb-C fusion protein (Rb residues 701 to 928) (Cell Signaling Technology, Beverly, Mass.) and 10 μCi of [^{32}P]ATP per sample (Amersham). Samples were incubated at 30°C for 30 min and separated by SDS-polyacrylamide gel electrophoresis. Phosphorylated Rb was visualized by autoradiography of the dried gels.

Immunofluorescence staining. Cells were fixed in 4% paraformaldehyde, blocked, and permeabilized in phosphate-buffered saline containing 4% fetal calf serum and 0.2% Triton-X. The anti-phospho-Rb antibody (specific for phosphorylation on Ser807/811 on human Rb) was obtained from Cell Signaling Technology. Alexa 594-conjugated or Alexa 488-conjugated secondary antibodies were used according to the recommendations of the manufacturer (Molecular

Probes). For BrdU incorporation, cells were labeled for 2 h with 10 μM BrdU prior to fixation. The anti-BrdU antibody was conjugated with Alexa 594 (Molecular Probes). Nuclear staining with 4′,6′-diamidino-2-phenylindole (DAPI) was used for total cell counts. The proportion of positive cells was determined by counting at least 200 cells per sample. Images were acquired with a 1350EX cooled charge-coupled device digital camera (QImaging, Burnaby, British Columbia, Canada) on a Zeiss Axioplan II Imaging inverted microscope (Carl Zeiss Canada Ltd., Toronto, Ontario, Canada) and analyzed with Northern Eclipse image analysis software (Empix Imaging, Mississauga, Ontario, Canada).

Statistical analysis. To determine statistical significance, a one-way analysis of variance with a Tukey test for multiple comparisons was used in all experiments except for the time course experiments. For the time course experiments, the Mann-Whitney U test was used. Statistical significance was taken at a P value of ≤ 0.05.

RESULTS

Activation of the Notch pathway induces cell cycle arrest in primary endothelial cells. The Notch1 and Notch4 receptors and the Notch ligands Dll4 and Jagged1 have been reported to be expressed in endothelial cells (12). To further define the expression patterns of Notch family members in endothelia of different vascular origins, we analyzed dermal microvascular endothelial cells transformed with SV40 large T antigen (HMEC-1), as well as primary endothelial cells from human dermis-derived microvasculature (HMVEC), human aorta (HAEC), and human umbilical vein (HUVEC). Primary human umbilical artery smooth muscle cells (UASMC) were also tested. Notch1, Notch2, Notch4, and Jagged1 were expressed in all endothelial cells examined (Fig. 1A). Interestingly, Dll4 mRNA was not detected in HMEC-1 and HUVEC, while Notch3 was expressed only in these cells. In agreement with previous reports suggesting that Notch4 is expressed selectively on endothelial cells, UASMC expressed mRNAs of the ligands tested and of all receptors except Notch4 (41).

Given that activation of Notch4 inhibits angiogenesis in vitro and in vivo, we sought to determine whether Notch4 regulates endothelial cell proliferation. Constitutively active Notch4 (Notch4IC) cDNA was inserted into a retroviral vector (MIY) in which the transgene is linked to yellow fluorescent protein (YFP) through an internal ribosomal entry site (17, 40). HUVEC were transduced with the empty MIY vector (HUVEC-vector) or with vector encoding Notch4IC (HUVEC-Notch4IC). In Fig. 1B we show analysis of the cell cycle distribution in HUVEC-vector and HUVEC-Notch4IC. In HUVEC-Notch4IC, YFP-positive cells (Notch4IC expressing) showed arrest in G_0/G_1 phase, whereas YFP-negative cells (lacking Notch4IC) showed cell cycle profiles similar to those of HUVEC-vector (Fig. 1B and data not shown). Further, in the HUVEC-Notch4IC cultures we observed a reduction of the proportion of YFP-positive cells (Notch4IC expressing) with serial passages, while this was not the case with HUVEC-vector (Fig. 1B [ungated region in the dot plot] and data not shown). This observation provides additional support for a growth-inhibitory effect of Notch4IC. As previously demonstrated, Notch4IC did not affect cell cycle progression in SV40 large-T-antigen-transformed HMEC-1 (data not shown) (17).

Jagged1 is expressed in the endothelial cells tested, and Jagged1 null mice die in utero due to vascular defects (43). To determine whether activation of the Notch pathway by the vascular ligand Jagged1 induces cell cycle arrest, we transduced HUVEC with MIY-Jagged1 (HUVEC-Jagged1) or MIY alone (HUVEC-vector). Transduced cells were not selected for YFP, so Jagged1-expressing cells (YFP positive) existed in coculture with parental HUVEC (YFP negative). We have previously shown that in endothelial cells the overexpression of Jagged1 induces activation of the Notch pathway in a CBF-1-dependent luciferase reporter assay (23). Cell cycle profiles from YFP-positive and YFP-negative populations were compared to study the effect of Jagged1 on cocultured parental HUVEC. In HUVEC-vector cocultures, YFP-nega-

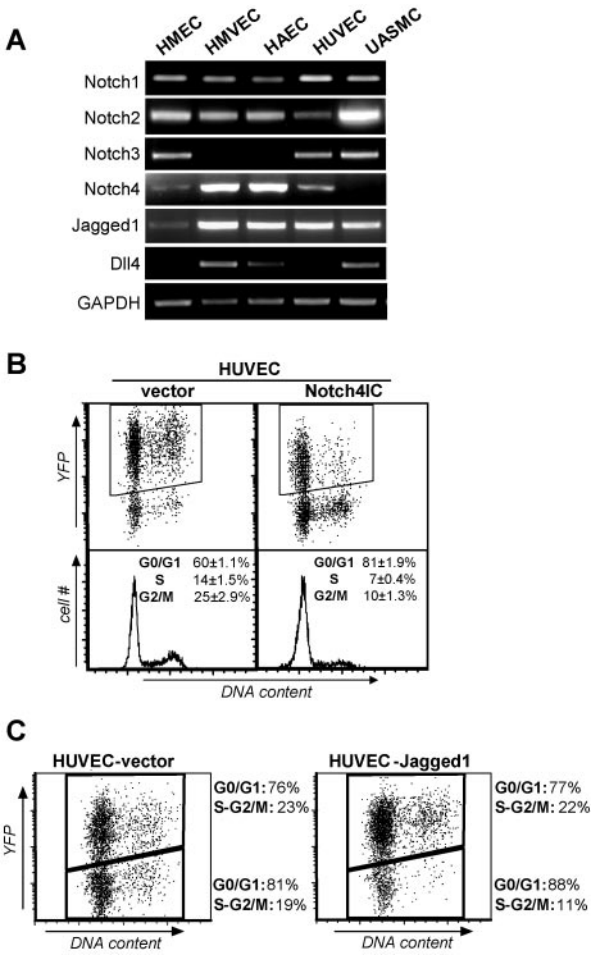

FIG. 1. Notch activation induces cell cycle arrest in primary endothelial cells. (A) RT-PCR for Notch receptors (Notch1, -2, -3, and -4) and ligands (Jagged1 and Dll4). Human endothelial cells from different vascular beds (HMEC, HMVEC, HAEC, and HUVEC) and UASMC were tested. GAPDH, glyceraldehyde-3-phosphate dehydrogenase. (B) Asynchronously growing HUVEC, transduced with MIY (vector) or MIY-Notch4IC (Notch4IC), were labeled with Hoechst 33342 and analyzed by flow cytometry. Dot plots show YFP expression (y axis) and DNA content (x axis). The gated population represents cells expressing YFP. Histograms illustrate cell cycle profiles of HUVEC positive for YFP. Proportions of cells in the G_0/G_1, S, and G_2/M phases of the cell cycle represent the means from four experiments ± standard errors of the means. (C) HUVEC transduced with MIY (HUVEC-vector) or MIY-Jagged1 (HUVEC-Jagged1) were labeled with Hoechst 33342 and analyzed by flow cytometry. Dot plots show YFP expression (y axis) and DNA content (x axis). Upper gates represent cells expressing YFP. Lower gates define the YFP-negative population. Cell cycle profiles were analyzed, and the proportions of cells in G_0/G_1 and S-G_2/M are indicated on the right of each gate. Experiments were repeated three times with similar results.

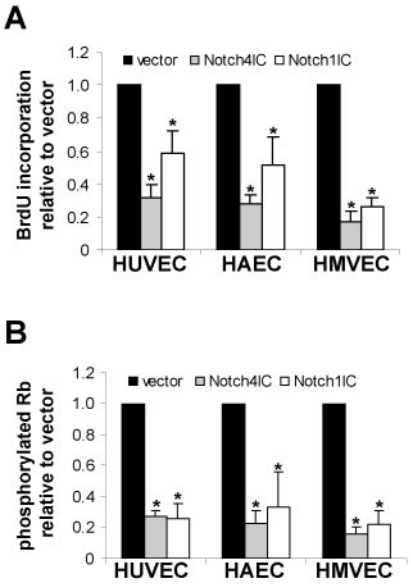

FIG. 2. Notch4IC and Notch1IC inhibit S-phase entry and Rb phosphorylation in endothelial cells from veins, arteries, and microvessels. HUVEC, HAEC, and HMVEC were transduced with MIY (vector), MIY-Notch4IC (Notch4IC), or MIY-Notch1IC (Notch1IC). Asynchronously growing cells were assayed for BrdU incorporation (A) (see also Fig. S2 in the supplemental material) and phosphorylated Rb (B) by immunofluorescence staining and enumerated by fluorescence microscopy. DAPI staining was used to define nuclear localization and for total cell counts. Graphs represent the means ± standard deviations from at least three experiments. *, $P < 0.05$ compared to vector.

tive and YFP-positive cells showed similar cell cycle profiles (Fig. 1C, left panel). In contrast, in HUVEC-Jagged1 cocultures, HUVEC receiving the Jagged1 signal (YFP-negative) had an increased proportion of cells in G_0/G_1 compared to that in the signaling cells (YFP positive) (Fig. 1C, right panel). Coculture experiments performed with HAEC confirmed similar results (data not shown). These data indicate that Notch inhibits proliferation in endothelial cells in which Notch is activated.

Notch4 and Notch1 inhibit Rb phosphorylation in primary endothelial cells of different vascular origins. Because of the demonstrated synergy of Notch4 and Notch1 in vivo during vascular development and the potential redundancy of some of their functions, we investigated whether Notch1 would also inhibit endothelial cell proliferation (15). We transduced HAEC, HMVEC, and HUVEC with MIY alone, MIY-Notch4IC, or MIY-Notch1IC. After sorting for YFP-positive cells, S-phase entry was assayed by BrdU incorporation, using immunofluorescence staining (see Fig. S2 in the supplemental material). In all endothelial cells tested, expression of activated Notch4 or Notch1 reduced the proportion of cells entering S phase (Fig. 2A).

During cell cycle progression, transition through the restriction point is blocked by unphosphorylated or hypophosphorylated Rb (32). Phosphorylation of Rb by cyclin-cdk complexes inactivates Rb and allows the cell to progress towards S phase (32). To determine whether Notch-mediated inhibition of S-phase entry was associated with reduced Rb phosphorylation, asynchronously growing HAEC, HMVEC, and HUVEC were transduced as described above, stained with an antibody against phosphorylated Rb, and examined by immunofluorescence microscopy. Activated Notch4 and Notch1 reduced the proportion of cells expressing phosphorylated Rb in all types of endothelial cells assayed (Fig. 2B). Hence, both Notch4 and Notch1 negatively regulate S-phase entry by a mechanism that prevents phosphorylation of Rb. This finding is consistent with our data showing the inability of activated Notch to overcome the proliferation advantage conferred by SV40 T antigen, which binds and inhibits Rb (4, 17).

Notch4 and Notch1 downregulate $p21^{Cip1}$ expression and inhibit cyclinD-cdk4 nuclear localization. Studies with murine keratinocytes have shown that Notch1-mediated cell cycle arrest is associated with upregulation of the cyclin-dependent kinase inhibitor (CKI) $p21^{Cip1}$ (26). In small-cell lung cancer cells, Notch-mediated cell cycle arrest is associated with induction of two members of the Cip/Kip CKI family, $p21^{Cip1}$ and $p27^{Kip1}$ (36). To determine whether activated Notch4 or Notch1 also upregulates $p21^{Cip1}$ or $p27^{Kip1}$ in endothelial cells, HUVEC-Notch4IC and HUVEC-Notch1IC were immunoblotted for $p21^{Cip1}$ and $p27^{Kip1}$. Surprisingly, both activated Notch4 and Notch1 inhibited $p21^{Cip1}$ expression in endothelial cells, whereas a statistically significant difference in expression of $p27^{Kip1}$ was not detected (Fig. 3A).

In keratinocytes, induction of $p21^{Cip1}$ expression by Notch depends on a mechanism that induces transcriptional activity of the $p21^{Cip1}$ promoter (26). To determine the effect of constitutively active Notch at the $p21^{Cip1}$ promoter in endothelial cells, we performed promoter-luciferase assays in HUVEC cotransfected with a p21-luc construct and with one of empty vector, Notch4IC or Notch1IC. In contrast to the findings reported for keratinocytes, Notch activation repressed $p21^{Cip1}$ promoter activity in HUVEC (Fig. 3B). These data demonstrate that Notch-mediated $p21^{Cip1}$ downregulation in endothelial cells is also dependent on a transcriptional mechanism, albeit with an opposite effect on the $p21^{Cip1}$ promoter compared to keratinocytes, and they implicate cell-specific nuclear events with respect to the $p21^{Cip1}$ promoter activity in the context of Notch activation.

In addition to acting as inhibitors of cdks, $p21^{Cip1}$ and $p27^{Kip1}$ have been shown to promote activation of cyclin D-dependent kinases, which initiate Rb phosphorylation during cell cycle progression (3, 16). The role of the Cip/Kip proteins as activators of cyclinD-cdk4 complexes depends, at least in part, on their ability to bind and target cyclin D and cdk4 to the nucleus (3, 16). To determine whether the lack of $p21^{Cip1}$ leads to decreased nuclear localization of cyclin D and cdk4 in HUVEC-Notch4IC and HUVEC-Notch1IC, asynchronously growing cells were stained with antibodies against cyclin D and cdk4 (Fig. 4A). Both activated Notch4 and Notch1 dramatically reduced nuclear localization of cdk4 and cyclin D (Fig. 4B). These data suggest that Notch activation may decrease Rb phosphorylation and S-phase entry, in part by preventing nuclear localization of cyclin D-cdk4 through the downregulation of $p21^{Cip1}$.

Nuclear localization of Notch4IC inhibits $p21^{Cip1}$ expression at early phases of cell cycle entry and delays activation of cyclinD-cdk4. Based on the findings described above, we further investigated the role of $p21^{Cip1}$ in Notch-mediated cell

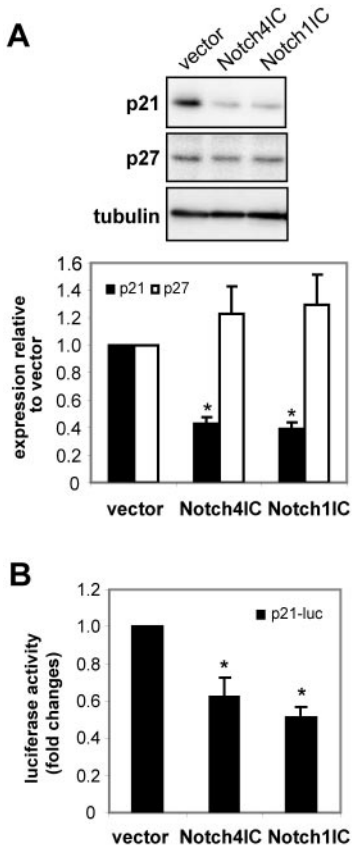

FIG. 3. Activated Notch downregulates $p21^{Cip1}$. (A) HUVEC transduced with MIY (vector), MIY-Notch4IC (Notch4IC), or MIY-Notch1IC (Notch1IC) were assayed by immunoblotting for $p21^{Cip1}$, $p27^{Kip1}$, and tubulin. Immunoblots were analyzed by densitometry and normalized for tubulin. Graphs represent the means ± standard errors of the means from three experiments. *, $P < 0.001$ compared to vector. (B) HUVEC were cotransfected with empty vector (vector), Notch4IC or Notch1IC, a p21 promoter-luciferase construct (p21-luc), and a constitutively active *Renilla* luciferase plasmid. The graphs show relative luciferase activity (means ± standard errors of the means from four experiments, each done in triplicate). *, $P < 0.01$ compared to vector.

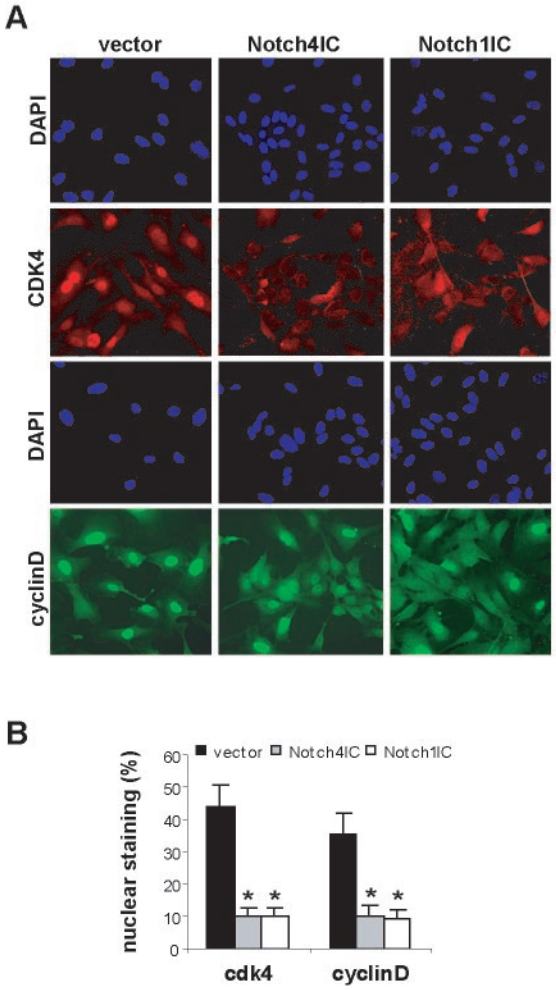

FIG. 4. Activated Notch inhibits nuclear localization of cdk4 and cyclin D. HUVEC transduced with MIY (vector), MIY-Notch4IC (Notch4IC), or MIY-Notch1IC (Notch1IC) were immunostained with antibodies for cdk4 and cyclin D, and the proportion of cells expressing nuclear cdk4 and cyclin D was enumerated by fluorescence microscopy. DAPI staining was used to define nuclear localization and for total cell counts. The graph represents proportions (means ± standard deviations) of cells with prevalent or exclusive nuclear staining from one experiment performed in triplicate. The experiments were repeated twice with similar results. *, $P < 0.01$ compared to vector.

cycle arrest. In order to mimic ligand-induced nuclear localization of Notch4IC, we used a tamoxifen (4-OHT)-inducible system based on the fusion of Notch4IC to the mutated ligand-binding domain of the ER (Notch4IC-ER) (29). HUVEC were transduced with the vector encoding Notch4IC-ER (HUVEC-Notch4IC-ER) or with vector alone (HUVEC-vector). Immunostaining demonstrated translocation of the Notch4IC-ER fusion protein to the nucleus following stimulation with 4-OHT (Fig. 5A). Cell counts at 3-day intervals for 9 days demonstrated reduced growth of 4-OHT-treated HUVEC-Notch4IC-ER compared to HUVEC-vector (Fig. 5B). To verify that reduced growth following nuclear translocation of Notch4IC-ER was associated with G_0/G_1 arrest, HUVEC-vector and HUVEC-Notch4IC-ER were assayed for BrdU incorporation and total DNA content in the absence or presence of 4-OHT. Flow cytometry demonstrated reduced S-phase entry in HUVEC-Notch4IC-ER treated with 4-OHT (Fig. 5C). We have recently shown that activation of Notch4 protects HUVEC against apoptosis, confirming that the inhibition of growth is due to decreased cell proliferation and not to increased apoptosis (19).

To test whether Notch4IC-ER nuclear localization inhibits Rb phosphorylation and to further study the role of Notch4 during cell cycle entry from quiescence, HUVEC were synchronized by serum starvation, pretreated with 4-OHT, and induced to reenter the cell cycle by the addition of serum. Cell cycle profiles were analyzed at the indicated time points, and cell lysates were tested by immunoblotting with an antibody that recognizes both hypophosphorylated and hyperphosphorylated Rb. As expected, upon mitogenic stimulation HUVEC-Notch4IC-ER treated with 4-OHT showed reduced S-phase entry coinciding with a delay in the initiation of Rb phosphorylation (Fig. 5D).

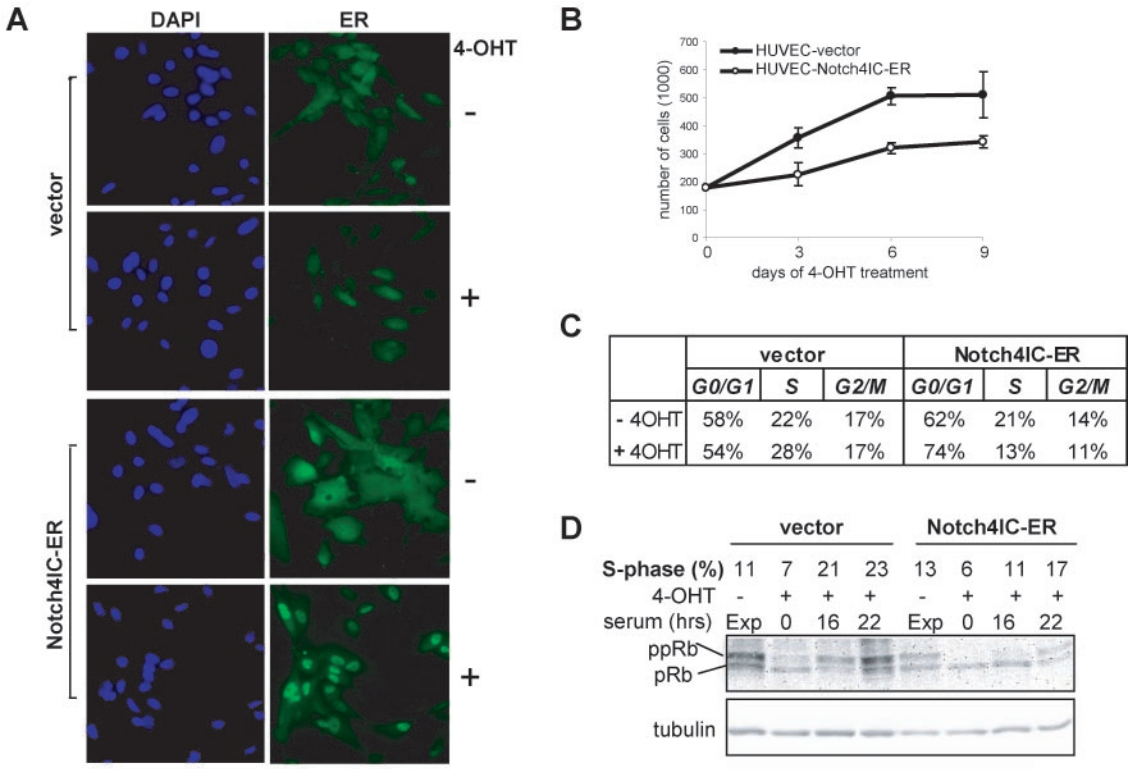

	vector			Notch4IC-ER		
	G0/G1	*S*	*G2/M*	*G0/G1*	*S*	*G2/M*
- 4OHT	58%	22%	17%	62%	21%	14%
+ 4OHT	54%	28%	17%	74%	13%	11%

FIG. 5. Translocation to the nucleus of the Notch4IC-ER fusion protein reduces S-phase entry and Rb phosphorylation in HUVEC. HUVEC were transduced with vector alone or vector encoding the Notch4IC-ER fusion protein and selected in puromycin. (A) Cells treated with 4-OHT (+) and treated with vehicle alone (−) were stained with an antibody against ER. DAPI was used for nuclear staining. (B) Cells (2×10^5) were plated (day 0), and medium containing 4-OHT was replaced daily. Cells were counted by trypan blue exclusion after 3, 6, and 9 days. By 6 days, HUVEC-vector reached confluence. The graph shows the means ± standard deviations for an experiment performed in triplicate. (C) Asynchronously growing HUVEC-vector and HUVEC-Notch4IC-ER were treated for 24 h with 4-OHT (+) or with vehicle alone (−). Cell cycle distributions were analyzed by flow cytometry for BrdU incorporation and DNA content. (D) HUVEC-vector or Notch4IC-ER were synchronized in quiescence by serum starvation and induced to reenter the cell cycle by addition of serum. Cells were treated with 4-OHT (+) to induce Notch4IC-ER nuclear translocation, and asynchronously growing untreated cells (−) were used as a control (Exp). HUVEC were analyzed at the indicated time points by flow cytometry for BrdU incorporation and DNA content and by immunoblotting with an antibody against hypophosphorylated (pRb) and hyperphosphorylated (ppRb) Rb. Tubulin was used as a loading control. The proportion of cells in S phase at each time point is indicated.

Interestingly, in several cell types, $p21^{Cip1}$ is induced following serum stimulation, consistent with a role for $p21^{Cip1}$ as an activator of cyclin D-cdk4 (3, 6, 16, 18, 24, 33). To determine whether serum stimulation upregulates $p21^{Cip1}$ in endothelial cells and whether Notch4 activation inhibits this induction, HUVEC were synchronized by serum starvation and treated as described above. Cells harvested at the indicated time points were tested by immunoblotting for $p21^{Cip1}$ expression. HUVEC-vector showed induction of $p21^{Cip1}$ between 2 and 12 h after serum stimulation, and as expected, this upregulation was inhibited by activation of Notch4IC-ER (Fig. 6A). In contrast, $p27^{Kip1}$ expression was downregulated following serum stimulation, but no differences between HUVEC-vector and HUVEC-Notch4IC-ER were detected (Fig. 6A). To test whether inhibition of $p21^{Cip1}$ induction by Notch4 was associated with reduction of cyclin D-cdk4 kinase activity, cyclin D-cdk4 kinase activity was determined by in vitro kinase assay on a C-terminal Rb fusion protein. Delayed and reduced cyclin D-cdk4 kinase activity was observed in HUVEC-Notch4IC-ER following mitogenic stimulation (Fig. 6B). However, there was no difference in cdk4 or cyclin D expression between control cells and HUVEC-Notch4IC-ER (Fig. 6C; see Fig. S3A in the supplemental material). We also confirmed that $p16^{INK4a}$ (Fig. 6D; see Fig. S3C in the supplemental material) and other CKIs of the INK4 family (data not shown) were not affected by Notch activation. The above data suggest that Notch impairs Rb phosphorylation by preventing induction of $p21^{Cip1}$ and nuclear localization and activation of cyclin D-cdk4 complexes.

$p21^{Cip1}$ is required for nuclear entry of cyclin D-cdk4. Given the inhibitory effect of activated Notch on endothelial cell proliferation and the downregulation of $p21^{Cip1}$ associated with decreased nuclear localization and activation of cyclin D-cdk4, we sought to determine whether reintroduction of $p21^{Cip1}$ into Notch-activated endothelial cells was sufficient to restore nuclear targeting of cyclin D and cdk4. HUVEC-Notch4IC-ER were transduced with MIY vector or MIY encoding $p21^{Cip1}$ (MIY-p21). YFP-positive cells were sorted by flow cytometry, and immunofluorescence staining was used to evaluate cyclin D and cdk4 nuclear expression. As expected, control cells (HUVEC-Notch4IC-ER transduced with MIY) treated with 4-OHT to activate Notch4 showed reduced cyclin D and cdk4 nuclear localization compared to vehicle-treated

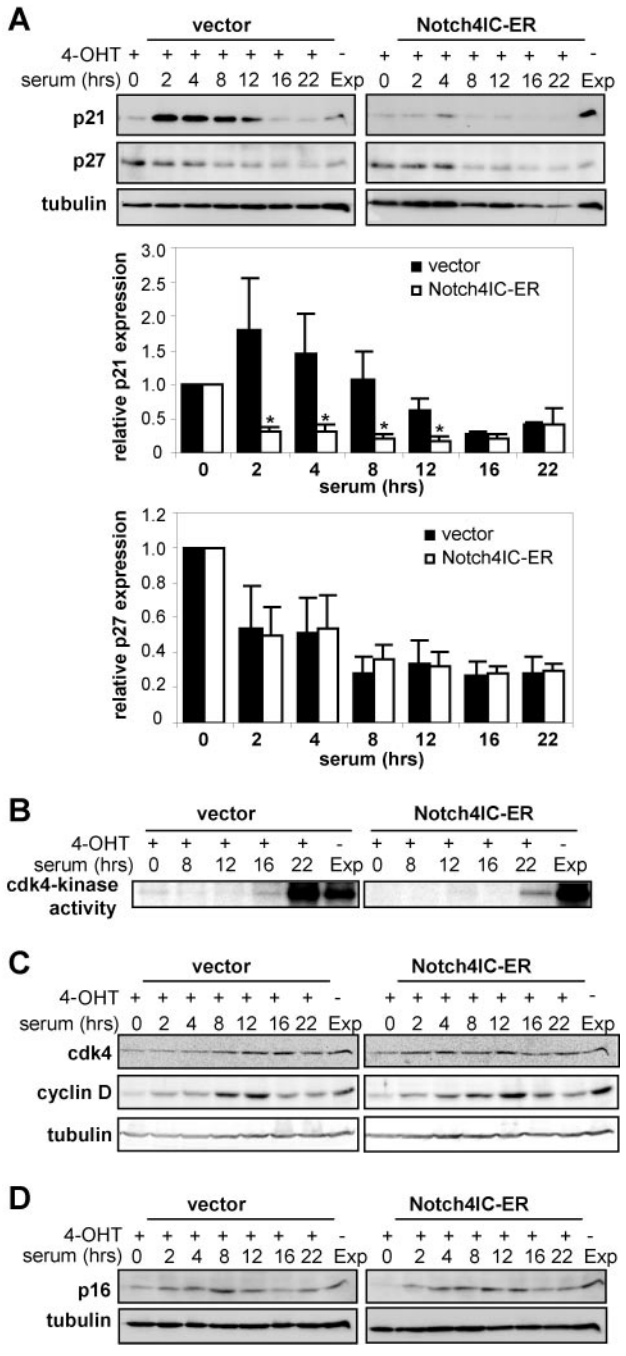

FIG. 6. $p21^{Cip1}$ is required for progression towards S phase in endothelial cells. HUVEC transduced with vector or Notch4IC-ER were synchronized in quiescence by serum starvation and induced to reenter the cell cycle by addition of serum. Cells were treated with 4-OHT (+) to induce Notch4IC-ER nuclear translocation. Untreated (−) asynchronously growing cells were used as a control (Exp). At the indicated times after serum stimulation, cells were assessed for expression of cell cycle regulators. (A) $p21^{Cip1}$ and $p27^{Kip1}$ expression was tested by immunoblotting, analyzed by densitometry, and normalized to tubulin. Graphs represent the means ± standard errors of the means for three experiments. *, $P < 0.001$. (B) Phosphorylation of a C-terminal Rb fusion protein was tested by in vitro kinase assay of immunoprecipitated cdk4 complexes. (C and D) Expression of cdk4 and cyclin D (C) and $p16^{INK4a}$ (D) was assayed by immunoblotting (see also Fig. S3 in the supplemental material).

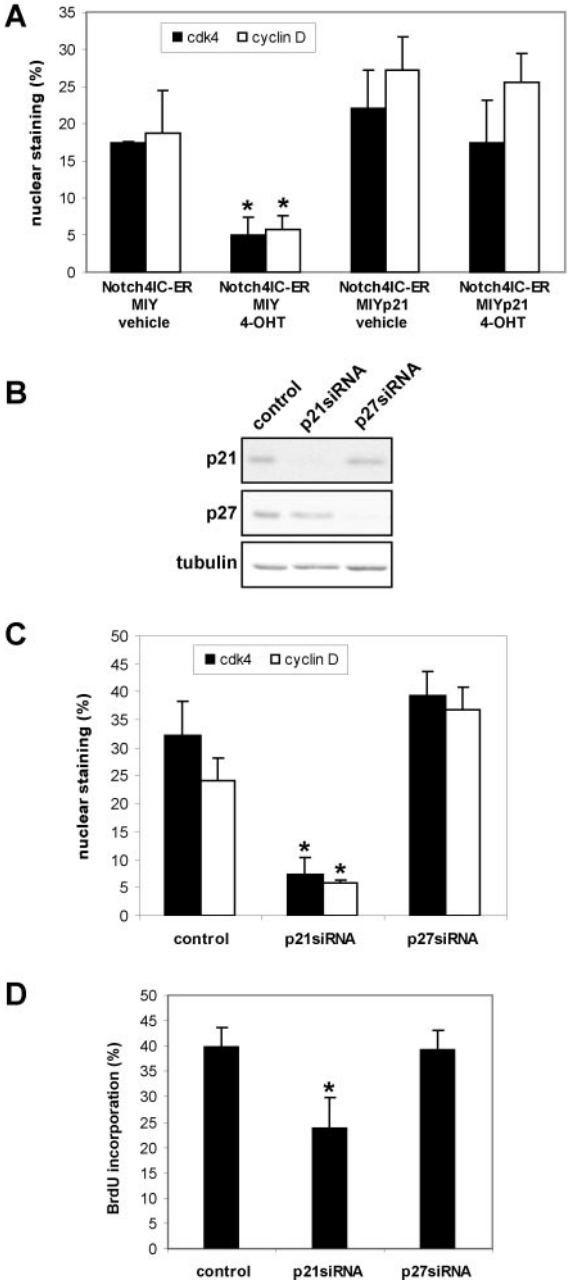

FIG. 7. $p21^{Cip1}$ is essential for cyclin D and cdk4 nuclear localization. (A and B) HUVEC-Notch4IC-ER were transduced with MIY vector (MIY) or MIY encoding $p21^{Cip1}$ (MIYp21). YFP-positive cells were sorted by flow cytometry. Immunofluorescence staining was used to evaluate cyclin D and cdk4 nuclear expression in the presence or absence of 4-OHT. (A) Proportion of cells with prevalent or exclusive cdk4 or cyclin D nuclear staining. The graph represents one experiment done in triplicate (means ± standard deviations) and is representative of two independent experiments. (B, C, and D) Following retroviral delivery of siRNA targeting either $p21^{Cip1}$ (p21siRNA) or $p27^{Kip1}$ (p27siRNA), cells were assayed for expression of $p21^{Cip1}$ and $p27^{Kip1}$ by immunoblotting (B), nuclear localization of cdk4 and cyclin D by immunofluorescence staining (C), and entry into S phase by monitoring BrdU incorporation (D). Empty vector was used as a control. The graph in panel C shows the means ± standard deviations from a single experiment done in triplicate and is representative of two independent experiments. The graph in panel D represents a single experiment done in triplicate (means ± standard deviations) and is representative of three independent experiments. *, $P < 0.05$.

HUVEC-Notch4IC-ER (Fig. 7A). In contrast, enforced expression of $p21^{Cip1}$ permitted cyclin D and cdk4 nuclear localization despite activation of Notch4 (HUVEC-Notch4IC-ER transduced with MIY-p21 and treated with 4-OHT).

Given the capacity of exogenous $p21^{Cip1}$ to rescue cyclin D-cdk4 nuclear localization, we tested whether downregulation of $p21^{Cip1}$ alone was sufficient to block nuclear localization of cyclin D and cdk4 and to impair cell cycle progression in endothelial cells. Retroviral vectors were used to express siRNA against $p21^{Cip1}$ (p21siRNA) or $p27^{Kip1}$ (p27siRNA) (7). HUVEC were infected with empty vector, p21siRNA, or p27siRNA. After antibiotic selection, exponentially growing cells were tested by immunoblotting for expression of Cip1/Kip1 proteins. In HUVEC, transduction of p21siRNA and p27siRNA specifically decreased expression of $p21^{Cip1}$ and $p27^{Kip1}$, respectively (Fig. 7B). While cells lacking $p21^{Cip1}$ were defective in targeting cdk4 and cyclin D to the nucleus, the absence of $p27^{Kip1}$ did not affect the nuclear translocation of cdk4 or cyclin D (Fig. 7C). This is not surprising given the fact that only $p21^{Cip1}$ is induced by mitogens in primary endothelial cells entering the cell cycle (Fig. 6A). Furthermore, the lack of $p21^{Cip1}$ was sufficient to reduce S-phase entry in endothelial cells, whereas targeted downregulation of $p27^{Kip1}$ had no effect on this process (Fig. 7D). Taken together, our data provide evidence for a role of $p21^{Cip1}$ in initiating endothelial cell cycle progression, as well as a mechanism for Notch-induced endothelial cell cycle arrest.

Endothelial cell-cell contact activates the Notch pathway and downregulates $p21^{Cip1}$ expression. As we have shown above, endothelial cells from different vascular beds express Notch receptors and their ligands. Cell fate control by Notch during development requires cell-cell contact in a process referred to as lateral inhibition (1). Thus, we hypothesized that endothelial cell-cell contact would activate Notch. To test this hypothesis HUVEC were plated at low density (~30% confluent), medium density (~60% confluent), and high density (100% confluent) and assayed for Notch activation. The Hairy-related transcription factor HRT1 is a target gene of Notch activation in endothelial cells (9, 39). To monitor Notch activation, expression of HRT1 was analyzed by RT-PCR. Upregulation of HRT1 correlated with increasing confluence of HUVEC (Fig. 8A; see Fig. S4A in the supplemental material) as well as HAEC and HMVEC (data not shown). To determine whether activation of endogenous Notch as a result of cell-cell contact would reduce $p21^{Cip1}$ expression, cell lysates from HUVEC at various levels of confluence were immunoblotted for $p21^{Cip1}$ and $p27^{Kip1}$. As expected, at high HUVEC density, Notch activation was associated with downregulation of $p21^{Cip1}$ (Fig. 8A; see Fig. S4B in the supplemental material), and as previously described for endothelial and other cell types, HUVEC showed induction of $p27^{Kip1}$ at increasing density (Fig. 8A; see Fig. S4C in the supplemental material) (10, 25). To confirm that the density-dependent downregulation of $p21^{Cip1}$ was mediated by activation of Notch, we used the γ-secretase inhibitor DFP-AA, which inhibits Notch activation by preventing ligand-dependent cleavage of Notch (21, 30, 42). Treatment with DFP-AA abolished downregulation of $p21^{Cip1}$ in HUVEC plated at high density, thus confirming the role of Notch activation (Fig. 8B; see Fig. S4D in the supplemental material). In contrast, induction of $p27^{Kip1}$ was not affected by DFP-AA (Fig. 8B; see Fig. S4E in the supplemental material), confirming that regulation of $p27^{Kip1}$ expression does not depend on Notch activation in endothelial cells. To determine whether maintenance of higher levels of $p21^{Cip1}$ as a result of Notch inhibition would promote Rb phosphorylation in confluent endothelial cells, HUVEC at high density were treated with DFP-AA for 2 days and stained by immunofluorescence with an antibody against phosphorylated Rb. The results show an increased proportion of cells expressing phosphorylated Rb in confluent endothelial cells treated with DFP-AA (Fig. 8C), suggesting that inhibition of Notch affects the capacity of confluent endothelial cells to impede cell cycle progression. These findings suggest that Notch activation may be involved in the phenomenon of contact inhibition, in part through downregulation of $p21^{Cip1}$.

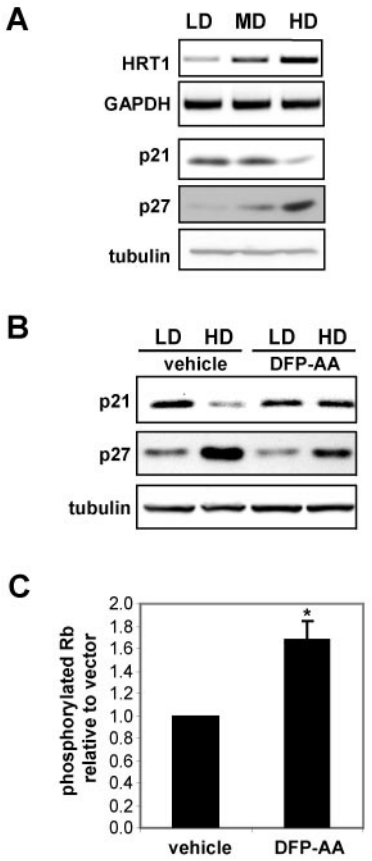

FIG. 8. Endothelial cell-cell interactions activate the Notch pathway and downregulate $p21^{Cip1}$. (A) HUVEC were plated at low (LD) (~30% confluent), medium (MD) (~60% confluent), and high (HD) (100% confluent) densities. mRNA expression of the Notch target gene HRT-1 and GAPDH was assayed by RT-PCR. Expression of $p21^{Cip1}$ and $p27^{Kip1}$ was assessed by immunoblotting. GAPDH, glyceraldehyde-3-phosphate dehydrogenase. (B) HUVEC at LD and HD were treated with the γ-secretase inhibitor DFP-AA (0.1 μM) or with vehicle alone, and $p21^{Cip1}$ and $p27^{Kip1}$ expression was assayed by immunoblotting. (C) HUVEC plated at HD underwent 48 h of treatment with DFP-AA (0.1 μM) or vehicle alone and were stained by immunofluorescence with an antibody against phosphorylated Rb. DAPI staining was used for total cell counts. Graphs represent the means ± standard errors of the means for four experiments. *, $P < 0.005$. See also Fig. S4 in the supplemental material.

DISCUSSION

The demonstration that Notch activation prevents mitogen-induced $p21^{Cip1}$ upregulation in endothelial cells provides a novel mechanism for Notch-mediated inhibition of proliferation. Our findings suggest that activation of the Notch pathway is involved in the phenomenon of contact inhibition in the endothelium, supporting the hypothesis that Notch participates in the control of vessel homeostasis by maintaining endothelial cell quiescence (9). Interestingly, it has previously been shown that $p21^{Cip1}$ is not expressed in the intima of quiescent adult vessels but is induced 7 days after balloon injury, when a high proportion of cells are proliferating (44). Given the requirement for endothelial cell proliferation during angiogenesis, the antiproliferative effect mediated by Notch explains, at least in part, the defects in vascular remodeling secondary to Notch4 activation in endothelial cells (17, 40). Further, the observation that Notch is not activated early in angiogenesis when endothelial cells begin to proliferate but is reactivated as vessels stabilize complements our data showing that Notch is activated at confluence with concomitant downregulation of $p21^{Cip1}$ (9).

Notch1 is also expressed on endothelial cells, and our data support the notion of a redundancy of function of Notch4 and Notch1 by demonstrating that both members of the Notch family regulate endothelial cell proliferation via a mechanism that converges on inhibition of Rb phosphorylation (15).

Previous studies demonstrate a dual function for $p21^{Cip1}$ that depends on the relative level of expression; low levels of $p21^{Cip1}$ activate cyclin D-ckd4, but at higher $p21^{Cip1}$/cyclin D-cdk4 stoichiometric ratios, $p21^{Cip1}$ becomes an inhibitor (16, 32). Our studies showing upregulation of $p21^{Cip1}$ upon serum stimulation and downregulation of $p21^{Cip1}$ in confluent endothelial cells imply that $p21^{Cip1}$ has a role in endothelial cell cycle progression. Our data indicate that one mechanism through which Notch interferes with the cell cycle machinery in endothelial cells is the downregulation of $p21^{Cip1}$, which impairs cyclin D-cdk4 nuclear localization and activation. We show that exogenous $p21^{Cip1}$ restores cyclin D-cdk4 nuclear localization in cells expressing activated Notch4. Accordingly, siRNA-targeted downregulation of endogenous $p21^{Cip1}$ hampers nuclear localization of cyclin D and cdk4 and also impairs the capacity of endothelial cells to enter S phase. Although both $p21^{Cip1}$ and $p27^{Kip1}$ have been reported to shuttle cyclin D and cdk4 to the nucleus, we show that only targeted knockdown of $p21^{Cip1}$ inhibits cyclin D and cdk4 nuclear localization in endothelial cells (3, 16). This is likely related to the fact that only $p21^{Cip1}$ is induced during progression towards S phase, whereas $p27^{Kip1}$ is downregulated following serum stimulation but is induced at confluence. Previous studies have shown that murine embryonic fibroblasts that are null for $p21^{Cip1}$ and $p27^{Kip1}$ demonstrate reduced cyclin D-cdk4 nuclear translocation and Rb kinase activity but no apparent defects in proliferation (3). It is likely that targeted downregulation of $p21^{Cip1}$ by RNA interference in adult cells has an acute effect that cannot be evaded by compensatory mechanisms, as may be seen in gene-targeted animals. Alternatively, $p21^{Cip1}$ may have a role in cell cycle regulation that is cell type specific. The fact that other cell types show upregulation of $p21^{Cip1}$ with Notch activation indicates that Notch-mediated regulation of expression is modulated by cell-type-specific factors (1, 38). Our data suggest that the specificity of action of Notch on the regulation of $p21^{Cip1}$ expression may depend on cell-type-specific partners of Notch that are involved in the control of the $p21^{Cip1}$ promoter.

Other signaling mechanisms must also be required for Notch-induced cell cycle arrest, since reduction of S-phase entry mediated by targeted downregulation of $p21^{Cip1}$ is not as efficient as the block mediated by Notch. Additionally, Notch must act in concert with other signaling mechanisms, as indicated by a Notch-independent upregulation of $p27^{Kip1}$ at confluence. In conclusion, our studies provide strong evidence that Notch activation participates in the phenomenon of endothelial cell contact inhibition, in part through downregulation of $p21^{Cip1}$.

ACKNOWLEDGMENTS

We thank F. Wong and I. Pollet for technical help, R. E. Durand and D. McDougal for assistance with flow cytometry and cell sorting, and K. G. Leong for reviewing the manuscript.

This research was supported by grants to A.K. from the Heart and Stroke Foundation of British Columbia and Yukon, the National Cancer Institute of Canada with funds from the Canadian Cancer Society, and the Canadian Institutes of Health Research and to B.E.C. from the NIH (CA84069). M.N. was supported by a fellowship from Fondazione Italiana per la Ricerca sul Cancro, a fellowship from the Canadian Institutes of Health Research, and a Research Trainee Award from the Michael Smith Foundation for Health Research. G.M. was supported by a Research Trainee Award from the Michael Smith Foundation for Health Research. B.E.C. is a W. M. Keck Distinguished Young Scholar in Medical Research. A.K. is a Clinician-Scientist of the Canadian Institutes of Health Research and a Scholar of the Michael Smith Foundation for Health Research.

REFERENCES

1. **Artavanis-Tsakonas, S., M. D. Rand, and R. J. Lake.** 1999. Notch signaling: cell fate control and signal integration in development. Science **284:**770–776.
2. **Carlesso, N., J. C. Aster, J. Sklar, and D. T. Scadden.** 1999. Notch1-induced delay of human hematopoietic progenitor cell differentiation is associated with altered cell cycle kinetics. Blood **93:**838–848.
3. **Cheng, M., P. Olivier, J. A. Diehl, M. Fero, M. F. Roussel, J. M. Roberts, and C. J. Sherr.** 1999. The p21(Cip1) and p27(Kip1) CDK 'inhibitors' are essential activators of cyclin D-dependent kinases in murine fibroblasts. EMBO J. **18:**1571–1583.
4. **DeCaprio, J. A., J. W. Ludlow, J. Figge, J. Y. Shew, C. M. Huang, W. H. Lee, E. Marsilio, E. Paucha, and D. M. Livingston.** 1988. SV40 large tumor antigen forms a specific complex with the product of the retinoblastoma susceptibility gene. Cell **54:**275–283.
5. **el-Deiry, W. S., T. Tokino, V. E. Velculescu, D. B. Levy, R. Parsons, J. M. Trent, D. Lin, W. E. Mercer, K. W. Kinzler, and B. Vogelstein.** 1993. WAF1, a potential mediator of p53 tumor suppression. Cell **75:**817–825.
6. **Firpo, E. J., A. Koff, M. J. Solomon, and J. M. Roberts.** 1994. Inactivation of a Cdk2 inhibitor during interleukin 2-induced proliferation of human T lymphocytes. Mol. Cell. Biol. **14:**4889–4901.
7. **Grandori, C., K. J. Wu, P. Fernandez, C. Ngouenet, J. Grim, B. E. Clurman, M. J. Moser, J. Oshima, D. W. Russell, K. Swisshelm, S. Frank, B. Amati, R. Dalla-Favera, and R. J. Monnat, Jr.** 2003. Werner syndrome protein limits MYC-induced cellular senescence. Genes Dev. **17:**1569–1574.
8. **Hanahan, D., and J. Folkman.** 1996. Patterns and emerging mechanisms of the angiogenic switch during tumorigenesis. Cell **86:**353–364.
9. **Henderson, A. M., S. J. Wang, A. C. Taylor, M. Aitkenhead, and C. C. Hughes.** 2001. The basic helix-loop-helix transcription factor HESR1 regulates endothelial cell tube formation. J. Biol. Chem. **276:**6169–6176.
10. **Hirano, M., K. Hirano, J. Nishimura, and H. Kanaide.** 2001. Transcriptional up-regulation of p27(Kip1) during contact-induced growth arrest in vascular endothelial cells. Exp. Cell Res. **271:**356–367.
11. **Hobson, B., and J. Denekamp.** 1984. Endothelial proliferation in tumours and normal tissues: continuous labelling studies. Br. J. Cancer **49:**405–413.
12. **Iso, T., Y. Hamamori, and L. Kedes.** 2003. Notch signaling in vascular development. Arterioscler. Thromb. Vasc. Biol. **23:**543–553.
13. **Jundt, F., I. Anagnostopoulos, R. Forster, S. Mathas, H. Stein, and B. Dorken.** 2002. Activated Notch1 signaling promotes tumor cell proliferation and survival in Hodgkin and anaplastic large cell lymphoma. Blood **99:**3398–3403.

14. **Karsan, A., E. Yee, G. G. Poirier, P. Zhou, R. Craig, and J. M. Harlan.** 1997. Fibroblast growth factor-2 inhibits endothelial cell apoptosis by Bcl-2-dependent and independent mechanisms. Am. J. Pathol. **151:**1775–1784.
15. **Krebs, L. T., Y. Xue, C. R. Norton, J. R. Shutter, M. Maguire, J. P. Sundberg, D. Gallahan, V. Closson, J. Kitajewski, R. Callahan, G. H. Smith, K. L. Stark, and T. Gridley.** 2000. Notch signaling is essential for vascular morphogenesis in mice. Genes Dev. **14:**1343–1352.
16. **LaBaer, J., M. D. Garrett, L. F. Stevenson, J. M. Slingerland, C. Sandhu, H. S. Chou, A. Fattaey, and E. Harlow.** 1997. New functional activities for the p21 family of CDK inhibitors. Genes Dev. **11:**847–862.
17. **Leong, K. G., X. Hu, L. Li, M. Noseda, B. Larrivee, C. Hull, L. Hood, F. Wong, and A. Karsan.** 2002. Activated Notch4 inhibits angiogenesis: role of beta 1-integrin activation. Mol. Cell. Biol. **22:**2830–2841.
18. **Li, Y., C. W. Jenkins, M. A. Nichols, and Y. Xiong.** 1994. Cell cycle expression and p53 regulation of the cyclin-dependent kinase inhibitor p21. Oncogene **9:**2261–2268.
19. **MacKenzie, F., P. Duriez, F. Wong, M. Noseda, and A. Karsan.** 2004. Notch4 inhibits endothelial apoptosis via RBP-Jkappa-dependent and -independent pathways. J. Biol. Chem. **279:**11657–11663.
20. **Mailhos, C., U. Modlich, J. Lewis, A. Harris, R. Bicknell, and D. Ish-Horowicz.** 2001. Delta4, an endothelial specific notch ligand expressed at sites of physiological and tumor angiogenesis. Differentiation **69:**135–144.
21. **Micchelli, C. A., W. P. Esler, W. T. Kimberly, C. Jack, O. Berezovska, A. Kornilova, B. T. Hyman, N. Perrimon, and M. S. Wolfe.** 2003. Gamma-secretase/presenilin inhibitors for Alzheimer's disease phenocopy Notch mutations in Drosophila. FASEB J. **17:**79–81.
22. **Nakajima, M., S. Yuasa, M. Ueno, N. Takakura, H. Koseki, and T. Shirasawa.** 2003. Abnormal blood vessel development in mice lacking presenilin-1. Mech. Dev. **120:**657–667.
23. **Noseda, M., G. McLean, K. Niessen, L. Chang, I. Pollet, R. Montpetit, R. Shahidi, K. Dorovini-Zis, L. Li, B. Beckstead, R. E. Durand, P. A. Hoodless, and A. Karsan.** 2004. Notch activation results in phenotypic and functional changes consistent with endothelial-to-mesenchymal transformation. Circ. Res. **94:**910–917.
24. **Nourse, J., E. Firpo, W. M. Flanagan, S. Coats, K. Polyak, M. H. Lee, J. Massague, G. R. Crabtree, and J. M. Roberts.** 1994. Interleukin-2-mediated elimination of the p27Kip1 cyclin-dependent kinase inhibitor prevented by rapamycin. Nature **372:**570–573.
25. **Polyak, K., J. Y. Kato, M. J. Solomon, C. J. Sherr, J. Massague, J. M. Roberts, and A. Koff.** 1994. p27Kip1, a cyclin-Cdk inhibitor, links transforming growth factor-beta and contact inhibition to cell cycle arrest. Genes Dev. **8:**9–22.
26. **Rangarajan, A., C. Talora, R. Okuyama, M. Nicolas, C. Mammucari, H. Oh, J. C. Aster, S. Krishna, D. Metzger, P. Chambon, L. Miele, M. Aguet, F. Radtke, and G. P. Dotto.** 2001. Notch signaling is a direct determinant of keratinocyte growth arrest and entry into differentiation. EMBO J. **20:**3427–3436.
27. **Reaume, A. G., R. A. Conlon, R. Zirngibl, T. P. Yamaguchi, and J. Rossant.** 1992. Expression analysis of a Notch homologue in the mouse embryo. Dev. Biol. **154:**377–387.
28. **Ronchini, C., and A. J. Capobianco.** 2001. Induction of cyclin D1 transcription and CDK2 activity by Notch(ic): implication for cell cycle disruption in transformation by Notch(ic). Mol. Cell. Biol. **21:**5925–5934.
29. **Ronchini, C., and A. J. Capobianco.** 2000. Notch(ic)-ER chimeras display hormone-dependent transformation, nuclear accumulation, phosphorylation and CBF1 activation. Oncogene **19:**3914–3924.
30. **Seiffert, D., J. D. Bradley, C. M. Rominger, D. H. Rominger, F. Yang, J. E. Meredith, Jr., Q. Wang, A. H. Roach, L. A. Thompson, S. M. Spitz, J. N. Higaki, S. R. Prakash, A. P. Combs, R. A. Copeland, S. P. Arneric, P. R. Hartig, D. W. Robertson, B. Cordell, A. M. Stern, R. E. Olson, and R. Zaczek.** 2000. Presenilin-1 and -2 are molecular targets for gamma-secretase inhibitors. J. Biol. Chem. **275:**34086–34091.
31. **Shen, J., R. T. Bronson, D. F. Chen, W. Xia, D. J. Selkoe, and S. Tonegawa.** 1997. Skeletal and CNS defects in Presenilin-1-deficient mice. Cell **89:**629–639.
32. **Sherr, C. J.** 2000. Cancer cell cycles revisited. Cancer Res. **60:**3689–3695.
33. **Sherr, C. J., and J. M. Roberts.** 1995. Inhibitors of mammalian G1 cyclin-dependent kinases. Genes Dev. **9:**1149–1163.
34. **Shirayoshi, Y., Y. Yuasa, T. Suzuki, K. Sugaya, E. Kawase, T. Ikemura, and N. Nakatsuji.** 1997. Proto-oncogene of int-3, a mouse Notch homologue, is expressed in endothelial cells during early embryogenesis. Genes Cells **2:**213–224.
35. **Shutter, J. R., S. Scully, W. Fan, W. G. Richards, J. Kitajewski, G. A. Deblandre, C. R. Kintner, and K. L. Stark.** 2000. Dll4, a novel Notch ligand expressed in arterial endothelium. Genes Dev. **14:**1313–1318.
36. **Sriuranpong, V., M. W. Borges, R. K. Ravi, D. R. Arnold, B. D. Nelkin, S. B. Baylin, and D. W. Ball.** 2001. Notch signaling induces cell cycle arrest in small cell lung cancer cells. Cancer Res. **61:**3200–3205.
37. **Taichman, D. B., K. M. Loomes, S. K. Schachtner, S. Guttentag, C. Vu, P. Williams, R. J. Oakey, and H. S. Baldwin.** 2002. Notch1 and Jagged1 expression by the developing pulmonary vasculature. Dev. Dyn. **225:**166–175.
38. **Talora, C., D. C. Sgroi, C. P. Crum, and G. P. Dotto.** 2002. Specific down-modulation of Notch1 signaling in cervical cancer cells is required for sustained HPV-E6/E7 expression and late steps of malignant transformation. Genes Dev. **16:**2252–2263.
39. **Taylor, K. L., A. M. Henderson, and C. C. Hughes.** 2002. Notch activation during endothelial cell network formation in vitro targets the basic HLH transcription factor HESR-1 and downregulates VEGFR-2/KDR expression. Microvasc. Res. **64:**372–383.
40. **Uyttendaele, H., J. Ho, J. Rossant, and J. Kitajewski.** 2001. Vascular patterning defects associated with expression of activated Notch4 in embryonic endothelium. Proc. Natl. Acad. Sci. USA **98:**5643–5648.
41. **Uyttendaele, H., G. Marazzi, G. Wu, Q. Yan, D. Sassoon, and J. Kitajewski.** 1996. Notch4/int-3, a mammary proto-oncogene, is an endothelial cell-specific mammalian Notch gene. Development **122:**2251–2259.
42. **Weng, A. P., Y. Nam, M. S. Wolfe, W. S. Pear, J. D. Griffin, S. C. Blacklow, and J. C. Aster.** 2003. Growth suppression of pre-T acute lymphoblastic leukemia cells by inhibition of notch signaling. Mol. Cell. Biol. **23:**655–664.
43. **Xue, Y., X. Gao, C. E. Lindsell, C. R. Norton, B. Chang, C. Hicks, M. Gendron-Maguire, E. B. Rand, G. Weinmaster, and T. Gridley.** 1999. Embryonic lethality and vascular defects in mice lacking the Notch ligand Jagged1. Hum. Mol Genet. **8:**723–730.
44. **Yang, Z. Y., R. D. Simari, N. D. Perkins, H. San, D. Gordon, G. J. Nabel, and E. G. Nabel.** 1996. Role of the p21 cyclin-dependent kinase inhibitor in limiting intimal cell proliferation in response to arterial injury. Proc. Natl. Acad. Sci. USA **93:**7905–7910.
45. **Zhang, W. W., S. Labrecque, E. Azoulay, R. Dudley, and G. Matlashewski.** 2001. Development of a p53 responsive GFP reporter; identification of live cells with p53 activity. J. Biotechnol. **84:**79–86.

THE JOURNAL OF BIOLOGICAL CHEMISTRY VOL. 284, NO. 29, pp. 19452–19462, July 17, 2009

Differential Regulation of Transforming Growth Factor β Signaling Pathways by Notch in Human Endothelial Cells*[S]

Received for publication, January 20, 2009, and in revised form, April 22, 2009 Published, JBC Papers in Press, May 27, 2009, DOI 10.1074/jbc.M109.011833

YangXin Fu[‡§1], Alex Chang[‡], Linda Chang[‡2], Kyle Niessen[‡2], Shawn Eapen[‡], Audi Setiadi[‡], and Aly Karsan[‡§3]

From the [‡]British Columbia Cancer Agency and the [§]Department of Pathology and Laboratory Medicine, University of British Columbia, Vancouver, British Columbia V5Z IL3, Canada

Notch and transforming growth factor β (TGFβ) play critical roles in endothelial-to-mesenchymal transition (EndMT), a process that is essential for heart development. Previously, we have shown that Notch and TGFβ signaling synergistically induce Snail expression in endothelial cells, which is required for EndMT in cardiac cushion morphogenesis. Here, we report that Notch activation modulates TGFβ signaling pathways in a receptor-activated Smad (R-Smad)-specific manner. Notch activation inhibits TGFβ/Smad1 and TGFβ/Smad2 signaling pathways by decreasing the expression of Smad1 and Smad2 and their target genes. In contrast, Notch increases *SMAD3* mRNA expression and protein half-life and regulates the expression of TGFβ/Smad3 target genes in a gene-specific manner. Inhibition of Notch in the cardiac cushion of mouse embryonic hearts reduces Smad3 expression. Notch and TGFβ synergistically upregulate a subset of genes by recruiting Smad3 to both Smad and CSL binding sites and cooperatively inducing histone H4 acetylation. This is the first evidence that Notch activation affects R-Smad expression and that cooperative induction of histone acetylation at specific promoters underlies the selective synergy between Notch and TGFβ signaling pathways.

During heart development, a subset of endocardial cells undergoes endothelial-to-mesenchymal transition (EndMT)[4] and migrates into the cardiac cushion to initiate valve formation (1). EndMT is regulated by multiple signaling pathways, including TGFβ and Notch (1). Although both pathways play critical roles in cardiovascular development (2–4), their functional interaction in endothelial cells remains to be fully investigated. We have previously shown that Notch and TGFβ synergistically induce expression of *SNAIL* and *HEY1* in endothelial cells (5), both of which play roles in cardiac cushion development (6, 7), suggesting functional integration between Notch and TGFβ signaling pathways in endothelial cells during heart development.

TGFβ is a multifunctional growth factor that is involved in many biological processes, including proliferation, differentiation, and apoptosis (8, 9). The TGFβ signal is transmitted through specific transmembrane type I and type II serine/threonine kinase receptors. Upon TGFβ binding, the constitutively active TGFβ type II receptor recruits and phosphorylates TGFβ type I receptor, and the latter phosphorylates receptor-activated Smads (R-Smads), including Smad1, Smad2, Smad3, Smad5, and Smad8. The phosphorylated R-Smads then form a complex with a common Smad, Smad4, and translocate into the nucleus to regulate target gene expression through interaction with other cofactors (10). In endothelial cells, TGFβ binds two distinct type I receptors, ALK1 (activin receptor-like kinase 1) and ALK5, to activate ALK1/Smad1/5/8 and ALK5/Smad2/3 signaling pathways. These two pathways regulate different genes and exert opposing biological functions in endothelial cells (11, 12).

The evolutionarily conserved Notch signaling pathway determines cell fate by regulating multiple cellular processes, including proliferation, differentiation, and apoptosis (13, 14). In mammals, four Notch receptors (Notch1–Notch4) and five ligands (Dll1 (Delta-like 1), Dll3, Dll4, Jagged1, and Jagged2) have been identified. Notch signaling is initiated by ligand binding, which triggers proteolytic cleavage of the transmembrane receptor and release of the Notch intracellular domain (NICD). Translocation of NICD into the nucleus results in association with the DNA-binding protein CSL and recruitment of coactivators, such as MAML (Mastermind-like) to initiate transcription (15–17).

Cross-talk between the Notch and TGFβ pathways has not been studied in endothelial cells, where both the Smad1/5/8 and Smad2/3 pathways can be activated in the same cell via ALK1 and ALK5 receptors, respectively (11, 12). Both synergy and antagonism between Notch and TGFβ signaling have been reported in other cell types, and the interaction between Notch and TGFβ signaling appears to be cell type- and context-dependent (18–24). Further, in previous studies, Notch signaling was activated by overexpression of the constitutively active NICD. In the current studies, we have attempted to understand the functional consequences of

* This work was supported in part by Canadian Institutes of Health Research Grant MOP-64354 and grants from the Heart and Stroke Foundation of British Columbia and the Yukon, the Canadian Cancer Society, Genome Canada, and Genome British Columbia.

[S] The on-line version of this article (available at http://www.jbc.org) contains supplemental Tables 1–4 and Figs. 1 and 2.

[1] Supported by postdoctoral awards from the Michael Smith Foundation for Health Research and the Stem Cell Network Centres of Excellence.

[2] Supported by doctoral research awards from the Michael Smith Foundation for Health Research.

[3] Senior Scholar of the Michael Smith Foundation for Health Research. To whom correspondence should be addressed: British Columbia Cancer Research Centre, 675W 10th Ave., Vancouver, British Columbia V5Z 1L3, Canada. Tel.: 604-675-8033; Fax: 604-675-8049; E-mail: akarsan@bccrc.ca.

[4] The abbreviations used are: EndMT, endothelial-to-mesenchymal transition; NICD, Notch intracellular domain; H3K4Me3, trimethylated histone 3 on lysine 4; TGF, transforming growth factor; R-Smad, receptor-activated Smad; SBE, Smad binding element; HA, hemagglutinin; HMEC, human microvascular endothelial cell(s); qRT, quantitative reverse transcription; qPCR, quantitative PCR; dnMAML1, dominant negative MAML1; En, embryonic day n; DAPI, 4′,6-diamidino-2-phenylindole; ChIP, chromatin immunoprecipitation; GAPDH, glyceraldehyde-3-phosphate dehydrogenase.

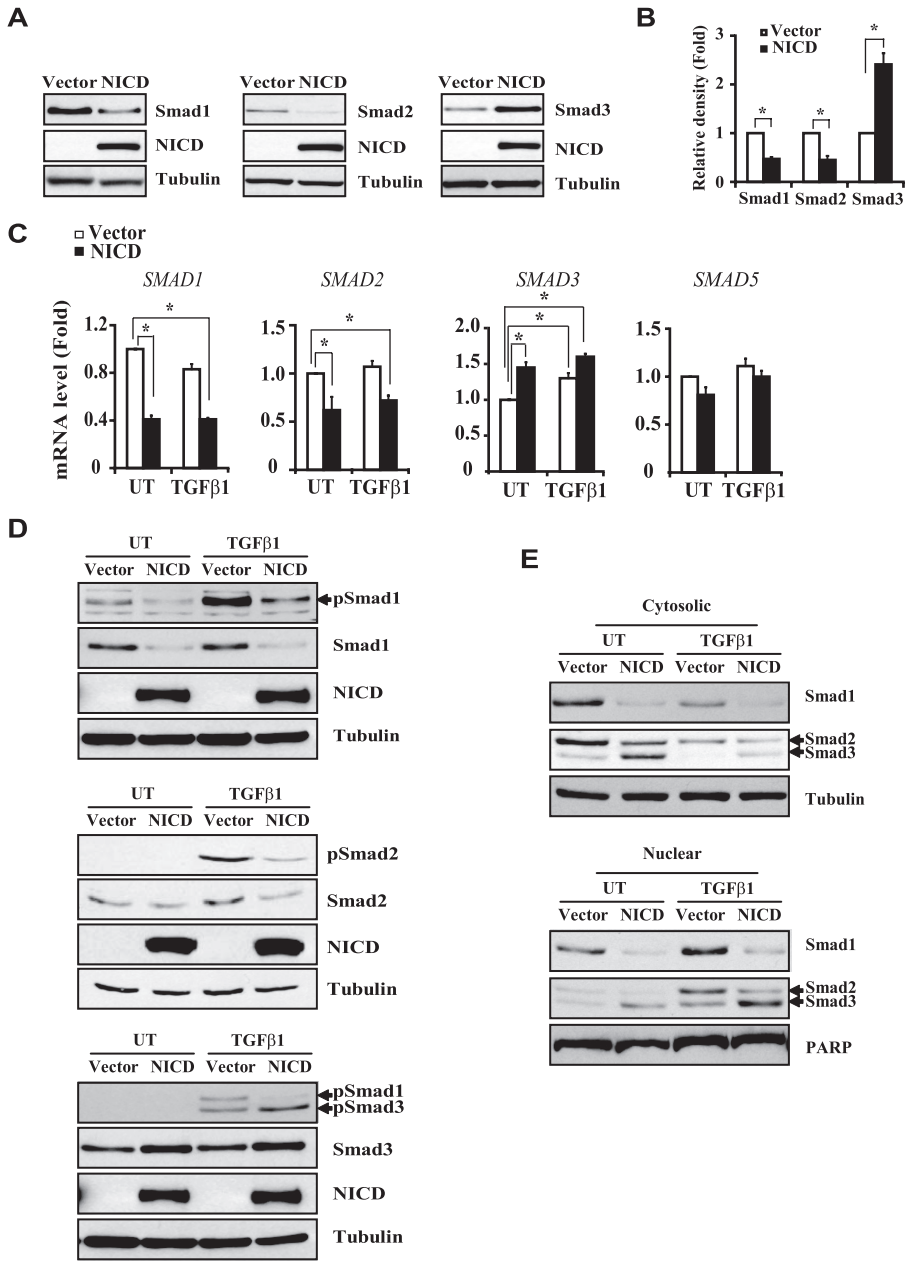

FIGURE 1. **NICD affects the expression and TGFβ-induced phosphorylation of R-Smads.** HMEC were transduced with empty vector or NICD. *A*, protein expression of R-Smads in whole cell lysates was examined by immunoblotting. *B*, R-Smad band intensity was measured by densitometry and normalized to tubulin. The relative density of R-Smad proteins was expressed as the -fold changes relative to the vector control and shown as the mean ± S.E. of three or four independent experiments. *, $p < 0.05$. *C*, HMEC transduced with empty vector or NICD were left untreated (*UT*) or treated with 2.5 ng/ml TGFβ1 for 2 h. R-Smad mRNA level was examined by qRT-PCR and normalized to GAPDH. mRNA levels were expressed as -fold changes relative to the untreated vector samples and shown as mean ± S.E. of three independent experiments. *, $p < 0.05$. *D*, HMEC transduced with empty vector or NICD were left untreated or treated with 2.5 ng/ml TGFβ1 for 1 h. The amount of total and phosphorylated R-Smad proteins in whole cell lysates was examined by immunoblotting. Tubulin was used as a loading control. *E*, R-Smad protein level in cytosolic and nuclear fractions was examined by immunoblotting. Tubulin and poly(ADP-ribose) polymerase (*PARP*) were used as loading controls for cytosolic and nuclear fractions, respectively.

coordinate TGFβ and Notch activation at physiologic levels in the endothelium.

Dll4 (Delta-like 4) is the major Notch ligand expressed in endothelial cells (25), and Dll4 activation of Notch plays an important role in cardiovascular development (26). Here, we report for the first time that in endothelial cells, Notch activation by either NICD expression or co-culture of Dll4-expressing cells regulates TGFβ ALK1/Smad1, ALK5/Smad2, and ALK5/Smad3 signaling pathways by differentially affecting the expression of these R-Smads. Notch activation decreases the expression of Smad1 and Smad2 and their target genes, whereas Notch increases expression of Smad3 and regulates target genes in a gene-specific manner. Notch not only increases *SMAD3* mRNA levels but also prolongs Smad3 protein half-life. *In vivo* endothelium-specific inhibition of Notch signaling by the expression of dominant negative MAML1 reduces Smad3 expression in the cardiac cushion of mouse embryonic hearts. Importantly, we demonstrate that simultaneous activation of TGFβ and Notch signaling recruits Smad3 to both Smad binding elements (SBEs) and CSL binding sites and cooperatively increases histone H4 acetylation at promoters in which consensus *cis* elements of both pathways are present. Our findings provide a molecular mechanism for the synergistic induction of a subset of TGFβ and Notch target genes, and demonstrate the crucial role of this interaction *in vivo*.

EXPERIMENTAL PROCEDURES

Antibodies—Rabbit anti-Smad1 and Smad2 antibodies were acquired from Zymed Laboratories Inc. (San Francisco, CA). Rabbit anti-Smad3, anti-Snail, and anti-histone H3 (trimethyl K4) antibodies were obtained from Abcam (Cambridge, MA). Rabbit anti-phospho-Smad1, phospho-Smad2, and phospho-Smad3 antibodies were acquired from Cell Signaling Technology (Beverly, MA). Rabbit anti-HA was obtained from Covance (Berkeley, CA). Mouse anti-HA and anti-tubulin were obtained from Sigma, and mouse anti-poly(ADP-ribose) polymerase was from Novus Biologicals, Inc. (Littleton, CO). Rabbit anti-acetyl-histone H4 antibody was obtained from Upstate Biotechnology, Inc. (Lake Placid, NY).

Cell Culture, Transfection, and TGFβ1 Treatment—The human microvascular endothelial cell line HMEC-1 (human microvascular endothelial cells (HMEC); Centers for Disease

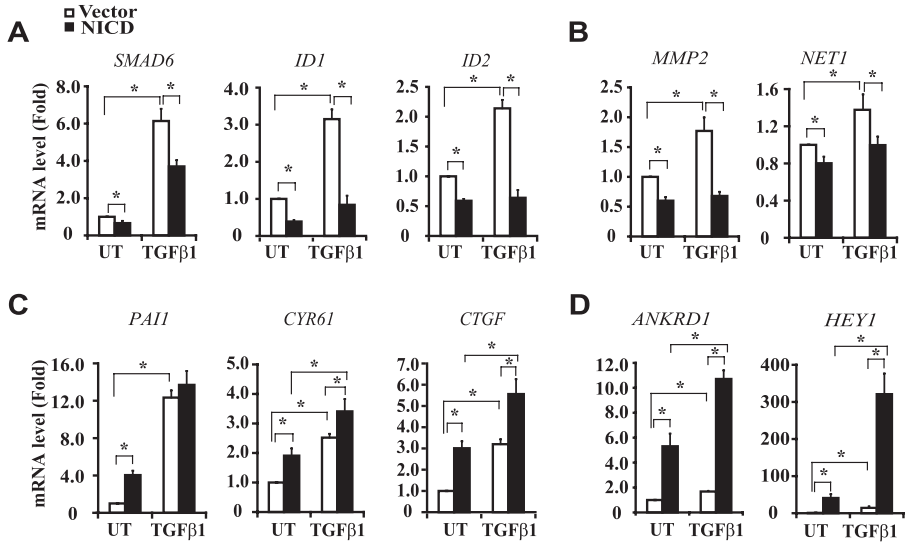

FIGURE 2. **NICD differentially affects TGFβ/Smad target gene expression.** HMEC transduced with empty vector or NICD were left untreated (*UT*) or treated with 2.5 ng/ml of TGFβ1 for 2 h. The mRNA level of target genes of TGFβ/Smad1 (*A*), TGFβ/Smad2 (*B*), and TGFβ/Smad3 (*C* and *D*) was examined by qRT-PCR and normalized to GAPDH. mRNA levels were expressed as -fold changes relative to the untreated vector samples and shown as mean ± S.E. of three independent experiments. *, $p < 0.05$.

Control and Prevention (Atlanta, GA)), the retroviral packaging cell line, Phoenix™-Ampho, and 293T cells were cultured as described previously (5). pLNCX-N4IC-HA, MIY-Dll4-HA, MSCV-Smad3, and MSCV-FLAG-Smad3 were used for retroviral infection of HMEC or transient transfection of 293T cells. TransIT-LT1 Transfection Reagent (Mirus, Madison, WI) or calcium phosphate was used for transfection of Phoenix™-Ampho and 293T cells. For TGFβ treatment, HMEC were cultured in MCDB medium containing 0.2% serum overnight and then left untreated or treated with 2.5 ng/ml of recombinant human TGFβ1 (R&D systems, Inc., Minneapolis, MN) for various times.

Preparation of Whole Cell Lysates and Cytosolic and Nuclear Fractions—Whole cell lysates were prepared using modified radioimmune precipitation buffer as described previously (27). For cytosolic and nuclear fraction preparations, cells were lysed using Buffer A (10 mM HEPES-KOH, pH 7.8, 1.5 mM $MgCl_2$, 10 mM KCl) containing 0.5% Nonidet P-40 and a protease inhibitor mixture (PIC; Roche Applied Science), incubated on ice for 10 min, and centrifuged at 12,000 × *g* for 15 min. The supernatant was collected as the cytosolic fraction. The pellet was resuspended in Buffer C (50 mM HEPES-KOH, pH 7.8, 50 mM KCl, 300 mM NaCl, 0.1 mM EDTA, 10% glycerol) containing 1% Triton X-100 and 1× PIC, incubated with rotating at 4 °C for 20 min, and centrifuged at 12,000 × *g* for 10 min. The supernatant was collected as the nuclear fraction. Proteins in cell lysates and cytosolic or nuclear fractions were quantified using the DC protein assay and used for immunoblotting.

RNA Isolation and Quantitative Reverse Transcription (qRT)-PCR—Total RNA was isolated using the GenElute™ Mammalian Total RNA Miniprep Kit (Sigma) and DNase-treated before cDNA was synthesized using SuperScript II reverse transcriptase reagent (Invitrogen) in the presence of RNase inhibitor. qRT-PCR was carried out using the SYBR green method on an Applied Biosystems 7900HT (Applied Biosystems, Foster City, CA). Sequences of the primers for qPCR are listed in supplemental Table 2.

Smad3 Expression in Mouse Cardiac Cushion Cells—Tet^{OS}-dominant negative MAML1 (dnMAML1) transgenic mice were generated in house and will be described elsewhere.[5] dnMAML1 mice were crossed with VE-cadherin-tTA mice (28) (gift of L. Benjamin, Harvard Medical School, Boston, MA), and in the double transgenic offspring, inducible expression of dnMAML1 blocks Notch activity in an endothelial cell-specific manner. Inhibition of Notch activity by dnMAML1 expression was initiated at embryonic day 8.5 (E8.5) or E9.5 by removal of tetracycline from the drinking water, cellularization of the cardiac cushion was examined at E10.5 by staining cells with DAPI, and cell number was quantified using ImageJ Software (National Institutes of Health). To examine Smad3 protein expression in the cardiac cushion cells, Notch activity was inhibited by dnMAML1 expression at E9.5, and Smad3 protein expression was examined at E10.5 by immunofluorescence staining. Smad3 protein expression was quantified using ImageJ software and normalized to total cell numbers by counting the DAPI-stained nuclei in the same area.

Co-immunoprecipitation Assay—To examine the interaction between Smad3 and NICD, HEK 293T cells were transiently transfected with pLNCX-N4IC-HA, MSCV-pac-Smad3, or both. After 48 h, cell lysates were prepared using lysis buffer (50 mM Tris-HCl, pH 7.6, 150 mM NaCl, 1 mM EDTA, 1% Triton X-100, 1% Nonidet P-40, and 0.1% deoxycholate) containing protease inhibitors. After preclearing, cell lysates were incubated with anti-Smad3 or anti-HA antibody at 4 °C overnight. The immunoprecipitation mixture was then incubated with protein A-agarose (for Smad3 antibody) or protein G-agarose (for HA antibody) beads for 2 h at 4 °C. After three washes with lysis buffer, the beads were resuspended with 20 μl of 2× SDS sample buffer and heated to 95 °C for 5 min. The supernatant was loaded onto 10% SDS-polyacrylamide gels for immunoblotting.

Analysis of Smad3 Protein Turnover—HMEC transduced with empty vector or NICD were treated with 50 μg/ml of cycloheximide and cell lysates were prepared at the indicated times. Smad3 protein levels were examined by immunoblotting. The relative density of each Smad3 band compared with tubulin was expressed as the percentage of the untreated sample.

[5] L. Chang and A. Karsan, unpublished data.

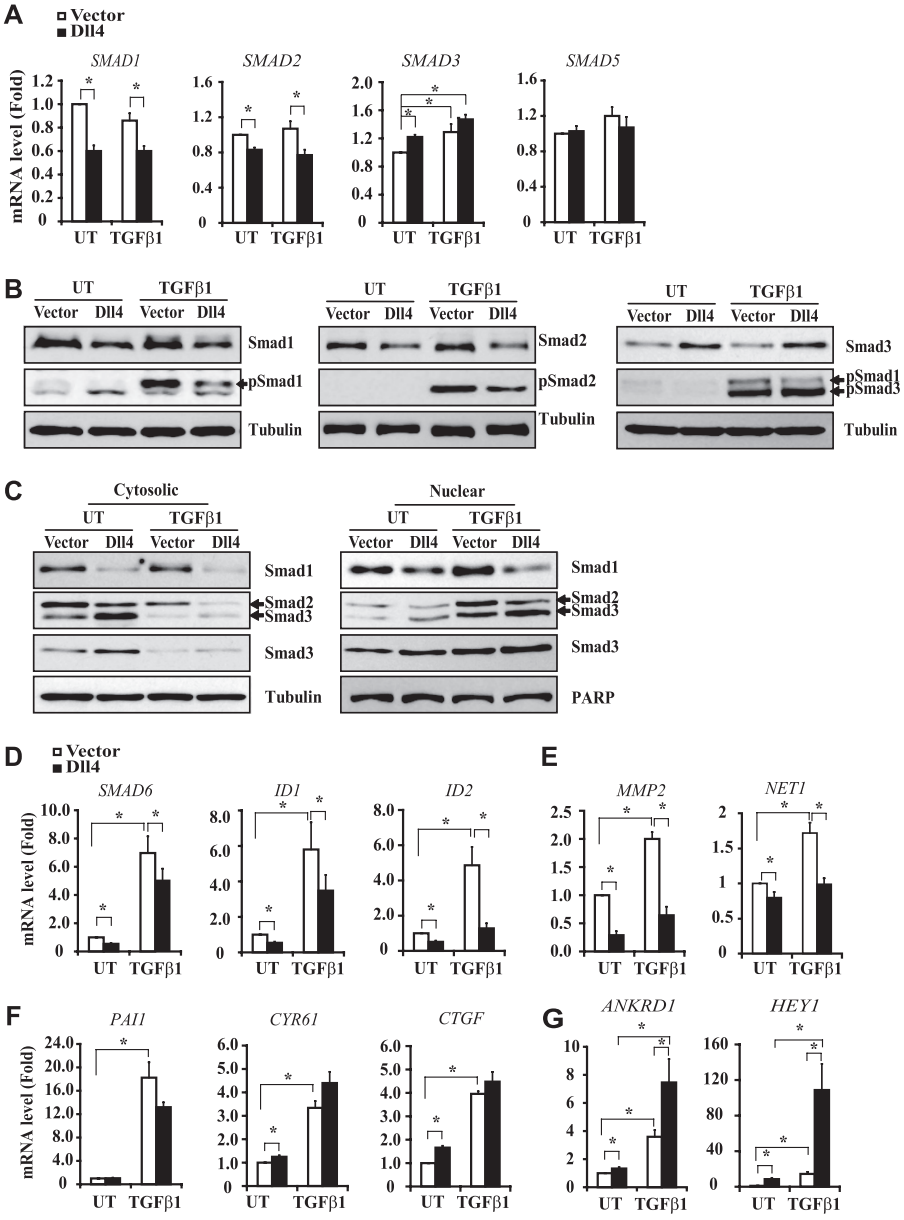

FIGURE 3. **Effects of Dll4-induced Notch activation on TGFβ signaling.** HMEC cocultured with Dll4-expressing HMEC at a 1:1 ratio were left untreated (*UT*) or treated with 2.5 ng/ml TGFβ1 for 1 h (*B* and *C*) or 2 h (*A*, *D*, *E*, *F*, and *G*). *A*, the mRNA level of Smad1, Smad2, Smad3, and Smad5 was examined by qRT-PCR and normalized to GAPDH. mRNA levels were expressed as -fold changes relative to the untreated vector sample and shown as mean ± S.E. of three independent experiments. *, $p < 0.05$. *B*, the amount of total and phosphorylated R-Smad proteins in whole cell lysates was examined by immunoblotting. Tubulin was used as a loading control. *C*, the R-Smad proteins in cytosolic and nuclear fractions were examined by immunoblotting. Tubulin and poly(ADP-ribose) polymerase (*PARP*) were used as loading control for cytosolic and nuclear fractions, respectively. *D–G*, the mRNA level of target genes of TGFβ/Smad1 (*D*), TGFβ/Smad2 (*E*), and TGFβ/Smad3 (*F* and *G*) was examined by qRT-PCR and normalized to GAPDH. mRNA levels were expressed as -fold changes relative to the untreated vector samples and shown as mean ± S.E. of three independent experiments. *, $p < 0.05$.

Chromatin Immunoprecipitation Assay—HMEC with or without Dll4 coculture were left untreated or treated with 2.5 ng/ml TGFβ1 for 1 h for Smad3 chromatin immunoprecipitation (ChIP) and 2 h for acetyl-histone H4 and trimethylated histone 3 on lysine 4 (H3K4Me3) ChIP. Cells were then cross-linked using 1% formaldehyde and harvested following lysis. After sonication, the lysates were diluted, and equal amounts of chromatin were used for ChIP with anti-Smad3, anti-acetyl-histone H4, or anti-histone H3 (trimethyl Lys^4) and rabbit IgG as a negative control. Enrichment of DNA around the SBE or CSL binding sites (for Smad3 ChIP) or the proximal promoter region and/or the 5′-end of the genes (for acetyl-histone H4 and H3K4Me3) was detected using qPCR and normalized against the respective input DNA. Primer positions and sequences are listed in supplemental Tables 3 and 4.

RESULTS

NICD Differentially Affects R-Smad Expression—Endothelial cells signal through two TGFβ type I receptor pathways, ALK1/Smad1/5/8 and ALK5/Smad2/3 (11, 12). To study the interaction between Notch and TGFβ, we examined the expression of R-Smads in HMEC transduced with activated Notch, NICD. Immunoblotting showed that NICD decreased Smad1 and Smad2 protein expression by 53 ± 3.9% and 55 ± 8.3%, respectively, but increased Smad3 protein 240 ± 22.9% (Fig. 1, *A* and *B*). Consistent with effects on protein expression, qRT-PCR revealed that NICD decreased mRNA levels of *SMAD1* and *SMAD2* by 59% ± 3.1% and 38% ± 13.7%, respectively, while increasing *SMAD3* mRNA 145 ± 7.3% and not affecting *SMAD5* mRNA (Fig. 1*C*).

TGFβ stimulation induces the phosphorylation of R-Smads, which then form protein complexes with Smad4 and translocate to the nucleus. Since NICD affects the expression of R-Smads, we expected that TGFβ-induced phosphorylation of R-Smads and nuclear translocation would be altered accordingly. As shown in Fig. 1*D*, NICD decreased phospho-Smad1 and phospho-Smad2 levels and increased phospho-Smad3 levels consistent with changes in total R-Smad protein expression. The differential effect of Notch activation on TGFβ-induced nuclear translocation of Smad1, Smad2, and Smad3 was confirmed by immunoblotting for Smad1, Smad2, and Smad3 in cytosolic and nuclear fractions after TGFβ treatment (Fig. 1*E*).

Effects of NICD on TGFβ Target Gene Expression are Pathway- and Gene-dependent—Since NICD affects the protein level, TGFβ-induced phosphorylation, and nuclear localization of R-Smads, we next examined the functional effects of NICD on the expression of TGFβ target genes. qRT-PCR showed that

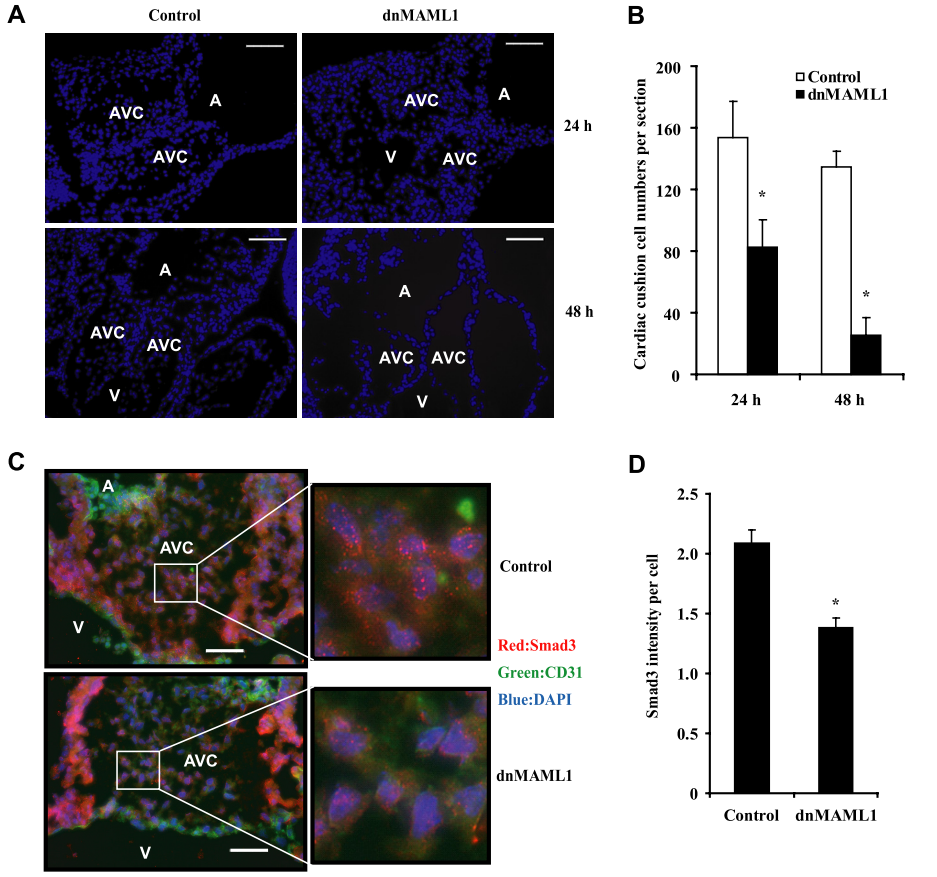

FIGURE 4. **Inhibition of Notch activity reduces Smad3 expression in mouse embryonic hearts.** Notch activity was inhibited by induction of dnMAML1 at E8.5 or E9.5, and cells in the cardiac cushion were stained by DAPI at E10.5 (*A*) and quantified using ImageJ software (*B*). *A*, atrium; *V*, ventricle; *AVC*, atrioventricular cushion. *Bars*, 50 μm. Ten sections of control hearts and six sections of dnMAML1 hearts at 24 h and three sections of control hearts and six sections of dnMAML1 hearts at 48 h were analyzed. Cardiac cushion cell number per section represents mean ± S.E. *, $p < 0.05$ compared with controls. *C*, Notch activity was inhibited by induction of dnMAML1 at E9.5, and Smad3 expression in cardiac cushion cells was examined at E10.5 by immunofluorescence staining using Smad3 antibody. *Red*, Smad3; *green*, CD31 (endocardium); *blue*, DAPI (nuclei). *Bars*, 50 μm. *D*, Smad3 expression in cardiac cushion cells from 13 sections of six control hearts and 15 sections of five dnMAML hearts were examined by immunofluorescence staining. The intensity of Smad3 staining was analyzed using ImageJ software, compared with the number of nuclei in the same area, and expressed as intensity per cell. Intensity per cell (arbitrary units) represents the means ± S.E. *, $p < 0.05$.

activated Notch significantly reduced the basal and TGFβ-induced levels of ALK1/Smad1 target genes *SMAD6*, *ID1*, and *ID2* (Fig. 2*A*), and two ALK5/Smad2-dependent targets, *MMP2* and *NET1* (29, 30) (Fig. 2*B*).

In contrast to inhibition of Smad1 and Smad2 targets, NICD alone up-regulated the ALK5/Smad3 target genes *PAI1*, *CTGF*, and *CYR61* (29, 31, 32). Costimulation of Notch and TGFβ only slightly induced (<2-fold) expression of *PAI1*, *CTGF*, and *CYR61* compared with TGFβ alone (Fig. 2*C*), suggesting a possible common signaling pathway through induction of Smad3. In contrast, a synergistic effect on the expression of *ANKRD1*, another TGFβ/Smad3 target gene (33), and *HEY1* was observed between NICD and TGFβ (Fig. 2*D*), similar to the effect we have previously noted for Snail (5). These results suggest that the effect of Notch activation on the expression of TGFβ/Smad3 targets is gene-specific.

Effects of Dll4-induced Notch Activation on the Expression of R-Smads and Their Target Genes—To examine whether ligand-induced Notch activation would have similar effects as NICD on TGFβ signaling pathways, we transduced HMEC with Dll4, the major Notch ligand in endothelial cells (25), and cocultured these cells with parental HMEC at a 1:1 ratio. In keeping with the NICD findings, qRT-PCR analysis showed that Dll4-induced Notch activation decreased *SMAD1* and *SMAD2* mRNA expression by 40 ± 4.8% and 17 ± 2.5%, respectively, and increased *SMAD3* mRNA expression 122 ± 3.2% but did not affect *SMAD5* mRNA expression (Fig. 3*A*). Consistent with mRNA expression, Smad1 and Smad2 protein levels were decreased and Smad3 protein levels were increased by Dll4-induced Notch activation (Fig. 3*B*). Additionally, TGFβ-induced phosphorylation and nuclear translocation of Smad1 and Smad2 were also decreased and that of Smad3 was increased by Dll4-induced Notch activation (Fig. 3, *B* and *C*). Given that the nuclear levels of the R-Smads were proportional to cytosolic expression, it is likely that the changes in R-Smad phosphorylation and nuclear translocation are a direct reflection of R-Smad levels.

Similar to NICD, Dll4-induced Notch activation inhibited the basal and TGFβ-induced mRNA levels of the ALK1/Smad1 target genes *SMAD6*, *ID1*, and *ID2* (Fig. 3*D*) and ALK5/Smad2 target genes *MMP2* and *NET1* (Fig. 3*E*). Dll4 minimally affected the basal mRNA levels of *CYR61*, *CTGF*, and *PAI1* (Fig. 3*F*). As with NICD, Dll4-induced Notch activation synergized with TGFβ upon inducing *ANKRD1* and *HEY1* expression (Fig. 3*G*) as well as on two classical direct Notch targets, *HEY2* and *HEYL* (see supplemental Fig. 1). To ensure that the effects we observed in coculture of parental HMEC and Dll4-expressing HMEC reflect Dll4-induced Notch activation in parental HMEC, we flow-sorted the cocultured cells into green fluorescent protein-positive (Dll4-expressing HMEC cells) and green fluorescent protein-negative (parental HMEC) populations after TGFβ treatment and examined mRNA expression of R-Smads and TGFβ target genes in these two populations by qRT-PCR. The results confirmed that the effect of Dll4 on TGFβ signaling is due to Notch activation, since the effects were more pronounced in parental HMEC (receiving the Notch signal) than in Dll4-expressing HMEC (see supplemental Fig. 2). Taken together, our data indicate that, similar to NICD, Dll4-induced Notch activation has an inhibitory effect on Smad1 and Smad2 pathways but a positive effect on Smad3 levels, with synergistic induction of a subset of Smad3 target genes.

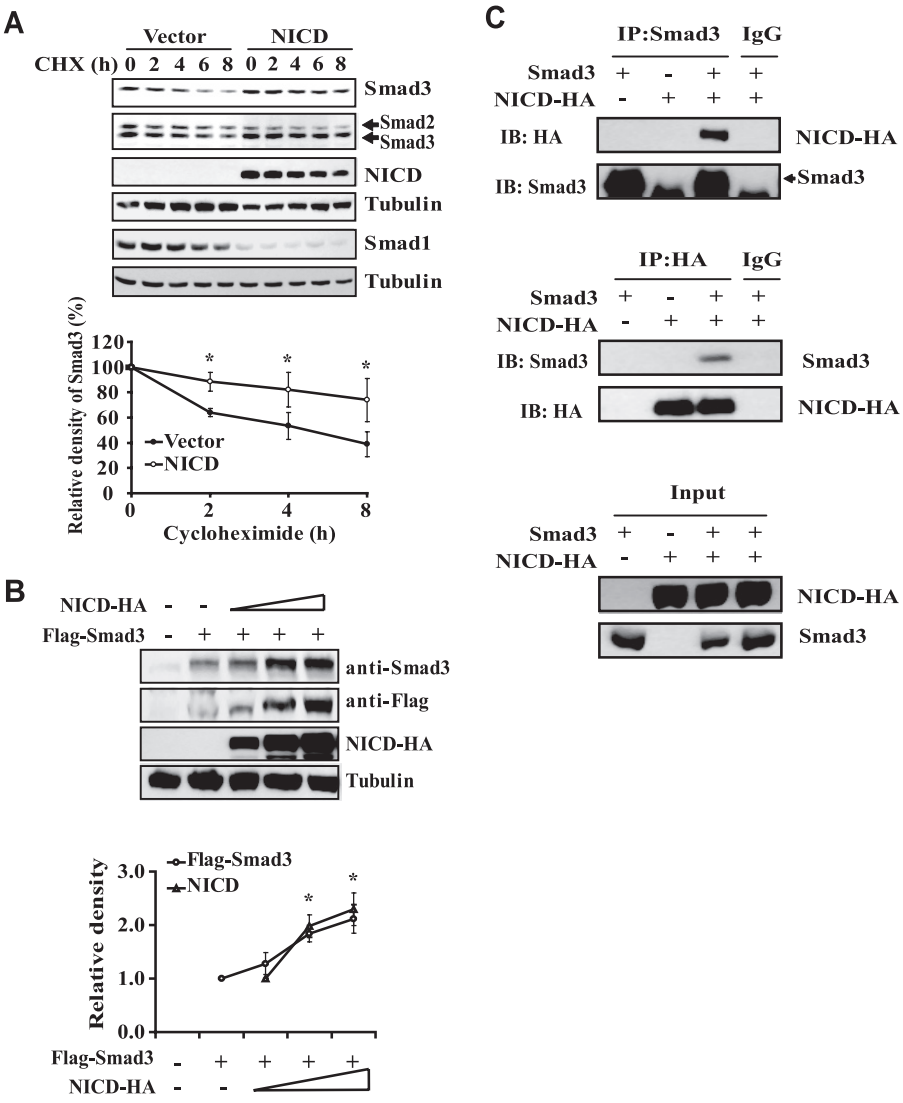

FIGURE 5. **NICD interacts with Smad3 and increases protein stability.** *A*, HMEC transduced with empty vector or NICD were treated with 50 μg/ml cycloheximide for various times. Smad1, Smad2, and Smad3 protein level in whole cell lysates was examined by immunoblotting. The density of the Smad3 bands was measured by densitometry and normalized to tubulin. The relative density of Smad3 protein at each time point is shown as the mean ± S.E. of four independent experiments. *, $p < 0.05$. *B*, 293T cells were transiently transfected with FLAG-Smad3 (2 μg) with or without cotransfection of various amounts of NICD-HA (1, 2, or 3 μg). Empty vector was used to equalize total plasmid concentration for each transfection. FLAG-Smad3 level was examined using anti-Smad3 or anti-FLAG antibodies. NICD expression was detected using anti-HA antibody. Tubulin was used as a loading control. The density of the FLAG-Smad3 and NICD bands was measured by densitometry and normalized to tubulin. The relative density of FLAG-Smad3 and NICD is shown as the mean ± S.E. of three independent experiments. The density of FLAG-Smad3 in cells transfected with FLAG-Smad3 alone and that of NICD in cells transfected with the lowest amount of NICD were designated as 1 for FLAG-Smad3 and NICD, respectively. *, $p < 0.05$. *C*, 293T cells were transiently transfected with Smad3, NICD-HA, or both for 48 h. Physical interaction between Smad3 and NICD was examined in the whole cell lysates by co-immunoprecipitation using anti-Smad3 or anti-HA antibodies. *IP*, immunoprecipitation; *IB*, immunoblot.

Inhibition of Notch Activity Reduces Smad3 Expression in the Mouse Embryonic Heart—A subset of endocardial cells initiates EndMT at E9.5 in the atrioventricular canal, which is regulated in part by Notch and TGFβ pathways (1, 5). To investigate whether Notch activity affects the expression of Smad3 during EndMT *in vivo*, we examined Smad3 expression in cardiac cushions of embryonic hearts from mice inducibly expressing the pan-Notch inhibitor, dnMAML1, from an endothelial promoter.[5] As the mesenchymal cells are derived from the endocardium, Notch inhibition carries through into the mesenchymal cells of the cardiac cushion (34).[5] We first examined the effect of Notch inhibition on cellularization of the cardiac cushion. Notch activity was inhibited by inducing expression of dnMAML1 at E8.5 or E9.5, and cardiac cushion cells were stained by DAPI and quantified at E10.5. Inhibition of Notch activity by dnMAML1 for 24 and 48 h resulted in a reduction of cell numbers in cardiac cushion by 46 ± 17.9 and 81 ± 11.3%, respectively, compared with littermate controls, demonstrating that inhibition of endocardial Notch activity blocks EndMT (Fig. 4, *A* and *B*). We then examined Smad3 expression in these cardiac cushion cells. Notch activity was inhibited by inducing expression of dnMAML1 at E9.5, and Smad3 protein expression in cardiac cushion cells was examined at E10.5 by immunofluorescent staining. There was reduced nuclear Smad3 localization in the cardiac cushion cells (Fig. 4*C*) and an overall reduction in Smad3 protein expression of 34 ± 9% per cell (Fig. 4*D*) when Notch activity was inhibited for 24 h compared with littermate controls. Thus, Notch activation regulates Smad3 expression in a physiologic context *in vivo*.

Notch Activation Stabilizes Smad3 Protein—Several pieces of data suggested to us that Notch also regulates Smad3 at the post-transcriptional level. First, Smad3 protein levels appeared disproportionately increased compared with the mRNA levels by NICD (Fig. 1, *A* and *B* compared with *C*) or by Dll4 (Figs. 3*B* and 6 compared with Fig. 3*A*). Additionally, TGFβ stimulation increased *SMAD3* mRNA to a similar level as that induced by Notch activation (Fig. 1*C* (131 ± 7.2%) and Fig. 3*A* (129 ± 11%)), but the increase of Smad3 protein was only observed in cells with active Notch and not in TGFβ-stimulated cells (Figs. 1*D* and 3*B*). To test whether NICD could increase Smad3 stability, we treated HMEC transduced with vector or NICD with 50 μg/ml cycloheximide to block new protein synthesis and analyzed Smad3 protein expression by immunoblotting. As shown in Fig. 5*A*, loss of Smad3 protein was much slower in NICD-expressing cells than in the vector control cells, suggesting that NICD increases Smad3 protein stability. In contract, NICD did not increase the stability of Smad1 and Smad2 (Fig. 5*A*). Next, we examined whether expression of NICD could increase the pro-

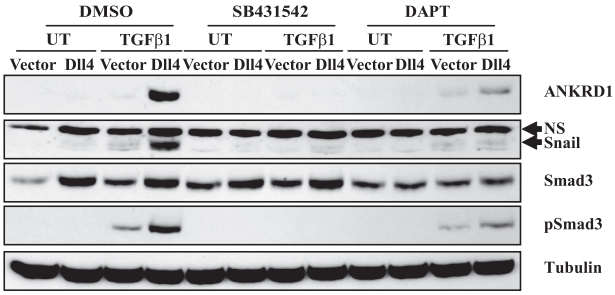

FIGURE 6. **Synergistic effect between Dll4 and TGFβ signaling requires both ALK5 and Notch activation.** HMEC with or without Dll4 coculture were pretreated with 10 μM SB431542 (ALK5 kinase inhibitor) or 10 μM DAPT (γ-secretase inhibitor) overnight and then left untreated (*UT*) or treated with 2.5 ng/ml TGFβ1 for 4 h in the presence of the inhibitors. ANKRD1, Snail, Smad3, and phospho-Smad3 expression was examined in whole cell lysates by immunoblotting. Tubulin was used as a loading control.

tein level of ectopically expressed Smad3 whose expression is controlled by the viral LTR rather than the endogenous promoter. Transient transfection of 293T cells with vector or FLAG-Smad3 co-transfected with increasing amounts of NICD showed that NICD increased protein levels of ectopically transfected FLAG-Smad3 (Fig. 5*B*). Since the expression of FLAG-Smad3 is not controlled by the endogenous Smad3 promoter, the increase of FLAG-Smad3 protein by NICD can be attributed to regulation at a post-translational level. Although we confirmed the physical interaction between NICD and Smad3 by co-immunoprecipitation in transiently transfected 293T cells (Fig. 5*C*) (18, 21), whether the stabilization of Smad3 by Notch is through physical interaction between Smad3 and NICD remains to be further investigated, because NICD has also been shown to interact with Smad1 and Smad2 (21, 35).

Synergism between Dll4 and TGFβ Signaling Requires both ALK5 and Activated Notch—To further study the synergy between Notch and TGFβ signaling, we pretreated HMEC-Dll4 cocultures with an ALK5 kinase inhibitor SB431542 or a γ-secretase inhibitor, DAPT, to block Notch activation prior to TGFβ1 stimulation. Immunoblotting showed that the synergistic up-regulation of ANKRD1 and Snail was abolished by either ALK5 or Notch inhibition (Fig. 6). However, ALK5 inhibition did not affect the induction of Smad3 by Dll4 but completely blocked TGFβ-induced Smad3 phosphorylation (Fig. 6), indicating that SB431542 effectively inhibits the TGFβ/ALK5/Smad3 signaling pathway, independent of the effect of Notch on Smad3 protein levels. In contrast, inhibition of Notch signaling by DAPT abolished the induction of Smad3 expression by Dll4 and reduced TGFβ-induced Smad3 phosphorylation to the level seen by TGFβ stimulation alone (Fig. 6). These data confirm the functional integration between Notch and TGFβ signaling pathways and highlight the synergistic effect of Notch on a subset of Smad3-inducible genes.

Smad3 Is Recruited to both SBEs and CSL Binding Sites in the Promoters of Target Genes with Combined TGFβ and Notch Activation—The finding that only a subset of TGFβ/Smad3 target genes is synergistically induced by the combination of Notch activation and TGFβ stimulation (Figs. 2*D* and 3*G*) prompted us to examine the mechanism underlying the selective synergy between Notch activation and TGFβ signaling. We selected *PAI1* as a primary TGFβ target gene that is only induced by TGFβ, but not by Dll4, and is not synergistically induced by the combination (Fig. 3*F*). *ANKRD1* and *HEY1* were chosen as TGFβ and Notch target genes that are synergistically induced by combined TGFβ stimulation and Dll4/NICD (Fig. 3*G*). Since Smad3 is induced by Notch activation, we first examined whether the combined activation of TGFβ and Notch pathways affects the level of occupancy of Smad3 on the promoters of these target genes. SBEs have been identified in *PAI1* (31), *ANKRD1* (33), and *HEY1* (19) promoters, and verified or potential CSL binding sites have been identified in *HEY1* (36) and *ANKRD1* promoters but not in the *PAI1* promoter up to 3 kb upstream of the transcriptional start site (see supplemental Table 1). To examine the occupancy of Smad3 on SBEs and CSL binding sites in these genes, we treated HMEC with or without Dll4 coculture with TGFβ1 for 1 h and examined Smad3 occupancy on SBEs and/or CSL binding sites in *PAI1*, *ANKRD1*, and *HEY1* promoters using a Smad3 ChIP assay followed by qPCR using primers amplifying the SBEs or CSL binding sites. Smad3 ChIP-qPCR results showed that the occupancy of Smad3 on the SBEs in the *PAI1* promoter was induced by TGFβ stimulation and was not further increased by Dll4-induced Notch activation (Fig. 7), consistent with the mRNA expression data (Fig. 3*F*). Similarly, TGFβ-induced Smad3 occupancy on the SBE in the *ANKRD1* promoter was not further increased by Dll4-induced Notch activation, suggesting that synergistic induction of *ANKRD1* mRNA expression by both TGFβ and Notch pathways is not through the regulation of Smad3 occupancy on the SBE in its promoter. In contrast, TGFβ-induced Smad3 occupancy on the CSL binding site in the *ANKRD1* promoter was further increased by Dll4-induced Notch activation (Fig. 7), which corresponds to the synergistic induction of *ANKRD1* mRNA expression by both pathways (Fig. 3*G*). Interestingly, Smad3 occupancy on both SBE and CSL binding sites in the *HEY1* promoter was induced only when both TGFβ and Notch pathways were activated (Fig. 7), which is consistent with our expression data indicating that the highest expression of *HEY1* mRNA was induced when both pathways were activated (Fig. 3*G*). These results suggest that the presence of CSL binding sites in Smad3-dependent promoters is the determining factor that allows the recruitment of Smad3 to not only SBEs but also to CSL binding sites by combined TGFβ stimulation and Notch activation, and this may explain the selective synergy between the TGFβ/ALK5/Smad3 and Notch pathways.

Dll4-induced Notch Activation and TGFβ Signaling Cooperatively Regulate Histone Acetylation—We next investigated whether histone modification by TGFβ and Notch could explain the synergistic up-regulation of specific target genes. Since both R-Smads and NICD interact with histone acetyltransferases (37, 38) and Smad3 is recruited to both SBEs and CSL binding sites (Fig. 7) in the promoters of *ANKRD1* and *HEY1* by combined TGFβ stimulation and Dll4-induced Notch activation, we examined whether TGFβ and Notch signaling pathways would cooperatively induce histone acetylation in these target genes. HMEC were cultured with combinations of Dll4 and TGFβ1 stimulation for 2 h, and histone H4 acetylation was examined by acetyl-histone H4 ChIP followed by qPCR to amplify the proximal promoter and/or 5′-end of target genes. As shown in Fig. 8*A*, histone H4 acetylation in the proximal

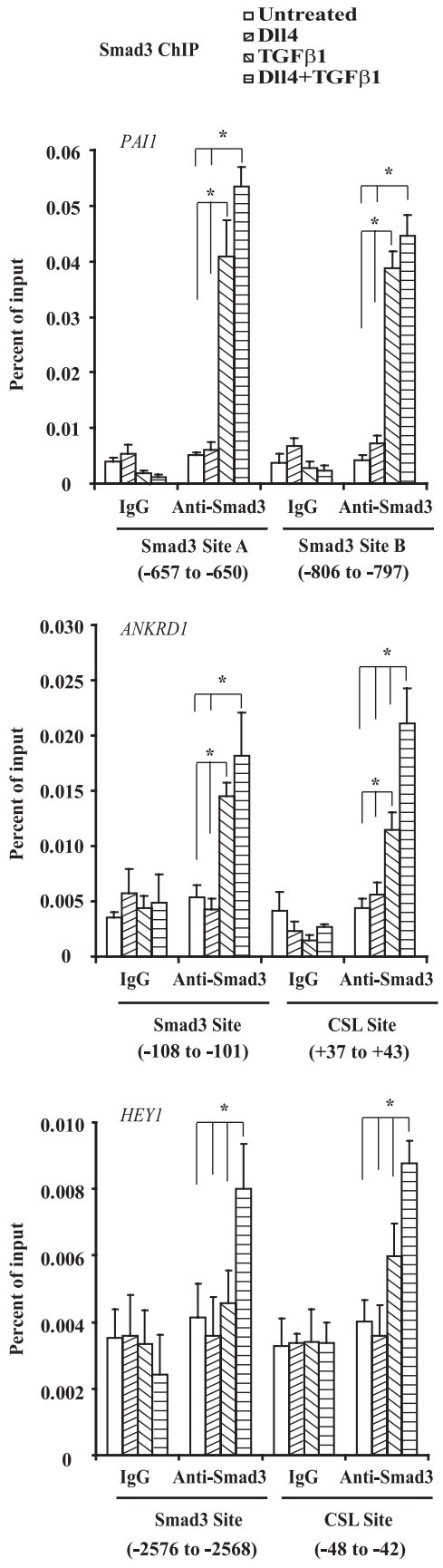

FIGURE 7. **Smad3 occupancy on SBE and CSL sites in the promoters of Smad3/CSL target genes.** HMEC with or without Dll4 co-culture were left untreated or treated with TGFβ1 for 1 h. Smad3 occupancy on SBE and/or CSL sites in *PAI1* (*top*), *ANKRD1* (*middle*), and *HEY1* promoter (*bottom*) was examined by Smad3 ChIP with IgG as a negative control. ChIP-qPCR was conducted using primers that amplify the SBE or CSL sites (see supplemental Tables 1 and 3 for SBE and CSL sites and primer sequences). Smad3 occupancy on these sites was normalized against the respective input DNA and expressed as a percentage of input DNA. Values were shown as mean ± S.E. of four independent experiments. *, $p < 0.05$.

promoter and 5′-end of *PAI1* was induced only by TGFβ stimulation and not by Dll4, and consistent with the expression data, the combination of both did not further increase histone H4 acetylation. In contrast, and in keeping with the expression data, the combination of Dll4 and TGFβ stimulation resulted in greater induction of histone H4 acetylation in the proximal promoter and/or 5′-end of *ANKRD1* and *HEY1* genes compared with either Dll4- or TGFβ-induced signaling alone (Fig. 8*A*). Thus, consistent with the simultaneous recruitment of Smad3 to both SBEs and CSL binding sites in *ANKRD1* and *HEY1* promoters (Fig. 7), our data demonstrate that combined TGFβ and Dll4 stimulation induces greater histone acetylation in the proximal promoter and 5′-end of these genes.

To examine whether combined TGFβ and Dll4 stimulation also affects H3K4Me3, which is another histone mark for active genes (39), histone H3K4Me3 ChIP-qPCR was performed and showed that TGFβ stimulation induced H3K4Me3 only in *PAI1* and not in *HEY1* and *ANKRD1* genes (Fig. 8*B*). Dll4 had no effect on H3K4Me3 in any of these genes (Fig. 8*B*). Thus, histone H4 acetylation, but not trimethylation of histone H3 Lys[4], is involved in the synergistic up-regulation of specific Smad3 targets following combined Dll4 and TGFβ stimulation.

DISCUSSION

In this study, we report that Notch activation differentially alters the expression of R-Smads. TGFβ activates ALK1/Smad1/5, ALK5/Smad2, and ALK5/Smad3 signaling pathways in endothelial cells. TGFβ/ALK1 and TGFβ/ALK5 pathways activate different target gene expression and play opposing roles in endothelial cells (11, 12). In this regard, ALK1 phosphorylates Smad1/5 and promotes proliferation and migration of endothelial cells, whereas ALK5 phosphorylates Smad2/3 and inhibits proliferation and migration of endothelial cells. Smad2 and Smad3 have been shown to have both overlapping and distinct roles in regulating the expression of TGFβ target genes and mediating TGFβ functions in a cellular context-dependent manner (29, 40, 41). Thus, modulation of the balance of TGFβ signaling pathways in certain cellular contexts can regulate distinct functional outcomes (42, 43). Here, we provide the first evidence that Notch activation not only modulates the balance between TGFβ/ALK1 and TGFβ/ALK5 signaling pathways, but also fine tunes the ALK5/Smad2 *versus* the ALK5/Smad3 pathways. These data reveal a novel mechanism by which Notch activation modulates TGFβ signaling pathways in an R-Smad-dependent manner in endothelial cells.

TGFβ signaling is regulated at multiple levels, including R-Smad expression. It has been shown that endoglin affects TGFβ signaling by increasing Smad2 protein levels without affecting its mRNA expression in endothelial cells, probably by inhibiting the ubiquitination and proteasome-dependent degradation of Smad2 protein (44). Here, we show that Notch acti-

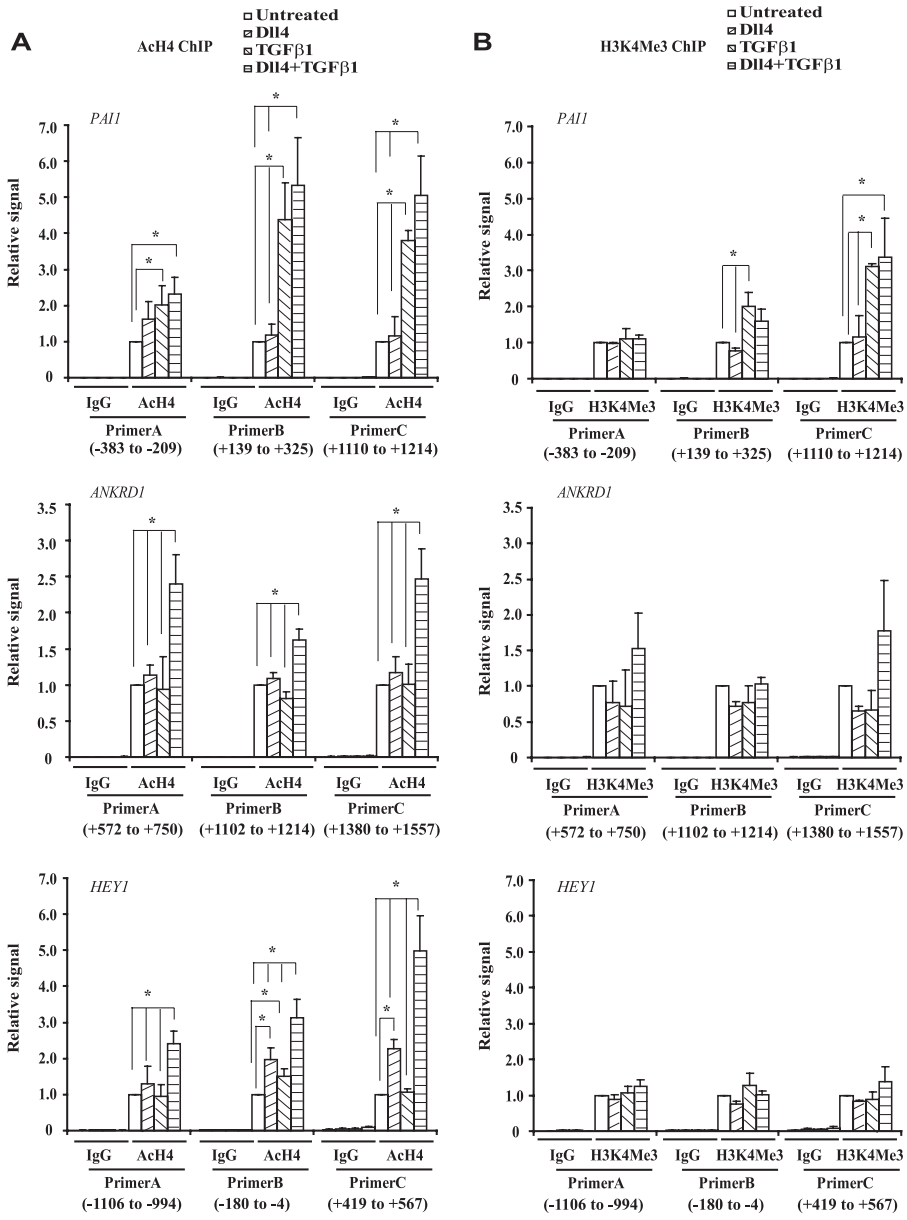

FIGURE 8. **Effects of TGFβ and Dll4-induced Notch activation on histone modification.** HMEC with or without Dll4 co-culture were left untreated or treated with TGFβ1 for 2 h. Histone H4 acetylation (*AcH4*) (*A*) and H3K4Me3 (*B*) were examined by ChIP followed by qPCR, using anti-acetyl-histone H4 and anti-histone H3 (trimethyl Lys[4]) antibodies, respectively, with IgG as a negative control. ChIP-qPCR was conducted using primers that amplify the proximal promoter regions and/or 5′-ends of the *PAI1* (*top*), *ANKRD1* (*middle*), and *HEY1* genes (*bottom*) (see supplemental Table 4 for primer sequences). The enrichment of these regions was calculated as a percentage of the respective input DNA concentration and expressed as relative signal after normalization against the untreated vector samples (designated as 1). Values are shown as the mean ± S.E. of four independent experiments. *, $p < 0.05$.

vation not only increases Smad3 mRNA levels but stabilizes Smad3 protein as well. Thus, our data demonstrate that Notch activation regulates Smad3 expression at both transcriptional and post-translational levels.

Dll4 is the major ligand that activates Notch signaling in endothelial cells (25). Our data indicate that Dll4-induced Notch activation has similar inhibitory effects as that of NICD on TGFβ/Smad1 and TGFβ/Smad2 pathways. But the effect of Dll4-induced Notch activation on TGFβ/Smad3 target gene expression is less potent than NICD (compare Figs. 2*C* and 3*F*). The discrepancy between Dll4-induced Notch activation and overexpression of NICD on *PAI1* expression suggests that the effects of Notch activation on TGFβ signaling are probably dose-dependent. Nevertheless, both NICD and Dll4-induced Notch activation show a strong synergistic effect with TGFβ signaling in the up-regulation of a subset of Smad3 target genes. Importantly, genes that are synergistically induced by Notch activation and TGFβ signaling, including *HEY1*, *HEY2*, *HEYL*, and *SNAIL*, have been shown to play critical roles in embryonic development (5, 7, 45–47). In this regard, targeted deletion of *Hey2*, or double knockout of *Hey1* and *Hey2* or *Hey1* and *HeyL* cause embryonic heart defects (7, 45, 46), and conditional deletion of *Snail* after E8.0 causes severe cardiovascular defects (47). Additionally, we have found that *ANKRD1*, a TGFβ/Smad3 target in smooth muscle cells (33), was synergistically induced by Notch activation and TGFβ signaling in endothelial cells. Interestingly, the association between the disruption of ANKRD1 expression and the pathogenesis of total anomalous pulmonary venous return (TAPVR), a congenital heart defect, has also been suggested in a recent study (48). Here we show that endothelium-specific inhibition of Notch activity by the overexpression of dnMAML1 *in vivo* blocks EndMT and reduces Smad3 expression in cardiac cushion cells of mouse embryonic hearts, and this impingement of Notch on a second distinct signaling pathway may explain the severe cardiac defects seen in targeted Notch1 mutants (6).

Although synergism between Notch and TGFβ signaling (18) and between Notch and BMP-6 (35) have been previously reported, the molecular mechanism underlying the synergy has not been clearly elucidated. In this study, we show that TGFβ-induced Smad3 occupancy on SBE in the *ANKRD1* promoter is not further increased by Dll4-induced Notch activation, suggesting that synergistic induction of *ANKRD1* by both TGFβ and Notch signaling is not mediated by Smad3 occupancy on the SBE of its promoter. Rather, we found that Dll4-induced Notch activation increases TGFβ-induced Smad3 occupancy on the CSL site in the *ANKRD1* promoter. Similarly, Smad3 occupancy on both SBE and CSL sites in the *HEY1* promoter is induced only when both TGFβ and

Notch pathways are activated, in keeping with higher expression of *HEY1* induced by combined TGFβ stimulation and Dll4-induced Notch signaling as compared with either signal alone. In contrast, TGFβ-induced Smad3 occupancy of SBEs in the *PAI1* promoter is not further increased by Notch activation, and a CSL binding site is not identified in the *PAI1* promoter up to 3 kb from the transcriptional start site. In keeping with Smad3 occupancy on both SBEs and CSL sites, we found that combined TGFβ stimulation and Dll4-induced Notch activation induces higher histone H4 acetylation in genes whose promoter contains both SBEs and CSL sites (*ANKRD1* and *HEY1*) but not in *PAI1* whose promoter contains only SBEs but not CSL binding sites. Since Dll4-induced Notch activation is required for Smad3 occupancy of CSL binding sites in the *ANKRD1* and *HEY1* promoters and the cooperative induction of histone acetylation surrounding the transcriptional start site of these genes, NICD must play a critical role in recruiting Smad3 to CSL binding sites, probably through the physical interaction between NICD and Smad3, as we have shown (Fig. 5*C*).

Because both Smad3 and NICD recruit histone acetyltransferases to their transcription complexes (37, 38), formation of the Smad3/NICD/CSL complex may recruit histone acetyltransferases more effectively than Smad3 or NICD alone and thereby facilitate increased levels of histone acetylation and more active gene expression. In support of this, we found that combined TGFβ and Dll4-induced Notch activation induces greater histone acetylation of *ANKRD1* and *HEY1* but not *PAI1*. Thus, the synergistic induction of a subset of target genes, such as *ANKRD1* and *HEY1*, by combined TGFβ stimulation and Notch activation is mediated by contemporaneous Smad3 occupancy on both SBEs and CSL binding sites in their promoters and consequently greater histone acetylation.

In summary, we demonstrate for the first time that Notch signaling differentially affects the expression of R-Smads and consequently modulates the balance between different TGFβ/Smad signaling pathways in endothelial cells. We also demonstrate that the synergistic induction of a subset of genes by Notch and TGFβ signaling is attributed to the simultaneous recruitment of Smad3 to both SBEs and CSL sites in the promoter of these target genes and the cooperative induction of histone acetylation. Our findings on the antagonism and synergy between Notch and TGFβ signaling pathways shed light on the molecular mechanism underlying the functional interaction between these two important pathways.

REFERENCES

1. Armstrong, E. J., and Bischoff, J. (2004) *Circ. Res.* **95,** 459–470
2. Niessen, K., and Karsan, A. (2008) *Circ. Res.* **102,** 1169–1181
3. ten Dijke, P., and Arthur, H. M. (2007) *Nat. Rev. Mol. Cell Biol.* **8,** 857–869
4. High, F. A., and Epstein, J. A. (2008) *Nat. Rev. Genet.* **9,** 49–61
5. Niessen, K., Fu, Y., Chang, L., Hoodless, P. A., McFadden, D., and Karsan, A. (2008) *J. Cell Biol.* **182,** 315–325
6. Timmerman, L. A., Grego-Bessa, J., Raya, A., Bertran, E., Pérez-Pomares, J. M., Díez, J., Aranda, S., Palomo, S., McCormick, F., Izpisúa-Belmonte, J. C., and de la Pompa, J. L. (2004) *Genes Dev.* **18,** 99–115
7. Fischer, A., Schumacher, N., Maier, M., Sendtner, M., and Gessler, M. (2004) *Genes Dev.* **18,** 901–911
8. Massagué, J. (2000) *Nat. Rev. Mol. Cell Biol.* **1,** 169–178
9. Attisano, L., and Wrana, J. L. (2000) *Curr. Opin. Cell Biol.* **12,** 235–243
10. Massagué, J., Seoane, J., and Wotton, D. (2005) *Genes Dev.* **19,** 2783–2810
11. Goumans, M. J., Lebrin, F., and Valdimarsdottir, G. (2003) *Trends Cardiovasc. Med.* **13,** 301–307
12. Goumans, M. J., Valdimarsdottir, G., Itoh, S., Rosendahl, A., Sideras, P., and ten Dijke, P. (2002) *EMBO J.* **21,** 1743–1753
13. Artavanis-Tsakonas, S., Rand, M. D., and Lake, R. J. (1999) *Science* **284,** 770–776
14. Bray, S., and Furriols, M. (2001) *Curr. Biol.* **11,** R217–R221
15. Wu, L., Sun, T., Kobayashi, K., Gao, P., and Griffin, J. D. (2002) *Mol. Cell Biol.* **22,** 7688–7700
16. Nam, Y., Weng, A. P., Aster, J. C., and Blacklow, S. C. (2003) *J. Biol. Chem.* **278,** 21232–21239
17. Nam, Y., Sliz, P., Song, L., Aster, J. C., and Blacklow, S. C. (2006) *Cell* **124,** 973–983
18. Blokzijl, A., Dahlqvist, C., Reissmann, E., Falk, A., Moliner, A., Lendahl, U., and Ibáñez, C. F. (2003) *J. Cell Biol.* **163,** 723–728
19. Zavadil, J., Cermak, L., Soto-Nieves, N., and Böttinger, E. P. (2004) *EMBO J.* **23,** 1155–1165
20. Niimi, H., Pardali, K., Vanlandewijck, M., Heldin, C. H., and Moustakas, A. (2007) *J. Cell Biol.* **176,** 695–707
21. Sun, Y., Lowther, W., Kato, K., Bianco, C., Kenney, N., Strizzi, L., Raafat, D., Hirota, M., Khan, N. I., Bargo, S., Jones, B., Salomon, D., and Callahan, R. (2005) *Oncogene* **24,** 5365–5374
22. Masuda, S., Kumano, K., Shimizu, K., Imai, Y., Kurokawa, M., Ogawa, S., Miyagishi, M., Taira, K., Hirai, H., and Chiba, S. (2005) *Cancer Sci.* **96,** 274–282
23. Ono, Y., Sensui, H., Okutsu, S., and Nagatomi, R. (2007) *J. Cell Physiol.* **210,** 358–369
24. Kennard, S., Liu, H., and Lilly, B. (2008) *J. Biol. Chem.* **283,** 1324–1333
25. Mailhos, C., Modlich, U., Lewis, J., Harris, A., Bicknell, R., and Ish-Horowicz, D. (2001) *Differentiation* **69,** 135–144
26. Krebs, L. T., Shutter, J. R., Tanigaki, K., Honjo, T., Stark, K. L., and Gridley, T. (2004) *Genes Dev.* **18,** 2469–2473
27. Fu, Y., Sies, H., and Lei, X. G. (2001) *J. Biol. Chem.* **276,** 43004–43009
28. Sun, J. F., Phung, T., Shiojima, I., Felske, T., Upalakalin, J. N., Feng, D., Kornaga, T., Dor, T., Dvorak, A. M., Walsh, K., and Benjamin, L. E. (2005) *Proc. Natl. Acad. Sci. U.S.A.* **102,** 128–133
29. Phanish, M. K., Wahab, N. A., Colville-Nash, P., Hendry, B. M., and Dockrell, M. E. (2006) *Biochem. J.* **393,** 601–607
30. Kretschmer, A., Moepert, K., Dames, S., Sternberger, M., Kaufmann, J., and Klippel, A. (2003) *Oncogene* **22,** 6748–6763
31. Dennler, S., Itoh, S., Vivien, D., ten Dijke, P., Huet, S., and Gauthier, J. M. (1998) *EMBO J.* **17,** 3091–3100
32. Chen, S. J., Ning, H., Ishida, W., Sodin-Semrl, S., Takagawa, S., Mori, Y., and Varga, J. (2006) *J. Biol. Chem.* **281,** 21183–21197
33. Kanai, H., Tanaka, T., Aihara, Y., Takeda, S., Kawabata, M., Miyazono, K., Nagai, R., and Kurabayashi, M. (2001) *Circ. Res.* **88,** 30–36
34. Alva, J. A., Zovein, A. C., Monvoisin, A., Murphy, T., Salazar, A., Harvey, N. L., Carmeliet, P., and Iruela-Arispe, M. L. (2006) *Dev. Dyn.* **235,** 759–767
35. Itoh, F., Itoh, S., Goumans, M. J., Valdimarsdottir, G., Iso, T., Dotto, G. P., Hamamori, Y., Kedes, L., Kato, M., and ten Dijke, P. (2004) *EMBO J.* **23,** 541–551
36. Maier, M. M., and Gessler, M. (2000) *Biochem. Biophys. Res. Commun.* **275,** 652–660
37. Itoh, S., Ericsson, J., Nishikawa, J., Heldin, C. H., and ten Dijke, P. (2000) *Nucleic Acids Res.* **28,** 4291–4298
38. Wallberg, A. E., Pedersen, K., Lendahl, U., and Roeder, R. G. (2002) *Mol. Cell Biol.* **22,** 7812–7819
39. Heintzman, N. D., Stuart, R. K., Hon, G., Fu, Y., Ching, C. W., Hawkins, R. D., Barrera, L. O., Van Calcar, S., Qu, C., Ching, K. A., Wang, W., Weng, Z., Green, R. D., Crawford, G. E., and Ren, B. (2007) *Nat. Genet.* **39,** 311–318
40. Piek, E., Ju, W. J., Heyer, J., Escalante-Alcalde, D., Stewart, C. L., Weinstein, M., Deng, C., Kucherlapati, R., Bottinger, E. P., and Roberts, A. B. (2001) *J. Biol. Chem.* **276,** 19945–19953
41. Brown, K. A., Pietenpol, J. A., and Moses, H. L. (2007) *J. Cell Biochem.* **101,**

9–33
42. Blanco, F. J., Santibanez, J. F., Guerrero-Esteo, M., Langa, C., Vary, C. P., and Bernabeu, C. (2005) *J. Cell Physiol.* **204,** 574–584
43. Lebrin, F., Goumans, M. J., Jonker, L., Carvalho, R. L., Valdimarsdottir, G., Thorikay, M., Mummery, C., Arthur, H. M., and ten Dijke, P. (2004) *EMBO J.* **23,** 4018–4028
44. Santibanez, J. F., Letamendia, A., Perez-Barriocanal, F., Silvestri, C., Saura, M., Vary, C. P., Lopez-Novoa, J. M., Attisano, L., and Bernabeu, C. (2007) *J. Cell Physiol.* **210,** 456–468
45. Donovan, J., Kordylewska, A., Jan, Y. N., and Utset, M. F. (2002) *Curr. Biol.* **12,** 1605–1610
46. Fischer, A., Steidl, C., Wagner, T. U., Lang, E., Jakob, P. M., Friedl, P., Knobeloch, K. P., and Gessler, M. (2007) *Circ. Res.* **100,** 856–863
47. Murray, S. A., and Gridley, T. (2006) *Proc. Natl. Acad. Sci. U.S.A.* **103,** 10300–10304
48. Cinquetti, R., Badi, I., Campione, M., Bortoletto, E., Chiesa, G., Parolini, C., Camesasca, C., Russo, A., Taramelli, R., and Acquati, F. (2008) *Hum. Mutat.* **29,** 468–474

Slug is a direct Notch target required for initiation of cardiac cushion cellularization

Kyle Niessen,[1,2] YangXin Fu,[1,3] Linda Chang,[1,2] Pamela A. Hoodless,[4,5] Deborah McFadden,[3] and Aly Karsan[1,2,3]

[1]Department of Medical Biophysics, British Columbia Cancer Agency, Vancouver V5Z 1L3, Canada
[2]The Experimental Medicine Program and [3]The Department of Pathology and Laboratory Medicine, University of British Columbia, Vancouver V6T 1Z4, Canada
[4]Terry Fox Laboratory, British Columbia Cancer Agency, Vancouver V5Z 1L3, Canada
[5]The Department of Medical Genetics, University of British Columbia, Vancouver V6T 1Z4, Canada

Snail family proteins are key regulators of epithelial-mesenchymal transition, but their role in endothelial-to-mesenchymal transition (EMT) is less well studied. We show that Slug, a Snail family member, is expressed by a subset of endothelial cells as well as mesenchymal cells of the atrioventricular canal and outflow tract during cardiac cushion morphogenesis. Slug deficiency results in impaired cellularization of the cardiac cushion at embryonic day (E)–9.5 but is compensated by increased *Snail* expression at E10.5, which restores cardiac cushion EMT. We further demonstrate that *Slug*, but not *Snail*, is directly up-regulated by Notch in endothelial cells and that *Slug* expression is required for Notch-mediated repression of the *vascular endothelial cadherin* promoter and for promoting migration of transformed endothelial cells. In contrast, transforming growth factor β (TGF-β) induces *Snail* but not *Slug*. Interestingly, activation of Notch in the context of TGF-β stimulation results in synergistic up-regulation of *Snail* in endothelial cells. Collectively, our data suggest that combined expression of *Slug* and *Snail* is required for EMT in cardiac cushion morphogenesis.

Introduction

Epithelial-mesenchymal transition is the process by which epithelial cells undergo phenotypic and morphological reorganization. Epithelial-mesenchymal transition is essential during embryogenesis for the formation of many tissues, including the formation of the mesoderm, the migration of neural crest cells, and the development of the heart valves and septa (Hay, 2005). Endothelial-to-mesenchymal transition (EMT) is a specific form of epithelial-mesenchymal transition that is initiated at embryonic day (E)–9.5 in the atrioventricular (AV) canal and E10.5 in the outflow tract (OFT) cardiac cushions, the two sites of EMT in the developing heart (Camenisch et al., 2002a). This process generates cells that contribute to the connective tissue of the valves and septa of the adult heart (Eisenberg and Markwald, 1995).

Recent studies have demonstrated a critical role of the Notch signaling pathway during cardiac EMT, and disruption of this pathway has been implicated in the pathogenesis of various cardiovascular diseases (Iso et al., 2003; Niessen and Karsan, 2007). In the mouse, targeted deletion of *Notch1* or its key nuclear partner *CSL* (*CBF1/Suppressor of Hairless/Lag-1*) results in cardiac cushion EMT defects (Oka et al., 1995; Timmerman et al., 2004). Further, targeted deletion of the downstream Notch/CSL effector *Hey2* or double-deficiency of *Hey1* and *Hey2* or *Hey1* and *HeyL* results in various congenital heart anomalies including cardiac cushion defects (Donovan et al., 2002; Fischer et al., 2004, 2007). In humans, mutations at the *Notch1* locus are associated with bicuspid aortic valve disease as well as mitral valve anomalies and tetralogy of Fallot (Garg et al., 2005). Further, patients with mutations of the Notch ligand Jagged1 develop Alagille syndrome, a polymalformative disorder which includes cardiac cushion defects (Li et al., 1997; Oda et al., 1997; Eldadah et al., 2001).

TGF-β–related pathways have also been shown to be essential for proper heart development through their role in regulating EMT (Azhar et al., 2003). Of particular interest, *BMP2* and *TGF-β2* are expressed by the AV canal cushion myocardium (Dickson et al., 1993; Zhang and Bradley, 1996). BMP2-deficient mice die before cardiac cushion development (Zhang

Correspondence to Aly Karsan: akarsan@bccrc.ca

Abbreviations used in this paper: AV, atrioventricular; ChIP, chromatin immunoprecipitation; E, embryonic day; EMSA, electrophoretic mobility shift assay; EMT, endothelial-to-mesenchymal transformation; HMEC, human mammary epithelial cell; HUVEC, human umbilical vein epithelial cell; OFT, outflow tract; qRT-PCR, quantitative RT-PCR; shRNA, short hairpin RNA; TSS, transcriptional start site; VE-cadherin, vascular endothelial cadherin.

The online version of this paper contains supplemental material.

The Rockefeller University Press $30.00
J. Cell Biol. Vol. 182 No. 2 315–325
www.jcb.org/cgi/doi/10.1083/jcb.200710067

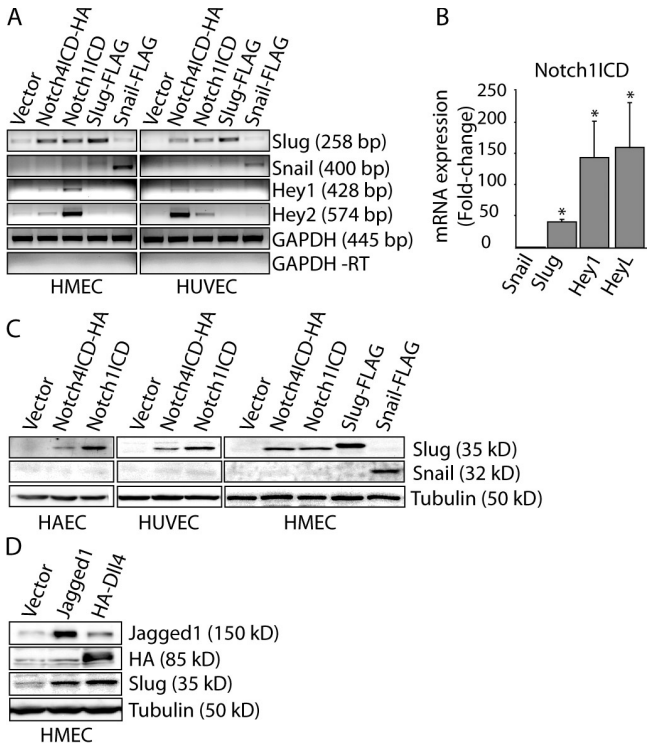

Figure 1. **Expression of *Slug*, but not *Snail*, is induced by Notch activation.** (A) Analysis of mRNA expression by semi–qRT-PCR in human mammary epithelial cells (HMEC) and human umbilical vein epithelial cells (HUVEC) expressing constitutively active Notch1 (Notch1ICD) or Notch4 (Notch4ICD). (B) Analysis of mRNA expression by qRT-PCR in HMEC expressing Notch1ICD. Results are normalized to the vector control ($n = 3$). *, $P < 0.05$. Error bars show SEM. (C) Immunoblots for Slug and Snail in HMEC, HUVEC, and human aortic endothelial cells (HAEC) transduced with Notch1ICD, Notch4ICD, or the empty vector. (D) HMEC expressing Jagged1 or Dll4 were cocultured with parental HMEC and immunoblotting for Slug was performed.

and Bradley, 1996); however, deficiency of the BMP2 receptor Alk2 results in AV canal EMT defects (Wang et al., 2005). *TGF-β2*–deficient mouse embryos do not display obvious cardiac cushion EMT defects, although later remodeling of the AV canal cushion is impaired (Dickson et al., 1993; Sanford et al., 1997; Bartram et al., 2001; Molin et al., 2002, 2003). However, using an ex vivo AV canal explant assay, TGF-β2–blocking antibodies or blocking antibodies for its coreceptor *TβRIII* inhibit AV canal EMT, suggesting redundancy of this pathway in vivo (Brown et al., 1999; Camenisch et al., 2002a). These data and others have established a clear role of TGF-β–related pathways during mammalian cardiac cushion development.

The Snail family members *Snail* (also known as *Snai1*) and *Slug* (also known as *Snai2*) encode zinc finger–containing transcriptional repressors that trigger EMT during embryonic development and tumor progression, in part by regulating expression of junctional proteins, most notably *E-cadherin* (Nieto, 2002). In the mouse, *Snail* has been shown to be expressed in the cardiac cushions from E9.5 onwards (Timmerman et al., 2004). Mice deficient for *Snail* die at E7.5, before cardiac development, and display defects in mesoderm formation (Carver et al., 2001). Conditional deletion of *Snail* after E8 results in lethality by E9.5, partially because of severe cardiovascular defects, but before the initiation of cardiac cushion EMT (Murray and Gridley, 2006). In the mouse, Slug is expressed in the cardiac cushions at E13.5, and mice deficient for *Slug* are viable but are growth retarded and display defects in pigmentation and hematopoiesis (Jiang et al., 1998; Inoue et al., 2002). To date, there is no direct evidence demonstrating the requirement for any Snail family member during mammalian heart development.

In this paper, we demonstrate that *Slug* is first expressed by a subset of endothelial cells as well as mesenchymal cells of the AV canal at E9.5, at the initiation of EMT. In keeping with a requirement for Slug during the initiation of cardiac EMT, the AV canal cushions show markedly reduced cellularization at E9.5, which normalizes by E10.5. Concordant with the in vivo findings, AV canal explant assays demonstrate that EMT in *Slug*-deficient embryos is impaired at E9.5 but not E10.5, as EMT in *Slug*-deficient embryos is rescued by an increase in *Snail* expression by E10.5. Accordingly, abolishing both *Slug* and *Snail* expression results in EMT defects at E10.5. In contrast to a previous study, we show that Notch signaling, through CSL, directly regulates the *Slug* promoter, resulting in the up-regulation of *Slug*, but not *Snail*, in endothelial cells (Timmerman et al., 2004). We further show that *Slug* directly binds and represses the *vascular endothelial cadherin* (*VE-cadherin*) promoter. Slug also promotes increased migration toward PDGF. In contrast, TGF-β2 and BMP2 induce *Snail* expression but minimal *Slug* expression. However, Notch synergistically induces *Snail* in concert with TGF-β2. Our data demonstrate that Notch-induced expression of *Slug* plays an important role in the initiation of EMT in the heart but that increased Snail compensates for the lack of Slug in *Slug*-targeted embryos as cardiac cushion morphogenesis progresses.

Results

Activation of the Notch pathway induces *Slug* but not *Snail* in endothelial cells

It has previously been suggested that EMT initiated by Notch may proceed through the induction of Snail; however, the degenerate primers used in that study amplify both Snail and Slug (Timmerman et al., 2004). To clarify which Snail family members are regulated by Notch signaling, we activated Notch in endothelial cells by ectopically expressing the Notch ligands Jagged1 or Dll4 or the constitutively active form of Notch1 or Notch4 (Notch1ICD and Notch4ICD, respectively), all of which are expressed in the cardiac cushion (Loomes et al., 1999; Noseda et al., 2004). Activated Notch up-regulated *Slug*, but not *Snail*, in all endothelial cells tested, as demonstrated by RT-PCR (Fig. 1 A), quantitative RT-PCR (qRT-PCR; Fig. 1 B), and immunoblotting (Fig. 1, C and D; and see Fig. 6 B). As a positive control, we confirmed that the known Notch targets *Hey1*, *Hey2*, and *HeyL* were induced by NotchICD (Fig. 1, A and B). Additional experiments with NotchICD deletion constructs revealed that the Ankyrin repeats of Notch are required for induction of Slug (Fig. S1, available at http://www.jcb.org/cgi/content/full/jcb.200710067/DC1). These findings indicate that Notch activation induces *Slug* but not *Snail* expression in endothelial cells.

Slug is expressed in a subset of endothelial cells and the mesenchymal cells of the AV canal, OFT, and valves of the embryonic mouse and human heart

It has been reported that *Slug* mRNA is not expressed at E9.5 in the cardiac cushion (Timmerman et al., 2004), which suggests that it is dispensable for cardiac EMT. Because Notch activation has been shown to be critical for EMT during cardiac cushion development (Noseda et al., 2004; Timmerman et al., 2004), we were interested in defining the expression of *Slug* during the period of cellularization of the mammalian cardiac cushions. We thus examined *Slug-lacZ* mice, which have the *lacZ* gene inserted into the *Slug* locus with concomitant deletion of the zinc finger DNA binding motifs. Expression of *lacZ* in this model has been shown to faithfully match expression of *Slug* mRNA in all tissues analyzed, as determined by in situ hybridization (Jiang et al., 1998). β-galactosidase staining of E9.5–11.5 embryos showed that *Slug*-expressing cells were abundant in the heart (Fig. 2 A) with expression within a subset of endothelial cells as well as the mesenchymal cells of the AV canal and OFT at E9.5, with increasing expression over E10.5 and 11.5 (Fig. 2 B). Detailed analysis of *Slug* expression around E9.5 revealed that *Slug* expression is induced in the AV canal at the 25–28-somite stage at the initiation of EMT (Fig. S2, available at http://www.jcb.org/cgi/content/full/jcb.200710067/DC1). Immunofluorescent staining for Slug protein at E11.5 confirmed expression in the cardiac cushion mesenchyme and a subset of endothelial cells that costained for CD31 (Fig. 2 C, arrowheads).

It has been suggested that EMT continues to take place to allow valvular remodeling later in development as well as in the adult (Armstrong and Bischoff, 2004). To confirm a role for Snail family members in the human heart, we examined expression of *Snail* and *Slug* in embryonic human hearts at various developmental stages (days 52–78 of gestation) with similar results at various stages. Fig. 2 D shows that *Snail* and *Slug* are both expressed in the tricuspid and mitral valves, the AV septum, and the interatrial septum in a 65-d human heart. This staining pattern is similar to *Slug* expression in later stages of mouse heart development (Oram et al., 2003). Higher magnification images revealed that the mesenchymal cells of the valves, as well as endothelial cells at the root of the valves, express *Snail* and *Slug* (Fig. 2 D), suggesting a role for Snail family members in human cardiac cushion development and remodeling.

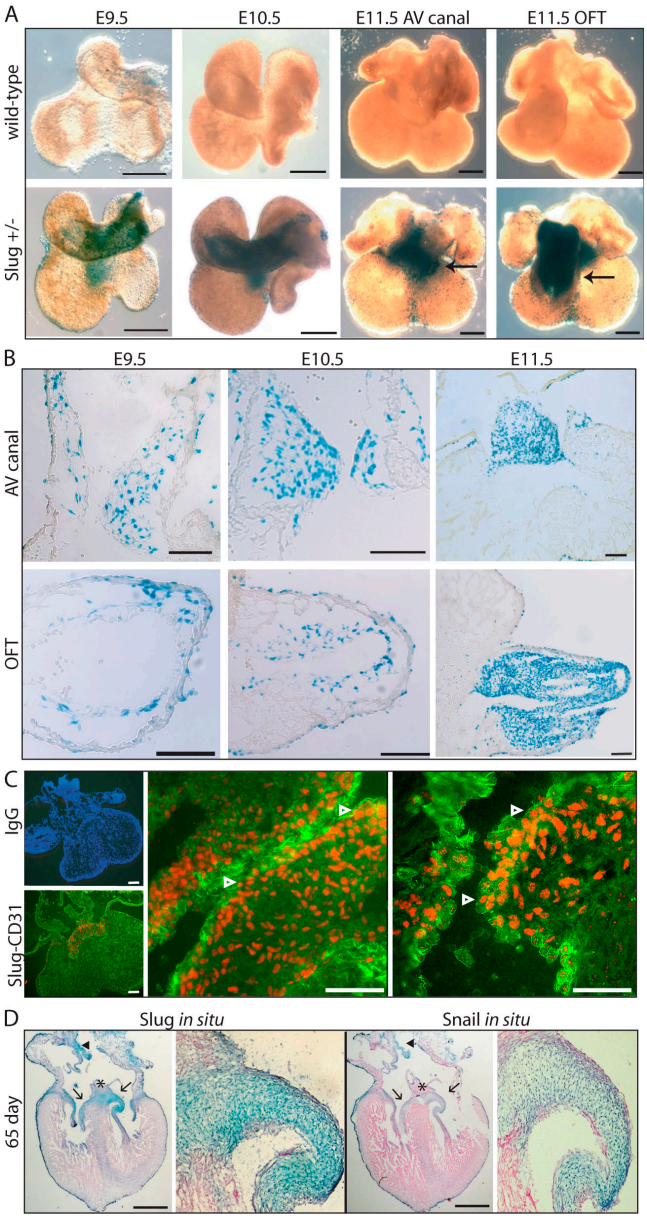

Figure 2. ***Slug* expression during cardiac cushion development.** (A) β-galactosidase staining (representing *Slug* expression) of whole-mounted hearts from *Slug-lacZ*$^{+/-}$ embryos from E9.5 to 11.5. Arrows point to the AV canal or OFT at E11.5. Bars, 250 µm. (B) Sections through the AV canal and OFT of β-galactosidase–stained *Slug-lacZ*$^{+/-}$ hearts from E9.5 to 11.5. Bars, 100 µm. (C) Immunofluorescence staining for Slug (red) and CD31 (green) in E11.5 embryonic mouse hearts. Arrowheads point to cells coexpressing Slug and CD31. Bars, 25 µm. (D) In situ hybridization for *Snail* and *Slug* in a 65-d human embryonic heart. Arrows point to the mitral and tricuspid valves, arrowheads indicate the interatrial septum, and the asterisk marks the AV septum. A higher magnification image of the heart valve is shown in the right panel of each analysis. Bars, 1 mm.

Slug is necessary for EMT in the cardiac cushions

To determine whether targeted disruption of the *Slug* gene has a functional effect on cardiac cushion development, the AV canal of E9.5 embryos were placed on collagen gels to monitor EMT ex vivo, as previously described (Camenisch et al., 2002a; Chang et al., 2004). Occasional endothelial cell outgrowths occur proximal to 100 µm of the AV canal explant. Therefore, only the morphologically distinct mesenchymal cells distal to 100 µm from the AV canal were quantitated to determine the degree of EMT. Homozygous *Slug-LacZ* mutants behave as *Slug*$^{-/-}$ (*Slug*-deficient) animals (Jiang et al., 1998; Inoue et al., 2002), and *Slug*$^{-/-}$ AV canal explants had significantly reduced migration and invasion compared with *Slug*$^{+/-}$ or wild-type controls at E9.5 (Fig. 3, A and B). Of the few *Slug*$^{-/-}$ cells that did migrate, many had a rounded morphology, and were not able to differentiate into spindled mesenchymal cells. Analysis of β-galactosidase activity in *Slug*$^{+/-}$ AV explants revealed *Slug* expression in the migrating cells as well as the proximal

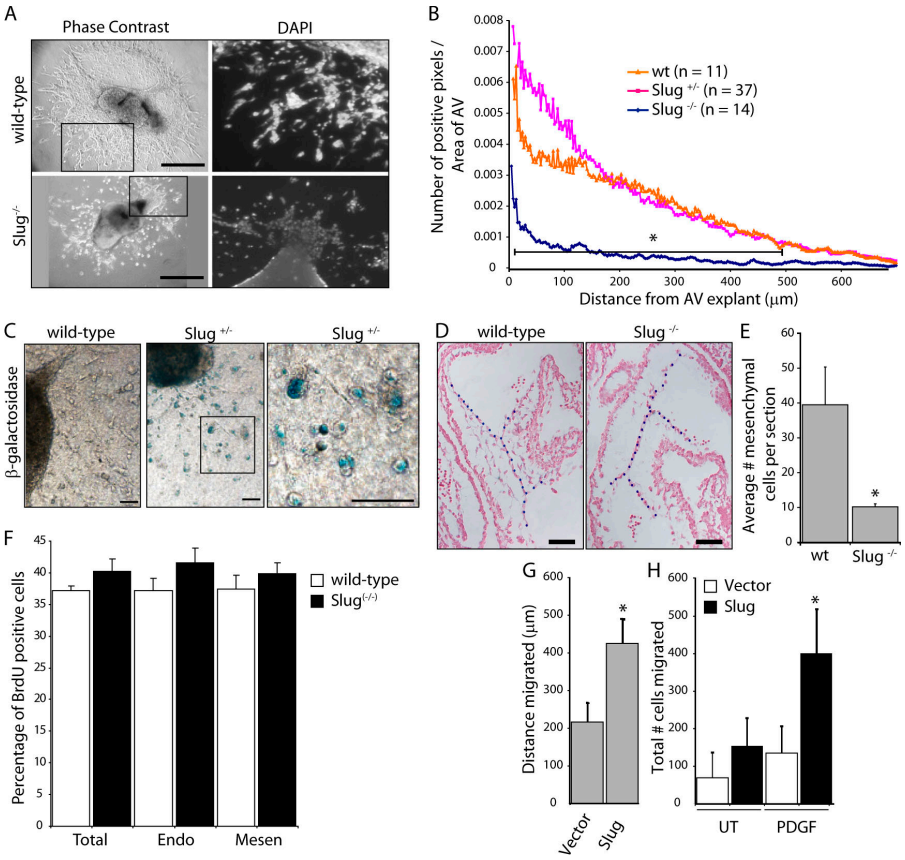

Figure 3. ***Slug*$^{-/-}$ embryos display defects in AV canal EMT at E9.5.** (A) Phase contrast (left) and DAPI (right) images of AV canal explants from wild-type and *Slug*$^{-/-}$ embryos. Bars, 250 μm. (B) Quantitative analysis of EMT in AV canal explants from E9.5 wild-type (wt), *Slug*$^{+/-}$, and *Slug*$^{-/-}$ embryos after 48 h in culture. Results represent the distance of a positive pixel (DAPI-stained nucleus) to the closest point of the AV canal normalized to the area of the AV canal tissue. *, $P < 0.05$. (C) *Slug* expression in the AV canal explant assay as visualized by β-galactosidase staining of wild-type and *Slug-lacZ*$^{+/-}$ AV explants. The rounded morphology of most of the LacZ^{+} cells is shown on the right. The black square indicates the region of higher magnification shown to the right. Bars, 50 μm. (D) Representative sections of wild-type and *Slug*$^{-/-}$ hearts counterstained with Nuclear Fast Red used for analysis in E. Dotted blue lines highlight the superior and inferior AV cushions. Bars, 50 μm. (E) Quantitation of the cellularity of the superior and inferior cushions in E9.5 wild-type (wt; $n = 3$) and *Slug*$^{-/-}$ ($n = 3$) embryos. Error bars show SEM. (F) BrdU analysis on the percentage of proliferating cells in wild-type ($n = 4$) and *Slug*$^{-/-}$ ($n = 6$) AV canal cardiac cushions (total), the AV canal endocardium (Endo), and AV canal mesenchymal cells (Mesen; 10–15 sections per embryo). Error bars show SEM. (G) Vector- or Slug-transduced HMEC were subjected to an endothelial wounding assay. Bars represent the distance migrated after 24 h ($n = 4$). *, $P < 0.05$. Error bars show SD. (H) Vector- or Slug-transduced HMEC were evaluated in a modified Boyden chamber assay with 20 ng/ml PDGF-BB present in the lower chamber. Bars represent the total number of cells migrated after 4 h ($n = 6$). *, $P < 0.05$. Error bars show SD.

cardiac endothelial cells (Fig. 3 C). Interestingly, the majority of β-galactosidase staining was seen in rounded cells, which is consistent with morphology of cells that are intermediate between endothelial and mesenchymal phenotype, as previously described (Camenisch et al., 2002b).

To confirm that cushion cellularization was impaired in Slug-deficient embryos in vivo, E9.5 hearts were serially sectioned (between 7 and 20 sections for each heart) and the number of cushion cells was quantitated in every section. At E9.5, *Slug*$^{-/-}$ embryos had significantly fewer mesenchymal cells in the cardiac cushions compared with wild-type controls (Fig. 3, D and E). However, by E10.5 there was no difference in cellularity of the cardiac cushions, and a defect in AV canal EMT ex vivo was not evident (Fig. S2). These findings implicate *Slug* in the early activation and migration of endothelial cells during cushion EMT with potential compensation by other factors later in cardiac cushion development. To investigate the reason for the normalization of cardiac cushion cellularization by E10.5, the degree of cardiac cushion apoptosis and proliferation was evaluated. AV canal endocardial and mesenchymal cell proliferation was measured by BrdU incorporation and no difference in S-phase entry was noted at E9.5 (unpublished data). However, analysis at E10.25 revealed that there is an increase in BrdU incorporation in both the endocardium and mesenchyme in *Slug*$^{-/-}$ embryos (Fig. 3 F). Although the increase in BrdU incorporation was small, a greater pool of endocardial cells able to undergo EMT combined with increased mesenchymal proliferation may be sufficient to normalize cushion cellularity by E10.5. In contrast, quantitation of active caspase-3 to enumerate the numbers of cells undergoing apoptosis did not reveal much cell death (< 1%) in either wild-type or *Slug*$^{-/-}$ AV canals, with no difference between the two groups (unpublished data).

To determine whether *Slug* is sufficient to promote a motile phenotype in endothelial cells, endothelial cells were transduced with vector or Slug, and an in vitro wound healing (scratch) assay was performed. The scratch assay revealed increased migration of Slug-expressing endothelial cells as early as 4 h and up to 24 h after wounding of the endothelial monolayer, resulting in Slug-expressing cells migrating almost twice as far after 24 h (Fig. 3 G). PDGF has been shown to be expressed in the cardiac cushions during EMT (Van Den Akker et al., 2005). Using a modified Boyden chamber assay with 20 ng/ml PDGF-BB present in the lower chamber, we found that Slug-expressing endothelial cells showed significantly increased directed migration toward PDGF-BB (Fig. 3 H). Thus, Slug expression in the endothelium appears to be sufficient for endothelial motility and directed migration.

Slug represses endothelial phenotype

Given our findings demonstrating the requirement of *Slug* in cardiac EMT, we sought to examine the role that *Slug* plays in modulating the endothelial phenotype. Enforced expression of Slug repressed expression of key endothelial genes such as *VE-cadherin*, *CD31*, and *Tie2* as determined by qRT-PCR, immunoblotting, and immunofluorescence (Fig. 4, A and B; and Fig. S3, available at http://www.jcb.org/cgi/content/full/jcb.200710067/DC1). However, in contrast to activated Notch, Slug did not induce the mesenchymal markers smooth muscle α-actin and h1-calponin (Fig. 4 B). These findings suggest that Slug expression promotes the initial phases of EMT associated with the loss of endothelial phenotype but is not sufficient to complete the transition into a mesenchymal cell that is mediated by Notch activation.

VE-cadherin is a key endothelial adherens junction protein that is required for maintenance of endothelial homeostasis and that must be down-regulated before endothelial remodeling (Crosby et al., 2005). We thus determined whether Slug was capable of directly repressing *VE-cadherin*. Promoter analysis of human *VE-cadherin* identified two putative Slug binding E2-box (CACCTG) motifs 5′ to the transcriptional start site (TSS), located at −306 to −311 and −379 to −384 (Prandini et al., 2005). As demonstrated by electrophoretic mobility shift assays (EMSA), Slug was capable of binding both E2-box motifs, but was unable to bind a CAGCTG E-box element located at −97 to −102 in the human *VE-cadherin* promoter (Fig. 4 C). Of the three cis elements tested in the human VE-cadherin promoter, only the −379 to −384 E2-box and the −97 to −102 E-box motifs are conserved in the mouse *VE-cadherin* promoter. Consistent with the EMSA result, mutation of the E2-box, but not the E-box motif, significantly reduced the ability of Slug to repress the mouse *VE-cadherin* promoter as measured by luciferase assays (Fig. 4 D). Thus, *VE-cadherin* transcription is directly repressed by Slug binding to the E2-box promoter elements in endothelial cells.

Notch acts through CSL to induce *Slug* and repress the endothelial phenotype

We next determined whether Notch induces *Slug* through the canonical CSL-dependent pathway or the less well-defined CSL-independent route (Ramain et al., 2001). Dll4-mediated induction of *Slug* mRNA and protein was dramatically reduced when *CSL* was knocked down using either of two lentiviral-delivered short hairpin RNA (shRNA) constructs, which target distinct regions of *CSL* (Fig. 5, A–C). As expected, induction of the Notch target *HeyL* was also abolished by *CSL* knockdown (Fig. 5 B). In addition, the ability of Notch activation to down-regulate the endothelial markers VE-cadherin and CD31 (Fig. 5 C) was abrogated when *CSL* was knocked down. We also targeted *Slug* using two distinct lentiviral-delivered shRNAs and found that the ability of Dll4-activated Notch to down-regulate VE-cadherin and CD31 was also reversed by Slug knockdown (Fig. 5 C and Fig. S3), thus demonstrating the requirement of CSL-mediated induction of *Slug* for Notch-mediated EMT. Furthermore, activation of CSL using a constitutively active CSL mutant (CSL-VP16; MacKenzie et al., 2004) demonstrated that CSL activation alone was sufficient to up-regulate *Slug* expression as well as the Notch target

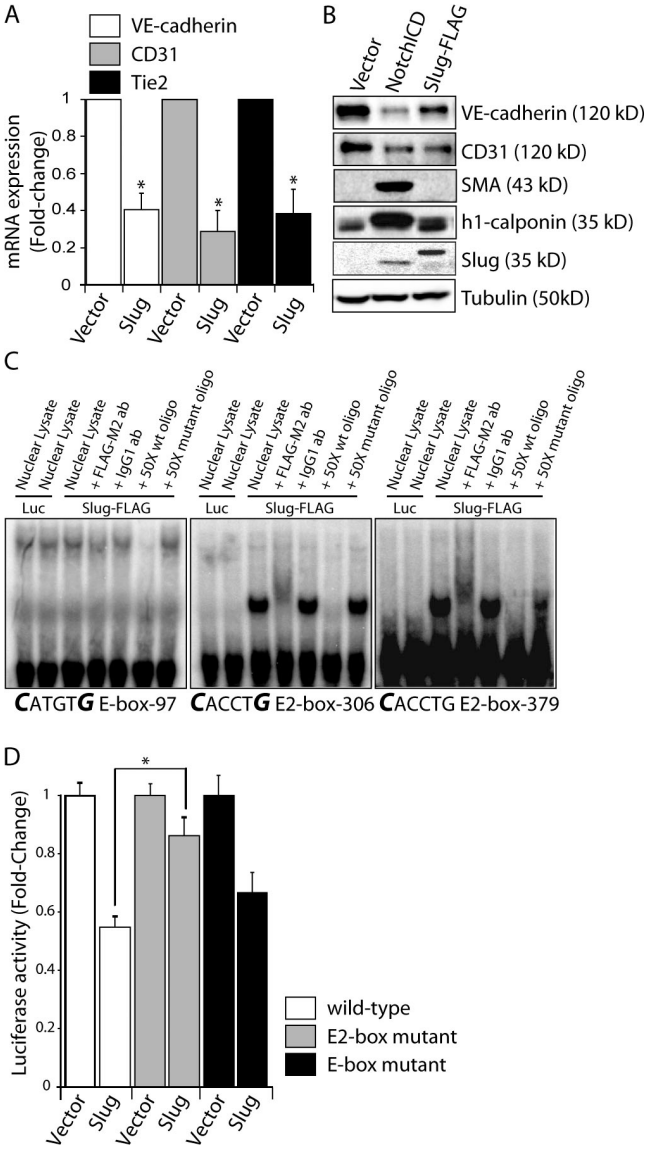

Figure 4. **Slug represses the endothelial phenotype and directly regulates the *VE-cadherin* promoter.** (A) Analysis of endothelial marker expression by qRT-PCR in Slug-transduced HMEC ($n = 3$). *, $P < 0.05$. (B) Immunoblots for endothelial and mesenchymal markers in empty vector–, NotchICD-, and Slug-expressing HMEC. (C) EMSA using in vitro–translated luciferase (Luc) or Slug-FLAG protein and ^{32}P-labeled double-stranded oligonucleotides for an E-box cis element (−97) or two putative *Slug* E2-box motifs (−306 and −379) in the human *VE-cadherin* promoter. Supershift assays with anti–FLAG-M2 or IgG control antibodies and competition assays with 50× wild-type (wt) or mutant probes are also shown. (D) Promoter activity in endothelial cells cotransfected with vector or Slug plasmids and wild-type, E2-box mutant, or E-box mutant mouse *VE-cadherin* promoter-luciferase constructs ($n = 4$; each experiment performed in triplicate). *, $P < 0.05$. Error bars show SEM.

HeyL (Fig. 5 D). However, enforced expression of the Notch targets Hey1 or Hey2, which have been implicated in cardiac EMT, did not up-regulate Slug or repress VE-cadherin (Fig. S3). Together, these findings indicate that Notch, via CSL, directly up-regulates *Slug* expression and that *Slug* is the Notch target responsible for repressing VE-cadherin expression.

Analysis of the human and mouse *Slug* promoters (−2,000 to +100 relative to the TSS) identified six putative CSL binding

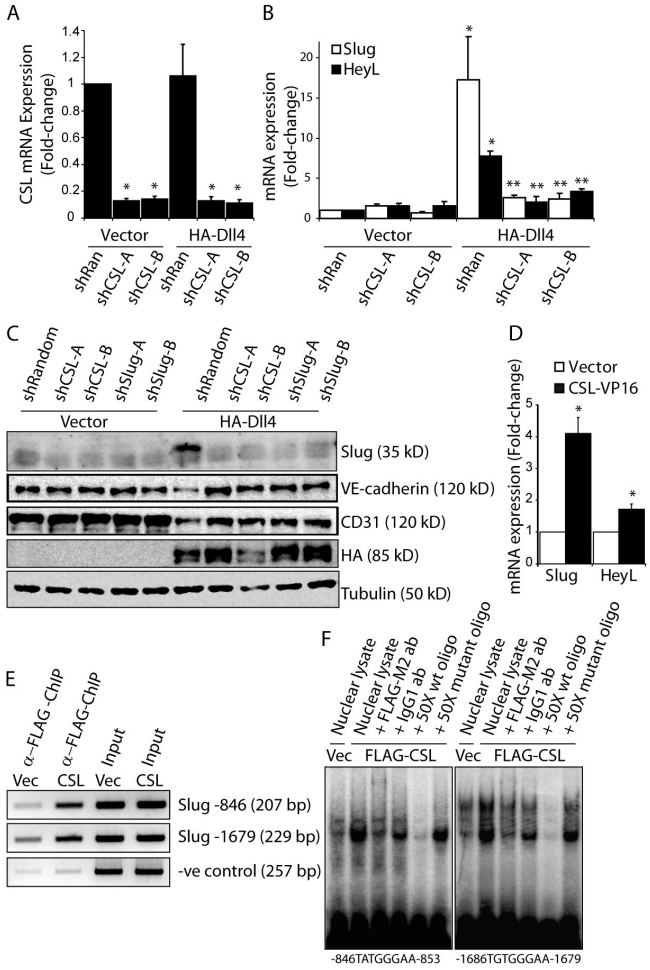

Figure 5. **Notch signaling regulates *Slug* expression through a CSL-dependent pathway.** (A) qRT-PCR analysis demonstrating efficient knockdown of *CSL* in HMEC with two different shRNAs targeting *CSL* (shCSL) compared with a random control sequence (shRan). (B) qRT-PCR of *Slug* and *HeyL* in vector- or Dll4-activated HMEC transduced with shCSL constructs ($n = 3$). *, $P < 0.05$ vector shRandom versus HA-D114 shRandom; **, $P < 0.05$ HA-D114 shRandom versus HA-D114 shCSL-A or shCSL-B. (C) Immunoblotting for Slug, VE-cadherin, and CD31 in vector- or Dll4-activated HMEC transduced with shCSL or shSlug constructs. (D) qRT-PCR of vector- or CSL-VP16–expressing HMEC for *Slug* and *HeyL* ($n = 3$). *, $P < 0.05$. (E) PCR after ChIP with anti–FLAG-M2 antibody on HMEC-expressing vector (vec) or FLAG-CSL (CSL) to demonstrate CSL binding to the human *Slug* promoter. The negative (-ve) control represents PCR of the *ZNF3* promoter after ChIP using FLAG-M2. (F) EMSA using nuclear lysates collected from vector- or FLAG-CSL–expressing HMEC and ^{32}P-labeled double-stranded oligonucleotides spanning each of the two CSL binding sites in the human *Slug* promoter. Supershift assays with anti–FLAG-M2 or IgG control antibodies, and competition assays with 50× wild-type (wt) or mutant probes are also shown. Error bars show SEM.

sites ((C/T)(A/G)TG(A/G/T)GA(A/G/T)) in the human and two putative CSL binding sites in the mouse. Of the six putative binding sites in the human *Slug* promoter, two were further investigated based on conservation of the *CSL* binding sites in the mouse *Slug* promoter. The first binding site (TATGGGAA) is located at −846 to −853, whereas the second binding site (TGTGGGAA) is located at −1,679 to −1,686 upstream of the TSS. Using chromatin immunoprecipitation (ChIP) followed by PCR with primers flanking the CSL elements, we found that CSL was capable of binding both CSL consensus motifs in the *Slug* promoter (Fig. 5 E). In contrast, PCR of the same ChIP DNA did not enrich the *ZNF3* promoter, which lacks a putative CSL binding site. EMSA of nuclear lysates harvested from FLAG-CSL–expressing endothelial cells confirmed that CSL is capable of binding both consensus elements present in the human *Slug* promoter (Fig. 5 F). Collectively, these data demonstrate that *Slug* is a direct target of Notch through a CSL-dependent pathway and that Slug induction is required for Notch-mediated repression of the endothelial phenotype.

Notch and TGF-β act synergistically to induce *Snail*

Components of the TGF-β pathway have been shown to be required for EMT and for the regulation of Snail family genes during heart development (Romano and Runyan, 2000; Camenisch et al., 2002a; Wang et al., 2005). Additionally, the Notch and TGF-β pathways have been shown to coregulate target gene expression in various cell types (Blokzijl et al., 2003; Zavadil et al., 2004). To investigate the relationship between the Notch and TGF-β pathways and Snail family member expression, endothelial cells cocultured with vector- or Dll4-transduced cells were treated with 2.5 ng/ml TGF-β2 or 20 or 50 ng/ml BMP2. TGF-β2 stimulation induced maximal induction of *Snail* mRNA and protein expression after 2 h of treatment in vector-transduced cells, followed by rapid down-regulation (Fig. 6, A and B). Although Dll4 stimulation alone did not induce *Snail*, combined activation of the Notch and TGF-β pathways resulted in a synergistic increase of *Snail* mRNA levels and maintenance of expression for at least 8 h after stimulation with TGF-β2 (Fig. 6 A). Protein expression of Snail peaked slightly later (4 h) and was sustained at a much higher level in the context of Dll4 and TGF-β2 costimulation compared with TGF-β2 stimulation alone (Fig. 6 B). In contrast, there was minimal induction of *Slug* by TGF-β2, whereas Notch activation alone dramatically up-regulated *Slug* (Fig. 6, B and C). Costimulation by Dll4 and TGF-β2 did not increase the level of *Slug* induction over that seen with Dll4 alone (Fig. 6, B and C).

To investigate the role of Notch activation in TGF-β2–mediated induction of *Snail*, we used the γ-secretase inhibitor DAPT to block ligand-activated Notch signaling. TGF-β2 treatment dramatically up-regulated the expression of *Snail*, but the addition of DAPT did not affect the ability of TGF-β2 to induce *Snail*, which is consistent with Notch-independent induction (Fig. 6 C). In the context of combined Notch and TGF-β2 activation, the synergistic up-regulation of *Snail* expression was reduced by DAPT to the level seen by TGF-β2 stimulation alone (Fig. 6 C). TGF-β2 had no effect on *Slug* levels, and the addition of DAPT abrogated *Slug* induction by Dll4, suggesting complete dependence on Notch activation for *Slug* up-regulation (Fig. 6 C). Similar results were observed with TGF-β1 treatment (Fig. S4, available at http://www.jcb.org/cgi/content/full/jcb.200710067/DC1). As expected, stimulation of endothelial cells with TGF-β2 induced expression of *Smad7*, a TGF-β target gene, to similar levels in control and Notch-activated cells (Fig. 6 C). Addition of DAPT appeared to block the ability of TGF-β2 to induce *Smad7*, but the results were variable and did not reach statistical significance for TGF-β2 or TGF-β1 (Fig. 6 C

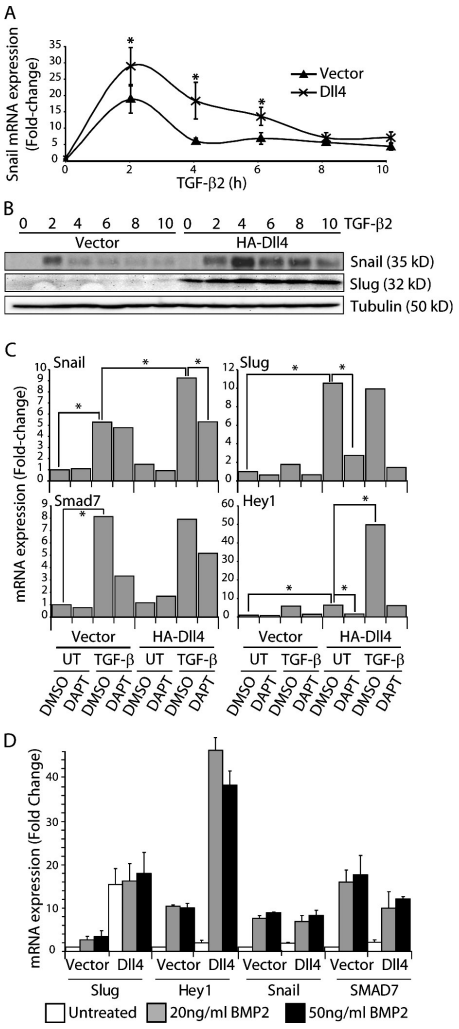

Figure 6. **Induction of *Snail* by TGF-β2 is synergistically enhanced in Dll4-activated endothelial cells.** (A) qRT-PCR for *Snail* mRNA in vector- or Dll4-activated HMEC treated with 2.5 ng/ml TGF-β2 for the indicated times ($n = 3$). *, $P < 0.05$. (B) Immunoblots for Snail and *Slug* in vector- or Dll4-activated HMEC treated with 2.5 ng/ml TGF-β2. (C) qRT-PCR for *Snail, Slug, Hey1,* and *Smad7* mRNA in vector- or Dll4-activated HMEC treated with 10 μM DMSO or DAPT for 16 h followed by treatment with 2.5 ng/ml TGF-β2 for 3 h ($n = 3$). *, $P < 0.05$. (D) qRT-PCR for *Snail, Slug, Hey1,* and *Smad7* mRNA in vector- or Dll4-activated HMEC treated with 20 or 50 ng/ml BMP2 ($n = 3$). Error bars show SEM.

and Fig. S4), suggesting a minimal role for Notch activation in TGF-β–induced *Smad7* induction. *Hey1* expression was induced by Notch signaling and TGF-β2 and was dependent on active Notch signaling (Fig. 6 C). Similar to what has been described for BMP4/6, *Hey1* was also synergistically induced to very high levels by TGF-β2 and Dll4 (Fig. 6 C; Dahlqvist et al., 2003; Itoh et al., 2004).

Similar to TGF-β2, when endothelial cells were stimulated with BMP2 there was dramatic up-regulation of *Snail* expression, minimal up-regulation of *Slug*, and synergistic activation of *Hey1* in Notch activated cells (Fig. 6 D). However, unlike TGF-β2, combined activation of the Notch pathway and BMP2 stimulation did not synergistically up-regulate *Snail* expression (Fig. 6 D). This suggests that a Smad3-dependent process is involved in the synergistic activation of *Snail* expression by the Notch and TGF-β pathways. These findings clearly confirm that *Slug* is a direct target of Notch and that *Snail* is not but that *Snail* is synergistically induced when Notch activation is superimposed on TGF-β stimulation.

Snail and *Slug* cooperatively induce cardiac EMT

Given that the cardiac EMT defect seen in *Slug*$^{-/-}$ mice at E9.5 was reduced by E10.5 (Fig. 3, A and B; and Fig. S2), we sought to determine whether *Snail* was compensating for the absence of *Slug* in vivo. qRT-PCR analysis of wild-type and *Slug*$^{-/-}$ hearts was conducted for *Snail* and *Slug*. *Slug* expression increased from E9.5 to 11.5 in the wild-type heart and its expression was abolished in the *Slug*$^{-/-}$ hearts. In contrast, *Snail* expression did not increase from E9.5 to 11.5 in the wild-type hearts. However, in the *Slug*$^{-/-}$ hearts Snail was up-regulated 3.6-fold by E11.5 (Fig. 7 A). In situ hybridization at E10.5 and 11.5 revealed *Snail* expression in the AV canal and OFT in both wild-type and *Slug*$^{-/-}$ hearts, with increased expression in the *Slug*$^{-/-}$ embryos (Fig. 7 B), suggesting that the region of *Snail* expression is not expanded but, rather, that the cells normally expressing *Snail* do so at a higher level in the *Slug*$^{-/-}$ hearts.

We next determined whether the TGF-β pathway, potentially through *Snail*, could compensate for *Slug* deficiency at E9.5. Treatment of E9.5 AV canal explants with 5 ng/ml TGF-β2 completely rescued the EMT defect seen in E9.5 *Slug*$^{-/-}$ embryos (Fig. 7 C). Given the increase in *Snail* expression noted at E10.5 and 11.5 in *Slug*$^{-/-}$ hearts (Fig. 7, A and B), the ability of *Snail* to compensate for the absence of *Slug* after E9.5 was directly assessed using a lentiviral-delivered shRNA to knock down *Snail* expression in *Slug*$^{-/-}$ E10.5 AV canal explants. Knockdown of *Snail* in wild-type or heterozygote *Slug* AV explants did not result in a decrease in the number or distance of migrating cells at E10.5 (Fig. 7 D). In contrast, knockdown of *Snail* in *Slug*$^{-/-}$ AV explants resulted in a significant reduction in the number of migrating/invading cells (Fig. 7 D). The degree of EMT is reduced in E10.5 AV canals compared with E9.5 AV canals, which is consistent with previous data (Dor et al., 2001; Chang et al., 2004). These data support the redundancy of *Slug* and *Snail* during the later stages of EMT in the cardiac cushions and suggest that parallel activation by the Notch and TGF-β–BMP pathways is required to maintain the appropriate level of expression of Snail family members in order for cushion development to proceed.

Discussion

The Notch signaling pathway has been found to be a key regulator of cardiac cushion EMT and has been implicated in the pathogenesis of various cardiovascular diseases (Niessen and Karsan, 2007). TGF-β–related pathways have also been shown to be essential for proper heart development through their role in regulating EMT (Azhar et al., 2003). Thus, there are clear requirements for both the Notch and TGF-β–related pathways during mammalian cardiac cushion development. However, there is limited detail of how these pathways function and interact with each other during cardiac development. Our findings suggest

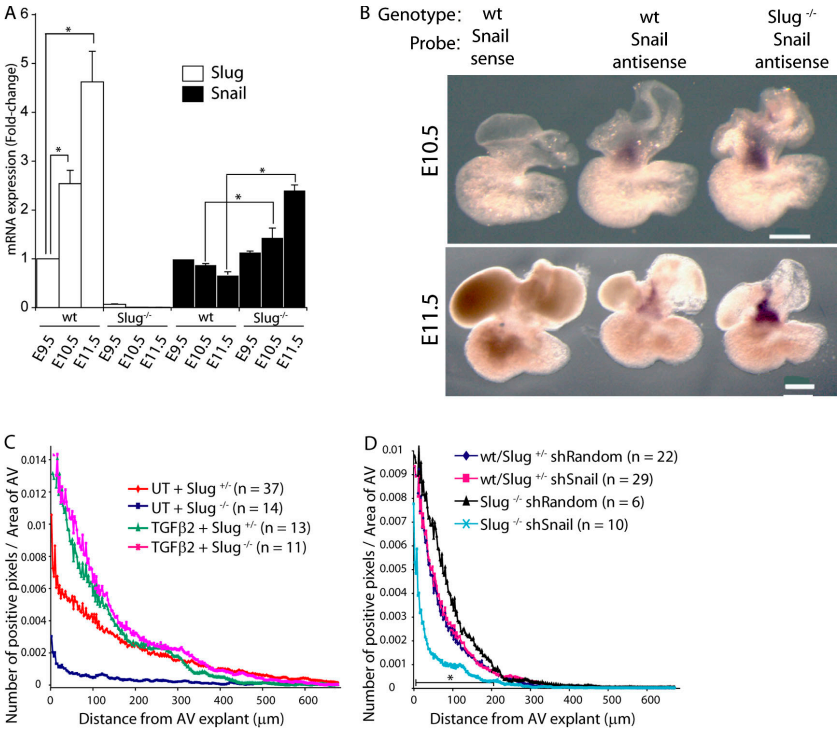

Figure 7. **Increased *Snail* expression compensates for *Slug* deficiency.** (A) qRT-PCR analysis for *Snail* and *Slug* of whole hearts isolated from E9.5, 10.5, and 11.5 wild-type (wt) and $Slug^{-/-}$embryos (n = 3). *, $P < 0.05$. Error bars show SEM. (B) In situ hybridization for *Snail* in E10.5 and 11.5 wild-type (wt) and $Slug^{-/-}$ hearts (n = 3; five embryos in each replicate). Bars, 250 μm. (C) Quantitation of EMT in AV canal explants from E9.5 wild-type (wt) or $Slug^{+/-}$ and $Slug^{-/-}$ embryos treated with 5 ng/ml TGF-β2 or vehicle (UT). (D) Quantitation of EMT in AV canal explants from E10.5 wild-type (wt) or $Slug^{+/-}$ and $Slug^{-/-}$ embryos transduced with shRandom or shSnail constructs.

cooperation between the Notch and TGF-β–BMP pathways during cardiac EMT, through the coordinate regulation of a group of genes such as the Snail family of transcription factors. In contrast to a previous study, we demonstrate that the transcriptional repressor *Slug*, but not *Snail*, is a direct target of the Notch pathway (Timmerman et al., 2004). Conversely, activation of the TGF-β pathway dramatically up-regulates the expression of *Snail* but not *Slug*, and *Slug* is not required for TGF-β–mediated EMT. Importantly we reveal synergistic up-regulation of *Snail* expression by the Notch and TGF-β pathways, despite the fact that *Snail* is not a direct target of Notch. This synergistic activation of TGF-β–induced *Snail* by Notch is consistent with the decrease in *Snail* expression seen in *CSL*-deficient embryos (Timmerman et al., 2004).

Interestingly, endothelial-specific gene targeting of the BMP receptor *Alk2* results in cardiac cushion defects that are associated with a decrease in the expression of *Snail*, but not *Hey2* or *Slug*, in the AV canal (Wang et al., 2005). In contrast, Notch-mediated EMT is cell autonomous and TGF-β independent (Noseda et al., 2004). Collectively, these findings support the data presented herein that *Slug* is a direct target of the Notch pathway and that *Snail* is a target of TGF-β–related pathways.

We show for the first time that *Slug* is expressed in a subset of cardiac endothelial cells and the mesenchyme of the AV canal and OFT from the onset of EMT at E9.5 and is essential for initiating cardiac cushion cellularization. We further demonstrate that Slug binds and represses the *VE-cadherin* promoter, inducing a motile phenotype. Taken with the defect in AV canal EMT at E9.5, the ability of Slug to bind and repress the *VE-cadherin* promoter and induce migration suggests that the activation phase of EMT in the endocardium is impaired by loss of *Slug*.

Using an AV canal explant model, we demonstrate that *Slug*-deficient hearts have a specific defect in cardiac cushion EMT at E9.5 but not at E10.5. In *Slug*-deficient hearts at E10.5, cardiac EMT is compensated for by a relative increase in *Snail* expression. Accordingly, inducing *Snail* expression by treatment with TGF-β2 at E9.5 rescues the EMT defect in *Slug*-deficient mice. Conversely, abolishing both *Slug* and *Snail* expression results in EMT defects at E10.5. Consistent with a requirement for both *Snail* and *Slug* during cardiac EMT, both members are expressed during mouse and human heart development with similar localization in a subset of endothelial cells and the mesenchymal cells of the AV canal and OFT. It is of interest that deletion of *Slug* results in up-regulation of *Snail*. This finding suggests that *Slug* may act to repress *Snail*, either by directly targeting the *Snail* promoter or through the repression of elements of the TGF-β–related or Notch pathways. Consistent with the latter hypothesis, we have seen that both *Hey2* and *Smad7* are up-regulated in *Slug*-deficient hearts at E11.5 (unpublished data). Additionally, it has been demonstrated that Slug does not affect *Snail*-promoter activity (Peiro et al., 2006), which we have verified (unpublished data). Our findings are concordant with a recent study showing that Snail heterozygosity increases the penetrance of palate defects in Slug-deficient mice, suggesting that Snail also compensates for Slug deficiency during palate development (Murray et al., 2007). In addition, the finding that there is increased *Slug* expression in the developing palate in *Snail*-deficient embryos (Murray et al., 2007) suggests reciprocal regulation of gene expression between *Slug* and *Snail*.

The interaction between the Notch and TGF-β pathways likely occurs at multiple levels and may be context-dependent. Targeting of *CSL* results in reduced *TGF-β2* and its receptor *TBRII* in the mouse heart (Timmerman et al., 2004). In contrast,

the Notch-ligand *Jagged1* has been shown to be induced by TGF-β at the onset of EMT in epithelial cells (Zavadil et al., 2004). Despite our evidence showing cooperation of the TGF-β and Notch pathways in cardiac cushion development, several studies have suggested that constitutively active NotchICD inhibits TGF-β signaling through the sequestration of Smad3 or the co-activator p300 (Masuda et al., 2005; Sun et al., 2005). However, overexpression of NotchICD may have resulted in artifactual sequestering of TGF-β signaling components. Alternatively, the outcome of Notch–TGF-β cross talk may be dependent on the context. Indeed, in mouse embryonic endothelial cells, BMP signaling synergizes with NotchICD through a ternary interaction between Smad5, NotchICD, and p/CAF (Itoh et al., 2004).

Combining the findings in this paper with published data, one can propose a model where endothelial Notch activation induces *Slug* and release of TGF-β and BMPs from the cushion myocardium activates the cardiac endothelium to up-regulate *Snail*, which is enhanced in Notch-activated cells. Based on the *Slug*-deficient hearts and RNAi studies in the AV explants, a minimal total dose of *Snail*/*Slug* is required in order for EMT to be initiated at E9.5, with a diminishing requirement at E10.5 as cushion development proceeds.

Materials and methods

Reagents
The mouse monoclonal antibody against the FLAG epitope (M2), mouse anti–h1-calponin, and mouse anti-tubulin were purchased from Sigma-Aldrich. Goat anti–VE-cadherin (C-19), goat anti-CD31 (C-20), and goat anti-Slug (G-18) were obtained from Santa Cruz Biotechnology Inc. Rabbit anti–Snail antibody was obtained from Abcam. Mouse anti–VE-cadherin (TEA1/31) was obtained from Beckman Coulter. Rabbit anti–α–smooth muscle actin antibody was obtained from Thermo Fisher Scientific.

Cell culture and gene transfer
The HMEC-1 human microvascular endothelial cell line, HUVEC, and human aortic endothelial cells were obtained and cultured as previously described (Noseda et al., 2004). Endothelial cells were transduced using the retroviral vectors pLNCX, pLNC-*Slug*-FLAG, pLNC-FLAG-*CSL*, MIY, MIY-*Slug*-FLAG, MIY-*Notch4IC*-HA, MIY-*Notch1IC*, and MIY-*CSL-VP16* as previously described (Karsan et al., 1996). pcDNA3-*Slug*-FLAG cDNA was a gift from E.R. Fearon (The University of Michigan Heath Systems, Ann Arbor, MI).

RNA collection and RT-PCR
RNA was isolated and cDNA was made as previously described (Noseda et al., 2004). PCR was performed on a PCR cycler (PTC-200 [Bio-Rad Laboratories] or 7900HT [Applied Biosystems]) with primers listed in Table S1 (available at http://www.jcb.org/cgi/content/full/jcb.200710067/DC1).

Luciferase reporter assay
8×10^4 HMEC was plated 24 h before transfection in 24-well plates. HMEC were transfected using SuperFect (QIAGEN) reagent, with 0.3125 µg of total plasmid DNA as per the manufacturer's recommendations. Each well was transfected with 0.3 µg of the VE-cadherin promoter plasmid or mutant VE-cadherin promoter constructs, 5 ng pcDNA3 or pcDNA3-*Slug*-FLAG, and 7.5 ng pRL-CMV (Promega). Luminescence was measured on a Lumat LB 9507 (EG&G Berthold) 24 h after transfection using dual luciferase reporter assays according to the manufacturer's recommendations (Promega).

EMSA
For Slug EMSA assays, in vitro–translated (TNT; Promega) Slug-FLAG or control luciferase protein was preincubated with FLAG-M2 antibody overnight at 4°C in 12 mM Hepes, pH 7.9, 4 mM Tris, pH 7.9, 133 mM KCl, 10% Glycerol, and 2 µg PolydI-dC binding buffer. 50-fold excess non-radioactive duplex oligos were preincubated for 15 min on ice, and then 150,000-cpm ^{32}P-labeled double-stranded oligo nucleotides were added and incubated for 30 min at room temperature. Binding reactions were run on 5% Tris-borate EDTA gels and exposed to a phosphorimager plate for 12–16 h. For CSL EMSA assays, nuclear lysates were collected from FLAG-CSL–overexpressing HMEC cells. Binding reaction and detection were the same as used for *Slug*-FLAG EMSA assays.

ChIP
HMEC were transduced with pLNCX or pLNC-FLAG-*CSL*, and ChIP assay was performed as previously described (Noseda et al., 2006). ChIP DNA was amplified for the *ZNF3* promoter or the two CSL binding sites in the human *Slug* promoter using primers listed in Table S1.

Mice and AV explant assay analysis
Slug-lacZ mice were provided by T. Gridley (Jackson Laboratories, Bar Harbor, ME). *Slug-lacZ*$^{+/-}$ mice were crossed to C57BL/6J mice for embryo collection. Embryos were assayed for β-galactosidase activity in situ using published protocols (Nagy et al., 2003). AV canal explants were performed as previously described (Camenisch et al., 2002a). Explants were cultured for 48 h and analyzed for the number and distance of migrating cells.

RNA interference
shRNAs targeting human *CSL*, *Snail*, and *Slug* were cloned into the HpaI–XhoI sites of the pLentilox3.7 vector (gift from L. Van Parijs, Massachusetts Institute of Technology, Cambridge, MA; Table S1). Constructs were sequence verified and validated for efficient knockdown.

Collection of human tissues
Human embryonic hearts were collected, after institutionally approved protocols and informed consent, at the Children's and Women's Health Sciences Centre (Vancouver, Canada). Tissue was fixed in 4% PFA overnight, embedded in OCT, and cryosectioned.

In situ hybridization
In situ hybridization was performed as previously described (Wilkinson, 1992). Mouse *Snail* probe (−55 to +454) was cloned into pBluescript. Human *Snail* and human *Slug* probes were comprised of the entire ORF cloned into pCDNA3.

BrdU analysis
Slug-lacZ$^{+/-}$ male and female mice were crossed and pregnant females were injected with 1,500 mg/ml BrdU (Sigma-Aldrich) 2 h before killing. Embryos were collected, paraffin embedded, and sectioned (6 µm) onto Histobond slides (Marienfeld Laboratory Glassware). Slides were boiled for 30 min in 0.1M citrate buffer, rinsed in water, and then denatured in 2N HCl for 45 min at 37°C. Slides were then rinsed in PBS, and BrdU staining was performed using mouse anti-BrdU (BU33; Sigma-Aldrich) and goat anti–mouse Alexa 488 (Invitrogen).

Online supplemental material
Fig. S1 shows that the ankyrin repeats of NotchICD are required for induction of Slug expression. Fig. S2 shows the Slug-lacZ expression in the 18 to 29 somite stage heart and that the AV canal EMT defect observed in Slug-deficient embryos at E9.5 is no longer present at E10.5. Fig. S3 shows that Slug represses endothelial cell phenotype in HMEC and HUVEC, that the knockdown of Slug expression in Notch-activated cells restores VE-cadherin and CD31 expression, and that the ectopic expression of Hey1 or Hey2 does not induce Slug expression or repress VE-cadherin expression. Fig. S4 shows that the induction of Snail by TGF-β1 is synergistically enhanced in Notch-activated endothelial cells. Table S1 is a list of primers used in this study. Online supplemental material is available at http://www.jcb.org/cgi/content/full/jcb.200710067/DC1.

We would like to thank Megan Abbott for help with the animal studies and Jennifer Baker and Alastair Kyle for help with the AV canal data analysis and immunohistochemistry studies.

This work was supported by grants from the Canadian Institutes of Health Research (MOP 64354), the Heart and Stroke Foundation of British Columbia and the Yukon, Genome Canada, and Genome British Columbia. K. Niessen and L. Chang are supported by Doctoral Research Awards and Y. Fu by a Postdoctoral Award from the Michael Smith Foundation for Health Research. A. Karsan and P.A. Hoodless are Senior Scholars of the Michael Smith Foundation for Health Research, and P.A. Hoodless is a Canadian Institutes of Health Research New Investigator.

Submitted: 11 October 2007
Accepted: 26 June 2008

References

Armstrong, E.J., and J. Bischoff. 2004. Heart valve development: endothelial cell signaling and differentiation. *Circ. Res.* 95:459–470.

Azhar, M., J. Schultz Jel, I. Grupp, G.W. Dorn II, P. Meneton, D.G. Molin, A.C. Gittenberger-de Groot, and T. Doetschman. 2003. Transforming growth factor beta in cardiovascular development and function. *Cytokine Growth Factor Rev.* 14:391–407.

Bartram, U., D.G. Molin, L.J. Wisse, A. Mohamad, L.P. Sanford, T. Doetschman, C.P. Speer, R.E. Poelmann, and A.C. Gittenberger-de Groot. 2001. Double-outlet right ventricle and overriding tricuspid valve reflect disturbances of looping, myocardialization, endocardial cushion differentiation, and apoptosis in TGF-beta(2)-knockout mice. *Circulation.* 103:2745–2752.

Blokzijl, A., C. Dahlqvist, E. Reissmann, A. Falk, A. Moliner, U. Lendahl, and C.F. Ibanez. 2003. Cross-talk between the Notch and TGF-β signaling pathways mediated by interaction of the Notch intracellular domain with Smad3. *J. Cell Biol.* 163:723–728.

Brown, C.B., A.S. Boyer, R.B. Runyan, and J.V. Barnett. 1999. Requirement of type III TGF-beta receptor for endocardial cell transformation in the heart. *Science.* 283:2080–2082.

Camenisch, T.D., D.G. Molin, A. Person, R.B. Runyan, A.C. Gittenberger-de Groot, J.A. McDonald, and S.E. Klewer. 2002a. Temporal and distinct TGFbeta ligand requirements during mouse and avian endocardial cushion morphogenesis. *Dev. Biol.* 248:170–181.

Camenisch, T.D., J.A. Schroeder, J. Bradley, S.E. Klewer, and J.A. McDonald. 2002b. Heart-valve mesenchyme formation is dependent on hyaluronan-augmented activation of ErbB2-ErbB3 receptors. *Nat. Med.* 8:850–855.

Carver, E.A., R. Jiang, Y. Lan, K.F. Oram, and T. Gridley. 2001. The mouse snail gene encodes a key regulator of the epithelial-mesenchymal transition. *Mol. Cell. Biol.* 21:8184–8188.

Chang, C.P., J.R. Neilson, J.H. Bayle, J.E. Gestwicki, A. Kuo, K. Stankunas, I.A. Graef, and G.R. Crabtree. 2004. A field of myocardial-endocardial NFAT signaling underlies heart valve morphogenesis. *Cell.* 118:649–663.

Crosby, C.V., P.A. Fleming, W.S. Argraves, M. Corada, L. Zanetta, E. Dejana, and C.J. Drake. 2005. VE-cadherin is not required for the formation of nascent blood vessels but acts to prevent their disassembly. *Blood.* 105:2771–2776.

Dahlqvist, C., A. Blokzijl, G. Chapman, A. Falk, K. Dannaeus, C.F. Ibanez, and U. Lendahl. 2003. Functional Notch signaling is required for BMP4-induced inhibition of myogenic differentiation. *Development.* 130:6089–6099.

Dickson, M.C., H.G. Slager, E. Duffie, C.L. Mummery, and R.J. Akhurst. 1993. RNA and protein localisations of TGF beta 2 in the early mouse embryo suggest an involvement in cardiac development. *Development.* 117:625–639.

Donovan, J., A. Kordylewska, Y.N. Jan, and M.F. Utset. 2002. Tetralogy of Fallot and other congenital heart defects in Hey2 mutant mice. *Curr. Biol.* 12:1605–1610.

Dor, Y., T.D. Camenisch, A. Itin, G.I. Fishman, J.A. McDonald, P. Carmeliet, and E. Keshet. 2001. A novel role for VEGF in endocardial cushion formation and its potential contribution to congenital heart defects. *Development.* 128:1531–1538.

Eisenberg, L.M., and R.R. Markwald. 1995. Molecular regulation of atrioventricular valvuloseptal morphogenesis. *Circ. Res.* 77:1–6.

Eldadah, Z.A., A. Hamosh, N.J. Biery, R.A. Montgomery, M. Duke, R. Elkins, and H.C. Dietz. 2001. Familial tetralogy of fallot caused by mutation in the jagged1 gene. *Hum. Mol. Genet.* 10:163–169.

Fischer, A., N. Schumacher, M. Maier, M. Sendtner, and M. Gessler. 2004. The Notch target genes Hey1 and Hey2 are required for embryonic vascular development. *Genes Dev.* 18:901–911.

Fischer, A., C. Steidl, T.U. Wagner, E. Lang, P.M. Jakob, P. Friedl, K.P. Knobeloch, and M. Gessler. 2007. Combined loss of Hey1 and HeyL causes congenital heart defects because of impaired epithelial to mesenchymal transition. *Circ. Res.* 100:856–863.

Garg, V., A.N. Muth, J.F. Ransom, M.K. Schluterman, R. Barnes, I.N. King, P.D. Grossfeld, and D. Srivastava. 2005. Mutations in NOTCH1 cause aortic valve disease. *Nature.* 437:270–274.

Hay, E.D. 2005. The mesenchymal cell, its role in the embryo, and the remarkable signaling mechanisms that create it. *Dev. Dyn.* 233:706–720.

Inoue, A., M.G. Seidel, W. Wu, S. Kamizono, A.A. Ferrando, R.T. Bronson, H. Iwasaki, K. Akashi, A. Morimoto, J.K. Hitzler, et al. 2002. Slug, a highly conserved zinc finger transcriptional repressor, protects hematopoietic progenitor cells from radiation-induced apoptosis in vivo. *Cancer Cell.* 2:279–288.

Iso, T., Y. Hamamori, and L. Kedes. 2003. Notch signaling in vascular development. *Arterioscler. Thromb. Vasc. Biol.* 23:543–553.

Itoh, F., S. Itoh, M.J. Goumans, G. Valdimarsdottir, T. Iso, G.P. Dotto, Y. Hamamori, L. Kedes, M. Kato, and P. ten Dijke Pt. 2004. Synergy and antagonism between Notch and BMP receptor signaling pathways in endothelial cells. *EMBO J.* 23:541–551.

Jiang, R., Y. Lan, C.R. Norton, J.P. Sundberg, and T. Gridley. 1998. The Slug gene is not essential for mesoderm or neural crest development in mice. *Dev. Biol.* 198:277–285.

Karsan, A., E. Yee, and J.M. Harlan. 1996. Endothelial cell death induced by tumor necrosis factor-alpha is inhibited by the Bcl-2 family member, A1. *J. Biol. Chem.* 271:27201–27204.

Li, L., I.D. Krantz, Y. Deng, A. Genin, A.B. Banta, C.C. Collins, M. Qi, B.J. Trask, W.L. Kuo, J. Cochran, et al. 1997. Alagille syndrome is caused by mutations in human Jagged1, which encodes a ligand for Notch1. *Nat. Genet.* 16:243–251.

Loomes, K.M., L.A. Underkoffler, J. Morabito, S. Gottlieb, D.A. Piccoli, N.B. Spinner, H.S. Baldwin, and R.J. Oakey. 1999. The expression of Jagged1 in the developing mammalian heart correlates with cardiovascular disease in Alagille syndrome. *Hum. Mol. Genet.* 8:2443–2449.

MacKenzie, F., P. Duriez, F. Wong, M. Noseda, and A. Karsan. 2004. Notch4 inhibits endothelial apoptosis via RBP-Jkappa-dependent and -independent pathways. *J. Biol. Chem.* 279:11657–11663.

Masuda, S., K. Kumano, K. Shimizu, Y. Imai, M. Kurokawa, S. Ogawa, M. Miyagishi, K. Taira, H. Hirai, and S. Chiba. 2005. Notch1 oncoprotein antagonizes TGF-beta/Smad-mediated cell growth suppression via sequestration of coactivator p300. *Cancer Sci.* 96:274–282.

Molin, D.G., U. Bartram, K. Van der Heiden, L. Van Iperen, C.P. Speer, B.P. Hierck, R.E. Poelmann, and A.C. Gittenberger-de-Groot. 2003. Expression patterns of Tgfbeta1-3 associate with myocardialisation of the outflow tract and the development of the epicardium and the fibrous heart skeleton. *Dev. Dyn.* 227:431–444.

Molin, D.G., M.C. DeRuiter, L.J. Wisse, M. Azhar, T. Doetschman, R.E. Poelmann, and A.C. Gittenberger-de Groot. 2002. Altered apoptosis pattern during pharyngeal arch artery remodelling is associated with aortic arch malformations in Tgfbeta2 knock-out mice. *Cardiovasc. Res.* 56:312–322.

Murray, S.A., and T. Gridley. 2006. Snail family genes are required for left-right asymmetry determination, but not neural crest formation, in mice. *Proc. Natl. Acad. Sci. USA.* 103:10300–10304.

Murray, S.A., K.F. Oram, and T. Gridley. 2007. Multiple functions of Snail family genes during palate development in mice. *Development.* 134:1789–1797.

Nagy, A.G., M. Gertsenstein, K. Vintersten, and R. Behringer. 2003. Manipulating the Mouse Embryo: A Laboratory Manual. Cold Spring Harbor Laboratory Press. 779 pp.

Niessen, K., and A. Karsan. 2007. Notch signaling in the developing cardiovascular system. *Am. J. Physiol. Cell Physiol.* 293:C1–C11.

Nieto, M.A. 2002. The snail superfamily of zinc-finger transcription factors. *Nat. Rev. Mol. Cell Biol.* 3:155–166.

Noseda, M., G. McLean, K. Niessen, L. Chang, I. Pollet, R. Montpetit, R. Shahidi, K. Dorovini-Zis, L. Li, B. Beckstead, et al. 2004. Notch activation results in phenotypic and functional changes consistent with endothelial-to-mesenchymal transformation. *Circ. Res.* 94:910–917.

Noseda, M., Y. Fu, K. Niessen, F. Wong, L. Chang, G. McLean, and A. Karsan. 2006. Smooth Muscle {alpha}-Actin Is a Direct Target of Notch/CSL. *Circ. Res.* 98:1468–1470.

Oda, T., A.G. Elkahloun, B.L. Pike, K. Okajima, I.D. Krantz, A. Genin, D.A. Piccoli, P.S. Meltzer, N.B. Spinner, F.S. Collins, and S.C. Chandrasekharappa. 1997. Mutations in the human Jagged1 gene are responsible for Alagille syndrome. *Nat. Genet.* 16:235–242.

Oka, C., T. Nakano, A. Wakeham, J.L. de la Pompa, C. Mori, T. Sakai, S. Okazaki, M. Kawaichi, K. Shiota, T.W. Mak, and T. Honjo. 1995. Disruption of the mouse RBP-J kappa gene results in early embryonic death. *Development.* 121:3291–3301.

Oram, K.F., E.A. Carver, and T. Gridley. 2003. Slug expression during organogenesis in mice. *Anat. Rec. A Discov. Mol. Cell. Evol. Biol.* 271:189–191.

Peiro, S., M. Escriva, I. Puig, M.J. Barbera, N. Dave, N. Herranz, M.J. Larriba, M. Takkunen, C. Franci, A. Munoz, et al. 2006. Snail1 transcriptional repressor binds to its own promoter and controls its expression. *Nucleic Acids Res.* 34:2077–2084.

Prandini, M.H., I. Dreher, S. Bouillot, S. Benkerri, T. Moll, and P. Huber. 2005. The human VE-cadherin promoter is subjected to organ-specific regulation and is activated in tumour angiogenesis. *Oncogene.* 24:2992–3001.

Ramain, P., K. Khechumian, L. Seugnet, N. Arbogast, C. Ackermann, and P. Heitzler. 2001. Novel Notch alleles reveal a Deltex-dependent pathway repressing neural fate. *Curr. Biol.* 11:1729–1738.

Romano, L.A., and R.B. Runyan. 2000. Slug is an essential target of TGFbeta2 signaling in the developing chicken heart. *Dev. Biol.* 223:91–102.

Sanford, L.P., I. Ormsby, A.C. Gittenberger-de Groot, H. Sariola, R. Friedman, G.P. Boivin, E.L. Cardell, and T. Doetschman. 1997. TGFbeta2 knockout

mice have multiple developmental defects that are non-overlapping with other TGFbeta knockout phenotypes. *Development.* 124:2659–2670.

Sun, Y., W. Lowther, K. Kato, C. Bianco, N. Kenney, L. Strizzi, D. Raafat, M. Hirota, N.I. Khan, S. Bargo, et al. 2005. Notch4 intracellular domain binding to Smad3 and inhibition of the TGF-beta signaling. *Oncogene*. 24:5365–5374.

Timmerman, L.A., J. Grego-Bessa, A. Raya, E. Bertran, J.M. Perez-Pomares, J. Diez, S. Aranda, S. Palomo, F. McCormick, J.C. Izpisua-Belmonte, and J.L. de la Pompa. 2004. Notch promotes epithelial-mesenchymal transition during cardiac development and oncogenic transformation. *Genes Dev.* 18:99–115.

Van Den Akker, N.M., H. Lie-Venema, S. Maas, I. Eralp, M.C. DeRuiter, R.E. Poelmann, and A.C. Gittenberger-De Groot. 2005. Platelet-derived growth factors in the developing avian heart and maturating coronary vasculature. *Dev. Dyn.* 233:1579–1588.

Wang, J., S. Sridurongrit, M. Dudas, P. Thomas, A. Nagy, M.D. Schneider, J.A. Epstein, and V. Kaartinen. 2005. Atrioventricular cushion transformation is mediated by ALK2 in the developing mouse heart. *Dev. Biol.* 286:299–310.

Wilkinson, D.G. 1992. In situ hybridization: a practical approach. Oxford University Press, New York. 224 pp.

Zavadil, J., L. Cermak, N. Soto-Nieves, and E.P. Bottinger. 2004. Integration of TGF-beta/Smad and Jagged1/Notch signalling in epithelial-to-mesenchymal transition. *EMBO J.* 23:1155–1165.

Zhang, H., and A. Bradley. 1996. Mice deficient for BMP2 are nonviable and have defects in amnion/chorion and cardiac development. *Development.* 122:2977–2986.

Smooth Muscle α-Actin Is a Direct Target of Notch/CSL

Michela Noseda, YangXin Fu, Kyle Niessen, Fred Wong, Linda Chang, Graeme McLean, Aly Karsan

Intercellular signaling mediated by Notch receptors is essential for proper cardiovascular development and homeostasis. Notch regulates cell fate decisions that affect proliferation, survival, and differentiation of endothelial and smooth muscle cells. It has been reported that Jagged1–Notch interactions may participate in endocardial cushion formation by inducing endothelial-to-mesenchymal transformation. Here, we show that Notch directly regulates expression of the mesenchymal and smooth muscle cell marker smooth muscle α-actin (SMA) in endothelial and vascular smooth muscle cells via activation of its major effector, CSL. Notch/CSL activation induces SMA expression during endothelial-to-mesenchymal transformation, and Notch activation is required for expression of SMA in vascular smooth muscle cells. CSL directly binds a conserved *cis* element in the SMA promoter, and this consensus sequence is required for Notch-mediated SMA induction. This is the first evidence of the requirement for Notch activation in the regulation of SMA expression.

Either loss or gain of function of the Notch pathway causes defects in cardiovascular development in human, mouse, and zebrafish.[1,2] Notch mediates intercellular signals that affect proliferation, survival, and differentiation of endothelial and vascular smooth muscle cells (SMC).[3–7] We and others have recently shown that Jagged1–Notch interactions may participate in endocardial cushion formation by inducing endothelial-to-mesenchymal transformation (EMT).[3,8]

Engagement of Notch receptors by their ligands results in a 2-step cleavage that releases the intracellular domain (NotchIC), permitting translocation to the nucleus. Presenilin-dependent γ-secretase activity is essential for the ultimate intramembrane clip that releases NotchIC.[9] Following nuclear localization, NotchIC interacts with the DNA-binding factor CSL (also known as RBP-Jκ and CBF1), resulting in transactivation of various promoters, such as those of the HES and HEY families.[10,11]

Notch-mediated mesenchymal transformation results in loss of endothelial markers and induction of mesenchymal proteins such as smooth muscle α-actin (SMA).[3] However, the mechanism of Notch-induced SMA expression has not been studied. SMA is the most abundant protein in SMC and appears to play an important role in mechanotransduction and generation of traction forces in SMC as well as myofibroblasts.[12] Here we demonstrate that Notch-mediated upregulation of SMA is directly dependent on the activation and binding of CSL to the SMA promoter. Importantly, not only is Notch/CSL-dependent induction of SMA involved in EMT, but it is also required for SMA expression in SMC.

Materials and Methods

Cell Culture

The human microvascular endothelial cell line HMEC-1 (HMEC), human aortic endothelial cells (HAEC), and human umbilical vein endothelial cells (HUVEC) were obtained as previously described.[3,5] Primary human foreskin fibroblasts (HFF) were provided by Dr C. Sherlock (St. Paul's Hospital, Vancouver, BC). Human aortic SMC (HASMC) were purchased from Cascade Biologics. Culture conditions are described in the expanded Materials and Methods section available in the online data supplement at http://circres.ahajournals.org.

Plasmids, Gene Transfer, and RNA Interference

Cells were transduced as previously described.[3,5] For a description of plasmids and details on small interfering RNA (siRNA), see the online data supplement.

Immunoblotting and Immunofluorescence Staining

Immunoblotting, immunostaining, and image acquisition were performed as described previously.[5] Antibodies are listed in the online data supplement.

Luciferase Assay

The SMA-promoter luciferase construct (gift of F. Dandre and G. K. Owens, University of Virginia Health Sciences Center, Charlottesville) has been previously described.[3,13] See the online data supplement for more details.

Chromatin Immunoprecipitation Assay

HMEC transduced with LNCX or vector expressing Flag-tagged CSL were fixed in 1% formaldehyde, lysed, and sonicated. One percent of total chromatin was used as positive control for PCR (online data supplement).

Results and Discussion

We first confirmed that Notch1IC induces SMA expression in endothelial cells by immunoblotting (Figure 1A). Activated Notch1 also induced expression of SMA in primary human fibroblasts (Figure 1B). Given that SMA is a marker of differentiation for SMC and that these cells express endogenous Notch1, Notch2, and Notch3, as well as the ligand Jagged1, we tested whether activated Notch and Jagged1-induced Notch activation would induce upregulation of SMA in HASMC.[5,14] Immunoblotting demonstrated that both

Original received March 23, 2006; revision received April 27, 2006; accepted May 18, 2006.

From the Departments of Medical Biophysics (M.N., Y.F., K.N., F.W., L.C., G.M., A.K.) and Pathology and Laboratory Medicine (A.K.), British Columbia Cancer Agency, Vancouver; and Department of Pathology and Laboratory Medicine (M.N., Y.F., A.K.) and Experimental Medicine Program (K.N., L.C., G.M., A.K.), University of British Columbia, Vancouver, Canada.

Correspondence to Aly Karsan, British Columbia Cancer Research Centre, 675 West 10th Ave, Vancouver, British Columbia V5Z 1L3, Canada. E-mail akarsan@bccrc.ca

(*Circ Res.* 2006;98:1468-1470.)

***Circulation Research* is available at http://circres.ahajournals.org**
DOI: 10.1161/01.RES.0000229683.81357.26

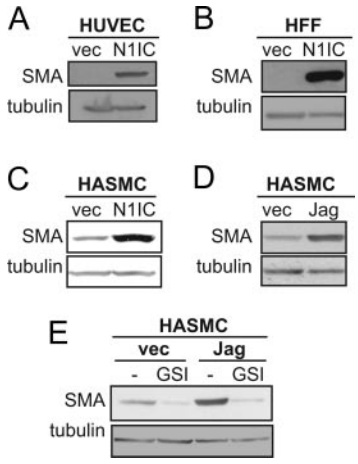

Figure 1. Activation of the Notch pathway induces expression of SMA. A through C, HUVEC, HFF, or HASMC were transduced with empty vector (vec) or vector encoding Notch1IC (N1IC), and SMA expression was analyzed by immunoblotting. D, HASMC-vector (vec) and HASMC-Jagged1 (Jag) were analyzed for expression of SMA by immunoblotting. E, HASMC-vector and HASMC-Jagged1 were treated with vehicle alone (-) or with GSI, and SMA expression levels were analyzed by immunoblotting. Tubulin was used as a loading control.

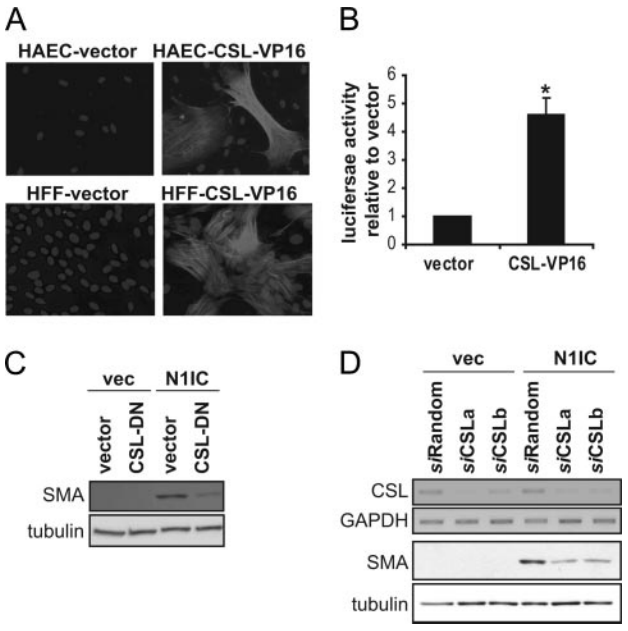

Figure 2. CSL activation is sufficient and necessary to induce SMA expression. A, HAEC and HFF were transduced with empty vector or vector encoding CSL-VP16. SMA expression was analyzed by immunofluorescence. Cell nuclei were counterstained with DAPI. B, HMEC were cotransfected with vector or CSL-VP16, SMA-WT, and constitutively active Renilla luciferase reporter. The graphs show relative luciferase activity (mean±SEM of 4 experiments, each done in triplicate). *$P<0.01$ compared with vector. C, HFF were transduced with Notch1IC (N1IC) or the empty vector (vec) and CSL-DN or its empty vector (vector) and analyzed by immunoblotting for expression of SMA. Tubulin was used as a loading control. D, HFF-vector (vec) and HFF-Notch1IC (N1IC) were infected with 1 of the 2 lentiviruses expressing siRNA targeting 2 different sequences of CSL (siCSLa and siCSLb) or control random siRNA (siRandom). Knockdown of CSL was confirmed by RT-PCR. Expression of SMA and tubulin were tested by immunoblotting.

Notch1IC and Jagged1-mediated Notch activation induced expression of SMA in SMC (Figure 1C and 1D). To determine whether Notch regulates SMA expression in SMC through endogenous Notch ligand–receptor interactions, HASMC transduced with vector alone (HASMC-vector) or Jagged1 (HASMC-Jagged1) were treated with vehicle or a γ-secretase inhibitor (GSI).[5,8] Inhibition of Notch processing blocked expression of SMA in control cells as well as in Jagged1 cocultures, indicating that in SMC the endogenous Notch pathway participates in the maintenance of SMA expression and that Jagged1-mediated induction of SMA is dependent on Notch activation (Figure 1E). These results indicate that the Notch pathway is a major regulator of the expression of SMA not only during EMT but also in fibroblasts and importantly in SMC.

Notch activation also induced expression of SMA mRNA and activated the SMA promoter as seen in a promoter-luciferase assay in HMEC and 293T cells (supplemental Figure I and data not shown), suggesting that Notch induces SMA through transcriptional activation.[3,13] The human SMA promoter contains a CSL consensus binding site (TGGGAA) beginning at −64 from the cap site that is conserved in apes and rodents (supplemental Figure II).[3,13] We thus tested whether CSL activation was sufficient to induce SMA expression. Transduction of constitutively active CSL (engineered by fusing CSL with the transcriptional activation domain of the herpes viral protein 16 [CSL-VP16]) was sufficient to induce expression of SMA in endothelial cells and fibroblasts (Figure 2A).[15] In addition, transfection of CSL-VP16 was sufficient to activate the SMA promoter in endothelial cells, as demonstrated by promoter-luciferase assay (Figure 2B).

To determine whether CSL is necessary for Notch-mediated SMA induction, HFF were double-transduced with Notch1IC and CSL-DN (dominant-negative CSL) or the empty vectors. Notch-induced morphological changes were lost in cells coexpressing Notch1IC and CSL-DN (data not shown). Immunoblotting showed decreased expression of SMA in cells transduced with CSL-DN and Notch1IC compared with cells transduced with Notch1IC and the empty vector (Figure 2C). Secondly, we used lentiviral transduction of short-hairpin RNAs to generate siRNAs targeting CSL (siCSL). Cells were infected with empty vector or Notch1IC and 1 of 2 lentiviral constructs targeting 2 different sequences of CSL (siCSLa or siCSLb) or a nonsilencing control (siRandom). Knock-down of CSL was confirmed by RT-PCR (Figure 2D). Cells infected with siCSLa or siCSLb and Notch1IC showed reduced expression of SMA compared with control cells (Figure 2D). Thus, Notch-mediated induction of SMA is mediated through activation of CSL.

To test whether the putative CSL-binding site in the SMA promoter is required for its activation, the consensus sequence was disrupted by site-directed mutagenesis. Endothelial cells were cotransfected with NotchIC or control vector and either the wild-type (SMA-WT) or CSL-binding site–mutated (SMA-mut) SMA-promoter luciferase constructs. Results show complete inhibition of Notch-dependent luciferase activation when the CSL-binding site is mutated (Figure 3A). To confirm a role for endogenous Notch/CSL signaling

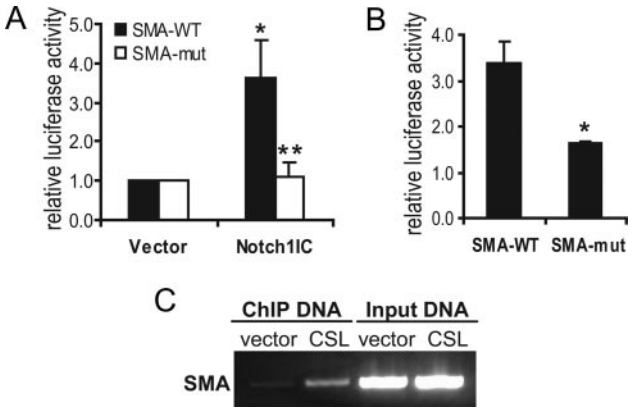

Figure 3. The CSL consensus binding site is required for SMA expression. A, HMEC were cotransfected with vector or NotchIC, firefly luciferase constructs with upstream wild-type (SMA-WT) or mutated SMA promoters (SMA-mut), and CMV-driven Renilla luciferase reporter. The graph shows relative luciferase activity (mean±SEM of 4 experiments, each done in triplicate). *$P<0.05$ compared with vector and **$P<0.05$ compared with SMA-WT NotchIC. B, SMC were transfected with vector, SMA-WT, or SMA-mut and Renilla luciferase reporter. Graphs show luciferase activity relative to vector (mean±SEM of 3 experiments, each done in triplicate). *$P<0.05$ compared with vector. C, ChIP assay in HMEC expressing Flag-tagged CSL (CSL) or vector control. PCR with primers flanking the CSL consensus sequence in the SMA promoter was performed following immunoprecipitation with the Flag antibody (ChIP DNA). One percent of total chromatin was used as a positive control for PCR (Input DNA).

in regulation of the SMA promoter in SMC, we transfected HASMC with SMA-WT or SMA-mut (Figure 3B). Luciferase assays demonstrate that mutation of the CSL-binding site significantly reduces activation of the SMA promoter in SMC, suggesting a critical role for endogenous CSL activity in inducing and maintaining expression of SMA. To confirm that CSL directly binds the SMA promoter, chromatin immunoprecipitation assay (ChIP) assays were performed in HMEC transduced with vector encoding Flag-tagged CSL or the empty vector. PCR of Flag immunoprecipitated DNA using primers flanking the CSL consensus site confirmed that CSL directly binds the SMA promoter (Figure 3C).

In summary, this study shows that Notch/CSL signaling directly regulates expression of SMA by a transcriptional mechanism that requires binding of CSL to the SMA promoter. Of note, Notch/CSL-mediated induction of SMA is involved in EMT and fibroblast acquisition of SMA, as well as in the maintenance of SMA expression in SMC. These data also trigger more questions regarding the role of Notch in the vasculature. For instance, what are the factors that determine cell-type and context-specific effects of Notch in the endothelial and mural compartments? Notch1 and Jagged1 have been detected in both endothelial cells and SMC, and whether specific Notch or ligand expression (eg, Notch3 in SMC and Notch4 and Dll4 in endothelial cells) contributes to these decisions remains to be investigated. On a broader perspective, given that Notch appears to play a role in tissue regeneration and that myofibroblasts and SMC appear to use SMA to transmit mechanical forces through the cell, our data provide a potential explanation of the role of Notch in wound healing and vascular remodeling.[12,16,17]

Acknowledgments

We thank Denise McDougal for assistance with cell sorting and Dana Wong for technical help.

Sources of Funding

This research was supported by grants to A.K. from the Heart and Stroke Foundation of British Columbia and the Yukon and the Canadian Institutes of Health Research. M.N. was supported by a fellowship from the Canadian Institutes of Health Research and a Research Trainee Award from the Michael Smith Foundation for Health Research. Y.F. and K.N. are supported by Research Trainee Awards from the Michael Smith Foundation for Health Research. A.K. is a scholar of the Michael Smith Foundation for Health Research.

Disclosures

None.

References

1. Shawber CJ, Kitajewski J. Notch function in the vasculature: insights from zebrafish, mouse and man. *Bioessays*. 2004;26:225–234.
2. Karsan A. The role of notch in modeling and maintaining the vasculature. *Can J Physiol Pharmacol*. 2005;83:14–23.
3. Noseda M, McLean G, Niessen K, Chang L, Pollet I, Montpetit R, Shahidi R, Dorovini-Zis K, Li L, Beckstead B, Durand RE, Hoodless PA, Karsan A. Notch activation results in phenotypic and functional changes consistent with endothelial-to-mesenchymal transformation. *Circ Res*. 2004;94:910–917.
4. MacKenzie F, Duriez P, Wong F, Noseda M, Karsan A. Notch4 inhibits endothelial apoptosis via RBP-Jkappa-dependent and -independent pathways. *J Biol Chem*. 2004;279:11657–11663.
5. Noseda M, Chang L, McLean G, Grim JE, Clurman BE, Smith LL, Karsan A. Notch activation induces endothelial cell cycle arrest and participates in contact inhibition: role of p21Cip1 repression. *Mol Cell Biol*. 2004;24:8813–8822.
6. Domenga V, Fardoux P, Lacombe P, Monet M, Maciazek J, Krebs LT, Klonjkowski B, Berrou E, Mericskay M, Li Z, Tournier-Lasserve E, Gridley T, Joutel A. Notch3 is required for arterial identity and maturation of vascular smooth muscle cells. *Genes Dev*. 2004;18:2730–2735.
7. Campos AH, Wang W, Pollman MJ, Gibbons GH. Determinants of Notch-3 receptor expression and signaling in vascular smooth muscle cells: implications in cell-cycle regulation. *Circ Res*. 2002;91:999–1006.
8. Timmerman LA, Grego-Bessa J, Raya A, Bertran E, Perez-Pomares JM, Diez J, Aranda S, Palomo S, McCormick F, Izpisua-Belmonte JC, de la Pompa JL. Notch promotes epithelial-mesenchymal transition during cardiac development and oncogenic transformation. *Genes Dev*. 2004;18:99–115.
9. Schroeter EH, Kisslinger JA, Kopan R. Notch-1 signalling requires ligand-induced proteolytic release of intracellular domain. *Nature*. 1998;393:382–386.
10. Jarriault S, Brou C, Logeat F, Schroeter EH, Kopan R, Israel A. Signalling downstream of activated mammalian Notch. *Nature*. 1995;377:355–358.
11. Kovall RA, Hendrickson WA. Crystal structure of the nuclear effector of Notch signaling, CSL, bound to DNA. *EMBO J*. 2004;23:3441–3451.
12. Wang J, Zohar R, McCulloch CA. Multiple roles of alpha-smooth muscle actin in mechanotransduction. *Exp Cell Res*. 2006;312:205–214.
13. Shimizu RT, Blank RS, Jervis R, Lawrenz-Smith SC, Owens GK. The smooth muscle alpha-actin gene promoter is differentially regulated in smooth muscle versus nonsmooth muscle cells. *J Biol Chem*. 1995;270:7631–7643.
14. Villa N, Walker L, Lindsell CE, Gasson J, Iruela-Arispe ML, Weinmaster G. Vascular expression of Notch pathway receptors and ligands is restricted to arterial vessels. *Mech Dev*. 2001;108:161–164.
15. Noseda M, Niessen K, McLean G, Chang L, Karsan A. Notch-dependent cell cycle arrest is associated with downregulation of minichromosome maintenance proteins. *Circ Res*. 2005;97:102–104.
16. Raya A, Koth CM, Buscher D, Kawakami Y, Itoh T, Raya RM, Sternik G, Tsai HJ, Rodriguez-Esteban C, Izpisua-Belmonte JC. Activation of Notch signaling pathway precedes heart regeneration in zebrafish. *Proc Natl Acad Sci U S A*. 2003;100(suppl 1):11889–11895.
17. Mitsiadis TA, Fried K, Goridis C. Reactivation of Delta-Notch signaling after injury: complementary expression patterns of ligand and receptor in dental pulp. *Exp Cell Res*. 1999;246:312–318.

KEY WORDS: endothelial cells ■ Notch ■ CSL ■ smooth muscle cells ■ smooth muscle actin ■ endothelial-to-mesenchymal transformation

Notch4-induced inhibition of endothelial sprouting requires the ankyrin repeats and involves signaling through RBP-Jκ

Farrell MacKenzie, Patrick Duriez, Bruno Larrivée, Linda Chang, Ingrid Pollet, Fred Wong, Calvin Yip, and Aly Karsan

Notch proteins comprise a family of transmembrane receptors. Ligand activation of Notch releases the intracellular domain of the receptor that translocates to the nucleus and regulates transcription through the DNA-binding protein RBP-Jκ. Previously, it has been shown that the Notch4 intracellular region (N4IC) can inhibit endothelial sprouting and angiogenesis. Here, N4IC deletion mutants were assessed for their ability to inhibit human microvascular endothelial cell (HMEC) sprouting with the use of a quantitative endothelial sprouting assay. Deletion of the ankyrin repeats, but not the RAM (RBP-Jκ associated module) domain or C-terminal region (CT), abrogated the inhibition of fibroblast growth factor 2 (FGF-2)– and vascular endothelial growth factor (VEGF)–induced sprouting by Notch4, whereas the ankyrin repeats alone partially blocked sprouting. The ankyrin repeats were also the only domain required for up-regulation of RBP-Jκ–dependent gene expression. Interestingly, enforced expression of the ankyrin domain alone was sufficient to up-regulate some, but not all, RBP-Jκ–dependent genes. Although N4IC reduced VEGF receptor-2 (VEGFR-2) and vascular endothelial (VE)–cadherin expression, neither of these events is necessary and sufficient to explain N4IC-mediated inhibition of sprouting. A constitutively active RBP-Jκ mutant significantly inhibited HMEC sprouting but not as strongly as N4IC. Thus, Notch4-induced inhibition of sprouting requires the ankyrin repeats and appears to involve RBP-Jκ–dependent and –independent signaling. (Blood. 2004;104:1760-1768)

Introduction

Notch proteins are a highly conserved family of transmembrane receptors involved in intercellular signaling that regulate cell fate.[1] Notch interacts with ligands presented on neighboring cells, triggering a 2-step proteolytic cleavage of the receptor that releases its C-terminal intracellular region (NIC).[2,3] NIC is then capable of translocating to the nucleus and up-regulating the transcription of target genes.[4,5] As a result of this signaling mechanism, enforced expression of the intracellular domain of the receptor provides constitutive Notch activity.[6,7]

In the nucleus, NIC regulates transcription through association with the DNA-binding protein RBP-Jκ (also known as CBF1, KBF2, or CSL). The primary gene targets of RBP-Jκ include members of the hairy and enhancer of split (HES) and hairy related transcription factor (HRT) families of basic-helix-loop-helix transcriptional repressors. In the absence of NIC, RBP-Jκ actively represses transcription by way of recruitment of a corepressor complex.[8] Nuclear translocation of NIC leads to dissociation of repressor proteins from RBP-Jκ and formation of a coactivator complex.[9-13]

RBP-Jκ–independent Notch signaling also exists. Studies on loss-of-function mutants indicate that the activity of Supressor of Hairless (Su(H)) and Lag-1–RBP-Jκ homologs in *Drosophila* and *Caenorhabditis elegans*, respectively, do not account for all observed Notch functions.[14-18] There is also growing support for the existence of RBP-Jκ–independent Notch signaling in mammals.[19-22]

Four mammalian Notch homologs have been identified to date and include Notch1, Notch2, Notch3, and Notch4.[23-28] The intracellular region of each homolog is composed of several discrete domains, including a RAM (RBP-Jκ–associated module) domain that has high affinity for RBP-Jκ and 6 ankyrin repeats that also bind RBP-Jκ as well as other components of the transcriptional coactivator complex.[9,13,29-31] The function of the region C-terminal to the ankyrin repeats is not well defined but includes a proline-glutamate-serine-threonine (PEST) motif that is involved in protein turnover.[32,33]

Functionally, Notch receptors and ligands are necessary for vascular development. Targeted deletion of Notch1 causes embryonic lethality because of defects in blood vessel development, and this phenotype is enhanced in Notch1/Notch4 double knock-out mice.[34,35] Paradoxically, similar vascular abnormalities occur in transgenic mice expressing a constitutively active Notch4 mutant in the endothelium, demonstrating the need for critical regulation of Notch activity during vascular development.[36] In these various mutant mice, the primary vascular plexus forms normally, but there is a failure to properly remodel this immature network, implicating a role for Notch in angiogenesis, the process of developing new blood vessels from the existing vasculature in response to various

From the Department of Pathology and Laboratory Medicine, University of British Columbia; the Experimental Medicine Program, University of British Columbia, Vancouver, BC, Canada; the Department of Medical Biophysics, British Columbia Cancer Agency; and the Department of Pathology and Laboratory Medicine, British Columbia Cancer Agency, Vancouver, BC, Canada.

Submitted December 15, 2003; accepted May 17, 2004. Prepublished online as *Blood* First Edition Paper, June 8, 2004; DOI 10.1182/blood-2003-12-4244.

Supported by grants from the Heart and Stroke Foundation of British Columbia and the Yukon (A.K.), the National Cancer Institute of Canada with funds from the Canadian Cancer Society (A.K.), and the Canadian Institutes of Health Research (A.K.). P.D. was supported by a Postdoctoral Fellowship Award from the Heart and Stroke Foundation of Canada. B.L. was supported by a Doctoral Research Award from the Heart and Stroke Foundation of Canada. A.K. is a Clinician-Scientist of the Canadian Institutes of Health Research and a Scholar of the Michael Smith Foundation for Health Research.

Reprints: Aly Karsan, Department of Medical Biophysics, British Columbia Cancer Research Centre, 601 West 10th Ave, Vancouver, BC, Canada V5Z 1L3; e-mail: akarsan@bccrc.ca.

The publication costs of this article were defrayed in part by page charge payment. Therefore, and solely to indicate this fact, this article is hereby marked "advertisement" in accordance with 18 U.S.C. section 1734.

factors such as vascular endothelial growth factor (VEGF, also VEGF-A) and fibroblast growth factor-2 (FGF-2).[37-39]

The regulatory role Notch4 plays in endothelial cells during angiogenesis is of particular interest because this receptor is primarily expressed in the vascular endothelium of embryonic and adult mammals.[27,40,41] Enforced expression of the Notch4 intracellular domain (N4IC) inhibits VEGF- and FGF-2–induced endothelial sprouting in 3-dimensional fibrin gels.[42] Activated Notch4 or Notch1, as well as a downstream Notch effector, HRT1, have each been shown to down-regulate VEGF receptor 2 (VEGFR-2) gene expression, which may provide one explanation of how Notch signals inhibit endothelial network formation.[43,44] However, the critical Notch4 domains required for its antiangiogenic activity have not been defined.

In the present study, the requirement of individual Notch4 domains to inhibit endothelial sprouting was investigated with the use of a quantitative assay.[42,45,46] Activated Notch4 was confirmed to inhibit human microvascular endothelial cell (HMEC) sprouting in response to FGF-2 and VEGF, as shown previously.[42] Inhibition of endothelial sprouting by Notch4 requires the ankyrin repeats, but not the RAM domain or C-terminal region (CT) as demonstrated by the expression of Notch4 mutants deleted in these individual domains. In parallel, enforced expression of only the ankyrin repeats of Notch4 partially inhibited sprouting. Similarly, activation of RBP-Jκ independently of Notch only partially inhibited endothelial sprouting. Deletion of the ankyrin repeats, but not the RAM domain or CT, abolished Notch4 induction of RBP-Jκ–dependent gene expression. Taken together, our findings indicate that Notch4-induced inhibition of endothelial sprouting requires the ankyrin repeats and likely involves signaling through both RBP-Jκ–dependent and –independent pathways.

Materials and methods

Cell culture

HMECs immortalized by the SV40 T antigen were provided by the Centers for Disease Control and Prevention (Atlanta, GA).[47] Cells were cultured in MCDB medium (Sigma, St Louis, MO) supplemented with 10% heat-inactivated fetal calf serum (FCS; HyClone, Logan, UT), 10 ng/mL epidermal growth factor (Sigma), and 50 U/mL penicillin and 50 μg/mL streptomycin (Gibco, Gaithersburg, MD) (HMEC medium). Cells were maintained at 37°C in 5% CO_2.

Plasmid constructs and gene transfer

The N4IC construct, described previously, contains a C-terminal hemagglutinin (HA) epitope tag and includes amino acids (aa's) 1476 to 2003 of the 2003 aa full-length Notch4.[42] The N4IC deletion mutants were constructed by polymerase chain reaction (PCR) with the use of N4IC as a template and also include C-terminal HA-tags. cDNAs were inserted into the LNCX retroviral vector, in which expression is controlled by the cytomegalovirus (CMV) immediate early enhancer/promoter. The N4IC mutants (Figure 1A) include constructs (1) lacking the entire RAM domain (ΔRAM; encodes aa 1518-2003), (2) lacking the RAM and N-terminally fused with an SV40-derived nuclear localization signal (NLS; NLS-ΔRAM; encodes aa 1518-2003), (3) lacking all 6 ankyrin repeats (ΔAnk encodes aa's 1476-1578 and 1801-2003), (4) lacking the C-terminal region (ΔCT; aa's 1475-1789), (5) composed of only the 6 ankyrin repeats (Ank; encodes aa's 1579-1789), and (6) composed of the 6 ankyrin repeats plus additional upstream sequence and fused with an N-terminal SV40 NLS (NLS-Ank; encodes aa's 1518-1789). The NLS sequence used encodes the amino acid sequence DPKKKRKV. N4IC was also cloned into the MSCV-IRES-YFP (MIY) retroviral vector, as was RBP-VP16, a constitutively active RBP-Jκ. In the MIY vector, gene expression is controlled by the murine stem cell virus long terminal repeats (LTRs). RBP-VP16 has an N-terminal FLAG-tag and was constructed by PCR amplification of the 3′ region of the mouse RBP-VP16 cDNA (gift of E. Manet, Institut National de la Santé et de la Recherche Médicale [INSERM], Lyon, France).[48] This PCR product, which includes the coding region for the VP16 transactivation domain, was digested with *Afl*II and ligated to the corresponding *Afl*II site of the cDNA for FLAG–RBP-Jκ, which itself was derived from the RBP-2N isoform of human RBP-Jκ (gift of R. Schmid, University of Ulm, Germany).[49] The 4xRBP-Jκ luciferase plasmid includes 4 copies of an RBP-Jκ binding element cloned into pGL2pro (Promega, Madison, WI), an SV40 promoter-driven firefly luciferase plasmid (gift of S.D. Hayward, Johns Hopkins School of Medicine, Baltimore, MD).[50] The HRT2 luciferase comprises a 10-kb fragment of the mouse HRT2 promoter cloned into pGL3basic (Promega), a promoterless firefly luciferase vector (gift of E.N. Olson, University of Texas Southwestern Medical Center, Dallas).[51]

HMECs were transduced with the empty vector control or vector with a cDNA insert as described previously.[52] Polyclonal HMEC lines were isolated by selection in 300 μg/mL G418 (Gibco) for the LNCX constructs and by sorting cells for yellow fluorescence protein (YFP) expression using a fluorescence activated cell sorter (FACS) 440 (Becton Dickinson [BD], San Jose, CA) for the MIY constructs.

Immunoblotting

Total cellular extracts were prepared from confluent cell monolayers and stored at −80°C until use. Total protein (40 μg) was separated by sodium dodecyl sulfate-polyacrylamide gel electrophoresis (SDS-PAGE) and transferred to nitrocellulose membranes. Primary antibodies used included a mouse anti-HA epitope monoclonal antibody (1:4000 dilution; Sigma), the M5 mouse anti-FLAG epitope monoclonal antibody (1:1000 dilution; Sigma), and a mouse anti–α-tubulin monoclonal antibody (1:5000 dilution; Sigma). The secondary antibody was horseradish peroxidase (HRP)–conjugated goat anti–mouse immunoglobulin G (IgG) antibody (Bio-Rad Laboratories, Hercules, CA).

Immunofluorescence

Transduced HMEC lines were cultured overnight on chamber slides (BD), fixed with 4% paraformaldehyde (Fisher Scientific, Suwannee, GA) for 15 minutes and then permeabilized with cold methanol (Fisher Scientific) for 3 minutes. Nonspecific binding was blocked by incubation with phosphate-buffered saline (PBS), 5% goat serum. Cells were stained with the mouse anti-HA monoclonal primary antibody (1:100 dilution) for 1 hour and then for 30 minutes with an AlexaFluor 488–conjugated goat anti–mouse IgG secondary antibody (1:500 dilution; Molecular Probes, Eugene, OR). Nuclei were counterstained with 4′,6′diamidino-2-phenylindole (DAPI) for 5 minutes, and coverslips were mounted with 50% glycerol. Slides were viewed through a 40× Neofluor objective (numerical objective 0.75) using a Zeiss Axioplan II Imaging inverted microscope (Carl Zeiss, Toronto, Canada), and images were captured with a 1350EX cooled charge-coupled device (CCD) digital camera (QImaging, Burnaby, BC, Canada) using Northern Eclipse software (Empix Imaging, Mississauga, ON, Canada).

Endothelial sprouting assay

Endothelial sprouting was assessed as previously described.[42,45,46] Briefly, microcarrier beads coated with gelatin were seeded with HMEC lines at a ratio of approximately 200 HMECs/bead and embedded in fibrin gels in 96-well plates (~ 50 beads/well). Fibrin gels were supplemented either with FGF-2 (15 ng/mL) or $VEGF_{165}$ (30 ng/mL) or with no angiogenic factor. The overlying medium contained either MCDB + 2% fetal bovine serum (FBS) alone (basal medium) or was supplemented with FGF-2 (15 ng/mL), or $VEGF_{165}$ (30 ng/mL). After 3 days of incubation with daily medium changes, the number of capillary-like tubes formed was quantitated by counting the number of tubelike structures more than 150 μm in length per microcarrier bead (sprouts/bead), counting all beads in every well. Images were captured with a Nikon Coolpix 950 camera (Nikon, Tokyo, Japan) through a 10× objective lens (numerical aperture 0.25).

Transient transfection and luciferase assays

Transient transfection of luciferase reporter plasmids was carried out by electroporation. Transduced HMEC lines were grown to approximately 80% confluence and then trypsinized and resuspended in HMEC medium. Cells (1.5×10^6/transfection) were pelleted at 200 *g* for 5 minutes, washed with PBS, pelleted as previous, and then resuspended in 0.4 mL electroporation buffer (20 mM HEPES [*N*-2-hydroxyethylpiperazine-*N*′-2-ethanesulfonic acid], 137 mM sodium chloride, 5 mM potassium chloride, 0.7 mM sodium phosphate, 6 mM D-glucose, pH 7.0 53) containing luciferase reporter plasmid DNA. The cell-DNA mixture was transferred to a 4-mm gap electroporation cuvette (Bio-Rad), left for 10 minutes at room temperature, and then electroporated at a fixed capacitance of 900 μF and 200 V using a Bio-Rad Gene Pulser II instrument. For each transfection, 2.5 μg 4xRBP-Jκ–binding promoter luciferase plus 1 μg RL-CMV (Promega) or 5 μg HRT2 promoter luciferase plus 1 μg RL-CMV were used. The RL-CMV reporter contains the renilla luciferase cDNA expressed under control of the CMV immediate early enhancer/promoter and serves as a normalization control for transfection efficiency. After electroporation, the cells were left for 10 minutes at room temperature before plating in prewarmed (37°C) HMEC medium. The medium was changed 24 hours later, and cells were harvested for assay 48 hours after transfection. Lysis and dual-luciferase reporter assays were performed according to the manufacturer's recommendations (Promega) with luminescence measured on a Tropix tube luminometer (BIO/CAN Scientific, Mississauga, ON, Canada). Luminescence values of mock transfections were subtracted from sample luminescence readings to give the net firefly and net renilla luciferase units. The net firefly units divided by the net renilla units determined the relative luciferase units (RLUs).

RNA isolation and RT-PCR

Total RNA was isolated from confluent cell monolayers with use of TRIzol Reagent (Invitrogen, Carlsbad, CA). First strand cDNA was synthesized with use of 50-μL reactions containing 2.5 μg RNA and 200 units SuperScript II reverse transcriptase (Invitrogen). Following RNAse H (2 U/reaction) (Invitrogen) treatment, PCR reactions were performed, and amplicons were resolved on Tris acetate ethylenediaminetetraacetic acid (TAE) agarose gels. No PCR products were detected in the negative control reactions performed without reverse transcriptase (RT). Following are the primers and reaction conditions used for amplification: HRT1, sense 5′-ggagaggcgccgctgtagtta-3′ and antisense 5′-caagggcgtgcgcgtcaaagta-3′ primers, 57°C annealing temperature, and 28 reaction cycles; HRT2, sense 5′-tgagcataggattccgagagtgc-3′ and 5′-antisense gaaggacagagggaagctgtgtg-3′ primers, 57°C annealing temperature, and 28 reaction cycles; HRT3, sense 5′-cactggtgggacaggattctttg-3′ and antisense 5′-gtaagcagccgaccctgtaggac-3′ primers, 57°C annealing temperature, and 30 reaction cycles; HES1, sense 5′-aggcggacattctggaaatg-3′ and 5′-antisense cggtacttccccagcacactt-3′ primers, 55°C annealing temperature, and 30 reaction cycles; HES4, sense 5′-caccgcaagtcctccaag-3′ and antisense 5′-tcacctccgccagacact-3′ primers, 53°C annealing temperature, and 30 reaction cycles; FGFR-1, sense 5′-agctccatattggacatc-3′ and antisense 5′-tatgatgctccaggtggc-3′ primers, 54°C annealing temperature, and 24 reaction cycles; VEGFR-2, sense 5′-agccctgtgcgctcaactgtc-3′ and antisense 5′-aagagaaacactaggcaaacc-3′ primers, 55°C annealing temperature, and 30 reaction cycles. GAPDH (glyceraldehyde-3-phosphate dehydrogenase), sense 5′-cccatcaccatcttccag-3′ and antisense 5′-atgaccttgcccacagcc-3′ primers, 55°C annealing temperature, and 22 reaction cycles.

Migration assay

The ability of HMECs to migrate toward FGF-2 and VEGF through collagen I–coated filters was measured with use of a Transwell filter assay as previously described.[42,53]

Statistics

Results were analyzed by analysis of variance (ANOVA) to ascertain differences between groups, followed by a Tukey test for multiple comparisons.

Results

Subcellular localization of Notch4 mutants

A series of deletion mutants of the human Notch4 intracellular region (N4IC) were constructed to determine the functional relevance of specific domains. The Notch4 deletion mutants included constructs lacking either the RAM domain (ΔRAM), all 6 ankyrin repeats (ΔAnk), or the C-terminal region (ΔCT), as well as a construct consisting of the ankyrin repeats alone (Ank) (Figure 1A). Each construct was C-terminally tagged with an HA epitope and stably expressed in HMECs, as confirmed by immunoblotting (Figure 1B).

Because activated Notch functions primarily by modulating transcription at promoter regulatory sites, it was important to ensure that each mutant localized to the nucleus. It has previously been reported that the RAM domain is required for nuclear targeting of Notch4 in mouse mammary epithelial cells.[54] As seen in Figure 1C, mutants lacking the RAM domain, including the ΔRAM and Ank constructs, localized predominantly to the cytoplasm in HMECs. Conversely, the intact N4IC, as well as the ΔAnk and ΔCT deletion mutants, were all predominantly expressed in the nucleus with varying degrees of cytoplasmic staining. Expression of the ΔCT and Ank mutants in HMECs were notably reduced compared with the other constructs as indicated by the immunoblotting (Figure 1B). Fusion of an SV40-derived NLS sequence to the N-terminus of ΔRAM and Ank restored the ability of these mutants to localize to the nucleus (Figure 1C). The NLS-ΔRAM mutant targeted to the nucleus with minimal cytoplasmic staining. In contrast, the NLS-Ank protein, although showing increased nuclear localization, still showed significant cytoplasmic distribution. To focus on Notch signaling in the nucleus, all subsequent experiments were carried out with the NLS-ΔRAM and NLS-Ank constructs rather than ΔRAM and Ank.

Notch4-induced inhibition of endothelial sprouting requires the ankyrin repeats

Notch4 is predominantly expressed in the vascular endothelium,[28,34,41] and constitutive activation of Notch4 in endothelial cells blocks angiogenesis.[36,42] Using an in vitro model of angiogenesis in which endothelial cells coated on microcarrier beads are induced to form cellular sprouts within a 3-dimensional fibrin gel, we have previously shown that N4IC inhibits serum-induced sprouting as well as that induced by FGF-2 and VEGF.[42] However, the structural elements of Notch4 that are required for regulating endothelial cell morphogenesis during vascular remodeling remain unknown. Figure 2A shows phase-contrast micrographs of microcarrier beads coated with either control cells or cells expressing activated Notch4 and incorporated into FGF-2-containing fibrin gels. Whereas extensive sprouting is observed in the control cells, there is minimal sprouting in the HMECs expressing N4IC (HMEC-N4IC). Transmission electron microscopy confirmed previous findings that this assay of morphogenesis mimics endothelial tube formation, because we detected the formation of lumina at the base of the sprouts (Figure 2B).[46] As quantitated in Figure 2C, mutants lacking either the RAM motif or the CT domain blocked endothelial sprouting as effectively as N4IC in response to all stimuli. Conversely, deletion of the Notch4 ankyrin repeats abrogated the ability of the receptor to inhibit endothelial sprouting. To determine whether the ankyrin repeats alone were sufficient for Notch4 function, HMECs sprouting in cells expressing the ankyrin repeats targeted to the nucleus (NLS-Ank) were determined. Sprouting of

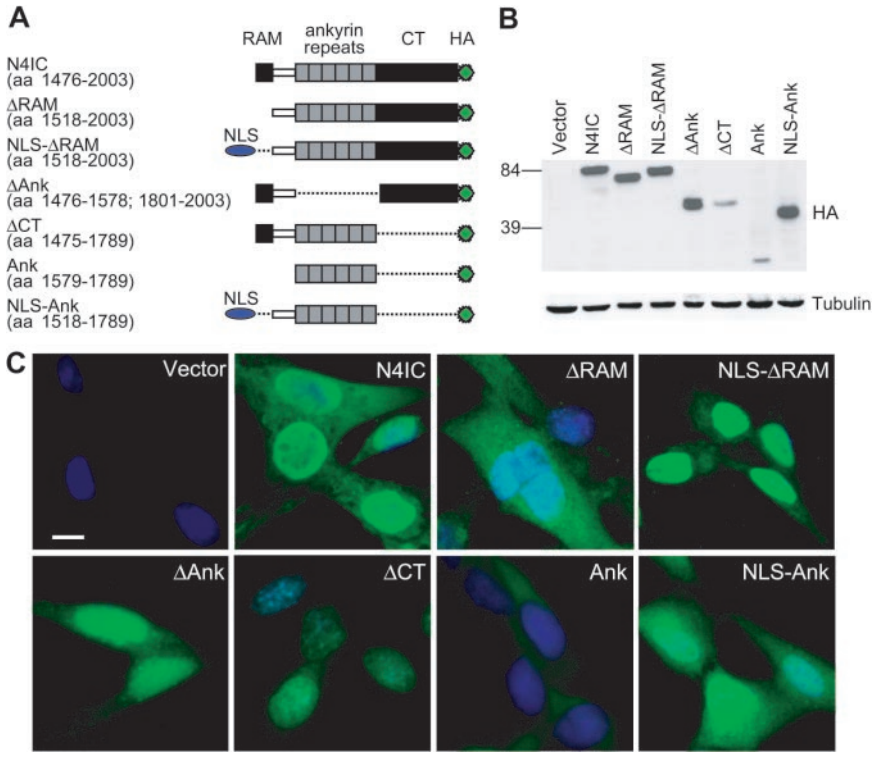

Figure 1. Deletion of the RAM domain inhibits Notch4 nuclear localization. (A) Structure diagrams of the HA epitope-tagged Notch4 intracellular region (N4IC) and related deletion constructs. The amino acid (aa) numbers from the 2003 residue human Notch4 protein that are included in each mutant are indicated in parentheses. NLS indicates nuclear localization signal. (B) Expression of the N4IC constructs in HMECs as detected by immunoblotting with anti-HA antibody. (C) Expression and subcellular localization of the N4IC constructs as detected by immunofluorescent staining of transduced HMEC lines with anti-HA antibody. Nuclei are counterstained with DAPI. Original magnification, × 400; bar = 10 μm.

HMEC-NLS-Ank was significantly less than control ($P < .001$), but significantly greater than N4IC-expressing endothelial cells ($P < .001$) for all stimuli (Table 1). Therefore, although the ankyrin repeats appear necessary for Notch4-induced inhibition of endothelial sprouting, this domain is only partially sufficient to inhibit sprouting in and of itself.

Induction of RBP-Jκ–dependent gene expression by Notch4 requires the ankyrin repeats

Activated Notch translocates to the nucleus and associates with the DNA-binding protein RBP-Jκ, thereby derepressing and/or coactivating the transcription of genes belonging to the HES and HRT families of basic helix-loop-helix factors.[55] Growing evidence suggests Notch may also signal through RBP-Jκ–independent pathways.[19-22] To determine the ability of the various Notch4 mutants to derepress/coactivate RBP-Jκ–dependent signaling, 2 distinct reporter plasmids containing promoters with RBP-Jκ–binding sites were used. In the first assay, HMEC-N4IC mutant cell lines were transiently transfected with a reporter construct containing 4 copies of an RBP-Jκ–binding element upstream of a minimal SV40 promoter driving the firefly luciferase gene (4xRBP-Jκ luciferase).[50] N4IC activation of the RBP-Jκ–dependent promoter-reporter (5.1-fold up-regulation) was abolished by deletion of the ankyrin domain, whereas mutants lacking the RAM (5.9-fold up-regulation) or CT (5.5-fold up-regulation) domains were fully able to activate the RBP-Jκ–dependent promoter (Figure 3A). However, although the ankyrin repeats alone appeared to slightly activate the 4xRBP-Jκ promoter (1.7-fold up-regulation), these results did not achieve statistical significance ($P = .9$).

With the use of a second RBP-Jκ–dependent reporter comprising a 10-kb fragment of the mouse HRT2 promoter driving the firefly luciferase gene (HRT2 luciferase),[51] similar results were seen. N4IC activated the HRT2 promoter (4.3-fold up-regulation), in a manner dependent on the ankyrin repeats but not the RAM motif (4.0-fold up-regulation of HRT2 luciferase with the ΔRAM mutant) (Figure 3B). ΔCT also up-regulated the HRT2 promoter (2.9-fold up-regulation), although activation was less than that induced by N4IC ($P < .001$), suggesting that the CT domain likely contributes in a differential manner to derepression/coactivation of individual RBP-Jκ–dependent genes. Again, the ankyrin repeats alone slightly activated the HRT2 promoter, but this was not statistically significant ($P = .9$).

As an independent measure of the ability of the Notch4 mutants to activate distinct RBP-Jκ–dependent promoters, mRNA levels of different members of the HRT and HES families of genes were analyzed. The *HRT* genes were the primary focus because their expression has been established in the mammalian vasculature.[56-58] As well, N4IC can induce HRT1 expression in cultured human endothelial cells.[43] HES1 was chosen because it has been the most extensively studied of all known Notch effectors.[55] HES4 was examined in addition to HES1 and the HRTs to determine whether there were any general differences in N4IC-mediated effects on HES family members compared with HRT family members. N4IC up-regulated all analyzed transcripts as determined by RT-PCR (Figure 3C). Specifically, HRT1 and HRT2 were strongly induced, whereas only slight induction of HRT3, HES1, and HES4 were detected. The ΔRAM and ΔCT mutants also induced each of the HRT and HES transcripts. Conversely, the ΔAnk mutant was incapable of inducing expression of any of the transcripts, verifying the requirement of the ankyrin repeats for RBP-Jκ derepression/coactivation in HMECs. Interestingly, NLS-Ank up-regulated HRT1, HRT2, and HES1 mRNA, but had no effect on expression of HRT3 or HES4 (Figure 3C). Quantitation of mRNA induction from 4 independent experiments verified that NLS-Ank up-regulated HRT2 but not HES4 mRNA, providing evidence for potentially different mechanisms of activation of different Notch-dependent promoters (Figure 3D-E).

Notch4-mediated inhibition of endothelial sprouting is independent of VEGFR-2 levels

The Notch signaling pathway down-regulates VEGF receptor-2 (VEGFR-2) mRNA expression in human capillary endothelial cells

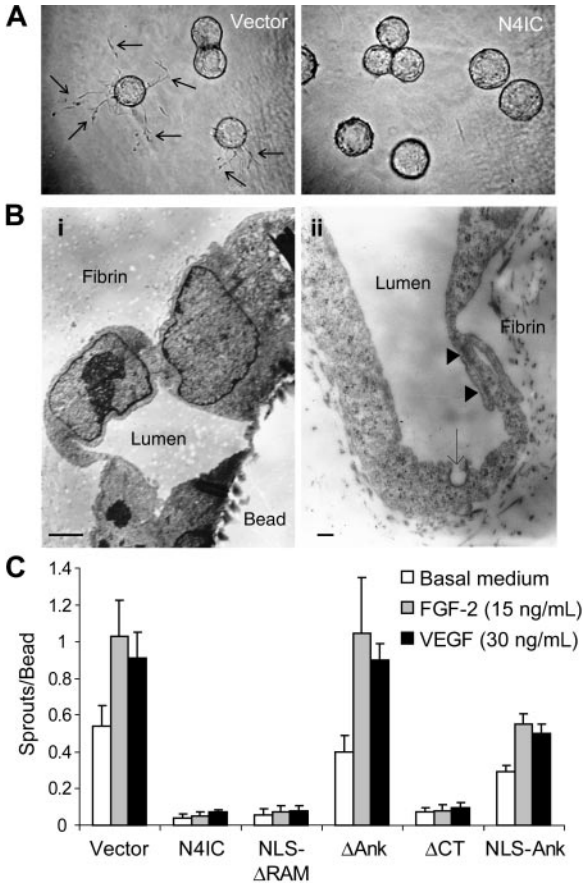

Figure 2. The ankyrin repeats are required for Notch4-mediated inhibition of endothelial sprouting. (A) Phase-contrast micrographs of microcarrier beads seeded with HMECs transduced with N4IC or empty vector control and stimulated with FGF-2. Arrows indicate capillary-like sprouts of sufficient length to be counted after 3 days of stimulation. Original magnification, × 100. (B) Transmission electron micrographs of sectioned fibrin gels containing sprouting HMECs. Panel i demonstrates the base of a sprout forming a lumen that excludes the fibrin gel (original magnification, × 9000; bar = 5 μm. Panel ii demonstrates another lumen formed by HMECs. Arrowheads point to adherens-like junctions and the arrow points to a coated pit (original magnification, × 54 000; bar = 1 μm. Electron microscopy was performed on a Philips 400 transmission electron microscope, and images were photographed with the built-in 3550 × objective (i) and the 21 500 × objective (ii). Images were scanned on an Epson Perfection scanner using Photoshop Element. (C) Quantitation of sprouting for the transduced cell lines after 3 days of stimulation with basal medium or medium supplemented with FGF-2 or VEGF. The number of sprouts per microcarrier bead (sprouts/bead) were counted and graphed as means + SD. Data are from a single experiment done in triplicate. The relative sprouting patterns are representative of at least 4 separate experiments.

and human umbilical vein endothelial cells and reduces the responsiveness of these cells to VEGF-induced proliferation.[43,44] We aimed to determine whether changes in VEGFR-2 expression were responsible for Notch4-mediated inhibition of sprouting in HMECs. In agreement with published results for other endothelial cell types, enforced expression of activated Notch4 down-regulated VEGFR-2 mRNA expression in HMECs (data not shown). However, expression of the FGF receptor 1 was not altered at the mRNA level (data not shown). Whether Notch also inhibits VEGFR-2 protein expression has not been reported. When examined by immunoblotting VEGFR-2 protein was down-regulated by N4IC as well as the NLS-ΔRAM construct, but the ΔCT construct had no effect (Figure 4A-B). These results indicate that the inhibition of endothelial sprouting by Notch4 is not solely dependent on the down-regulation of VEGFR-2 expression.

Inhibition of endothelial sprouting by Notch4 is independent of VE-cadherin expression

Recently, we have shown that enforced expression of N4IC causes an endothelial-to-mesenchymal transformation in various endothelial cell types, including HMECs.[59] This phenotypic switch of endothelial cells is defined by the down-regulation of vascular endothelial (VE)–cadherin and up-regulation of smooth muscle α-actin (SMA) expression. Because lack of VE-cadherin disrupts angiogenesis, VE-cadherin protein levels in the HMEC-N4IC mutant cell lines were compared to determine whether endothelial transdifferentiation correlated with inhibition of sprouting.[60] As detected by immunoblotting, only N4IC and NLS-ΔRAM down-regulated VE-cadherin (Figure 5A-B). ΔCT did not alter VE-cadherin expression, but fully inhibited endothelial cell sprouting. NLS-Ank, which partially inhibits sprouting, was similarly unable to regulate VE-cadherin. Collectively, these results strongly suggest that Notch4-initiated inhibition of endothelial sprouting includes events in addition to VE-cadherin down-regulation.

Constitutively-active RBP-Jκ inhibits endothelial sprouting

Given that the Notch4 deletion mutants that were able to activate RBP-Jκ–dependent genes were also able to inhibit endothelial sprouting, we attempted to determine whether Notch-independent activation of RBP-Jκ–dependent gene expression could inhibit endothelial sprouting. Attempts were made to determine to what degree Notch4-induced inhibition of sprouting was mediated by RBP-Jκ. To this end, a dominant-negative human RBP-Jκ was constructed on the basis of RBP-Jκ R218H, an established dominant-negative mouse RBP-Jκ that cannot bind DNA.[61] Cotransduction of dominant-negative human RBP-Jκ and N4IC into HMECs only partially blocked RBP-Jκ–dependent gene activation, as seen by RBP-Jκ–dependent promoter-reporter assays and RT-PCR (data not shown). This is due to at least 2 reasons: The first is that even with retrovirally mediated gene transfer, in our hands, the proportion of selected cells expressing a given transgene can vary from 50% to 80%. Secondly, the vast excess of dominant-negative RBP-Jκ protein expression required to inhibit Notch function is likely not achievable using this strategy. Transient transfections in which the dominant-negative can be added in large excess are not practical because of the low efficiency of these methods in endothelial cells.

Thus, an alternative approach to determine the role of RBP-Jκ in Notch-mediated inhibition of endothelial sprouting was attempted. A constitutively active RBP-Jκ was constructed on the basis of an established mutant that fuses the transactivation domain

Table 1. Statistical analysis of the effect of Notch 4 mutants on HMEC sprouting

	Comparisons of each N4IC construct to empty vector control, *P*					Comparison of N4IC vs NLS-Ank, *P*
	N4IC	NLS-ΔRAM	ΔAnk	ΔCT	NLS-Ank	
Medium	< .001	< .001	< .05	< .001	< .001	< .001
FGF-2	< .001	< .001	< .05	< .001	< .001	< .001
VEGF	< .001	< .001	< .05	< .001	< .001	< .001

Table shows multiple comparisons of different cell lines receiving a given growth factor stimulus.

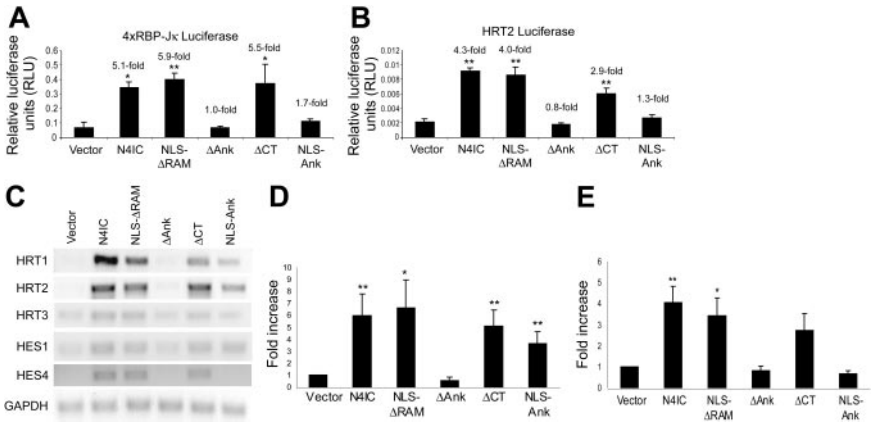

Figure 3. Notch4 induction of RBP-Jκ–dependent gene expression requires the ankyrin repeats. Reporter assays using a reporter construct with 4 copies of a RBP-Jκ–binding element upstream of an SV40 promoter-driven firefly luciferase gene (4xRBP-Jκ luciferase) (A) or a HRT2 promoter-driven firefly luciferase gene (HRT2 luciferase) (B). Reporter plasmids were electroporated into the HMEC-N4IC mutant cell lines along with a CMV promoter-driven renilla luciferase plasmid used as a normalization control for transfection efficiency. Cell lysates were harvested 48 hours after electroporation, and the relative luciferase units (RLUs) were determined as the ratio of firefly-derived luminescence over renilla-derived luminescence. Data are means + SD for a single experiment done in triplicate. Fold increases are reported for each N4IC construct cell line as compared with the empty vector control cell line. *$P < .01$ and **$P < .001$ for sample means compared with the empty vector control. The relative RLU patterns are representative of at least 3 separate experiments. (C) RT-PCR was performed using single-stranded cDNA reverse-transcribed from total RNA isolated from the HMEC-N4IC mutant cell lines. PCR amplifications were done with primers specific for fragments of the HRT1-3, HES1, HES4, and GAPDH cDNA sequences. Quantitation of 4 independent experiments was performed by densitometry of HRT2 (D) and HES4 (E) with levels normalized to GAPDH expression. *$P < .05$ and **$P < .01$ for sample means compared with the empty vector control.

of the herpes simplex virus transcription factor VP16 to the C-terminus of RBP-Jκ (RBP-VP16).[48] FLAG-tagged RBP-VP16 or HA-tagged N4IC were transduced into HMECs, and their expression was confirmed by immunoblotting (Figure 6A). Activation of the 4xRBP-Jκ luciferase reporter and up-regulation of endogenous transcripts confirmed RBP-VP16 activity. RBP-VP16 (4.0-fold up-regulation) and N4IC (3.4-fold up-regulation) induced similar levels of reporter activity (Figure 6B). RBP-VP16 and N4IC also induced similar levels of HRT1 and HRT2 expression (Figure 6C).

In keeping with activation of the RBP-Jκ–dependent promoters, RBP-VP16 inhibited endothelial sprouting in response to basal medium, as well as medium supplemented with FGF-2 and VEGF (Figure 6D). However, inhibition of sprouting by RBP-VP16 was significantly less than that induced by activated Notch4 for all stimuli ($P < .05$). These findings suggest that constitutively active RBP-Jκ partially mimics the Notch4-mediated inhibition of endothelial sprouting and imply that Notch4 may block morphogenesis through both RBP-Jκ–dependent and RBP-Jκ–independent pathways.

Inhibition of endothelial migration partially explains the antisprouting effect of Notch4

We have previously shown that Notch4 does not affect HMEC proliferation.[42] Similarly, RBP-VP16 did not decrease HMEC

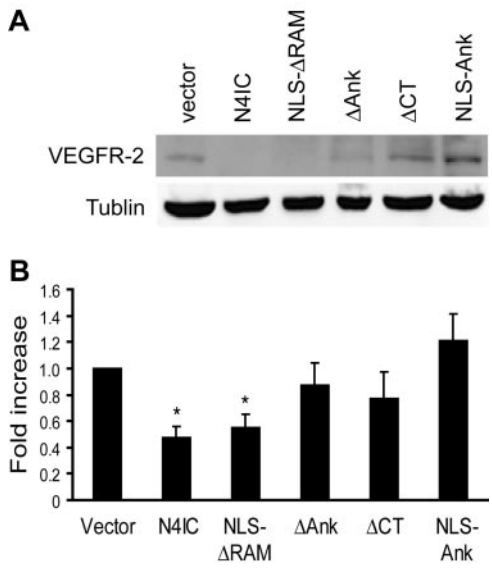

Figure 4. Notch4-induced inhibition of endothelial sprouting is independent of VEGFR-2 expression. (A) Total protein harvested from each of the Notch mutant cell lines was assayed for expression of VEGFR-2 protein by immunoblotting. Immunoblotting for α-tubulin demonstrates equivalent loading of total protein. Results are representative of 5 separate experiments and quantitation of the 3 experiments was performed by densitometry with VEGFR-2 levels normalized to α-tubulin (B). *$P < .01$ for sample means compared with the empty vector control.

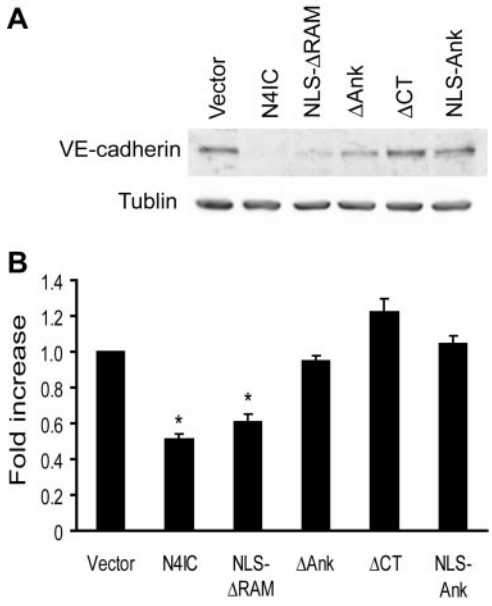

Figure 5. Inhibition of endothelial sprouting by Notch4 is independent of VE-cadherin expression. (A) Total protein harvested from each of the Notch mutant cell lines was assayed for expression of VE-cadherin protein by immunoblotting. Immunoblotting for α-tubulin demonstrates equivalent loading of total protein. Results are representative of 3 separate experiments, and quantitation of the 3 experiments was performed by densitometry with VE-cadherin levels normalized to α-tubulin (B). *$P < .001$ for sample means compared with the empty vector control.

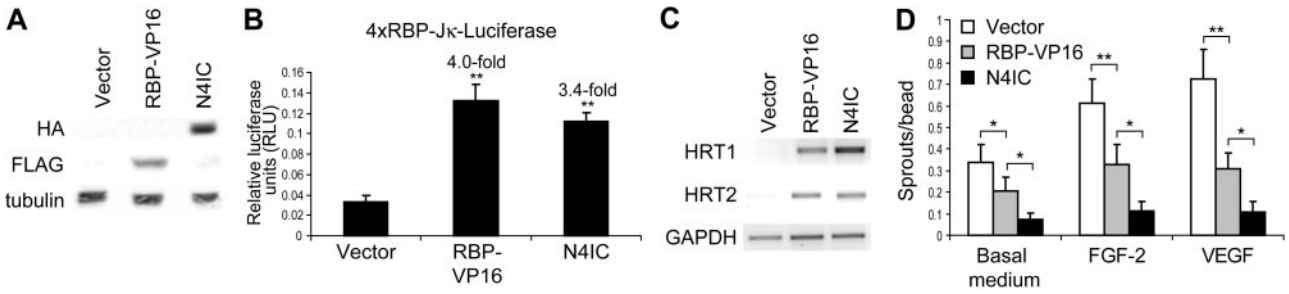

Figure 6. Constitutively active RBP-Jκ inhibits endothelial sprouting. (A) Expression of RBP-VP16 and N4IC in HMECs was detected by immunoblotting of total cellular lysates with a monoclonal anti-FLAG antibody and a monoclonal anti-HA antibody, respectively. Immunoblotting for tubulin demonstrates equivalent loading of total protein. (B) 4xRBP-Jκ luciferase reporter activity in HMECs transduced with RBP-VP16, N4IC, or empty vector control. Data are means + SD for a single experiment done in triplicate. Fold increases are reported for RBP-VP16 and N4IC cell lines as compared with the empty vector control. $^{**}P < .001$ for sample means compared with the empty vector control. The relative RLU patterns are representative of at least 3 separate experiments. (C) RT-PCR was performed by using single-stranded cDNA reverse-transcribed from total RNA isolated from HMECs transduced with RBP-VP16, N4IC, or empty vector control. PCR amplifications were done with primers specific for fragments of the HRT1-3 and GAPDH cDNA sequences. Amplification of the GAPDH fragment demonstrates equivalent levels of cDNA input. The relative patterns of mRNA expression are representative of at least 3 separate experiments. (D) Endothelial sprouting assay for HMECs transduced with RBP-VP16, N4IC, or empty vector control. Assays were quantitated and graphed as means + SE for an average of 4 experiments, each done in triplicate. $^{*}P < .05$ and $^{**}P < .001$ for the indicated comparisons.

proliferation in response to VEGF (30 ng/mL) or FGF-2 (15 ng/mL). In response to VEGF, RBP-VP16 HMECs showed a 1.88 ± 0.27-fold increase in cell number over 72 hours compared with 1.70 ± 0.10-fold increase in vector-transduced cells. FGF-2–stimulated HMECs showed a 2.00 ± 0.25-fold and 1.97 ± 0.14-fold increase in RBP-VP16 and vector-transduced HMECs, respectively.

The ability of Notch4 to inhibit endothelial sprouting is in part related to the inhibition of HMEC migration across collagen but not fibrinogen.[42] To investigate the effect of the various Notch4 mutants and RBP-VP16 on HMEC migration, a Transwell filter assay was carried out. Although Notch4IC inhibited migration, as expected, the NLS-Ank mutant had no effect on migration (Figure 7), despite a significant effect on sprouting (Figure 2C). In contrast, RBP-VP16 had a significant inhibitory effect on HMEC migration across collagen even though the antisprouting effect was not as potent as that of Notch4IC. These studies highlight the multiple steps required for an endothelial sprout to form and provide further evidence that Notch must act at several steps to block angiogenesis.

Discussion

Angiogenesis, the development of new blood vessels from the existing microvasculature, contributes to the pathogenesis of many human diseases, including cancer and cardiovascular disease.[62] Notch4 functions in endothelial cells to regulate angiogenic remodeling of the vasculature. Notch4 is predominantly expressed in the vascular endothelium and loss of Notch4 function in mice enhances the vascular remodeling defects caused by loss of Notch1 function.[34] Intriguingly, a similar failure in mouse vascular development occurs when constitutively active Notch4 is targeted to the endothelium under control of the regulatory elements of the *VEGFR-2* gene.[36] Enforced expression of activated Notch4 also blocks angiogenesis in vivo in the chick chorioallantoic membrane and inhibits endothelial sprouting in vitro, pointing to a requirement for fine regulation of Notch signaling in vascular homeostasis.[42]

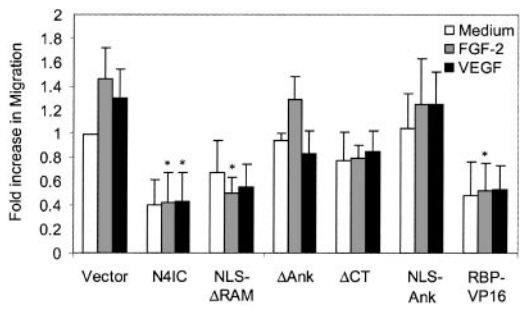

Figure 7. Constitutively active RBP-Jκ inhibits endothelial migration. HMEC migration was assayed by a Transwell filter assay in response to basal medium, FGF-2 (15 ng/mL), or VEGF (30 ng/mL). Cells migrating to the underside of the filter were quantitated and graphed as means + SE for the average of 3 experiments, each done in duplicate. $^{*}P < .05$ compared with the vector control.

The elucidation of the functional domains required for Notch4-mediated inhibition of angiogenesis in this study identifies the ankyrin repeats as the crucial motif for Notch4 function. The necessity of the ankyrin repeats for Notch4 function in HMECs is not entirely surprising, given the established significance of this domain for the activity of Notch proteins across species.[7,63-66] In particular, deletions or loss-of-function mutations of this motif invariably abolish transactivation of RBP-Jκ–dependent genes.[29,65-68] The requirement of the ankyrin repeats for RBP-Jκ–dependent signaling probably owes to the interaction with multiple factors in the coactivator complex, including RBP-Jκ, SKIP (Ski-interacting protein), MAML (Mastermind-Like-1), and the histone acetyltransferases, PCAF (p300/CBP-associated factor) and GCN5 (general control of amino-acid synthesis 5).[9,13,29,31]

Although the ankyrin repeats are necessary for Notch4 function in HMECs, they only provide partial activity on their own. Numerous studies have shown that the Notch1 ankyrin repeats are insufficient for transactivation of RBP-Jκ–dependent reporter constructs.[19,20,69,70] Our results with Notch4 using RBP-Jκ–dependent promoter-reporter assays are consistent with this finding. However, the ankyrin repeats do elevate expression of certain endogenous RBP-Jκ–dependent genes. The ankyrin repeats have been reported to be sufficient for Notch-induced inhibition of C2C12 myoblast differentiation and Notch-induced neoplastic transformation of RK3E rat kidney cells.[20,69] In both instances, the ankyrin domain-mediated effects were proposed to be RBP-Jκ independent, based largely on the fact that this motif could not activate luciferase reporters driven by promoters containing multimerized RBP-Jκ–binding elements. As shown here, it cannot be assumed that a given Notch mutant is unable to regulate all endogenous RBP-Jκ–dependent genes based solely on the fact that the mutant does not activate a reporter construct with RBP-Jκ–binding sites in its promoter.

The varying ability of the ankyrin domain alone to transactivate distinct RBP-Jκ–dependent genes suggests that different targets require varying degrees or aspects of Notch function for their transcription. Genetic studies in *Drosophila* support the theory that the transcription of some genes only requires Notch to relieve the repression mediated by RBP-Jκ, whereas other targets require both depression and the recruitment of coactivators for transcription.[71] Alleviation of RBP-Jκ–mediated repression may be sufficient for transcriptional activation when Notch-independent transcriptional activators are available or already in place, but are inhibited by the RBP-Jκ corepressor complex. It is possible that in such instances the Notch ankyrin domain alone may be sufficient to disrupt the corepressor complex and allow transcription. However, the ankyrin repeats may not be sufficient to activate regulatory sites that require Notch-mediated derepression and coactivation. Regardless of the specific requirements of individual promoters, the finding that the ankyrin repeats alone were able to significantly inhibit endothelial sprouting, despite having a minimal effect on migration, suggests that multiple distinct events play roles in Notch4-mediated angiogenesis inhibition. That multiple events are required for Notch4-directed antiangiogenic activity is bolstered by the fact that constitutive activation of RBP-Jκ, albeit having a significant effect, is also not sufficient for complete inhibition of endothelial sprouting.

In this regard, the ability of Notch4 to block both FGF-2 and VEGF-induced sprouting is significant because these growth factors are able to induce angiogenesis through distinct pathways. For example, Src-family kinases were shown to be required for angiogenesis induced by VEGF, but not FGF-2, in chick embryo and mouse in vivo models.[72] Although Notch activation has been shown to down-regulate VEGFR-2 expression, this in itself is not sufficient to explain inhibition of VEGF-induced sprouting, because the ΔCT mutants inhibit sprouting to the same degree without affecting VEGFR-2 levels. Moreover, FGFR-1 mRNA expression is not affected by Notch4 activation, thus precluding receptor down-regulation as the principal mode of Notch-mediated antiangiogenic function. Finally, the demonstration that mutants that do not down-regulate VE-cadherin still inhibit endothelial sprouting provides additional evidence for Notch inhibiting endothelial sprouting through multiple pathways.

The RAM and CT domains are not required for Notch4-induced inhibition of endothelial sprouting and are largely dispensable for up-regulation of RBP-Jκ–dependent genes. The primary function of the RAM domain is to bind RBP-Jκ, although this activity is not strictly required for interaction between Notch and RBP-Jκ.[30,31] Presumably, multiple contacts between the other Notch domains, in particular the ankyrin repeats, and the RBP-Jκ–coactivator complex can compensate for loss of the RAM. Nevertheless, the RAM domain does provide specific functional activity in endothelial cells. For instance, we have seen in other studies, that deletion of the RAM domain reduces the antiapoptotic activity provided by Notch4.[73] The CT domain of Notch1, but not Notch4, has intrinsic transcriptional activation capability when analyzed in COS7, NIH3T3, and C2C12 cells.[65] The CT is the least conserved region among human Notch proteins and this divergence may explain the differential responses evolved by Notch1 and Notch4. The RAM and CT domains are not completely superfluous because the addition of either motif to the ankyrin repeats greatly enhances the inhibition of endothelial sprouting and the activation of RBP-Jκ (Figures 2C and 3). The RAM and CT motifs may directly potentiate the activity of the ankyrin repeats or, alternatively, the ankyrin repeats may only require one of the RAM or CT for proper protein folding following translation.

In conclusion, Notch4-induced inhibition of endothelial sprouting requires the ankyrin repeats and appears to involve RBP-Jκ–dependent and –independent signaling. Of interest, it appears that down-regulation of VEGFR-2 and VE-cadherin, and functionally inhibition of migration, by Notch4 is not sufficient to explain the inhibitory effects of Notch4 on endothelial sprouting and indicate that Notch uses multiple pathways to restrict vascular morphogenesis and angiogenesis.

Acknowledgments

We thank E. Manet, R. Schmid, S.D. Hayward, and E.N. Olson for providing plasmids, and D. Walker for assistance with electron microscopy.

References

1. Artavanis-Tsakonas S, Rand MD, Lake RJ. Notch signaling: cell fate control and signal integration in development. Science. 1999;284:770-776.
2. Auerbach R, Lewis R, Shinners B, Kubai L, Akhtar N. Angiogenesis assays: a critical overview. Clin Chem. 2003;49:32-40.
3. Brou C, Logeat F, Gupta N, et al. A novel proteolytic cleavage involved in Notch signaling: the role of the disintegrin-metalloprotease TACE. Mol Cell. 2000;5:207-216.
4. Struhl G, Adachi A. Nuclear access and action of Notch in vivo. Cell. 1998;93:649-660.
5. Schroeter EH, Kisslinger JA, Kopan R. Notch-1 signalling requires ligand-induced proteolytic release of intracellular domain. Nature. 1998;393:382-386.
6. Greenwald I. Structure/function studies of lin-12/Notch proteins. Curr Opin Genet Dev. 1994;4:556-562.
7. Rebay I, Fehon RG, Artavanis-Tsakonas S. Specific truncations of Drosophila Notch define dominant activated and dominant negative forms of the receptor. Cell. 1993;74:319-329.
8. Lai EC. Notch cleavage: Nicastrin helps Presenilin make the final cut. Curr Biol. 2002;12:R200–202.
9. Uyttendaele H, Closson V, Wu G, Roux F, Weinmaster G, Kitajewski J. Notch4 and Jagged-1 induce microvessel differentiation of rat brain endothelial cells. Microvasc Res. 2000;60:91-103.
10. Zhou S, Hayward SD. Nuclear localization of CBF1 is regulated by interactions with the SMRT corepressor complex. Mol Cell Biol. 2001;21:6222-6232.
11. Oswald F, Tauber B, Dobner T, et al. p300 acts as a transcriptional coactivator for mammalian Notch-1. Mol Cell Biol. 2001;21:7761-7774.
12. Donovan J, Kordylewska A, Jan YN, Utset MF. Tetralogy of Fallot and other congenital heart defects in Hey2 mutant mice. Curr Biol. 2002;12:1605-1610.
13. Kurooka H, Honjo T. Functional interaction between the mouse notch1 intracellular region and histone acetyltransferases PCAF and GCN5. J Biol Chem. 2000;275:17211-17220.
14. Lecourtois M, Schweisguth F. The neurogenic suppressor of hairless DNA-binding protein mediates the transcriptional activation of the enhancer of split complex genes triggered by Notch signaling. Genes Dev. 1995;9:2598-2608.
15. Ligoxygakis P, Yu SY, Delidakis C, Baker NE. A subset of notch functions during Drosophila eye development require Su(H) and the E(spl) gene complex. Development. 1998;125:2893-2900.
16. Lambie EJ, Kimble J. Two homologous regulatory genes, lin-12 and glp-1, have overlapping functions. Development. 1991;112:231-240.
17. Christensen S, Kodoyianni V, Bosenberg M, Friedman L, Kimble J. lag-1, a gene required for lin-12 and glp-1 signaling in Caenorhabditis elegans, is homologous to human CBF1 and Drosophila Su(H). Development. 1996;122:1373-1383.
18. Wang S, Younger-Shepherd S, Jan LY, Jan YN. Only a subset of the binary cell fate decisions mediated by Numb/Notch signaling in Drosophila sensory organ lineage requires Suppressor of Hairless. Development. 1997;124:4435-4446.
19. Shawber C, Nofziger D, Hsieh JJ, et al. Notch signaling inhibits muscle cell differentiation through a CBF1-independent pathway. Development. 1996;122:3765-3773.
20. Nofziger D, Miyamoto A, Lyons KM, Weinmaster G. Notch signaling imposes two distinct blocks in the differentiation of C2C12 myoblasts. Development. 1999;126:1689-1702.
21. Yamamoto N, Yamamoto S, Inagaki F, et al. Role

of Deltex-1 as a transcriptional regulator downstream of the Notch receptor. J Biol Chem. 2001; 276:45031-45040.

22. Kao HY, Ordentlich P, Koyano-Nakagawa N, et al. A histone deacetylase corepressor complex regulates the Notch signal transduction pathway. Genes Dev. 1998;12:2269-2277.
23. Ellisen LW, Bird J, West DC, et al. TAN-1, the human homolog of the Drosophila notch gene, is broken by chromosomal translocations in T lymphoblastic neoplasms. Cell. 1991;66:649-661.
24. del Amo FF, Gendron-Maguire M, Swiatek PJ, Jenkins NA, Copeland NG, Gridley T. Cloning, analysis, and chromosomal localization of Notch-1, a mouse homolog of Drosophila Notch. Genomics. 1993;15:259-264.
25. Weinmaster G, Roberts VJ, Lemke G. Notch2: a second mammalian Notch gene. Development. 1992;116:931-941.
26. Lardelli M, Dahlstrand J, Lendahl U. The novel Notch homologue mouse Notch 3 lacks specific epidermal growth factor-repeats and is expressed in proliferating neuroepithelium. Mech Dev. 1994; 46:123-136.
27. Uyttendaele H, Marazzi G, Wu G, Yan Q, Sassoon D, Kitajewski J. Notch4/int-3, a mammary proto-oncogene, is an endothelial cell-specific mammalian Notch gene. Development. 1996; 122:2251-2259.
28. Achen MG, Jeltsch M, Kukk E, et al. Vascular endothelial growth factor D (VEGF-D) is a ligand for the tyrosine kinases VEGF receptor 2 (Flk1) and VEGF receptor 3 (Flt4). Proc Natl Acad Sci U S A. 1998;95:548-553.
29. Zhou S, Fujimuro M, Hsieh JJ, Chen L, Hayward SD. A role for SKIP in EBNA2 activation of CBF1-repressed promoters. J Virol. 2000;74:1939-1947.
30. Tamura K, Taniguchi Y, Minoguchi S, et al. Physical interaction between a novel domain of the receptor Notch and the transcription factor RBP-J kappa/Su(H). Curr Biol. 1995;5:1416-1423.
31. Mizutani T, Taniguchi Y, Aoki T, Hashimoto N, Honjo T. Conservation of the biochemical mechanisms of signal transduction among mammalian Notch family members. Proc Natl Acad Sci U S A. 2001;98:9026-9031.
32. Oberg C, Li J, Pauley A, Wolf E, Gurney M, Lendahl U. The Notch intracellular domain is ubiquitinated and negatively regulated by the mammalian Sel-10 homolog. J Biol Chem. 2001;276: 35847-35853.
33. Iso T, Sartorelli V, Poizat C, et al. HERP, a novel heterodimer partner of HES/E(spl) in Notch signaling. Mol Cell Biol. 2001;21:6080-6089.
34. Krebs LT, Xue Y, Norton CR, et al. Notch signaling is essential for vascular morphogenesis in mice. Genes Dev. 2000;14:1343-1352.
35. Huppert SS, Le A, Schroeter EH, et al. Embryonic lethality in mice homozygous for a processing-deficient allele of Notch1. Nature. 2000;405:966-970.
36. Uyttendaele H, Ho J, Rossant J, Kitajewski J. Vascular patterning defects associated with expression of activated Notch4 in embryonic endothelium. Proc Natl Acad Sci U S A. 2001;98:5643-5648.
37. Senger DR, Galli SJ, Dvorak AM, Perruzzi CA, Harvey VS, Dvorak HF. Tumor cells secrete a vascular permeability factor that promotes accumulation of ascites fluid. Science. 1983;219:983-985.
38. Compagni A, Wilgenbus P, Impagnatiello MA, Cotten M, Christofori G. Fibroblast growth factors are required for efficient tumor angiogenesis. Cancer Res. 2000;60:7163-7169.
39. Colville-Nash PR, Willoughby DA. Growth factors in angiogenesis: current interest and therapeutic potential. Mol Med Today. 1997;3:14-23.
40. Villa N, Walker L, Lindsell CE, Gasson J, Iruela-Arispe ML, Weinmaster G. Vascular expression of Notch pathway receptors and ligands is restricted to arterial vessels. Mech Dev. 2001;108:161-164.
41. Shirayoshi Y, Yuasa Y, Suzuki T, et al. Proto-oncogene of int-3, a mouse Notch homologue, is expressed in endothelial cells during early embryogenesis. Genes Cells. 1997;2:213-224.
42. Leong KG, Hu X, Li L, et al. Activated Notch4 inhibits angiogenesis: role of beta 1-integrin activation. Mol Cell Biol. 2002;22:2830-2841.
43. Taylor KL, Henderson AM, Hughes CC. Notch activation during endothelial cell network formation in vitro targets the basic HLH transcription factor HESR-1 and downregulates VEGFR-2/KDR expression. Microvasc Res. 2002;64:372-383.
44. Henderson AM, Wang SJ, Taylor AC, Aitkenhead M, Hughes CC. The basic helix-loop-helix transcription factor HESR1 regulates endothelial cell tube formation. J Biol Chem. 2001;276:6169-6176.
45. Pollet I, Opina CJ, Zimmerman C, Leong KG, Wong F, Karsan A. Bacterial lipopolysaccharide directly induces angiogenesis through TRAF6-mediated activation of NF-κB and c-Jun N-terminal kinase. Blood. 2003;102:1740-1742.
46. Nehls V, Drenckhahn D. A novel, microcarrier-based in vitro assay for rapid and reliable quantification of three-dimensional cell migration and angiogenesis. Microvasc Res. 1995;50:311-322.
47. Ades EW, Candal FJ, Swerlick RA, et al. HMEC-1: establishment of an immortalized human microvascular endothelial cell line. J Invest Dermatol. 1992; 99:683-690.
48. Waltzer L, Bourillot PY, Sergeant A, Manet E. RBP-J kappa repression activity is mediated by a co-repressor and antagonized by the Epstein-Barr virus transcription factor EBNA2. Nucleic Acids Res. 1995;23:4939-4945.
49. Oswald F, Liptay S, Adler G, Schmid RM. NF-kappaB2 is a putative target gene of activated Notch-1 via RBP-Jkappa. Mol Cell Biol. 1998;18:2077-2088.
50. Hsieh JJ, Henkel T, Salmon P, Robey E, Peterson MG, Hayward SD. Truncated mammalian Notch1 activates CBF1/RBPJk-repressed genes by a mechanism resembling that of Epstein-Barr virus EBNA2. Mol Cell Biol. 1996;16:952-959.
51. Koyano-Nakagawa N, Kim J, Anderson D, Kintner C. Hes6 acts in a positive feedback loop with the neurogenins to promote neuronal differentiation. Development. 2000;127:4203-4216.
52. Karsan A, Yee E, Harlan JM. Endothelial cell death induced by tumor necrosis factor-alpha is inhibited by the Bcl-2 family member, A1. J Biol Chem. 1996;271:27201-27204.
53. Celis JEE. Cell biology: a laboratory handbook. 2nd ed. New York: Academic Press; 1998.
54. Lee JS, Haruna T, Ishimoto A, Honjo T, Yanagawa SI. Intracisternal type A particle-mediated activation of the Notch4/int3 gene in a mouse mammary tumor: generation of truncated Notch4/int3 mRNAs by retroviral splicing events. J Virol. 1999;73:5166-5171.
55. Iso T, Kedes L, Hamamori Y. HES and HERP families: multiple effectors of the Notch signaling pathway. J Cell Physiol. 2003;194:237-255.
56. Leimeister C, Schumacher N, Steidl C, Gessler M. Analysis of HeyL expression in wild-type and Notch pathway mutant mouse embryos. Mech Dev. 2000;98:175-178.
57. Chin MT, Maemura K, Fukumoto S, et al. Cardiovascular basic helix loop helix factor 1, a novel transcriptional repressor expressed preferentially in the developing and adult cardiovascular system. J Biol Chem. 2000;275:6381-6387.
58. Nakagawa O, Nakagawa M, Richardson JA, Olson EN, Srivastava D. HRT1, HRT2, and HRT3: a new subclass of bHLH transcription factors marking specific cardiac, somitic, and pharyngeal arch segments. Dev Biol. 1999;216:72-84.
59. Noseda M, McLean G, Niessen K, et al. Notch activation results in phenotypic and functional changes consistent with endothelial-to-mesenchymal transformation. Circ Res. 2004;94:910-917.
60. Carmeliet P, Lampugnani MG, Moons L, et al. Targeted deficiency or cytosolic truncation of the VE-cadherin gene in mice impairs VEGF-mediated endothelial survival and angiogenesis. Cell. 1999;98:147-157.
61. Chung CN, Hamaguchi Y, Honjo T, Kawaichi M. Site-directed mutagenesis study on DNA binding regions of the mouse homologue of Suppressor of Hairless, RBP-J kappa. Nucleic Acids Res. 1994;22:2938-2944.
62. Carmeliet P. Mechanisms of angiogenesis and arteriogenesis. Nat Med. 2000;6:389-395.
63. Roehl H, Bosenberg M, Blelloch R, Kimble J. Roles of the RAM and ANK domains in signaling by the C. elegans GLP-1 receptor. EMBO J. 1996;15:7002-7012.
64. Lieber T, Kidd S, Alcamo E, Corbin V, Young MW. Antineurogenic phenotypes induced by truncated Notch proteins indicate a role in signal transduction and may point to a novel function for Notch in nuclei. Genes Dev. 1993;7:1949-1965.
65. Kurooka H, Kuroda K, Honjo T. Roles of the ankyrin repeats and C-terminal region of the mouse notch1 intracellular region. Nucleic Acids Res. 1998;26:5448-5455.
66. Kato H, Taniguchi Y, Kurooka H, et al. Involvement of RBP-J in biological functions of mouse Notch1 and its derivatives. Development. 1997; 124:4133-4141.
67. Aster JC, Robertson ES, Hasserjian RP, Turner JR, Kieff E, Sklar J. Oncogenic forms of NOTCH1 lacking either the primary binding site for RBP-Jkappa or nuclear localization sequences retain the ability to associate with RBP-Jkappa and activate transcription. J Biol Chem. 1997;272:11336-11343.
68. Jarriault S, Brou C, Logeat F, Schroeter EH, Kopan R, Israel A. Signalling downstream of activated mammalian Notch. Nature. 1995;377:355-358.
69. Dumont E, Fuchs KP, Bommer G, Christoph B, Kremmer E, Kempkes B. Neoplastic transformation by Notch is independent of transcriptional activation by RBP-J signalling. Oncogene. 2000; 19:556-561.
70. Redmond L, Oh SR, Hicks C, Weinmaster G, Ghosh A. Nuclear Notch1 signaling and the regulation of dendritic development. Nat Neurosci. 2000;3:30-40.
71. Bray S, Furriols M. Notch pathway: making sense of suppressor of hairless. Curr Biol. 2001;11: R217–221.
72. Eliceiri BP, Paul R, Schwartzberg PL, Hood JD, Leng J, Cheresh DA. Selective requirement for Src kinases during VEGF-induced angiogenesis and vascular permeability. Mol Cell. 1999;4:915-924.
73. MacKenzie F, Duriez P, Wong F, Noseda M, Karsan A. Notch4 inhibits endothelial apoptosis via RBP-Jkappa-dependent and -independent pathways. J Biol Chem. 2004;279:11657-11663.

Notch-Dependent Cell Cycle Arrest Is Associated With Downregulation of Minichromosome Maintenance Proteins

Michela Noseda, Kyle Niessen, Graeme McLean, Linda Chang and Aly Karsan

Circ. Res. 2005;97;102-104; originally published online Jun 23, 2005;
DOI: 10.1161/01.RES.0000174380.06673.81
Circulation Research is published by the American Heart Association. 7272 Greenville Avenue, Dallas, TX 72514
 Print ISSN: 0009-7330. Online ISSN: 1524-4571

Notch-Dependent Cell Cycle Arrest Is Associated With Downregulation of Minichromosome Maintenance Proteins

Michela Noseda, Kyle Niessen, Graeme McLean, Linda Chang, Aly Karsan

Perturbation of the Notch signaling pathway has been implicated in the pathogenesis of human cardiovascular diseases, and animal models have confirmed the requirement of Notch during cardiovascular development. We recently demonstrated that Notch activation delays S-phase entry and contributes to endothelial contact inhibition. Minichromosome maintenance (MCM) proteins, components of the prereplicative complex (pre-RC), are essential for DNA replication. Here, we report that Notch-mediated cell cycle arrest is associated with downregulation of MCM2 and MCM6 in endothelial cells and human fibroblasts. Downregulation of MCM proteins is also observed on activation of C promoter binding factor (CBF1) and is mediated by inhibition of Rb phosphorylation, as demonstrated using a constitutively active Rb mutant. Although the effects of the Notch pathway are cell-type specific and context-dependent, in cell types where Notch has an antiproliferative effect, downregulation of MCM proteins may be a common mechanism to inhibit DNA replication.

Intercellular signaling mediated by Notch receptors is essential for proper development and homeostasis of the cardiovascular system; indeed, perturbations of the Notch pathway have been implicated in the pathogenesis of several cardiovascular diseases.[1–3] We have recently shown that activation of Notch in endothelial cells has an antiproliferative effect which may explain the defects of vascular remodeling consequent to dysregulation of Notch activation.[3,4] In endothelial cells, Notch delays progression toward S-phase through a mechanism that depends, at least in part, on improper subcellular localization of the cyclin D-cdk4 complex secondary to downregulation of $p21^{Cip1}$.[4] Given that this mechanism seems to be endothelial-specific and targeted downregulation of $p21^{Cip1}$ by short interfering RNA induces a less efficient block of S-phase entry compared with Notch activation, we postulated that additional mechanisms may contribute to Notch-mediated cell cycle arrest.[4]

Minichromosome maintenance (MCM) proteins 2 to 7 form a complex with helicase activity and participate in the formation of prereplicative complexes (pre-RCs) that allow chromatin licensing to ensure that DNA replication initiates at specific sites.[5] Thus, MCM proteins are essential for DNA replication and cell cycle progression.[5]. Indeed, inactivation of MCM2 in *Drosophila* reduces proliferation in the developing central nervous system and microinjection of antibodies targeting MCM3 and MCM2 inhibits DNA replication.[5] Here, we identify repression of MCM2 and MCM6 as a mechanism of Notch-mediated cell cycle arrest.

Materials and Methods

Cell Culture

The human microvascular endothelial cell line, HMEC-1 (HMEC) and human umbilical vein endothelial cells (HUVEC) were cultured as previously described.[4,6] Primary human foreskin fibroblasts (HFF) were cultured in Dulbecco's modified Eagle's medium with 10% heat inactivated fetal bovine serum (HyClone).

Plasmids and Gene Transfer

HUVEC and HFF were transduced using Ampho-Phoenix packaging cells.[4] Expression of Notch4IC, Notch1IC, CBF1-VP16, and RbΔK11 proteins were confirmed by immunoblotting (data not shown). For a description of plasmids, see Material and Methods in the online data supplement at http://circres.ahajournals.org.

Immunoblotting and Immunofluorescence

Immunostaining was performed as previously described.[4] For list of antibodies used see Material and Methods in the online data supplement.

Statistical Analysis

To determine statistical significance, a Student *t* test for comparison between 2 groups was used, whereas a 1-way ANOVA with a Tukey test was used for multiple comparisons. Statistical significance was taken at $P=0.05$.

Results and Discussion

To identify new pathways mediating the Notch antiproliferative effect, HMEC transduced with vector alone (HMEC-pLNCX) or vector encoding the active intracellular portion of the endothelial-specific Notch4 (HMEC-pLNC-Notch4IC) were analyzed using high-throughput immunoblotting (Power Blot, BD Pharmingen).[7] MCM2 and MCM6 were consistently downregulated in the HMEC-pLNC-Notch4IC compared with HMEC-pLNCX (online Table I). As we have previously shown, fibronectin was found to be highly upregulated in HMEC-pLNC-Notch4IC (online Table I).[8] These findings were validated in HUVEC transduced with empty vector, vector encoding activated Notch4 (Notch4IC) or Notch1 (Notch1IC), because both Notch family members block S-phase entry.[4] Both active Notch4 and Notch1 downregulated MCM2 and MCM6 (Figure 1A and online Figure

Original received March 24, 2005; revision received June 9, 2005; accepted June 9, 2005.

From the Department of Medical Biophysics (M.N., K.N., G.M., L.C., A.K.), Department of Pathology and Laboratory Medicine (A.K.), British Columbia Cancer Agency, Vancouver, Canada; and the Department of Pathology and Laboratory Medicine (M.N., A.K.), Experimental Medicine Program (K.N., G.M., L.C., A.K.), University of British Columbia, Vancouver, Canada.

Correspondence to A. Karsan, British Columbia Cancer Research Centre, 675 W 10th Ave, Vancouver, British Columbia, Canada V5Z 1L3. E-mail akarsan@bccrc.ca

(*Circ Res*. 2005;97:102-104.)

Circulation Research is available at http://circres.ahajournals.org
DOI: 10.1161/01.RES.0000174380.06673.81

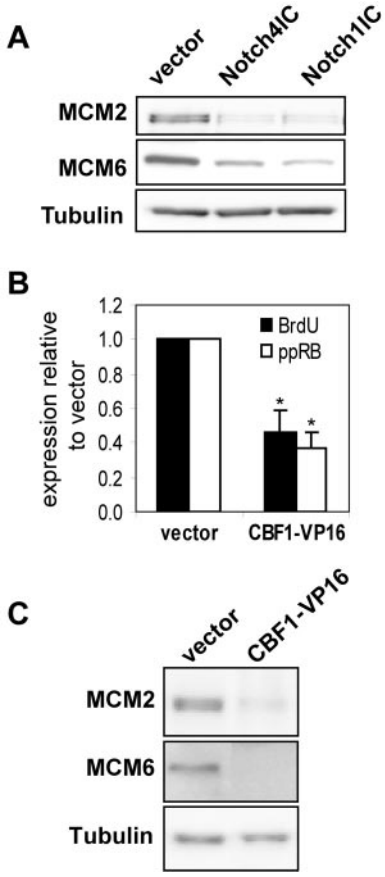

Figure 1. Notch-dependent downregulation of MCM2 and MCM6 is mediated by CBF1 in endothelial cells. A, HUVEC were transduced with empty vector (vector), Notch4IC, or Notch1IC, and cell lysates were analyzed for MCM2, MCM6, and α-tubulin expression by immunoblotting. B, BrdU incorporation and expression of phosphorylated Rb was quantitated using immunofluorescent staining in asynchronously growing HUVEC-vector and HUVEC-CBF1-VP16 cells. Bars represent the Mean$\pm$SD. *$P<0.05$ compared with vector. C, Immunoblots of cell lysates from HUVEC-vector and HUVEC-CBF1-VP16 probed for MCM2, MCM6, and α-tubulin.

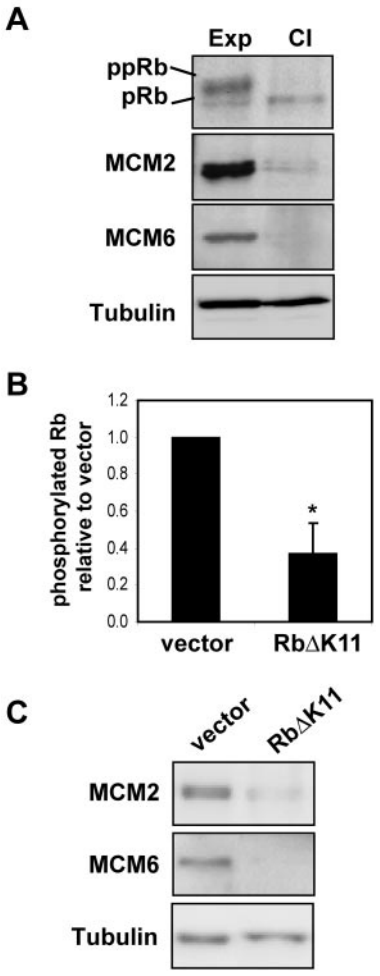

Figure 2. Inhibition of Rb phosphorylation represses MCM2 and MCM6 expression in HUVEC. A, Lysates from exponentially growing (Exp) and contact-inhibited (CI) HUVEC were analyzed by immunoblotting for Rb, MCM2, MCM6, and α-tubulin. pRb indicates hypophosphorylated Rb; ppRb, hyperphosphorylated Rb. B, HUVEC transduced with empty vector or vector encoding RbΔK11 were analyzed by immunofluorescence with an antibody against phosphorylated Rb. Cells expressing phosphorylated Rb are represented as a proportion relative to HUVEC-vector (Mean$\pm$SD). *$P<0.05$ compared with vector. C, HUVEC-vector and HUVEC-RbΔK11 were assayed by immunoblotting for expression of MCM2, MCM6, and α-tubulin.

SIA). Together with previous studies, these data suggest that Notch-mediated endothelial cell cycle arrest is effected by multiple pathways that impinge on DNA replication via downregulation of members of the pre-RC.

Binding of NotchIC to CBF1, the best described effector of the Notch pathway, induces derepression/activation of CBF1 target gene transcription.[9] Notch activation in endothelial cells triggers CBF1 activity, and the Notch pathway induces endothelial quiescence partly by a mechanism that impedes phosphorylation of Rb.[4,10] We used a constitutively-active form of CBF1, obtained by fusing the CBF1 cDNA with the transcriptional activation domain of herpes virus protein, VP16 (CBF1-VP16), to determine whether Notch-mediated cell cycle arrest could be mimicked by CBF1 activation alone.[10] HUVEC-CBF1-VP16 showed reduction of the proportion of cells entering S-phase and of cells expressing phosphorylated Rb, compared with the HUVEC-vector, suggesting that CBF1-VP16 impedes cell cycle progression at least in part via inhibition of Rb phosphorylation (Figure 1B). As well, CBF1-VP16 markedly repressed MCM2 and MCM6 expression (Figure 1C and online Figure SIB). These data demonstrate that activation of CBF1 is sufficient to inhibit Rb phosphorylation and repress MCM2 and MCM6.

MCM proteins are essential for progression of the cell cycle, but the expression of MCM2 and MCM6 in proliferating and arrested endothelial cells has not been examined. Rb phosphorylation can be used as an indicator of actively proliferating cells, because it is required for progression toward S-phase. Rb phosphorylation was abolished in contact-inhibited compared with logarithmically growing HUVEC. Rb hypophosphorylation directly correlated with the downregulation of MCM2 and MCM6 (Figure 2A). Thus, expression of MCM2 and MCM6 is regulated in concert with Rb phosphorylation and the proliferative status of endothelial cells.

Overexpression of E2F transcription factors, which are released on Rb phosphorylation, induce MCM expression.[11,12] Because both Notch activation and activated CBF1 inhibit Rb phosphorylation, we tested whether persistently hypophosphorylated Rb, which does not release E2F, is sufficient to repress MCM2 and MCM6 expression. Expression of a phosphorylation-resistant Rb mutant with 11 serine/threonine to alanine substitutions (RbΔK11) inhibits cell proliferation and E2F transcriptional activity similar to the constitutively-active and hypophosphorylated native Rb (data not shown).[13] Attenuation of phosphorylation of endogenous Rb in endothelial cells expressing RbΔK11, using an antibody specific for 2 phospho-acceptor sites that have been mutated in RbΔK11, confirmed that this construct maintains Rb in a hypophosphorylated state (Figure 2B). HUVEC transduced with RbΔK11 (HUVEC-RbΔK11) show downregulation of MCM2 and MCM6 compared with cells transduced with vector alone (HUVEC-vector) (Figure 2C). Hence, Notch-mediated CBF1-dependent inhibition of Rb phosphorylation appears sufficient to mediate downregulation of MCM2 and MCM6.

The effects of Notch activation on proliferation can be stimulatory or inhibitory depending on the cell type, and the mechanisms mediating cell cycle inhibition can be cell-type specific.[4,14] Thus, we sought to determine whether the Notch/CBF1/Rb-dependent mechanism impeding cell cycle progression is conserved in fibroblasts. Active Notch1 reduced Rb phosphorylation, reduced the proportion of HFF entering S-phase, and downregulated MCM2 and MCM6 (online Figure SIC, SIIA, and SIIB). Similarly, constitutively active CBF1-VP16 inhibited S-phase entry and Rb phosphorylation, as well as downregulated MCM2 and MCM6 expression (online Figure SID, SIIC, and SIID). Finally, we confirmed that RbΔK11 also downregulates MCM2 and MCM6 in HFF (online Figure SID and SIIE). Together these results suggest that inhibition of Rb phosphorylation and downregulation of MCM proteins via a CBF1-dependent mechanism are conserved elements of Notch-mediated cell cycle arrest in at least 2 different cell types.

Taken together our results suggest that Notch activation triggers an axis of events that, through the activation of CBF1, interferes with Rb phosphorylation and results in downregulation of MCM2 and MCM6 in endothelial cells and fibroblasts. However, fibroblasts do not show suppression of $p21^{Cip1}$ after Notch activation (data not shown). Hence, repression of MCM proteins may represent a common downstream mechanism for Notch-mediated cell cycle arrest in some cell types. It remains to be established what the effect on MCM expression is in cell types that are stimulated to grow after Notch activation. However, Notch- and CBF1-dependent hypophosphorylation of Rb with consequent downregulation of MCM proteins could be a downstream effect of the arrest in G0/G1 caused by mechanisms that remain to be elucidated. Nevertheless, these results show that there is a functional correlation between 2 highly conserved cellular pathways: the Notch pathway that regulates cell fate through an intercellular signaling mechanism and the ancestral MCM proteins that are essential for initiation of DNA replication.

Acknowledgments

This research was supported by grants to A.K. from the National Cancer Institute of Canada with funds from the Canadian Cancer Society and the Heart and Stroke Foundation of British Columbia and the Yukon. M.N. was supported by a fellowship from the Canadian Institutes of Health Research and a Research Trainee Award from the Michael Smith Foundation for Health Research and G.M. by a Research Trainee Award from the Michael Smith Foundation for Health Research. A.K. is a Scholar of the Michael Smith Foundation for Health Research. We thank Denise McDougal for assistance with cell sorting and Dr B. Larrivée for providing HFF.

References

1. Joutel A, Tournier-Lasserve E. Notch signalling pathway and human diseases. *Semin Cell Dev Biol*. 1998;9:619–625.
2. Krebs LT, Xue Y, Norton CR, Shutter JR, Maguire M, Sundberg JP, Gallahan D, Closson V, Kitajewski J, Callahan R, Smith GH, Stark KL, Gridley T. Notch signaling is essential for vascular morphogenesis in mice. *Genes Dev*. 2000;14:1343–1352.
3. Uyttendaele H, Ho J, Rossant J, Kitajewski J. Vascular patterning defects associated with expression of activated Notch4 in embryonic endothelium. *Proc Natl Acad Sci U S A*. 2001;98:5643–5648.
4. Noseda M, Chang L, McLean G, Grim JE, Clurman BE, Smith LL, Karsan A. Notch activation induces endothelial cell cycle arrest and participates in contact inhibition: role of p21Cip1 repression. *Mol Cell Biol*. 2004;24:8813–8822.
5. Tye BK. MCM proteins in DNA replication. *Annu Rev Biochem*. 1999;68:649–686.
6. Leong KG, Hu X, Li L, Noseda M, Larrivee B, Hull C, Hood L, Wong F, Karsan A. Activated Notch4 inhibits angiogenesis: role of beta 1-integrin activation. *Mol Cell Biol*. 2002;22:2830–2841.
7. Krummrei U, Baulieu EE, Chambraud B. The FKBP-associated protein FAP48 is an antiproliferative molecule and a player in T cell activation that increases IL2 synthesis. *Proc Natl Acad Sci U S A*. 2003;100:2444–2449.
8. Noseda M, McLean G, Niessen K, Chang L, Pollet I, Montpetit R, Shahidi R, Dorovini-Zis K, Li L, Beckstead B, Durand RE, Hoodless PA, Karsan A. Notch activation results in phenotypic and functional changes consistent with endothelial-to-mesenchymal transformation. *Circ Res*. 2004;94:910–917.
9. Artavanis-Tsakonas S, Rand MD, Lake RJ. Notch signaling: cell fate control and signal integration in development. *Science*. 1999;284:770–776.
10. MacKenzie F, Duriez P, Wong F, Noseda M, Karsan A. Notch4 inhibits endothelial apoptosis via RBP-Jkappa-dependent and -independent pathways. *J Biol Chem*. 2004;279:11657–11663.
11. Leone G, DeGregori J, Yan Z, Jakoi L, Ishida S, Williams RS, Nevins JR. E2F3 activity is regulated during the cell cycle and is required for the induction of S phase. *Genes Dev*. 1998;12:2120–2130.
12. Ohtani K, Iwanaga R, Nakamura M, Ikeda M, Yabuta N, Tsuruga H, Nojima H. Cell growth-regulated expression of mammalian MCM5 and MCM6 genes mediated by the transcription factor E2F. *Oncogene*. 1999;18:2299–2309.
13. Jiang Z, Zacksenhaus E. Activation of retinoblastoma protein in mammary gland leads to ductal growth suppression, precocious differentiation, and adenocarcinoma. *J Cell Biol*. 2002;156:185–198.
14. Rangarajan A, Talora C, Okuyama R, Nicolas M, Mammucari C, Oh H, Aster JC, Krishna S, Metzger D, Chambon P, Miele L, Aguet M, Radtke F, Dotto GP. Notch signaling is a direct determinant of keratinocyte growth arrest and entry into differentiation. *Embo J*. 2001;20:3427–3436.

KEY WORDS: minichromosome maintenance proteins ■ cell cycle ■ Notch ■ endothelial cells ■ retinoblastoma protein

Supplementary material, Material and Methods

Antibodies used for immunoblotting and immunofluorescence staining. Anti-MCM2, anti-MCM6 and anti-Rb (clone G3-245) antibodies were all obtained from BD Pharmingen (Bedford, MA). Anti- α-tubulin antibody was purchased from Sigma. The anti-BrdU antibody conjugated with Alexa 594 was purchased from Molecular Probes. The anti-phospho Rb antibody (specific for phosphorylation on Ser807/811 of human Rb corresponding to Ser800/804 of murine Rb) was from Cell Signaling Technologies (Beverly, MA).

Plasmids. pLNCX and pLNC-Notch4IC plasmids were previously described (Leong KG et al; *Mol Cell Biol*. 2002;22:2830-41.) To transduce HUVEC and HFF we used constructs encoding the C-terminal HA-tagged Notch4IC, Notch1IC and Flag-tagged CBF1-VP16 subcloned into the MSCV-IRES-YFP vector (MIY). cDNA encoding RbΔK11 (gift of Dr. E. Zacksenhaus, University of Toronto, Toronto, ON) was also subcloned into MIY.

Supplementary data, Table 1

Table 1

Protein	Fold change[1]		
	Run 1	**Run 2**	**Run 3**
MCM2	0.49	0.49	0.28
MCM6	0.15	0.12	0/(+)[2]
Fibronectin	(+)/0[3]	4.47	7.39

[1]**Fold change** is a semiquantitative value that represents the general trend in protein changes representing expression in HMEC-pLNC-Notch4IC relative to HMEC-pLNCX.

[2]**0/(+)** represents absence of a protein in HMEC-pLNC-Notch4IC versus presence in HMEC-pLNCX (fold change unmeasurable).

[3]**(+)/0** represents presence of a protein in HMEC- pLNC-Notch4IC versus absence in control cells (fold change unmeasurable).

Supplementary data, Figure S1

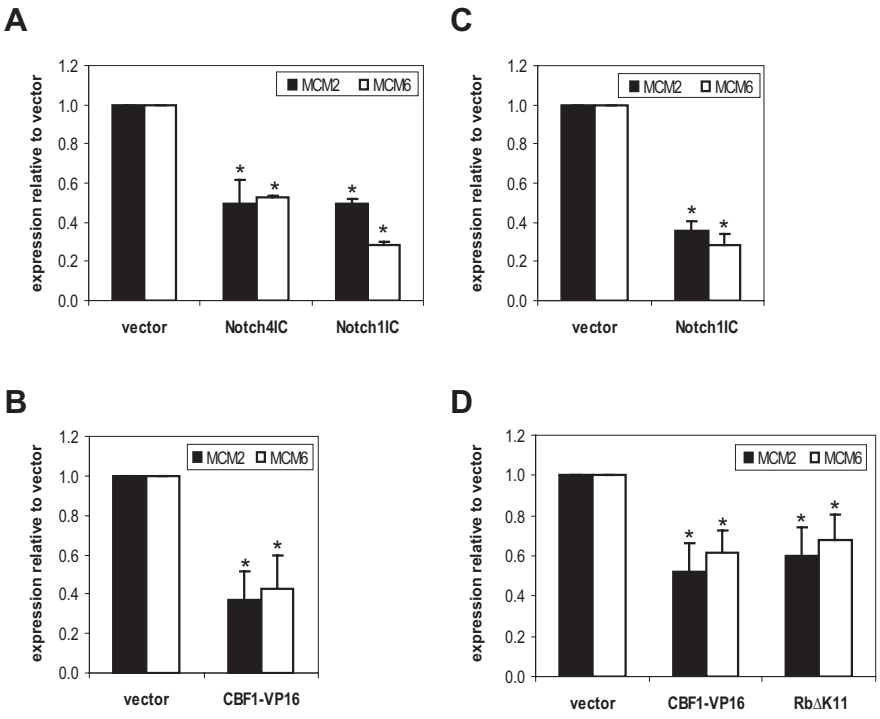

Densitometric analysis shows relative expression of MCM2 ad MCM6.
(A and B) HUVEC transduced with vector alone, Notch4IC, Notch1IC or CBF1-VP16 were lysed and tested by immunobloting for expression of MCM2, MCM6 and tubulin as a loading control. Expression was analyzed by densitometry and quantification of MCM2 and MCM6 was normalized to tubulin. (B and C) HFF transduced with vector, Notch1IC, CBF1-VP16 and RbΔK11 were analyzed as described for HUVEC. Graphs represent the mean ± SEM of at least three experiments.*P<0.05 compared to vector.

Supplementary data, Figure S2

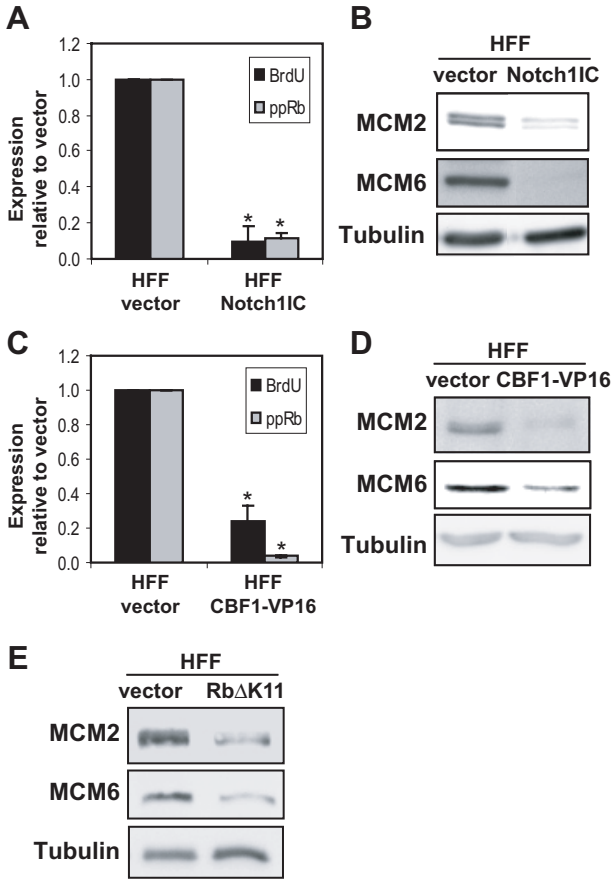

Notch activation inhibits proliferation of human fibroblasts via CBF1- and Rb-dependent repression of MCM2 and MCM6.
(A) HFF-vector and HFF-Notch1IC were examined by immunofluorescence for BrdU incorporation and Rb phosphorylation. The proportion of cells incorporating BrdU and expressing phosphorylated Rb (ppRb) is presented relative to HFF-vector (mean ± SD). (B) Immunoblotting for MCM2, MCM6 and α-tubulin. (C) Immunofluorescence for BrdU incorporation and expression of phosphorylated Rb (ppRb) in HFF transduced with empty vector or CBF1-VP16. (D) Lysates from HFF-vector or HFF- CBF1-VP16 were analyzed by immunoblotting for MCM2, MCM6 and α-tubulin. (E) Lysates from HFF-vector or HFF-RbΔK11 were analyzed by immunoblotting for MCM2, MCM6 and α-tubulin.